Monitoring the Performance of Bioretention and Permeable Pavement Stormwater Controls in Northern Ohio: Hydrology, Water Quality, and Maintenance Needs

Prepared for:

Chagrin River Watershed Partners, Inc. under NOAA award No. NA09NOS4190153

Prepared by:

Ryan J. Winston, PhD Candidate, P.E., Biological and Agricultural Engineering, North Carolina State University

Jay D. Dorsey, PhD, P.E., Water Resources Engineer, Ohio Department of Natural Resources, Division of Soil and Water Resources

William F. Hunt, PhD, P.E., William Neal Reynolds Distinguished Professor, Extension Specialist, and University Faculty Scholar, Biological and Agricultural Engineering, North Carolina State University

August 15, 2015

This final report is based upon work supported by the University of New Hampshire under Cooperative Agreement No. NA09NOS4190153 (CFDA No. 11.419) from the National Oceanic and Atmospheric Association. Any opinions, findings, and conclusions or recommendations expressed in this publication are those of the author(s) and do not necessarily reflect the views of the University of New Hampshire or the National Oceanic and Atmospheric Association.

This work was completed as part of a NERRS Science Collaborative project led by Old Woman Creek NERR, Chagrin River Watershed Partners, Inc., Ohio Department of Natural Resources- Division of Soil and Water Resources, North Carolina State University, Erie Soil and Water Conservation District, and Consensus Building Institute. The "Implementing Credits and Incentives for Innovative Stormwater Management" project promoted the implementation of low impact development (LID) stormwater control measures (SCMs) that reduce the impacts of stormwater runoff on Ohio's coastal communities and Lake Erie and worked to improve state and local stormwater policies. A Collaborative Learning Group of municipal and consulting engineers, stormwater utilities, and regulators provided feedback on this project.

TABLE OF CONTENTS

FIGURES

TABLES

LIST OF ACRONYMS AND ABBREVIATIONS

ADP – antecedent dry period
Al – aluminum
ARI – average recurrence interval
ASTM – American Society for Testing and Materials
BRC – bioretention cell
Ca - calcium
Cl – chloride
CN – curve number
Cu – copper
ESP – exchangeable sodium percentage
ET - evapotranspiration
Fe - iron
HLR – hydrologic loading ratio
IWS – internal water storage
K_{sat} – saturated hydraulic conductivity
LID – Low Impact Development
MDL – method detection limit
Mg – magnesium
Mn - manganese
NCSU – North Carolina State University
NERR – National Estuarine Research Reserve
NO_{2-3} – nitrate and nitrite nitrogen
NPDES – National Pollutant Discharge Elimination System
ON – organic nitrogen
OP – orthophosphate
OWC – Old Woman Creek National Estuarine Research Reserve
Pb - lead
PBP – particulate bound phosphorus
PC – pervious concrete
PICP – permeable interlocking concrete pavement
PQL – practical quantification limit
QA/QC – Quality Assurance, Quality Control
SAR – sodium adsorption ratio
SCM – stormwater control measure
SIR – surface infiltration rate
SIT – simple infiltration test
SWMM – Storm Water Management Model
TAN – total ammoniacal nitrogen
TKN – total Kjeldahl nitrogen
TMDL – total maximum daily load
TN – total nitrogen
TP – total phosphorus
TSS – total suspended solids

UC – Ursuline College
US EPA – United States Environmental Protection Agency
USGS – United States Geological Survey
Zn - zinc

1 EXECUTIVE SUMMARY

Urban stormwater management is a critical part of non-point source pollution abatement. Traditionally, engineers have used pipe-and-pond methodologies to meet urban drainage permit requirements. Over the past 15 years, the Low Impact Development (LID) philosophy embraced the use of distributed stormwater control measures (SCMs) to treat runoff at the source and reduce the effective impervious area. While LID practices have been monitored under other conditions, the clay soils and cold climate of northern Ohio pose perceived challenges to the use of typical LID SCMs. Under the guidance of a Collaborative Learning Group of stormwater professionals, the project team focused on monitoring and modeling bioretention and permeable pavement stormwater controls in this region. This report details the results of the intensive monitoring of three bioretention cells and four permeable pavement applications. It also includes results on an innovative SCM treatment train – using permeable pavement as a pretreatment device to an underground cistern. Hydrologic and water quality results are presented for both bioretention and permeable pavements, as well as a study on surface clogging of permeable pavements.

Volume reduction for the three permeable pavements that treated run-on varied from 16% at Willoughby Hills (Small application) to 53% at Perkins Township, considered excellent given the low drawdown rates (<0.014 in/hr) and hydrologic loading ratios (HLR, ratio of watershed area to SCM surface area) of at least 5:1. The effective curve numbers for these three sites were 1-4 points lower than pre-SCM implementation conditions. At Orange Village, drainage volume from the permeable pavement was 99% less than rainfall volume; this site had improved performance because: (1) it treated only direct rainfall, (2) it had soils with saturated hydraulic conductivity ranging from 0.01 to 1.54 in/hr, and (3) a curtain drain was present below the

permeable pavement cross-section, which perhaps enhanced exfiltration. Inclusion of an internal water storage (IWS) zone, permeable underlying soils, and low HLRs were cited as major contributing factors for improved volume reduction. Peak flow mitigation was observed even during the largest storm events for those sites where the pavement did not clog. Overall, results showed permeable pavement can be employed successfully over clay soils and in the harsh winter climate of northern Ohio.

For the permeable pavements studied, soil saturated hydraulic conductivity measured during construction was *similar to* measured post-construction drawdown rates. Post-construction drawdown rates generally followed linear trends, suggesting lateral exfiltration and evaporation are relatively minor factors in permeable pavement performance. Saturated hydraulic conductivities of the soil underlying the bioretention cells measured during construction were *less than* the measured post-construction drawdown rates for all three bioretention cells. Potential reasons for this difference between bioretention and permeable pavement were: head driven flow during exfiltration due to the 15-24 inch depth IWS zones in the bioretention cells, lateral exfiltration from the side walls of the bioretention cells, and minor amounts of evapotranspiration. While the soils surrounding the bioretention cells were mapped as Hydrologic Soil Group (HSG) D, measured post-construction drawdown rates were in the range of HSG C soils (0.065-0.17 in/hr).

The permeable pavements at Willoughby Hills also were extensively monitored for water quality performance. Leaching of sediment was observed, perhaps due to either a maturation period after construction or due to the application of deicing salt, which may have deflocculated the underlying subgrade clay soil. The permeable pavements reduced the mass loading of nutrients and of most metals; water quality performance was generally better for the Large

application, which had a lower HLR and therefore increased hydraulic retention time. The permeable pavement and cistern treatment train provided excellent capture of every nutrient studied except $NO_{2\text{-}3}$, which was converted from NH_3 under the aerobic conditions present in the SCM. Total and dissolved phosphorus, solids, and heavy metals capture was greater than 60% in all cases. These results suggested the addition of a cistern provided additional hydraulic retention time, improving the functionality of the system for water quality treatment. For all permeable pavements studied, leaching of Ca and Mg was observed, perhaps due to the dolomitic limestone used as the aggregate beneath the pavement course.

Runoff reduction for the Ursuline College, Holden South, and Holden North bioretention cells was 60%, 42%, and 36%, and primarily was related to the exfiltration rate of the underlying soil. Outflow from these SCMs did not occur until 0.63, 0.32, and 0.25 inches of rainfall occurred, respectively, showing their promise for mitigation of small storm events. For all bioretention cells studied, the watershed curve number was reduced by approximately 5 points from the value derived from the pre-SCM implementation watershed land use. Peak flows were mitigated for both small and large storm events, since the peak rainfall intensity often occurred before the bioretention surface storage was full, even during the largest and most intense rainfall events. Peak flow mitigation and volume reduction were shown to occur when bioretention cells are sited over poorly draining soils; the implementation of an IWS zone allows for augmented exfiltration over long inter-event periods.

The water quality performance of the bioretention cell at Ursuline College was monitored over a small sample size of 7 storm events. The bioretention cell leached nutrients, suggesting the type and/or amount of organic matter in the typical bioretention media blend in Ohio may need to be adjusted to prevent this from occurring in the future. Because of the 60% volume

reduction provided through exfiltration and evapotranspiration, mass loadings of sediment, inorganic nitrogen, and most metals were retained by the bioretention cell.

A study was conducted which focused on the rate and spatial progression of clogging over time at three permeable pavement sites in Ohio and two in North Carolina. For monitoring sites without clogging stressors (run-on from impermeable pavement, presence of trees, sediment from pervious areas, etc.), no significant clogging occurred over the 1 year monitoring period. The permeable/impermeable interface, defined as the location that first receives run-on from a watershed, was the location most apt to clog and will need frequent maintenance (3-4 times per year) over the life of the pavement. A simple infiltration test was developed which uses materials purchased from a home improvement store, and was shown to be a good substitute for ASTM methods for determination of surface infiltration rate (and therefore maintenance needs). Maintenance performed with street sweepers with a vacuum component resulted in significantly improved surface infiltration rates but did not produce surface infiltration rates similar to newly constructed permeable pavements, suggesting maintenance was not 100% effective.

These results suggested both bioretention and permeable pavement SCMs are viable for control of the water quality volume over poorly draining, HSG D soils. When critical design parameters are met, such as proper media selection for bioretention and prevention of surface clogging for permeable pavement, these systems provide mitigation of stormwater volume and peak flow rate as well as improve the stormwater quality discharged from an urban watershed.

KEYWORDS

Bioretention, permeable pavement, cistern, urban stormwater, volume, peak flow, nutrients, metals, sediment

1 PERMEABLE PAVEMENT HYDROLOGY

1.1 Review of Literature

Urban runoff can impair waterways through increased stream instability and pollutant loading (USEPA 2003; Line and White 2007). The construction of impervious surfaces and urban drainage networks augment the rate and volume of stormwater runoff that reaches receiving water bodies, resulting in stream bank erosion and degradation of aquatic health (Meyer et al. 2005; Schueler et al. 2009). To combat these deleterious effects, Low Impact Development (LID) strategies have been adopted to attempt to more closely mimic pre-development rate, volume, and duration of flow in the built environment (Dietz and Clausen 2008; Page et al. 2015). Stormwater managers implement stormwater control measures (SCMs), such as permeable pavement, to achieve these goals.

Permeable pavement consists of a permeable surface course of concrete, asphalt, or interlocking concrete pavers that allows water to infiltrate the pavement surface and access underlying aggregate storage layers (Figure 1). Permeable pavements usually have an underdrain serving to drain the aggregate void spaces inter-event. Stormwater entering permeable pavement can exit through four hydrologic pathways: evaporation, exfiltration to the native soil, drainage through the underdrain, and surface runoff or bypass.

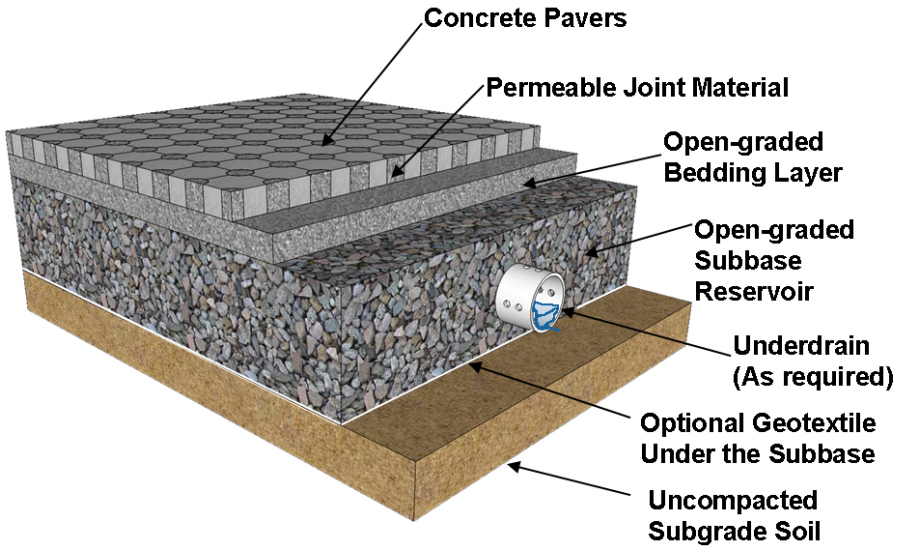

Figure 1. Schematic cross-section of permeable pavement (courtesy Matthew Jones, NCSU).

To date, most published studies on permeable pavement focused on systems designed to treat only direct rainfall and were located over permeable, sandy soils (Pratt et al. 1995; James and Thompson 1997; Rushton 2001; Brattebo and Booth 2003; Dreelin et al. 2006; Gilbert and Clausen 2006; Bean et al. 2007). Permeable pavements have been shown to substantially reduce flow volumes and peak flow rates under these conditions (Bean et al. 2007; Collins et al. 2008; Ball and Rankin, 2009). Mean curve numbers (CN) for three permeable pavement sites located over sandy soils in eastern North Carolina were 44, 77, and 80 – much lower than the standard CN of 98 for impermeable asphalt (Bean et al. 2007).

However, relatively little research has been completed on permeable pavement systems situated over clay soils (Tyner et al. 2009; Fassman and Blackbourn, 2010; Drake et al. 2014). The median estimated volumetric runoff coefficient (defined as the ratio of outflow volume to inflow volume) for permeable pavement in one study with clay underlying soils was 0.49, while that for standard asphalt was 0.85 (Fassman and Blackbourn, 2010). In a study of four types of permeable pavements located over sandy clay loam soils, a Hydrologic Soil Group (HSG) C soil,

mean runoff reductions of >98% were observed (Collins et al. 2008). Drake et al. (2014) studied runoff reduction provided by three permeable pavements located over clayey soils treating direct rainfall in Vaughn, Ontario, Canada, and found the permeable pavement reduced runoff volume by 43% and was able to capture storm events less than 0.28-in depth. Runoff reduction in clay soils was enhanced when the subgrade was treated with ripping or trenching to alleviate compaction and improve exfiltration (Tyner et al. 2009). These studies suggested permeable pavements provide the hydrologic mitigation to move a site toward pre-development hydrology, even over HSG D soils.

In poorly draining soils, the drainage fraction of the long-term hydrology can be quite significant. Inclusion of an internal water storage (IWS) zone within the aggregate has been suggested as a mechanism to increase exfiltration into the *in situ* soils and reduce drain flow (Collins et al. 2008; Wardynski et al. 2012). In clay soils, if the underdrain is located at the bottom of the cross-section, the drainage rate will be many times greater than the exfiltration rate. By storing water in the aggregate using an upturned elbow in the underdrain, stormwater has time to drain (albeit slowly) both intra- and inter-event. Permeable pavement was studied under varying drainage configurations by Wardynski et al (2012) at a single site over sandy loam texture, compacted urban fill. The study included events with rainfall depths up to 4.01 inches. Over the yearlong monitoring period, the conventionally drained cell (i.e. underdrain at the bottom of the cross-section) reduced runoff by 77%. The system with a 6-in deep IWS zone (i.e. 6 inches of ponding within the aggregate is needed for drainage to occur) reduced runoff by 99.5%. The cell with a 12-in deep IWS zone eliminated outflow entirely. This proof-of concept study suggested an IWS zone has the potential to be a boon to hydrologic mitigation for permeable pavements sited over clay soils.

The primary goals of this study were to study permeable pavements in a location with cold winters, over clay soils (HSG D), and under high hydrologic loading ratios to assess how well this SCM functions under "worst-case" conditions. Additionally, this study aimed to test how the inclusion of an IWS zone within the permeable pavement cross-section affected the long-term water balance. This was accomplished using four field monitored permeable pavement applications in northern Ohio.

1.2 Site Descriptions

Four permeable pavement SCMs were monitored for hydrologic performance at three sites in northern Ohio (Figure 2). Characteristics of the four monitored permeable pavements and their contributing watershed areas are shown in Table 1. Three of the permeable pavements accepted run-on from impermeable surfaces, while Orange Village treated only direct rainfall. Additionally, all of the permeable pavement applications included a 6-in IWS zone within the aggregate (Table 2). All SCMs were located over poorly draining HSG D soils according to soil surveys (Soil Survey Staff 2015). The IWS zone forced extended ponding within the aggregate, allowing for both vertical and lateral exfiltration into the *in situ* soils. Without the IWS zone, the drainage rate of the underdrain would be orders of magnitude higher than that of the underlying clay soil, and nearly all of the inflow would leave the permeable pavement as drainage. The sites were built as retrofits (Willoughby Hills) or redevelopment (Perkins Township and Orange Village), and there was fill soil present at all three sites. The following equation was used to calculate the hydrologic loading ratio (HLR) for each permeable pavement SCM:

$$HLR = \frac{A_{PP}+A_{WS}}{A_{PP}} \quad (1.1)$$

where A_{PP} is the surface area of the permeable pavement and A_{WS} is the surface area of the watershed. One of the purposes of this study was to tax the permeable pavements with much higher HLRs than the 3:1 HLR currently specified as the maximum allowable in the *Ohio Rainwater and Land Development Manual* (ODNR 2006). Two different loading ratios were calculated for each permeable pavement: one for clogging and one for hydrology, or exfiltration. The HLR for clogging related the watershed area draining onto the permeable pavement surface area; this value was 1.6 at Perkins Township (because the run-on to the permeable pavement was only the center drive aisle, while roof runoff was routed to the subgrade of the permeable pavement, eliminating the potential for additional surface clogging) and 1.0 at Orange Village (since it had no run-on). The Willoughby Hills Large application represented the Ohio standard for permeable pavement run-on, while the Small application heavily taxed the permeable pavement in terms of clogging and hydraulics. The HLR for exfiltration was based on the relationship between watershed area and infiltrative surface area (Table 1). At Perkins Township, the subgrade aggregate reservoir was larger than the pervious concrete surface area, allowing for additional infiltration. The stepped subgrade at Willoughby Hills Large application had the opposite effect, because the design of the steps did not cause internal ponding over the entire subgrade area.

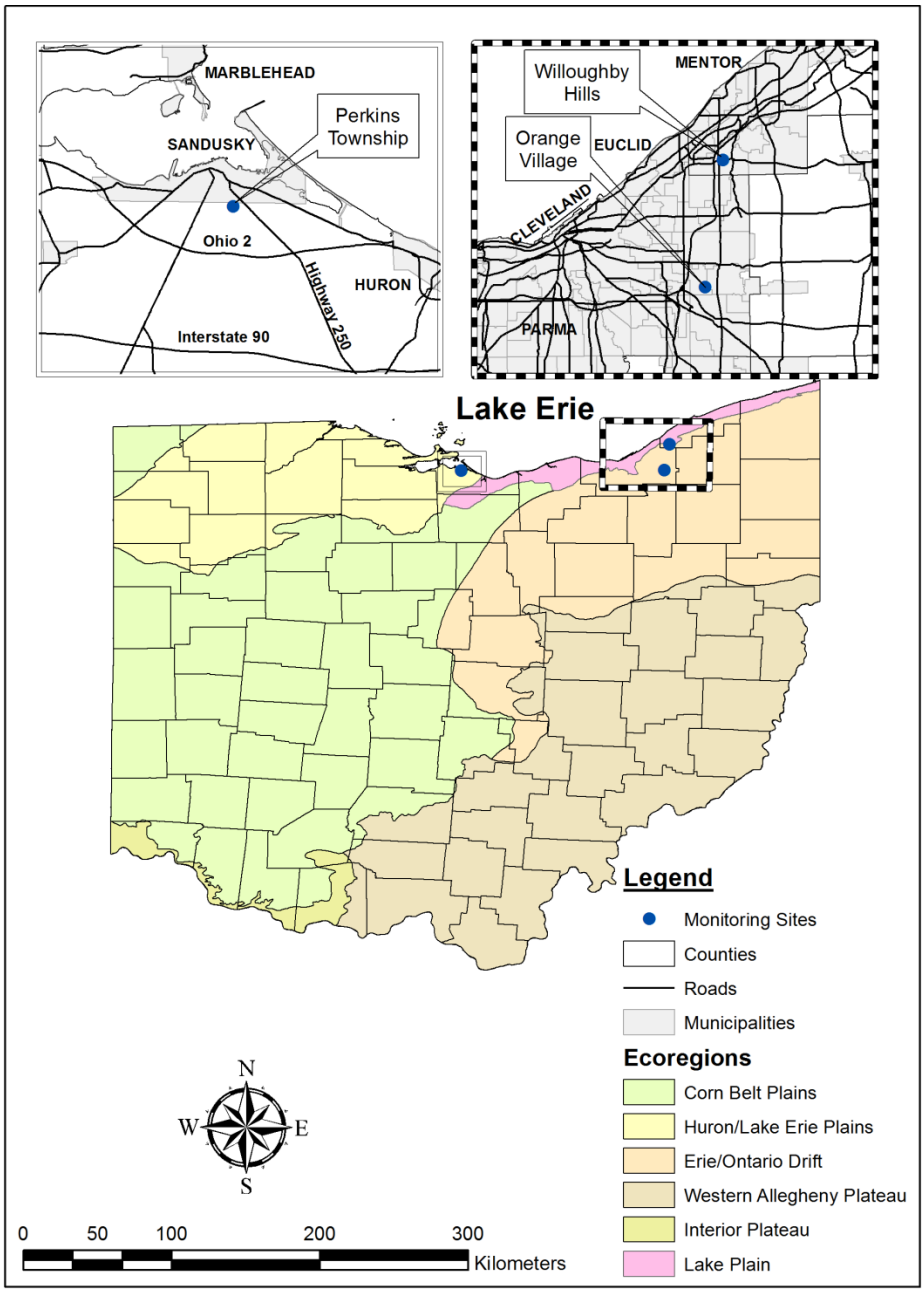

Figure 2. Permeable pavement monitoring sites in northern Ohio.

Table 1. Characteristics of the permeable pavements and their watersheds.

Site Name	Cell Name	Contributing Watershed Area (ac)	Surface Area of Permeable Pavement (ft^2)	Infiltrative Surface Area (ft^2)	Hydrologic Loading Ratio: Clogging	Hydrologic Loading Ratio: Exfiltration	Catchment Percentage Impervious
Perkins Township	-	0.53	2600	4820	1.6	5.8	81
Willoughby Hills	Small	0.08	480	480	8.2	8.2	100
	Large	0.22	4420	2210*	3.2*	5.3	100
Orange Village	-	0	9490	9490	1.0	N/A	N/A

*this represents the footprint of the IWS zone at Willoughby Hills Large

Table 2. Soil and cross-sectional characteristics for each permeable pavement.

Site Name	Cell Name	Surface Course	Mapped Underlying Soil Type	Hydrologic Soil Group	Total Aggregate Depth (in)	IWS zone depth (in)
Perkins Township	-	PC	Bennington silty clay loam	C/D	15-18	6
Willoughby Hills	Small	PICP	Mahoning silt loam	D	20	6
	Large	PICP	Mahoning silt loam	D	20	6
Orange Village	-	PICP	Wadsworth silt loam	D	23-29	6

The monitored pervious concrete system at Perkins Township was installed as part of a redevelopment in October-December 2012 adjacent to the township administration building. Two areas of pervious concrete parking stalls, with a total PC surface area of 2600 ft^2, were separated by and received runoff from an impermeable concrete drive aisle (Figure 3 and Figure 4). The design included open-graded aggregate beneath the impermeable concrete drive aisle, and thus the effective infiltrative surface area was increased to 4,820 ft^2 (Table 1). Runoff from the rooftop of the adjacent administration building (0.43 acres, shown in gray in Figure 4) was routed from the downspouts into the aggregate of the permeable pavement. A small (0.1 acre) pervious area drained to a catch basin with a surface inlet, then connected to the pipe delivering roof runoff to the aggregate beneath the pavement. This resulted in a total drainage area of 0.53 acres. Given this, the HLR for exfiltration for the Perkins Township pervious concrete

application was 5.8. Total aggregate depth varied from 15-18 inches, with a flat infiltrative surface over to the *in situ* soil.

Figure 3. Pervious concrete monitoring site at Perkins Township, Ohio.

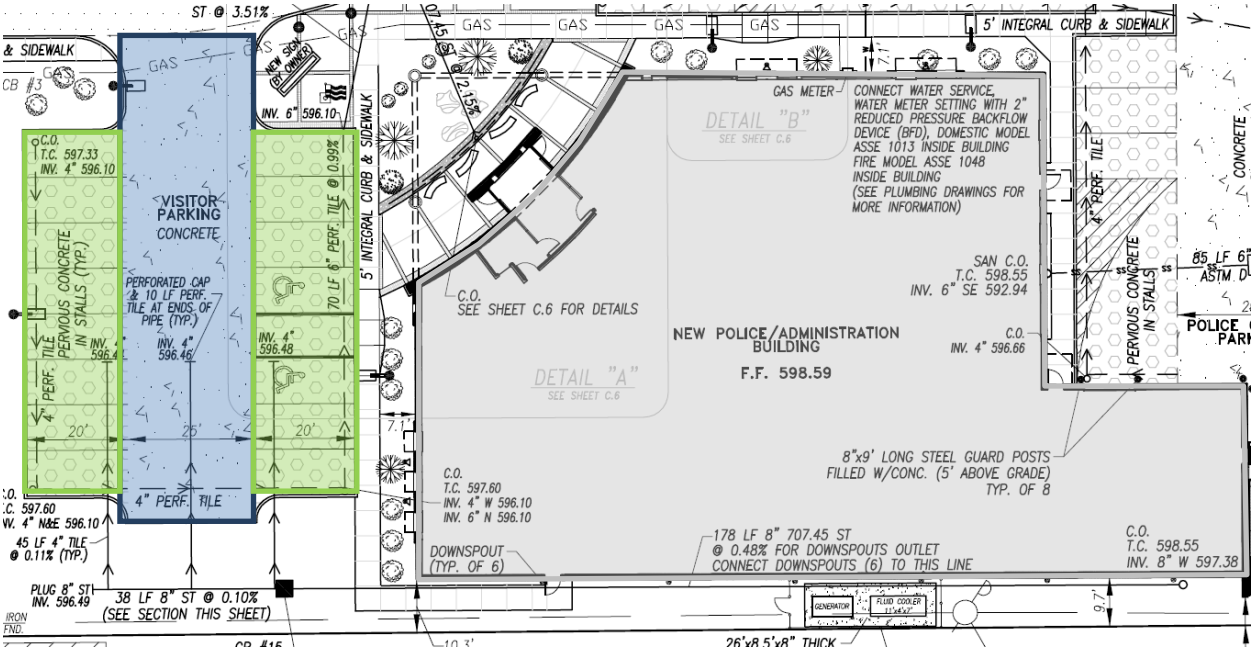

Figure 4. Schematic of Perkins Township site. The pervious concrete is hatched in green, the impermeable concrete in blue, and the building in grey. The single underdrain is shown as a dashed line.

Two permeable interlocking concrete pavement (PICP) applications were retrofitted into the parking lot at the Willoughby Hills community center during September-October 2013. The two applications, hereafter referred to as Small and Large, were monitored separately to characterize

the water balance (Figure 5 and Figure 6). Both cells employed a 20-in total aggregate depth. The Small application, 480 ft^2 in surface area, had a flat infiltrative surface (Table 1). The HLR for exfiltration for the Small application was 8.2, the largest HLR monitored in this work. The Large application (surface area of 4420 ft^2) had a stepped subgrade to make up for the 1-2% surface slope; this resulted in four steps in the subgrade with the underdrain at the bottom of the cross-section (i.e. no IWS in the stepped portion of the subgrade). Thus, the effective infiltrative surface area was reduced to 2210 ft^2. The HLR for clogging was near the maximum recommended value of 3.0 for Ohio, at 3.2 (ODNR 2006). Due to the stepped subgrade, however, the HLR for exfiltration was 5.3. The contributing drainage areas for both the Small and Large applications were impermeable asphalt, except for parking lot islands and a Small portion of concrete sidewalk in the Small application watershed.

Figure 5. Small (left) and Large (right) permeable pavement applications at Willoughby Hills.

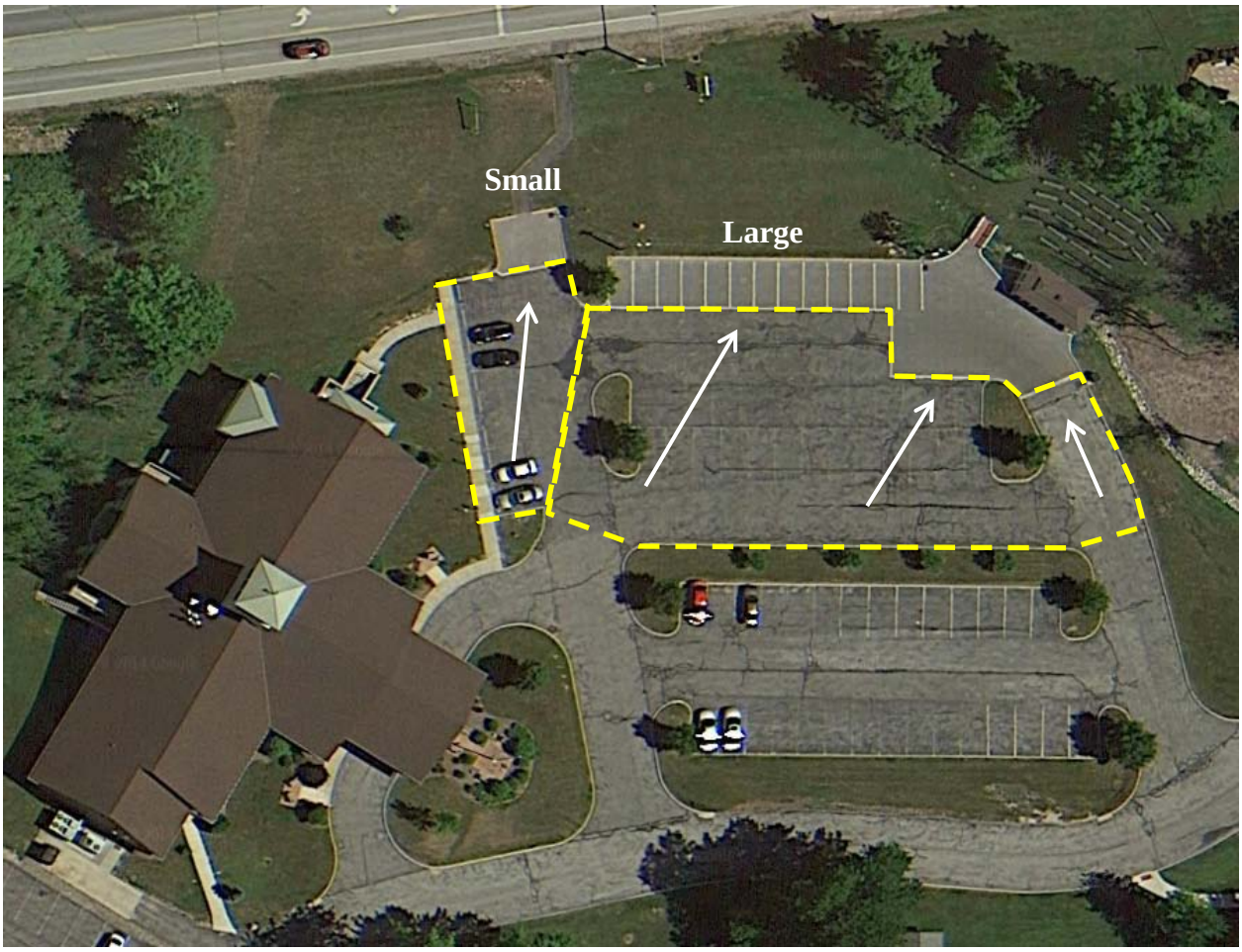

Figure 6. Willoughby Hills site plan view. Watersheds are outlined in yellow dashed lines, with general flow paths shown with white arrows. The Small and Large PICP applications are located along the northern edge of the parking lot. Photo credit: Google earth.

A newly constructed PICP parking lot was built at the Orange Village recycling facility during September-October 2013 (Figure 7 and Figure 8). The total aggregate depth at the site varied from 23-29 inches. This site was unique since it had no run-on from impermeable pavement (i.e. the parking lot treated only direct rainfall), resulting in an HLR for both clogging and exfiltration of 1.0 (Table 1). The total surface area of the parking lot was 9,490 ft^2, and a 6-in IWS zone was incorporated in the cross-section. Additionally, two 6-in diameter curtain drains were installed 2.75 feet below the permeable pavement cross-section (~5 feet below ground surface) to mitigate a potentially high water table at the site. The approximate locations

of the curtain drains are shown in yellow in Figure 8. These curtain drains probably increased the drainage capacity of the site, improving the exfiltration rate of the permeable pavement at Orange Village. Because of this, conservativism should be applied in interpreting the monitoring results from Orange Village.

Figure 7. Photos of the Orange Village PICP parking lot.

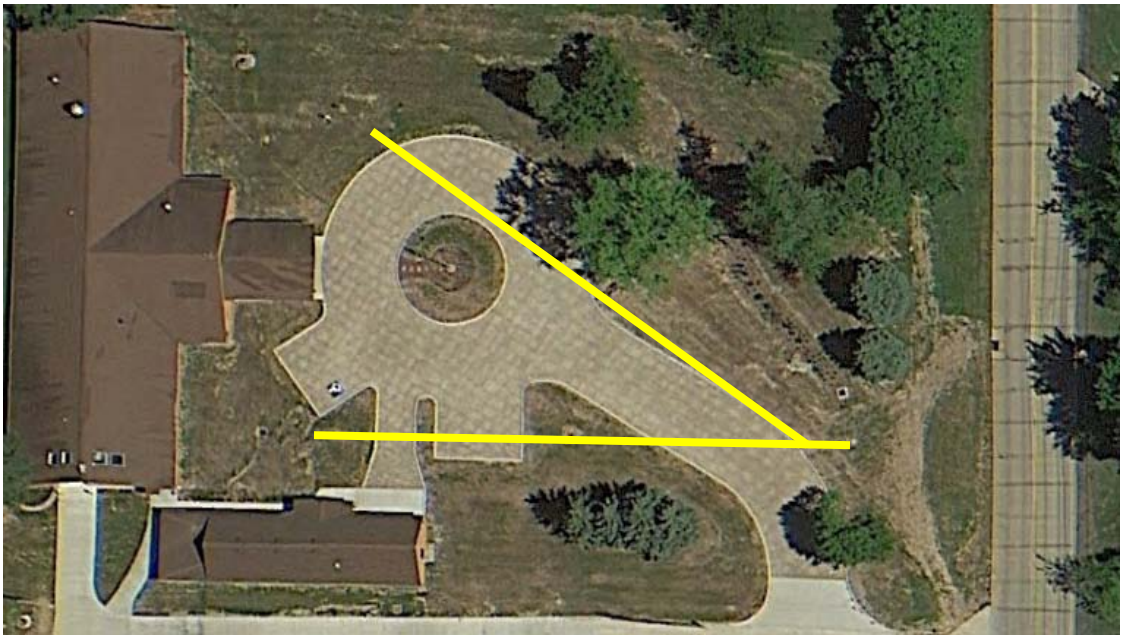

Figure 8. Plan view of the PICP parking lot at the Orange Village recycling facility. Note that the entire lot is PICP, with no run-on from impermeable pavement. Locations of the curtain drains are shown in yellow. Photo credit: Google earth.

1.3 Materials and Methods

2.3.1 Data Collection

Each site was instrumented to monitor rainfall, climatic parameters, and the hydrologic performance of each permeable pavement application. Rainfall was measured at each site using a 0.01-inch resolution tipping-bucket rain gauge affixed approximately 6 feet above the ground (Davis Instruments, Hayward, California). Rainfall data were stored in the Hobo U30 data logger attached to the nearby weather station (Figure 9). The weather station deployed at each site was a 6-ft tall, Hobo weather station that included separate sensors for wind speed, wind direction, air temperature, relative humidity, and solar radiation (Figure 9, Onset Computer Corporation, Bourne, MA). Rain gauges and weather stations were located in an open area, free from overhanging trees. All rainfall and climatic parameters were recorded on a 1-minute interval.

Figure 9. Hobo U30 data logger attached to weather station mast (left). Photo of rain gauge and weather station located at Perkins Township (right).

Underdrain flow from each permeable pavement application was measured directly using a weir box and a Hobo U20 pressure transducer (Onset Computer Corporation, Bourne, MA). Each weir box had an internal baffle to still the flow and the pressure transducer was placed as far from the weir as possible within each weir box. Weir boxes were purpose-built for each monitoring location and utilized sharp crested, v-notch weirs for greater low flow accuracy

(Figure 10). A variety of v-notch weirs were utilized depending on the expected flow rates from the underdrain (Table 3). No overflow occurred during the monitoring period at Perkins Township or Orange Village. At Willoughby Hills, overflow monitoring began on August 5, 2014 after an overflow event was observed the week prior due to surface clogging.

Water level within the aggregate base was measured as a function of time using a Hobo U20 pressure transducer within a 1" diameter water table well located at the Perkins Township and Willoughby Hills Small and Large applications. A construction oversight at Orange Village meant a monitoring well was not installed, resulting in the inability to monitor post-construction drawdown rates. Since the pressure transducers were non-vented, an additional U20 pressure transducer was placed in the rain gauge housing at each site to measure local barometric pressure. All pressure transducer measurements were obtained on a 2-minute interval. Data at each site were downloaded approximately every 3 weeks. Upon arrival at the office, data QA/QC was performed, data were backed up on a server, and data sent to NCSU staff for analysis.

Figure 10. Weir boxes at Willoughby Hills Small application (left) and Orange Village (right). Note 6" underdrain tying into weir box at left. Note presence of three weir boxes at right. The upper weir box is connected to the underdrain for the permeable pavement, while the middle and lower ones measure drainage from the bioretention cell and the curtain drains at Orange Village.

Table 3. Devices used to monitor hydrology and climatic parameters by site.

Measurement	**Perkins Township**	**Willoughby Hills Small**	**Willoughby Hills Large**	**Orange Village**
Rainfall	Davis 0.01" tipping bucket	Davis 0.01" tipping bucket		Davis 0.01" tipping bucket
Climatic Parameters	Hobo weather station	Hobo weather station		Hobo weather station
Drainage	60˚ v-notch weir	30˚ v-notch weir	60˚ v-notch weir	30˚ v-notch weir
Overflow	NA*	30˚ v-notch weir	60˚ v-notch weir	NA*
Internal Water Level	Yes	Yes	Yes	NA **

*Not Applicable - no overflow during monitoring period

**Not Applicable - water table well not installed during construction

2.3.2 Data Analysis

Data QA/QC was performed in Hoboware Pro version 3.7.0 (Onset Computer Corporation, Bourne, MA) by visually checking for anomalies in the data while in the field. This allowed for replacement of any broken data loggers without an additional trip to the field site. Rainfall and weather parameters were immediately exported from Hoboware Pro and stored in separate spreadsheets for analysis. Discrete storm events were identified by a minimum antecedent dry

period (ADP) of 6 hours and a minimum rainfall depth of 0.1 inches (Driscoll 1989). Rainfall data were further analyzed for total storm event rainfall depth (inches), rainfall duration (hours), average rainfall intensity (in/hr), peak 5-minute rainfall intensity (in/hr), and antecedent dry period (days).

Since inflow to each permeable pavement application was not directly measureable at a precise location using a weir or flume, the amount of water entering each permeable pavement was calculated using estimation methods. For Orange Village, the volume of direct rainfall onto the pavement was calculated as the product of rainfall depth and pavement surface area. For the remaining sites, a rainfall-runoff model, the NRCS Curve Number method, was used to estimate inflow (NRCS 1986):

$$Q = \frac{(P-I_a)^2}{(P-I_a+S)} * A \quad (1.2)$$

where Q is runoff volume (ft^3), P is precipitation depth (in), I_a is the initial abstraction (inches) in the watershed (I_a = 0.2*S), CN is the curve number for the watershed, A is the surface area of the watershed, and S is the potential maximum soil moisture retention (inches) and is related to the CN by:

$$S = \frac{1000}{CN} - 10 \quad (1.3)$$

Using equations 2 and 3, inflow volumes were calculated for each runoff producing event (i.e. $P > I_a$). Impervious areas within each watershed were assigned the standard CN of 98 (i.e. almost all rainfall becomes runoff; Fangmeier et al. 2006), while pervious areas were represented by a CN of 80 (only present at Perkins Township). Additionally, antecedent moisture corrections were applied to the CN for dry and wet moisture conditions using methods in NRCS (2004).

ADPs less than two days and greater than 5 days were considered wet and dry antecedent moisture conditions, respectively.

Peak inflow rates were estimated using the Rational Method (Mulvany 1851), a commonly used engineering method that relates rainfall intensity to flow rate:

$$Q_p = C * i * A \tag{1.4}$$

where Q_p is the peak flow rate (ft^3/s), C is the rational runoff coefficient, i is the rainfall intensity measured during the storm (in/hr), and A is the watershed area (acres). The rational coefficient is customarily taken to be 0.9 for impervious areas, while pervious areas were given a rational coefficient of 0.2, equivalent to that for lawns on average slope and heavy soil (Chin 2006).

Hoboware Pro software was utilized to offset all pressure transducer measurements by barometric pressure measured by a separate, on-site logger. This corrected pressure was then converted to feet of water, and exported to a spreadsheet for further analysis. Weir equations corresponding to the particular weir geometries (Table 3) were utilized to calculate discharge as a function of depth of flow above the weir crest (Grant and Dawson 2001):

$$Q = 0.676 * H^{2.5}, 30^{\circ} \text{ v-notch weir} \tag{1.5}$$

$$Q = 1.443 * H^{2.5}, 60^{\circ} \text{ v-notch weir} \tag{1.6}$$

where Q is flow rate (ft^3/s) and H is head (ft) above the weir crest. Flow rates were calculated on a 2-minute interval, and the area under the hydrograph integrated over time to calculate total outflow volumes on a storm-by-storm basis. The peak outflow rate was taken to be the instantaneous 2-minute maximum value over each storm event. Annual inflow and outflow volumes were calculated as the sum of the storm-by-storm volumes.

Water level within the aggregate of each permeable pavement was utilized to determine the drawdown rate, a combined measure of inter-event exfiltration and evaporation. Following each storm, the water level and date/time of the end of drainage (i.e. when the water level reached the invert of the underdrain) was recorded. Immediately preceding the commencement of the following rain event, the water level and date/time were also recorded. This allowed for a total drawdown time and depth to be calculated. The drawdown rate is defined as the quotient of these values, which were compared against single-ring, constant head saturated hydraulic conductivity tests performed during construction. The sum of exfiltration and evaporation can then be calculated by:

$$V_{EE} = \frac{\sum_{i=1}^{n}(Q_{DD,i} * DD_{time,i} * \phi) * f_{drain} * A_{IS}}{12} \quad (1.7)$$

Where V_{EE} is the stormwater volume exfiltrated or evaporated over the monitoring period (ft^3), n is the total number of rainfall events, Q_{DD} is the drawdown rate (in/hr), DD_{time} is the inter-event period (hr), ϕ is the porosity of the aggregate (equal to 0.4), f_{drain} is the quotient of total time in the monitoring period to sum of the dry period durations, and A_{IS} is the area of the infiltrative surface. This allowed for the estimation of drawdown while drainage was occurring for inclusion in the overall water balance calculations.

1.4 Results and Discussion

1.4.1. Rainfall

Over the course of the approximately two-year monitoring period (April 2013-November 2014) at Perkins Township, 87 storm events were monitored to quantify hydrologic performance of the pervious concrete SCM. The monitoring period at both Willoughby Hills and Orange Village lasted nine months from October 2013 through November 2014, during which 77

separate storms were observed at Willoughby Hills and Orange Village. Climatic and hydrologic data were collected during the winter months of December 2013 through March 2014, but were deemed unreliable due to equipment failure or error induced by sub-freezing temperatures. Summary statistics for rainfall event depth, average intensity, peak five-minute intensity, and antecedent dry period are presented in Table 4. Total rainfall depths over the monitoring periods were 50.59, 39.17, and 36.53 inches at Perkins Township, Willoughby Hills, and Orange Village, respectively.

Median and mean rainfall depths during the monitoring periods were near 0.35 and 0.50 inches at all three sites. Maximum observed rainfall depths were 2.6 inches at Perkins Township and around 3.5 inches for the sites located in the Chagrin River Watershed (Willoughby Hills and Orange Village). For all but the most extreme events, average and peak 5-minute rainfall intensities were lower at Orange Village than the other two monitoring sites. Median and mean antecedent dry periods varied by watershed: 4-6 days for Perkins Township (located in the Pipe Creek watershed) and 2.5-4 days for the sites in the Chagrin River watershed. This meant the IWS zone at Perkins Township typically had additional time to dewater between events.

At Perkins Township, the 82nd percentile rainfall depth was representative of the 0.75-in water quality event in Ohio. Given the run-on from the adjacent building rooftop and an empty IWS zone at the onset of rainfall, drainage would be expected to begin after 0.42 inches of rainfall. This was approximately the 58th percentile event depth recorded during the monitoring period. At Willoughby Hills, the 79th percentile monitored event depth was equivalent to the 0.75-in water quality event. With the loading ratios and 6-in IWS zones employed in the Small and Large applications (assuming the IWS zones were empty at the onset of rainfall and nearly all rainfall is transmitted as runoff from impervious surfaces), drainage would be expected at

Willoughby Hills Small and Large applications after 0.29 and 0.37 inches of rainfall, respectively. These were the 43rd and 55th percentile monitored rainfall depths. However, this neglects soil storage in the stepped portion of the subgrade at Willoughby Hills Large application. The 82nd percentile event was representative of the 0.75-in water quality event during the monitoring period at Orange Village. Because the Orange Village permeable pavement treated only direct rainfall (i.e. no run-on from impermeable surfaces), it could store the 2.4-in event without drainage (assuming the IWS zone was empty at the onset of rainfall). This represented the 99th percentile rainfall event during the monitoring period. Willoughby Hills and Perkins Township had slow drawdown rates, resulting in many storm events where the IWS zone had not dewatered at the commencement of rainfall.

Table 4. Summary statistics for rainfall events at Perkins Township, Willoughby Hills, and Orange Village.

Monitoring Site	Statistic	Depth (in)	Average Intensity (in/hr)	Peak 5-minute Intensity (in/hr)	Antecedent Dry Period (days)
Perkins Township	Minimum	0.10	0.01	0.12	0.3
	Median	0.35	0.06	1.02	4.2
	Mean	0.53	0.12	1.33	5.7
	90th percentile	1.19	0.29	3.13	13.4
	Maximum	2.60	0.87	5.04	24.8
Willoughby Hills	Minimum	0.10	0.01	0.12	0.3
	Median	0.35	0.04	0.48	2.6
	Mean	0.53	0.10	1.00	3.5
	90th percentile	1.16	0.19	2.59	7.9
	Maximum	3.42	0.86	6.60	18.6
Orange Village	Minimum	0.10	0.01	0.12	0.3
	Median	0.34	0.05	0.72	2.9
	Mean	0.48	0.09	0.96	4.2
	90th percentile	0.98	0.14	1.80	8.4
	Maximum	3.51	1.20	6.00	24.4

1.4.2 Drawdown Rate

During the design phase, understanding *in situ* soil properties is critical to the determination of post-construction permeable pavement performance. Sandy underlying soils, such as those studied in Bean et al. (2007), transmit water at higher rates than soils with higher silt and clay contents, such as those in Fassman and Blackbourn (2010). The underlying soil saturated hydraulic conductivity (K_{sat}) results in vast differences in runoff reduction for permeable pavement studies in the literature (Bean et al. 2007; Ball and Ranking 2010; Fassman and Blackbourn 2010; Drake et al. 2013; Drake et al. 2014). Pre-construction soil testing is critical to proper design and crediting of a permeable pavement SCM, as local variability in soils and site conditions greatly impact performance (Wardynski et al. 2012; Olson et al. 2013). Testing for saturated hydraulic conductivity (hydrologic design) and California Bearing Ratio (structural design) have been suggested as two soil tests important for ensuring successful permeable pavements (Eisenberg et al. 2015). Additionally, methods of soil de-compaction following construction have been used to rejuvenate soil K_{sat} (Tyner et al. 2009; Wardynski et al. 2012).

During the installation of each of the four permeable pavement SCMs, construction was halted for one day as the excavation reached the final subgrade elevation to undertake soil infiltration testing (Figure 11). Between two and six single-ring, constant head hydraulic conductivity tests were completed in the subsoils beneath each of the permeable pavement applications (Table 5). In some cases, the subsoils had been raked with the excavator bucket teeth prior to the commencement of soil testing to reduce compaction; if this was the case, then a garden hoe (hand-held) was used to remove loose soil and the test run on the uncompacted subsoil. A Mariotte bottle was used to keep a constant head on the soil, and mathematical

corrections were used based on methods in Reynolds et al. (2002) to offset for lateral water flow. Thus, the tests provided estimates of only the vertical component of the soil K_{sat}.

Figure 11. Single ring, constant head hydraulic conductivity test with Mariotte syphon (left) and hydraulic conductivity tests being carried out at the Willoughby Hills Large application (right).

All three permeable pavement monitoring sites were located over mapped HSG D soils (Table 2). At Perkins Township, *in situ* soil saturated hydraulic conductivities measured at the subgrade elevation during construction were between 0.01-0.05 in/hr, while those for the Small and Large applications at Willoughby Hills were between 0.01-0.05 in/hr and 0-0.06 in/hr, respectively. These were all within the expected range for an HSG D soil. Post-construction drawdown rate, measured by taking the slope of the linear water table drawdown following a storm event (Figure 12), was 0.013 in/hr at Perkins Township. Post-construction drawdown rates were within the range of those measured during construction at this site, suggesting the soil de-compaction implemented at the subgrade elevation was successful. However, both the Willoughby Hills Small and Large applications had post-construction drawdown rates on the low end of those measured during construction (Table 5). Soil conditions must have changed after the single ring

K_{sat} tests. The contractor was very diligent in breaking up compaction of the subsoil imparted by construction equipment at Willoughby Hills, so it is surmised this was not the cause of reduced K_{sat}. A possible explanation was the application of salt to the watersheds; salt was sparingly applied during winter weather at Perkins Township, while it was liberally applied at Willoughby Hills. The application of sodium-based deicing salts increases the interaction of sodium with the clayey subsoils; this in turn augments both sodium adsorption ratio (SAR) and exchangeable sodium percentage (ESP). These chemical soil parameters are measures of the amount of sodium as a function of other cations, such as Ca^{2+}, Mg^{2+}, and K^{+}. As SAR and ESP increase, deflocculation of clay particles occurs, increasing soil dispersibility. Agassi et al. (1981) found that the impacts of rain drops cause greater dispersion under sodic soil conditions; Frenkel et al. (1978) found "caking" of fine textured soils under these conditions, reducing infiltration rate and saturated hydraulic conductivity. This result is supported by others (e.g. McNeal and Coleman 1966; Pupisky and Shainberg 1979; Shainberg et al. 1981); decreases in soil hydraulic conductivity were particularly pronounced for 2:1 layer silicates, such as montmorillonites (McNeal and Coleman 1966). This may be a pathway for the apparent decreases in K_{sat} post-construction at Willoughby Hills.

Table 5. Comparing saturated hydraulic conductivity of the subsoil measured during construction to post-construction drawdown rates for each of the permeable pavement applications.

Site	**Mapped Soil**	**K_{sat} Measured during Construction (in/hr)**	**Post-Construction Drawdown Rate (in/hr)**
Perkins Township	Bennington	0.01, 0.01, 0.04,0.05	0.013
Orange Village	Wadsworth	0.01, 0.03, 0.05, 0.06, 0.72, 1.54	N/A
Willoughby Hills	Mahoning	Small – 0.01, 0.05 Large – 0, 0.01, 0.04, 0.06	Small – 0.002 Large – 0.002-0.006

Water table depth data were collected in the monitoring wells located in the Perkins Township and Willoughby Hills permeable pavements; water table data over a two month period for Perkins Township are presented in Figure 12. The interface between the aggregate storage layer and the *in situ* soil was located at 0 feet relative elevation, while the top of the IWS zone (i.e. invert of the underdrain) was at 0.5 feet elevation. The duration of drainage measurement in the weir box was nearly identical to the duration the water table was above the invert of the underdrain. The IWS zone at Perkins Township completely dewatered once during the two year monitoring period, which maximized the amount of exfiltration from the site.

Below the invert of the underdrain, exfiltration and evaporation were the controlling factors for water table drawdown. Unlike the results for the bioretention cells (see section 2.4.2), drawdown from all three permeable pavements could be modeled with a linear regression, suggesting vertical exfiltration was the dominant pathway. There was proportionally less lateral (i.e. side wall) surface area than in the bioretention cells that had both a smaller footprint and deeper IWS; when the IWS zone was full, it represented 3%, 5%, and 9%, respectively, of the infiltrative surface area at Perkins Township, Willoughby Hills Small, and Willoughby Hills Large. Even if there were substantial anisotropy in soil hydraulic conductivity (Bathke and Cassel 1991), the small lateral surface area for exfiltration would make the vertical hydraulic conductivity the critical component in permeable pavement performance. The lateral hydraulic conductivity becomes more important as the IWS zone depth is increased from 6 inches; the converse holds true as well.

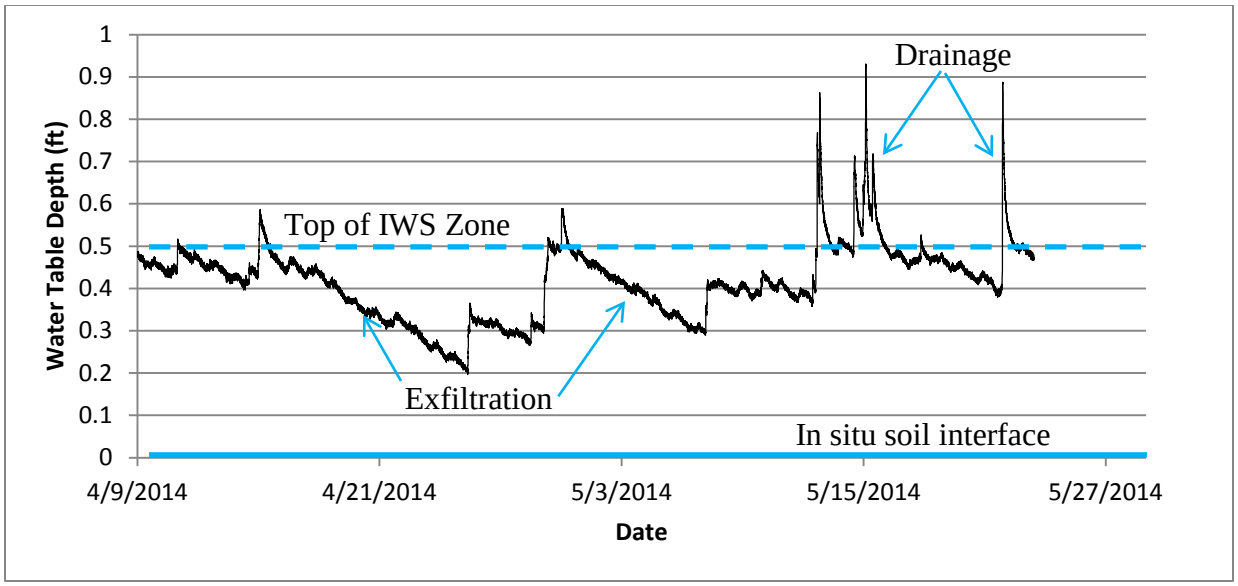

Figure 12. Water table depth as a function of time for the Perkins Township pervious concrete site. The top of the IWS zone is marked with a blue dashed line, while the in situ soil interface is located at the blue solid line.

Measured drawdown rates for the Willoughby Hills permeable pavements were <0.01 in/hr, and could be represented with a linear regression, similar to Perkins Township (Figure 12). The IWS zones at the Small and Large applications at Willoughby Hills never dewatered entirely during the monitoring period. Post-construction drawdown rates at Orange Village were not measured because monitoring wells were inadvertently not installed during construction.

1.4.3 Volume Reduction

Runoff reduction, or the sum of exfiltration and evaporation, varied from 16-99% across the four monitored permeable pavements. The Willoughby Hills Small application, which had the highest HLR for exfiltration and lowest exfiltration rate (0.002 in/hr), reduced runoff by only 16%. Willoughby Hills Large, with a slightly higher average exfiltration rate (0.004 in/hr) and lower HLR for exfiltration, reduced runoff by 32%. Perkins Township had a comparably “high” infiltration rate (0.014 in/hr) and 5.3 HLR for exfiltration, resulting in a 53% volume reduction.

Orange Village, which treated only direct rainfall and had pre-construction K_{sat} values up to 1.5 in/hr, performed by far the best, with 99% volume reduction. The curtain drains beneath the permeable pavement at Orange Village probably enhanced exfiltration and thus reduced the fraction of drainage. The Orange Village curtain drains produced a total of 64.8 watershed inches of drainage (while only 36.5 inches of rainfall occurred during the monitoring period), suggesting the curtain drains were draining other parts of the site beyond the permeable pavement. Modeling of permeable pavement in DRAINMOD showed that the inclusion of an IWS zone substantially improves the fraction of exfiltration over HSG D soils (Smolek et al. 2015).

Table 6. Summary statistics for volume and percentage of inflow, drainage, overflow, and exfiltration+evaporation.

Site Name	Cell Name	Total Inflow (ft^3)	Drainage (ft^3)	Overflow (ft^3)	Exfiltration + Evaporation (ft^3)	Drainage (%)	Overflow (%)	Runoff Reduction (%)
Perkins Township	-	59700	28300	0	31400	47.4	0	52.6
Willoughby Hills	Small	7700	5800	644	1220	75.6	8.4	15.9
	Large	24900	11000	6040	7900	44.2	24.2	31.6
Orange Village	-	28900	353	0	28500	1.2	0	98.8

At Perkins Township and Orange Village, overflow did not occur during the monitoring period; this was because the extremely high initial surface infiltration rates (800-1200 in/hr) were maintained through the monitoring period due to the low HLRs for clogging (1.6 and 1.0, respectively) at these two sites (see additional discussion in chapter 6). Therefore, runoff not reduced through exfiltration or evaporation drained through the underdrain. The elevated HLR for clogging for the Small application at Willoughby Hills resulted in 8% surface bypass (or overflow) over the monitoring period.

While the Large application at Willoughby Hills had an HLR for clogging near the standard 3 commonly approved in Ohio, substantial clogging occurred in one region of the parking lot (Figure 13). Stormwater from the upgradient portions of the watershed concentrated along the curb line of a parking lot island. Three parking stalls ended up draining an area approximately 25% of the total watershed area, creating an effective clogging HLR of 6.4. Because the parking lot also had a substantial surface slope (4.5%), stormwater had enough velocity to pass over the clogged pavement surface, flow to the curb, and then overflow into the catch basin (see chapter 6 for additional details). At the cessation of monitoring, the water balance did not sum to 100%. Since overflow was not monitored over most of the monitoring period, the authors had to back-calculate an estimate of overflow, 24% of the water balance.

To determine if this was indeed the fraction of overflow, a calibrated and validated DRAINMOD model for the Willoughby Hills Small application was used to estimate an "effective drainage area" using monitored drainage volumes for the Large application, as the basis for calibration (because underlying soils were similar for the two applications). The contributing drainage area (and associated drain spacing, drainage area to permeable pavement area ratio, etc.) was adjusted based on an assumed percentage of clogged permeable pavement. This percentage was altered until the modeled drainage best matched measured drainage for the Large application. Based on this analysis, approximately 13% of the PICP was determined to be clogged (550 ft^2). It was estimated 4400 ft^2 of the drainage area flowed to the clogged permeable pavement resulting in surface runoff equivalent to 24% of the overall water balance. Valuable insight was gained by applying DRAINMOD as a tool to determine the clogged percentage of the permeable pavement surface. This is an example of how the modeling efforts informed analysis of the monitoring results (Smolek et al. 2015).

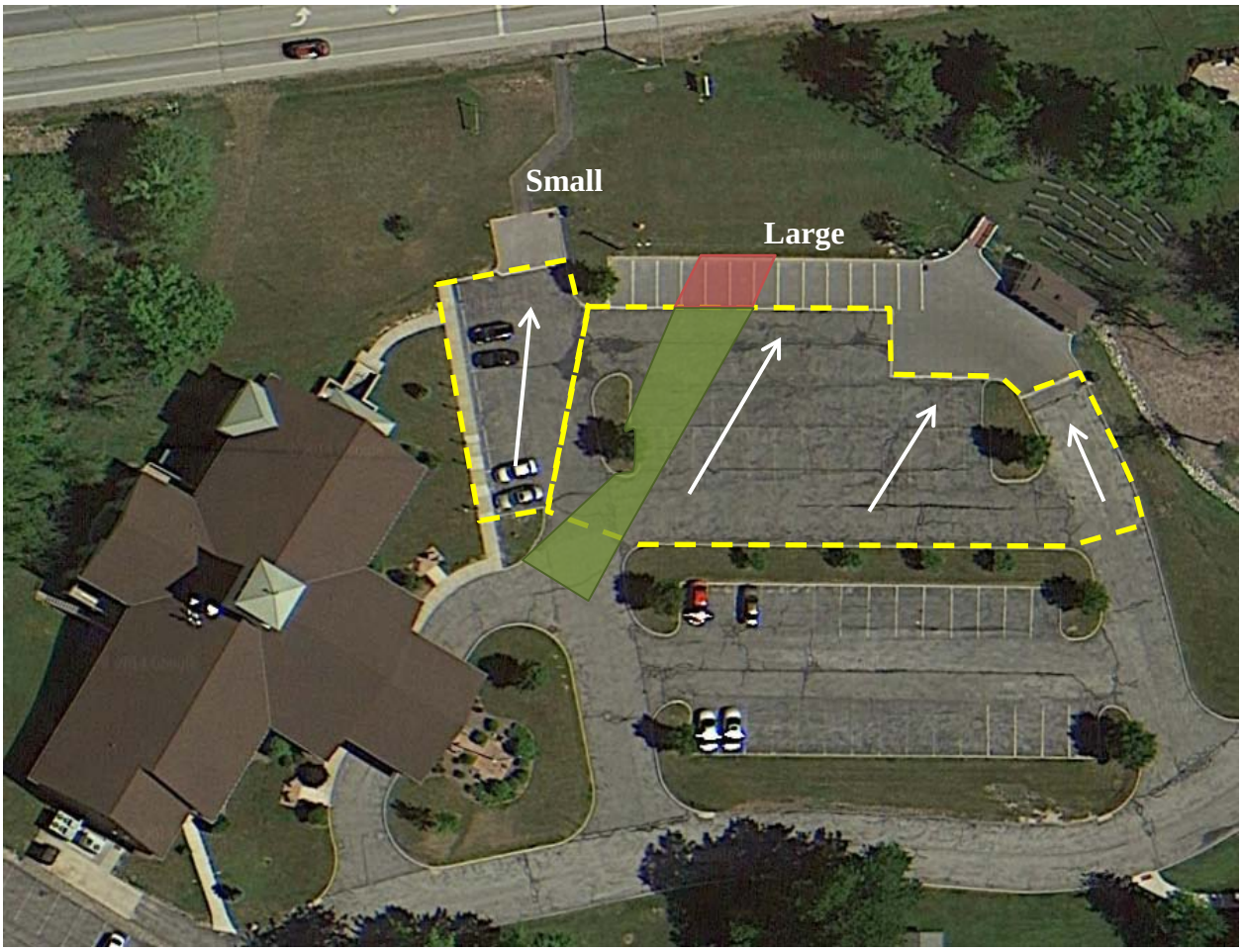

Figure 13. Estimated clogged PICP surface area (red) and contributing drainage area to the clogged PICP (green).

One of the tenets of an LID strategy is to move a development site toward pre-development hydrology. In order to do so, an SCM must capture and infiltrate or evapotranspire a substantial fraction of the smallest events to meet the pre-development initial abstraction provided by the soil and vegetation (Ahiablame et al. 2012). The number of events completely captured over the monitoring periods was summarized in Table 7. The percentage of events varied widely among the permeable pavements, with only 4% of events producing no outflow at Willoughby Hills Small application, while the Orange Village permeable pavement eliminated outflow during 78% of events. The maximum rainfall depths that did not produce outflow were 0.13, 0.42, 0.50, and

1.02 inches, respectively, for Willoughby Hills Small, Willoughby Hills Large, Perkins Township, and Orange Village. Because the IWS zone depths were the same among sites, two factors impacted the number and depth of completely captured storms: (1) the exfiltration-based HLR of the system and (2) the exfiltration rate, a function of the underlying soil characteristics. The Willoughby Hills applications had the lowest exfiltration rates and moderate to high HLRs for exfiltration, resulting in the worst performance for completely captured events. Orange Village, with an HLR of 1.0 and relatively permeable soils (based on pre-construction infiltration testing), had the best overall performance. This suggests: (1) siting these systems over the most permeable soils on a development site and (2) reducing the HLR as much as practicable will improve volume mitigation.

Table 7. Completely captured storm events (i.e. no outflow) for the four permeable pavement applications.

Site Name	Cell Name	Events Completely Captured (#)	Percentage of Events Completely Captured	Storm Size of Completely Captured Events (in)
Perkins Township	-	17/87	19.5	0.1-0.5
Willoughby Hills	Small	3/77	4	0.11-0.13
	Large	30/77	39	0.1-0.42
Orange Village	-	60/77	78	0.1-1.02

Permeable pavement performance has been shown to vary across rainfall depth, with the fraction of outflow increasing as a function of increasing rainfall depth (Fassman and Blackbourn 2010). When an IWS zone is included in the design, the available storage volume within the system increases, and subsequently the exfiltration and evaporation fractions are augmented over the long-term (Smolek et al. 2015). The discharge threshold, defined herein as the minimum rainfall depth to produce outflow from a permeable pavement, was determined by plotting outflow volume against rainfall depth and using piecewise linear regression in Figure 14

(Vieth 1989). The discharge threshold is the point where the linear trend line through the events with substantial outflow intersects the horizontal axis. For the four permeable pavement data sets, discharge thresholds were 0.11 inches at Willoughby Hills Small, 0.31 inches at Willoughby Hills Large, 0.35 inches at Perkins Township, and 0.99 inches at Orange Village. The discharge threshold was impacted by the HLR for exfiltration, the drawdown rate of the SCM (a function of the underlying soil), and antecedent dry period (ADP). Greater HLR for exfiltration and reduced drawdown rate resulted in diminished discharge threshold. Because extended ADP (5-10 days) results in greater drawdown of the IWS zone, events larger than the discharge threshold were captured by each of the permeable pavements (Table 7); the opposite also occurred. Nearly an order of magnitude difference existed between the smallest and largest discharge threshold, which speaks to the variability in the hydrologic performance of permeable pavements (Bean et al. 2007; Ball and Ranking 2010; Fassman and Blackbourn 2010; Drake et al. 2013; Drake et al. 2014). Thus, there is a need for a long-term hydrologic model to accurately represent the hydrology of these SCMs as a function of design (Smolek et al. 2015).

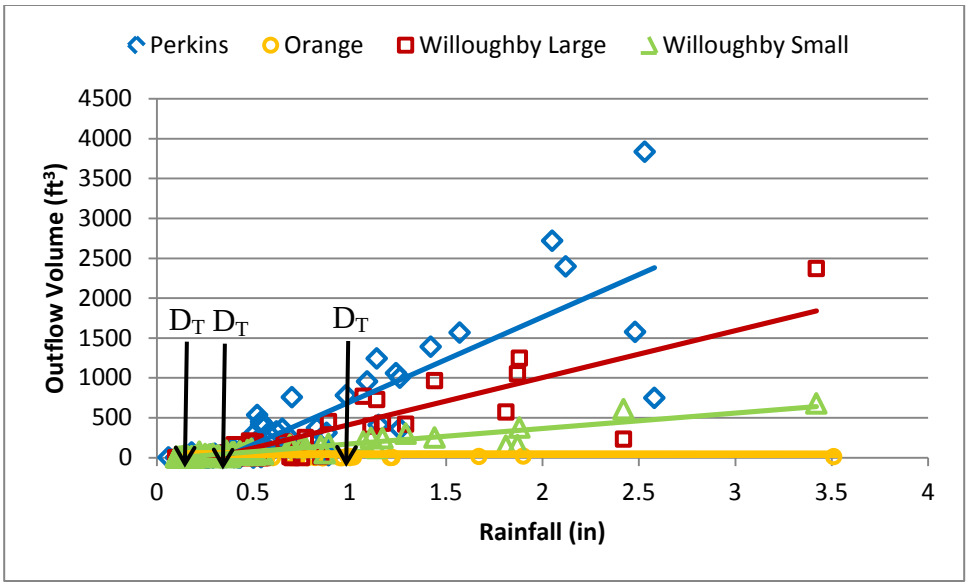

Figure 14. Determination of the discharge threshold at each permeable pavement monitoring site.

Exceedance probability plots present the ranked volume of inflow and outflow (i.e. sum of drainage and overflow) over the monitoring period (Figure 15). Since data are ranked, corresponding inflow and outflow points are not necessarily from the same storm event. However, the distribution of data allow for general conclusions about SCM performance. For Orange Village, only 17 events (or 22% of the total) had measurable outflow, and only one event had more than 100 ft^3 of outflow. Higher exfiltration rates and a lower HLR at Orange Village improved hydrologic performance, albeit the curtain drain probably had some influence on these results. The Willoughby Hills Large application completely captured a larger fraction of events than the Perkins Township site, perhaps due to a lower overall HLR and minor soil storage in the stepped portions of the subgrade. However, Perkins Township reduced runoff to a greater extent due to the higher measured exfiltration rates. For Willoughby Hills Small application, measured inflow and outflow were nearly equivalent over the range of event sizes, with substantial volume reductions occurring for only 5% of monitored storms.

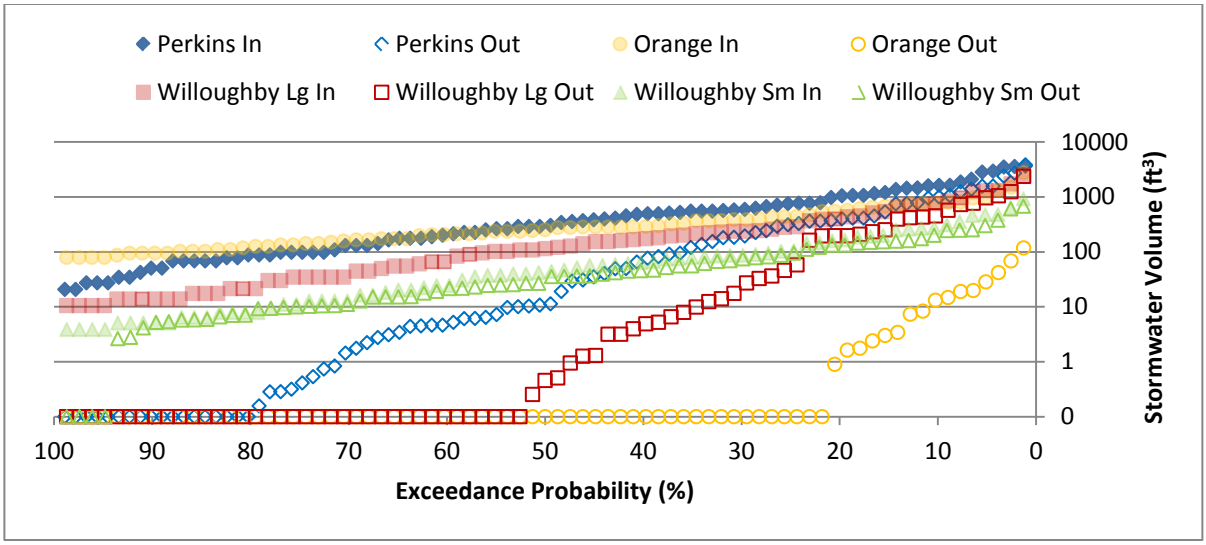

Figure 15. Exceedance probability for inflow and outflow volumes over the monitoring periods.

Engineers typically use curve numbers (CN) to determine expected volumes of runoff from a development project (NRCS 1986). CNs vary from 30 for a forested watershed in good condition located in sandy soils to 98 for an impervious parking lot or rooftop. While volumes of data exist on CNs as a function of land use and HSG, little data are available on the effect of permeable pavement on CN, especially as a function of HLR. For instance, Bean et al. (2007) calculated median CNs of 45-89 for permeable pavements treating direct rainfall and located over sandy soils in coastal North Carolina. The site with the highest CN had no gravel storage layer (i.e. pervious concrete directly on sandy underlying soils), and the authors suggested the inclusion of aggregate reservoirs in the design may reduce CN. Schwartz (2010) suggested a CN of 87 for permeable pavements over poorly draining soils, but this was for permeable pavements with only a 2.0 HLR.

The 100% impervious watersheds at Willoughby Hills had a CN of 98 (Table 8). The effective CN for the Perkins Township site was 94.6, while Orange Village had no drainage area (and therefore no watershed CN). Back-calculated CNs for the watersheds post-permeable

pavement installation are presented in Table 8; methods used for this calculation are discussed in Hawkins (1993). The storage parameter, S, was calculated using a quadratic formula originally proposed by Hawkins (1973):

$$S = 5 * [P + 2Q - (4Q^2 + 5PQ)^{1/2}] \quad (1.8)$$

where P is rainfall and Q is runoff (i.e. outflow from the permeable pavement). Using equation 3, a CN is then back-calculated for each rainfall event. In all cases, CNs were near 100 for the smallest events, and then approached a horizontal asymptote when rainfall depths were greater than 2 inches. This asymptotically-approached value is the CN used for design. Using the field-collected data, median watershed CNs post-permeable pavement implementation were between 93-94 for permeable pavements with run-on, a decrease of 1-4 points from pre-SCM implementation. Mean CNs varied from 88-92. These values were in the range of open space in poor condition over an HSG D soil (Fangmeier et al. 2006). For Orange Village, the site with no run-on, the median and mean CNs were 59; the curtain drain probably impacted the performance of this site.

These post-SCM installation CNs could be compared against a surrogate CN for pre-development hydrology in Ohio, such as that for a forest in good condition over an HSG D soil (i.e. CN of 77, NRCS 1986). The permeable pavements accepting run-on do not meet this criterion, and would need to be paired with another runoff reduction SCM in a treatment train to approach pre-development runoff volumes (Wilson et al. 2015). However, the site treating only direct rainfall was easily able to meet this metric, and in fact produced a CN near that for a fair quality forested condition over an HSG B soil. This shows the effect of HLR on system performance during large rainfall depths, where the IWS zone is quickly filled and drain flow commences earlier in the hyetograph.

Table 8. Comparing pre- and post-permeable pavement implementation curve numbers for the watersheds.

Effective Curve Number			
Site	Watershed	Median with Permeable Pavement	Mean with Permeable Pavement
Perkins Township	94.6	93.6	88.5
Willoughby Hills Small	98	94	91.5
Willoughby Hills Large	98	93.3	90.2
Orange Village	N/A	59	58.6

1.4.4 Peak Flow Mitigation

The peak runoff rate is substantially enlarged when impervious surfaces are constructed, resulting in erosion of stream banks and loss of in-stream habitat (Finkenbine et al. 2000). Reducing the peak runoff rate from an urban catchment is one key goal of flood-control regulations. Detention practices are often used for peak mitigation. There is significant interest from the design community to use permeable pavement to meet peak flow requirements, since it moves the SCM underground freeing valuable land for other beneficial uses.

For each monitored storm event, peak inflow was estimated and peak outflow measured from each permeable pavement. Summary statistics for inlet and outlet peak flow rate as well as peak flow percent reduction are presented in Table 9. Inflow rates were proportional to the size of the watershed, while outflow rates were mitigated substantially by storage in the IWS, lateral flow to the drain, and the single 6-in underdrain within each permeable pavement system. The 90^{th} percentile peak flow rate, which might be used as a surrogate for stream protection (Tillinghast et al. 2011) was below 0.2 cfs for three of the permeable pavements. Clogging of a portion of the Willoughby Hills Large pavement surface caused elevated 90^{th} percentile and maximum peak effluent rates, with magnitudes twice those of Perkins Township. Because Perkins Township had a watershed area more than twice that of Willoughby Hills Large, this

shows the importance of preventing overflow through prescriptive maintenance to prevent or remove clogging layers that form in the pavement. However, soil storage within the stepped portion of the subgrade in the Willoughby Hills Large application aided in its performance during small events, with frequent runoff capture (Figure 16). If the stormwater infiltrates the pavement, then peak flow mitigation is nearly assured through storage in the IWS zone and attenuation provided by the underdrain. If runoff or surface bypass occurs for a substantial portion of the watershed, as at the Willoughby Hills Large application, then the section of the watershed draining to the clogged area may receive little peak mitigation. Median and average percent peak flow reductions were still higher for the Willoughby Hills Large application when compared to the Small, due to differences in HLR. Perkins Township and Orange Village had minimum peak flow reductions of 45 and 92% during the monitoring periods, which shows the capability of these systems for peak mitigation if (1) surface clogging does not occur to a great extent allowing water to fully infiltrate the pavement (i.e. no bypass), and (2) the IWS zone is able to dewater between storm events, providing storage below the underdrain invert.

Table 9. Statistics for peak flow mitigation at the Perkins Township, Willoughby Hills, and Orange Village permeable pavement applications.

Site Name	Cell Name	Location	Median Peak Flow Rate (cfs)	75th Percentile Peak Flow Rate (cfs)	90th Percentile Peak Flow Rate (cfs)	Maximum Peak Flow Rate (cfs)	Median Peak Flow Reduction (%)	Range of Peak Flow Reduction (%)
Perkins Township	-	Inlet	0.40	0.80	1.21	1.95	98.3	45-100
		Outlet	0.01	0.03	0.18	0.47		
Willoughby Hills	Small	Inlet	0.04	0.10	0.19	0.48	71.8	16-100
		Outlet	0.01	0.04	0.11	0.20		
	Large	Inlet	0.09	0.28	0.50	1.29	100	0-100
		Outlet	*	0.14	0.35	0.82		
Orange Village	-	Inlet	0.14	0.24	0.35	1.18	100	92-100
		Outlet	0	0	*	0.1		

*Flow occurring but below lowest measurable value (0.01 cfs)

Peak ratio, defined as the ratio of the outlet peak to the inlet peak, is a useful metric for evaluation of peak reduction on an event-by-event basis (Davis 2008). Exceedance probability for peak ratio was plotted in Figure 16 for the four monitored permeable pavements. Davis (2008) suggested a 0.33 peak ratio should be targeted, as this is the ratio of the rational runoff coefficient for the pre-development condition (0.3) to that for an impervious surface (0.9). Mean and median peak ratios were less than 0.33 for every site, although Willoughby Hills Small approached this value with mean and median peak ratios of 0.31 and 0.28, respectively. However, this site had an HLR of 8.2, which would not typically be recommended due to concerns with surface clogging. This suggested for most events and typical design HLRs, peak flow mitigation was excellent. The percentage of events meeting the 0.33 target for LID was 55% for Willoughby Hills Small, 72% for Willoughby Hills Large, 98% for Perkins Township, and 100% for Orange Village. This suggested if stormwater infiltrates the pavement surface, peak flow mitigation will be 67% or greater in all but the largest events. Other studies of permeable pavement hydrology have generally observed excellent peak flow mitigation, albeit often with no run-on to the permeable pavement from an impervious watershed (Bean et al. 2007; Brattebo and Booth 2003; Roseen et al. 2009; Fassman and Blackbourn 2010; Roseen et al. 2012).

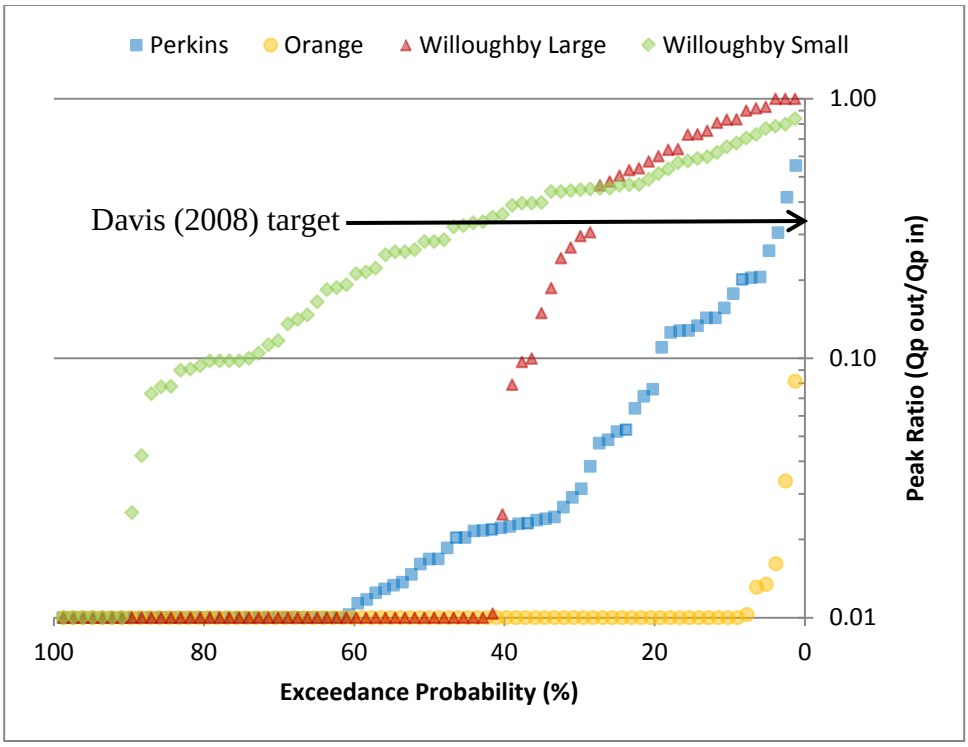

Figure 16. Analysis of peak ratio for monitored storm events at Perkins Township, Willoughby Hills, and Orange Village.

For compliance with flood control regulations, engineers are required to mitigate peak flows from developed watersheds; matching the post-development peak flow to the pre-development peak flow from a 1-year or 10-year storm is often required by municipalities. Rainfall intensities are typically derived from NOAA Atlas 14 databases for design purposes (NOAA 2015); design rainfall event intensities were obtained for Cleveland Hopkins International airport, the nearest reliable source of long term data (located approximately 53 miles from Perkins Township, 28 miles from Willoughby Hills and 22 miles from Orange Village). Because the times of concentration from the catchments of interest were small (i.e. less than 5 minutes), a 5-minute rainfall duration was used for the analysis that follows. During the monitoring periods, a minimum of two events occurred at each monitoring site that exceeded the 1-yr, 5-minute rainfall intensity (Table 10). A dichotomy in peak flow mitigation performance existed for these

high intensity rainfall events. For Perkins Township and Orange Village, peak flow mitigation exceeded 84% in all cases, as stormwater was essentially routed to an underground storage reservoir, and detained there with its outflow rate limited by the proportionally large abstraction capacity of the IWS, tortuous flow path, and the metering effect of the underdrain.

A permeable pavement site with a 2:1 loading ratio located over impermeable clay soils was studied in Auckland, New Zealand (Fassman and Blackbourn 2010). During two design rainfall events (5 and 10 yr ARI), peak flow rate was reduced by 40-50% from pre-development, considerably less than the peak mitigation observed at Perkins Township and Orange Village; however, this site did not employ an IWS zone and had a subgrade canted on a 5% slope to direct water to the underdrain.

At Willoughby Hills, substantial clogging occurred along curbs and in areas receiving increased run-on due to parking lot islands. For portions of each application, surface infiltration rates were less than 100 in/hr, limiting infiltration and causing surface bypass (Table 6). Surface bypass and the low drawdown rates for the Willoughby Hills permeable pavements were likely the reasons for the lower peak flow mitigation observed at the Small (27-61%) and Large (17-36%) applications during these design storm events. The application with the higher loading ratio had the greater peak flow mitigation – this is due to less surface clogging at this site, which routed more water to the aggregate base. Across the research sites, the peak precipitation rate occurred before the centroid of the rainfall depth for approximately 80% of the design storm events. This resulted in greater storage within the aggregate reservoir, and provided greater peak flow mitigation than if the systems received a centrally-weighted Type II rainfall distribution (NRCS 1986).

Table 10. Distribution of storm events greater than design rainfall intensities and peak flow mitigation during these events at the four permeable pavement research sites.

Statistic	Perkins	Willoughby Large	Willoughby Small	Orange
No. Events >1yr storm (3.88 in/hr)	5	3	3	0
No. Events >2yr storm (4.63 in/hr)	1	0	0	2
No. Events >5yr storm (5.56 in/hr)	0	0	0	1
No. Events >10yr storm (6.3 in/hr)	0	1	1	0
Peak Flow Reduction (%)	84-98	17-36	27-61	92-99

Flow duration curves are used to summarize the hydraulic response of permeable pavements by combining flow rates measured on a 2-minute interval across all observed storm events into a single distribution (Figure 17; Davis et al. 2012). The distributions can be compared against critical outflow rates for stream health or against rainfall or monitoring period duration to determine whether the SCM is elongating or shortening the duration of outflow. Total monitoring period durations were 609 days at Perkins Township and 423 days at both Willoughby Hills and Orange Village. Outflow occurred from the Orange Village permeable pavement for 269 hours, or 2.6% of the monitoring period due to the high *in situ* soil K_{sat}, lack of run-on to the permeable pavement, and six inch IWS zone. The Willoughby Hills Large application had the second largest number of completely captured events (Table 7), perhaps due to soil storage in the stepped portions of the subgrade. This resulted in a similar duration of outflow (291 hours) to Orange Village, representing 2.9% of the monitoring period. Surface bypass at the Willoughby Hills Large application also reduced the fraction of water passing through the underdrain, reducing total drainage time. Drainage from the Perkins Township permeable pavement occurred during 6.6% (967 hours) of the monitoring period. This was perhaps greater than Willoughby Hills Large due to the lack of bypass at Perkins Township and greater HLR for exfiltration at Perkins Township, causing increased drain time. The Willoughby

Hills Small application had drainage or overflow over 1283 hours, representing 12.6% of the monitoring period. Because the HLR was 8.2 for this application and the drawdown rate was very low, the drainage period was greatly elongated. The total rainfall durations at Perkins Township, Willoughby Hills, and Orange Village were 732, 796, and 645 hours, respectively.

Perkins Township and Willoughby Hills Small application increased the overall duration of outflow when compared to rainfall duration. These two sites had the highest HLRs for exfiltration (Table 2) and had very low drawdown rates (<0.014 in/hr), causing elongation of the drainage time. The sites with lower HLRs and more permeable soils decreased the duration of outflow, which may be a key metric for stream health (Walsh et al. 2012). It is suggested the duration of outflow from permeable pavements is related to the underlying soil exfiltration rate, the depth of the IWS zone, the diameter of the underdrain, the overall depth of the aggregate, and the percentage of surface bypass that occurs due to clogging.

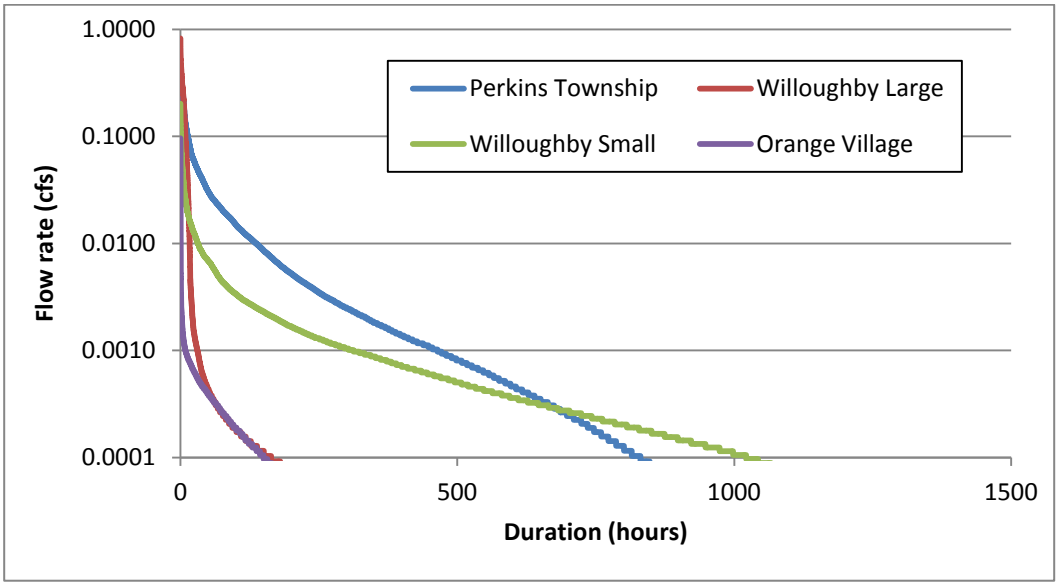

Figure 17. Flow duration curves for outflow from the monitored permeable pavement applications.

1.5 Summary and Conclusions

In order to inform improved design and crediting of permeable pavement SCMs in Ohio, the monitoring of four permeable pavements was undertaken across northern Ohio. The systems were extensively monitored to quantify the water balance and hydrologic functionality of each system. Based on the data analysis presented above, the following conclusions can be drawn from this work:

1) Soil saturated hydraulic conductivity measured during construction was representative of HSG D soils at two of the research sites, but varied over 3 orders of magnitude at the third. This shows the spatial variability of soils (especially fill soils) and the need for site-scale infiltration testing for infiltration-based practices. Post-construction drawdown rates generally followed linear trends, which contrasted with drawdown patterns for the bioretention cells monitored in this work. The post-construction drawdown rates were similar to those measured during construction, suggesting lateral exfiltration and evaporation are relatively minor factors in permeable pavement performance.

2) Volume reduction varied from 16% at Willoughby Hills Small to 53% at Perkins Township, considered excellent given the low drawdown rates (<0.014 in/hr) and HLRs of at least 5:1 for exfiltration. At Orange Village, drainage volume from the permeable pavement was 98.8% less than rainfall volume; as a consequence, results from this site may not be representative of sites without curtain drains on similar soils. Inclusion of a 6-in IWS zone in each SCM was identified as a major contributing factor for the volume reduction through exfiltration and evaporation. Overall, results showed permeable pavement can be employed successfully over clay soils and in the harsh winter climate of northern Ohio.

3) Between 4-80% of storm events were completely captured by the permeable pavements. Lower HLR for exfiltration and higher drawdown rates positively impacted the percentage of completely captured events. Discharge thresholds for each site varied from a minimum of 0.11 inches at Willoughby Hills Small (highest HLR for exfiltration) to 0.99 inches at Orange Village (which treated only direct rainfall). This substantial variability in performance suggests: (1) pre-construction soil infiltration testing is critical to understanding the performance of these systems over the long-term, (2) minimizing the HLR will provide the best hydrologic mitigation while reducing surface clogging, and (3) implementing an IWS zone will drastically improve hydrologic performance.

4) Effective curve numbers for the watersheds were reduced by 1-4 points with the retrofit of the permeable pavements. Sites treating run-on from impermeable surfaces had CNs between 88-94. Orange Village, which treated only direct rainfall, was best represented by a runoff CN of 59, which was similar to a forested condition in fair condition situated over an HSG B soil.

5) Peak flow mitigation was observed for all rainfall events not producing surface bypass across all sites. This included 10 events across the three monitoring sites that exceeded the 1-year, 5-minute design rainfall intensity for the Cleveland, Ohio area. Median event peak flow reduction was between 72-100%. Peak flow mitigation was at minimum 45 and 92% for the two sites which did not experience overflow during the monitoring periods. The fraction of rainfall infiltrating the pavement surface and the HLR were the governing factors for peak flow mitigation.

1.6 References

Agassi, M., Shainberg, I., and Morin, J. (1981). "Effect of electrolyte concentration and soil sodicity on infiltration rate and crust formation." *Soil Science Society of America Journal*. *45*(5), 848-851.

Ahiablame, L.M., Engel, B.A., and Chaubey, I. (2012). "Effectiveness of low impact development practices: literature review and suggestions for future research." *Water, Air, and Soil Pollution*. 223(7), 4253-4273.

Ball, J.E., and Rankin, K. (2010). "The hydrological performance of a permeable pavement." *Urban Water Journal*. 7(2), 79-90.

Bathke, G.R., and Cassel, D.K. (1991). "Anisotropic variation of profile characteristics and saturated hydraulic conductivity in an Ultisol landscape." *Soil Science Society of America Journal*. 55(2), 333-339.

Bean, E.Z., Hunt, W.F., and Bidelspach, D.A. (2007). "Evaluation of four permeable pavement sites in eastern North Carolina for runoff reduction and water quality impacts." *Journal of Irrigation and Drainage Engineering*. 133(6), 583-592.

Brattebo, B.O., and Booth, D.B. (2003). "Long-term stormwater quantity and quality performance of permeable pavement systems." *Water Research.* 37(18), 4369-4376.

Chin, D.A. (2006). *Water resources engineering*. 2nd edition. Pearson Prentice Hall, Upper Saddle River, NJ.

Collins, K.A., Hunt, W.F., and Hathaway, J.M. (2008). "Hydrologic comparison of four types of permeable pavement and standard asphalt in eastern North Carolina." *Journal of Hydrologic Engineering.* 13(12), 1146-1157.

Davis, A.P. (2008). "Field performance of bioretention: hydrology impacts." *Journal of Hydrologic Engineering*. 13(2), 90-95.

Davis, A.P., Stagge, J.H., Jamil, E., and Kim, H. (2012). "Hydraulic performance of grass swales for managing highway runoff." *Water Research*. 46(20), 6775-6786.

Dietz, M. E., and Clausen, J. C. (2008). "Stormwater runoff and export changes with development in a traditional and low impact subdivision." *Journal of Environmental Management*. 87(4), 560-566.

Drake, J., Bradford, A., and Marsalek, J. (2013). "Review of environmental performance of permeable pavement systems: state of the knowledge." *Water Quality Research Journal of Canada*. 48(3), 203-222.

Drake, J., Bradford, A., and Van Seters, T. (2014). "Hydrologic performance of three partial-infiltration permeable pavements in a cold climate over low permeability soil." *Journal of Hydrologic Engineering*, 19(9), 04014016-1.

Dreelin, E.A., Fowler, L., and Carroll, C.R. (2006). "A test of porous pavement effectiveness on clay soils during natural storm events." *Water Research*. 40(4), 799-805.

Driscoll, E. (1989). *Analysis of Storm Event Characteristics for Selected Rainfall Gages Throughout the United States: Draft.* US Environmental Protection Agency, 1989.

Eisenberg, B.E., Lindow, K.C., Smith, D.R. (2015). *Permeable pavements*. 1st Ed., American Society of Civil Engineers, Reston, VA.

Fangmeier, D.D., Elliot, W.J., Workman, S.R., Huffman, R.L., and Schwab, G.O. (2006). *Soil and water conservation engineering*. 5th edition. Thomson Delmar learning, Clifton Park, NY.

Fassman, E.A., and Blackbourn, S. (2010). "Urban runoff mitigation by a permeable pavement system over impermeable soils." *Journal of Hydrologic Engineering.* 15(6), 475-485.

Finkenbine, J.K., Atwater, J.W., and Mavinic, D.S. (2000). "Stream health after urbanization." *Journal of the American Water Resources Association*. 36(5), 1149-1160.

Frenkel, H., Goertzen, J.O., and Rhoades, J.D. (1978). "Effects of clay type and content, exchangeable sodium percentage, and electrolyte concentration on clay dispersion and soil hydraulic conductivity." *Soil Science Society of America Journal*, 42(1), 32-39.

Gilbert, J.K., and Clausen, J.C. (2006). "Stormwater runoff quality and quantity from asphalt, paver, and crushed stone driveways in Connecticut." *Water Research*. *40*(4), 826-832.

Grant, D.M. and Dawson, B.D. (2001). *Isco open channel flow measurement handbook.* 5th edition. Isco, Inc., Lincoln, NE.

Hawkins, R.H. (1973). "Improved prediction of storm runoff in mountain watersheds." *Journal of the Irrigation and Drainage Division*. 99(4), 519-523.

Hawkins, R.H. (1993). "Asymptotic determination of runoff curve numbers from data." *Journal of Irrigation and Drainage Engineering.* 119(2), 334-345.

James, W., and Thompson, M.K. (1997). "Contaminants from four new pervious and impervious pavements in a parking lot." *Advances in modeling and management of stormwater impacts*. W. James, ed., CHI, Guelph, Canada, 207–222.

Line, D.E., and White, N.M. (2007). "Effects of development on runoff and pollutant export." *Water Environment Research.* 79(2), 185–190.

McNeal, B.L., and Coleman, N.T. (1966). "Effect of solution composition on soil hydraulic conductivity." *Soil Science Society of America Journal*. 30(3), 308-312.

Meyer, J.L., Paul, M.J., and Taulbee, W.K. (2005). "Stream ecosystem function in urbanizing landscapes." *Journal of the North American Benthological Society*, 24(3), 602–612.

Mulvany, T.J. (1851). "On the use of self-registering rain and flood gauges in making observations of the relation of rainfall and flood discharges in a given catchment." *Transactions of the Institution of Civil Engineers of Ireland*, 4, 18-33.

National Oceanic and Atmospheric Administration (NOAA). (2015). *NOAA Atlas 14 point precipitation frequency estimates, Ohio.* Hydrometeorological Design Studies Center, Precipitation Frequency Data Server. Available: http://dipper.nws.noaa.gov/hdsc/pfds/pfds_map_cont.html?bkmrk=oh

Natural Resources Conservation Service (NRCS). (1986). *Urban hydrology for small watersheds*. Technical Release 55 (TR-55). 2nd edition. United States Department of Agriculture (USDA), Natural Resources Conservation Service, Conservation Engineering Division.

Natural Resources Conservation Service (NRCS). (2004). "Estimation of direct runoff from storm rainfall." *National engineering handbook*, Chapter 10: hydrology. Washington, DC, pgs. 1–22.

Ohio Department of Natural Resources (ODNR), Division of Soil and Water Conservation. (2006). *Rainwater and land development: Ohio's standards for stormwater management, low impact development, and urban stream protection*. 3rd edition. Ed: John Mathews.

Olson, N.C., Gulliver, J.S., Nieber, J.L., and M. Kayhanian. (2013). "Remediation to improve infiltration into compact soils." *Journal of Environmental Management*. 117,85–95.

Page, J.L., Winston, R.J., Mayes, D.B., Perrin, C., and Hunt, W.F. (2015). "Hydrologic mitigation of impervious cover in the municipal right-of-way through innovative stormwater control measures." *Journal of Hydrology.* 527, 923-932.

Pratt, C.J., Mantle, J.D.G., and Schofield, P.A. (1995). "UK research into the performance of permeable pavement, reservoir structures in controlling stormwater discharge quantity and quality." *Water Science and Technology.* 32(1), 63–69.

Pupisky, H., and Shainberg, I. (1979). "Salt effects on the hydraulic conductivity of a sandy soil." *Soil Science Society of America Journal*. 43(3), 429-433.

Reynolds, W.D., Elrick, D.E., Youngs, E.G., and Amoozegar, A. (2002). "Ring or cylinder infiltrometers (vadose zone)." *Methods of Soil Analysis - Part 4: Physical Methods*, J.H. Dane and G.C. Topp, eds., Soil Science Society of America. Madison, WI.

Roseen, R.M., Ballestero, T.P., Houle, J.J., Avellaneda, P., Briggs, J., Fowler, G., and Wildey, R. (2009). "Seasonal performance variations for storm-water management systems in cold climate conditions." *Journal of Environmental Engineering*. 135(3), 128-137.

Roseen, R.M., Ballestero, T.P., Houle, J.J., Briggs, J.F., and Houle, K.M. (2012). "Water quality and hydrologic performance of a porous asphalt pavement as a storm-water treatment strategy in a cold climate." *Journal of Environmental Engineering*. 138(1), 81-89.

Rushton, B.T. (2001). “Low-impact parking lot design reduces runoff and pollutant loads.” *Journal of Water Resources Planning and Management.* 127(3), 172–179.

Schueler, T.R., Fraley-McNeal, L., and Cappiella, K. (2009). “Is impervious cover still important? Review of recent research.” *Journal of Hydrologic Engineering.* 14(4), 309–315.

Schwartz, S.S. (2010). “Effective curve number and hydrologic design of pervious concrete storm-water systems.” *Journal of Hydrologic Engineering*. 15(6), 465-474.

Shainberg, I., Rhoades, J.D., and Prather, R.J. (1981). “Effect of low electrolyte concentration on clay dispersion and hydraulic conductivity of a sodic soil.” *Soil Science Society of America Journal*. 45(2), 273-277.

Smolek, A.P., Winston, R.J., Dorsey, J.D., and Hunt, W.F. (2015). *Modeling the hydrologic performance of bioretention and permeable pavement stormwater controls in northern Ohio using DRAINMOD: Calibration, validation, sensitivity analysis, and future climate scenarios.* Final report submitted to the University of New Hampshire and the Chagrin River Watershed Partners, Inc. In fulfilment of NOAA Award number NA09NOS4190153. *These authors contributed equally to this work.

Soil Survey Staff, Natural Resources Conservation Service, United States Department of Agriculture. (2015). Web Soil Survey. http://websoilsurvey.nrcs.usda.gov/. Accessed 28 January 2015.

Tillinghast, E.D., Hunt, W.F., and Jennings, G.D. (2011). “Stormwater control measure (SCM) design standards to limit stream erosion for Piedmont North Carolina.” *Journal of Hydrology*. 411(3), 185-196.

Tyner, J.S., Wright, W.C., and Dobbs, P.A. (2009). “Increasing exfiltration from pervious concrete and temperature monitoring.” *Journal of Environmental Management.* 90(8), 2636-2641.

United States Environmental Protection Agency (USEPA). (2003). “Protecting water quality from urban runoff.” *EPA 841-F-03-003*, Washington, DC.

Vieth, E. (1989). “Fitting piecewise linear regression functions to biological responses.” *Journal of Applied Physiology*. 67(1), 390-396.

Walsh, C.J., Fletcher, T.D., and Burns, M.J. (2012). “Urban stormwater runoff: a new class of environmental flow problem.” *PLOS ONE.* 7(9): e45814. doi:10.1371/journal.pone.0045814

Wardynski, B.J., Winston, R.J., and Hunt, W.F. (2012). “Internal water storage enhances exfiltration and thermal load reduction from permeable pavement in the North Carolina mountains.” *Journal of Environmental Engineering*, 139(2), 187-195.

Wilson, C.E., Hunt, W.F., Winston, R.J., and Smith, P. (2015). “Comparison of runoff quality and quantity from a commercial low-impact and conventional development in Raleigh, North Carolina.” *Journal of Environmental Engineering*. 141(2), 05014005.

2 BIORETENTION HYDROLOGY

2.1 Review of Literature

Urban development brings about the construction of impervious surfaces, causing changes to the hydrological cycle (e.g. hydromodification), including reduced infiltration and evapotranspiration and augmented runoff fraction (Bledsoe and Watson 2001; Booth et al. 2002). Within a watershed, impervious fractions of 10% or more have been shown to negatively impact stream ecology, including declines in habitat and water quality (Wang et al. 2001; Schueler et al. 2009). Through incision and bank erosion, cross-sectional area of urban streams was 3.8 times larger than those of rural watersheds in Piedmont Pennsylvania (Hammer 1972; Booth 1990). To mitigate these impacts, engineers have installed large scale detention and retention basins to reduce peak flow rates for flood protection; however, recent studies have shown these practices may amplify the duration of critical erosion-causing discharges, furthering degradation of streams (Palhegyi 2009; Tillinghast et al. 2011). As a result, engineers have looked to Low Impact Development (LID) technologies, such as bioretention and permeable pavement, to replicate pre-development hydrology, including duration, rate, and volume of flow (USEPA 2007).

Bioretention cells (BRC) are biologically-based media filters designed to temporarily store and treat the first flush (i.e. 0.75 inch event in Ohio) from highly impervious watersheds (ODNR 2006). Typically, they pond 9-12 inches of stormwater in their bowl storage, have 2-4 ft of engineered soil media, and, when underlying soils are poorly drained, have an underdrain surrounded by a gravel drainage layer to allow for inter-event drainage (Davis 2008; Li et al. 2009; Davis et al. 2009; Figure 18). Bioretention soil media are a mixture of sand (usually the vast majority of the media), fines (silt and clay), and organic matter, with 2-4 inches/hr typically

targeted as a design infiltration rate (Emerson and Traver, 2008; Dietz and Clausen, 2005; Brown and Hunt, 2011a). The media supports the growth of plants, typically trees, shrubs, forbs, and/or grasses that are chosen for their ability to withstand primarily droughty but also inundated conditions (Bratieres et al. 2008). These plants are critical in promoting evapotranspiration (ET) and for maintaining the soil infiltration rate over time, with root macropores appearing to offset the negative effects of media compaction and sediment deposition (Gilbert Jenkins 2010). Bioretention cells are often able to capture smaller storms in their entirety (Davis 2008; Hunt et al. 2008; Li et al. 2009; Jones and Hunt 2009), which translates into substantial abstraction of long-term stormwater volume. For storms larger than the water quality volume, a bypass or overflow structure typically is provided to connect the SCM to the storm or combined sewer network.

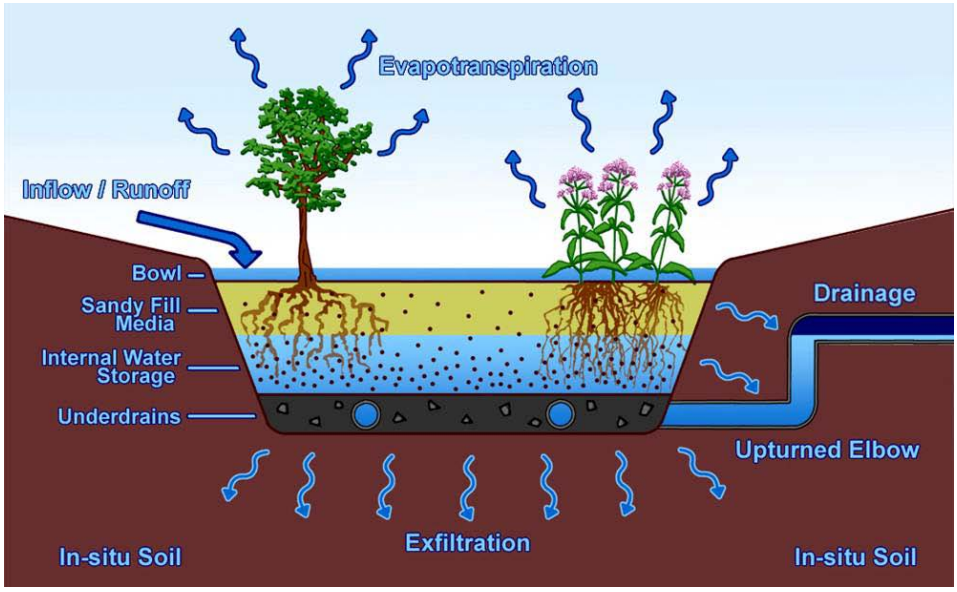

Figure 18. Schematic of a bioretention cell with an internal water storage (IWS) zone (courtesy Shawn Kennedy, NCSU)

Stormwater may leave a bioretention cell through one of four potential pathways: exfiltration to the native or *in situ* soil, ET, drainage through the underdrain, and overflow/bypass. Previous

research has shown good retention of smaller (typically <1 inch events), resulting in substantial volume reduction over the long-term. For instance, Dietz and Clausen (2005) found that 98.8% of inflow to two bioretention cells in Connecticut left as drainage and 0.8% overflowed. Peak flows were also successfully mitigated in these cells. Luell (2011) studied two bioretention cells located over sandy clay loam soils, one sized to treat the 1 inch event and one to treat the 0.5 inch event. The cells reduced runoff volume by 30% and 20%, respectively. Deeper media depths have been found to promote infiltration and evapotranspiration better than shallow media depths, better matching pre-development hydrology (Li et al. 2009; Brown and Hunt 2011a). Brown and Hunt (2011a) also observed deeper media depths promote more exfiltration (37% loss in the 3 ft media depth versus 26% loss in the 2 ft media depth, with cells located over the same soil type). Peak flow mitigation in a BRC is directly associated with its surface area, the infiltration rate of the media, the exfiltration rate, and the potential for water storage within the soil pores (Davis et al. 2009; Hunt et al. 2008). Hunt et al. (2012) suggested to treat the larger design storms (>2 year average return interval), BRC may be paired with above or below-ground detention systems.

One design feature in a BRC is the underdrain configuration, which may employ a standard, straight underdrain at the bottom of the cross-section or an internal water storage zone (IWS); an IWS zone is created through an upturned elbow in the underdrain, forcing internal ponding within the media, especially less-permeable soils (Figure 18). The IWS zone was originally recommended to promote the reduction of nitrate through denitrification from stormwater (Hunt et al. 2006; Dietz and Clausen 2006; Davis 2008; Passeport et al. 2009), but have also been shown to substantially improve exfiltration and evapotranspiration from BRCs (Dietz and Clausen 2006; Brown and Hunt 2011b; Brown et al. 2013). Li et al. (2009) reported that a BRC

with an IWS zone produced outflow during 37% of storms, while a neighboring, otherwise identical cell with no IWS zone produced outflow for 65% of storms. The internal storage of water within the media and gravel layers allows for inter-event exfiltration, which reduced total outflow from these SCMs. The IWS zone is typically 18-36 inches deep (Hunt et al., 2006; Passeport et al., 2009); in heavier soils, a zone of aerobic media should be retained above the IWS zone to allow plants to grow.

While research studies have informed bioretention design (e.g. Hunt et al. 2012), the hydrology of bioretention systems over poorly draining soils has not been studied in the field to-date. These infiltration-based SCMs are often specified in HSG A and B soils, with some governing bodies disallowing their use in poorly draining soils. The goals of this study were to test bioretention cell hydrologic performance in locations with cold winters, over poorly draining soils, and with the inclusion of an IWS zone. This was accomplished using three bioretention cell field monitoring sites in northeastern Ohio.

2.2 Site Descriptions

For the purposes of this study, three BRCs were monitored at two locations in northeastern Ohio (Figure 19). The water balance was determined on a storm-by-storm basis for two BRCs at Holden Arboretum (HA) and one at Ursuline College (UC). The surface area of the BRCs were intended to be 5% of their contributing impervious catchment area and to capture the 0.75 inch water quality volume from the watershed in their bowl storage, per guidance in the *Ohio Rainwater and Land Development Manual* (ODNR 2006). All three bioretention cells were located over HSG D soils per the Ohio soil survey (Platea and Pierpont silty clay loam at Holden Arboretum and Mahoning silt loam at Ursuline College, Soil Survey Staff 2015).

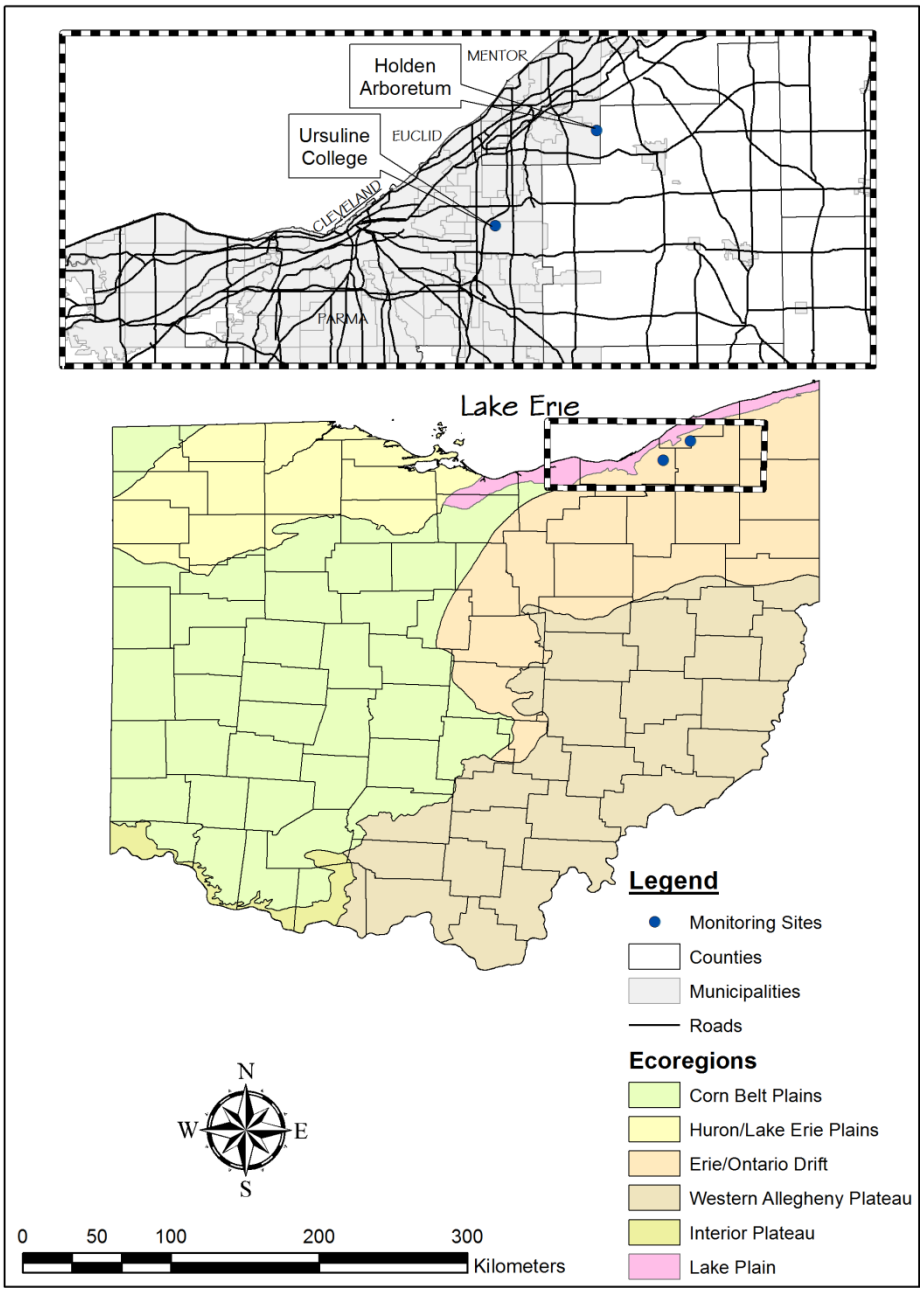

Figure 19. Location of bioretention cell monitoring sites in northeast Ohio.

A bioretention cell was constructed during April-May of 2014 on the campus of UC to treat a 0.89 acre, 77.1% impervious watershed consisting of a parking lot and associated pervious areas (Table 11 and Figure 20). The as-built filter bed surface area of the BRC was 1960 ft^2; this SCM was slightly over-designed per ODNR specifications at 6.5% of the contributing impervious

watershed area (ODNR 2006). The as-built bowl storage was surveyed with a total station and provided an average of 11.7 inches of ponding before overflow occurred. This resulted in a total storage volume of 2120 ft^3 below the overflow structure, compared to the water quality volume of 1380 ft^3; therefore, the BRC actually was sized to store the 1.16 inch storm event in its bowl storage volume (Table 12). Equation 10 was used to calculate the hydrologic loading ratio (HLR) in Table 11 for each BRC.

$$HLR = \frac{A_{BRC}+A_{WS}}{A_{BRC}} \quad (2.1)$$

Where A_{BRC} is the surface area of the bioretention cell and A_{WS} is the surface area of the watershed. The HLR for the Ursuline BRC was 21.4, and all of the impervious area was directly connected (Figure 21).

Figure 20. Photographs of the Ursuline College bioretention cell six months post-construction.

Figure 21. Watershed overview for the Ursuline College bioretention cell site. The watershed is outlined in green and the bioretention cell in blue.

Table 11. Watershed characteristics of bioretention cell monitoring sites.

Site Name	Cell Name	Contributing Impervious Watershed Area (ac)	Contributing Pervious Watershed Area (ac)	Surface Area of Bioretention Cell (ft^2)	Hydrologic Loading Ratio (HLR)	Catchment Percentage Impervious
Ursuline College	-	0.69	0.2	1960	21	77
Holden Arboretum	South	0.28	0.2	610	35	58
	North	0.39	0.28	850	35	58

The bioretention soil mix was locally sourced, and third party testing showed that the mineral fraction was 87% sand, 4% silt, and 9% clay, or a loamy sand soil texture (Table 13). Organic matter made up 4.3% of the media by mass. The bioretention media at UC was 2 feet thick and was underlain by 3 inches of medium coarse sand, 3 inches of pea gravel, and 12 inches of #57 gravel bedding around the underdrain. The media contained 3 distinct layers: 6 inches of Osorb amendment and media mixed together sandwiched between two 9 inch layers of standard bioretention media. Approximately 0.1% Osorb was mixed into the media on a mass basis. A single 6-in diameter underdrain was utilized to drain the BRC, which was tied into the outlet

structure, where outflow monitoring occurred. An upturned elbow in the underdrain created a 24-in deep IWS zone that extended through the gravel and sand layers and 6 inches into the bioretention soil media. This created a minimum 18 inches of aerobic soil. The bioretention cell was planted with a mixture of 1450 one-inch plugs spaced 15 inches on center and a 3-in layer of hardwood mulch was spread over the media (Table 14). During the monitoring period, the plants were juvenile and developed shoots that were less than 1 foot in height; therefore, plant processes were not expected to play a major role in the results presented below.

Table 12. As-built characteristics of the bioretention cells at Ursuline College and Holden Arboretum.

Site Name	Cell Name	Avg. Bowl Depth (in)	Volume of Rainfall Stored (in)	Media Depth (ft)	Choking Stone + Sand Layer (in)	#57 Aggregate Storage Layer (in)	IWS Zone depth (in)
Ursuline College	-	11.7	1.16	2	6	12	24
Holden Arboretum	South	15.3	1.78	2.75	6	12	15
	North	15.9	1.76	3	6	12	18

Table 13. Physical and chemical characteristics of the soil media at Ursuline College and Holden Arboretum.

Parameter	Ursuline College	Holden Arboretum
% Sand	87	88
% Silt	4	2
% Clay	9	10
% Organic Matter	4.3%	1.4% and 1.0%
Texture Class	Loamy Sand	Loamy Sand
Soil Test P (mg/kg)	70	34 and 30
pH	7.5	7.7
K_{sat} (in/hr)	6.6	4

Table 14. Planting lists for the bioretention cells at Ursuline College and Holden Arboretum.

UC	HA North	HA South
Carex comosa	*Clethra alnifolia*	*Anemone canadensis*
Carex crinita	*Cornus alba*	*Panicum virgatum*
Carex grayl	*Gleditsia triacanthos*	*Symphyotrichum novi-belgii*
Carex lurida	*Ilex glabra*	*Heliopsis helianthoides*
Carex vulpinoidea	*Itea virginica*	*Baptisia australis*
Elymus virginicus	*Myrica pensylvanica*	*Matteuccia struthiopteris*
Scirpus atrovirens	*Thuja occidentalis*	*Camassia leichtlinii cearulea*
Scirpus validus	*Vaccinium macrocarpon*	
Asclepias incarnata		
Aster novae-angliae		
Echinacea purpurea		
Eupatorium maculatum		
Hellanthus grosseserratus		
Iris versicolor		
Liatris spicata		
Lobelia cardinalis		
Lobelia siphilitica		
Mimulus ringens		
Monarda fistulosa		
Physostegia virginiana		
Veronicastrum virginicum		

Two bioretention cells at Holden Arboretum (HA) were constructed in September 2013 (Table 11 and Figure 22). The South bioretention cell had a watershed area of 0.48 acres, while that of the North cell was 0.67 acres (Figure 23). The two cells each had an HLR of 35; however, 42% of the watershed that drained to each BRC was pervious and well vegetated with turfgrass and mature trees. The cells were surveyed with a total station. Filter bed surface area of the South bioretention cell was 610 ft^2, while that of the North cell was 850 ft^2; these values represented 5% of their respective impervious watershed areas. The South and North cells were built with 15.3 and 15.9-in ponding depths due to a construction mishap wherein the thickness of the metal frame and grate on the overflow structure was not taken into account (Table 12). This resulted in a total South cell storage volume of 1220 ft^3 below the overflow structure compared

with the water quality volume of 515 ft^3; therefore, the BRC was actually sized for the 1.78 inch storm event. For the North cell, total as-built storage was 1690 ft^3, considerably more than the 720 ft^3 water quality volume. This resulted in the BRC being effectively sized to capture the 1.76 inch event without overflow.

Figure 22. Photographs of the Holden Arboretum South (at left) and North (at right) bioretention cells 13 months post-construction.

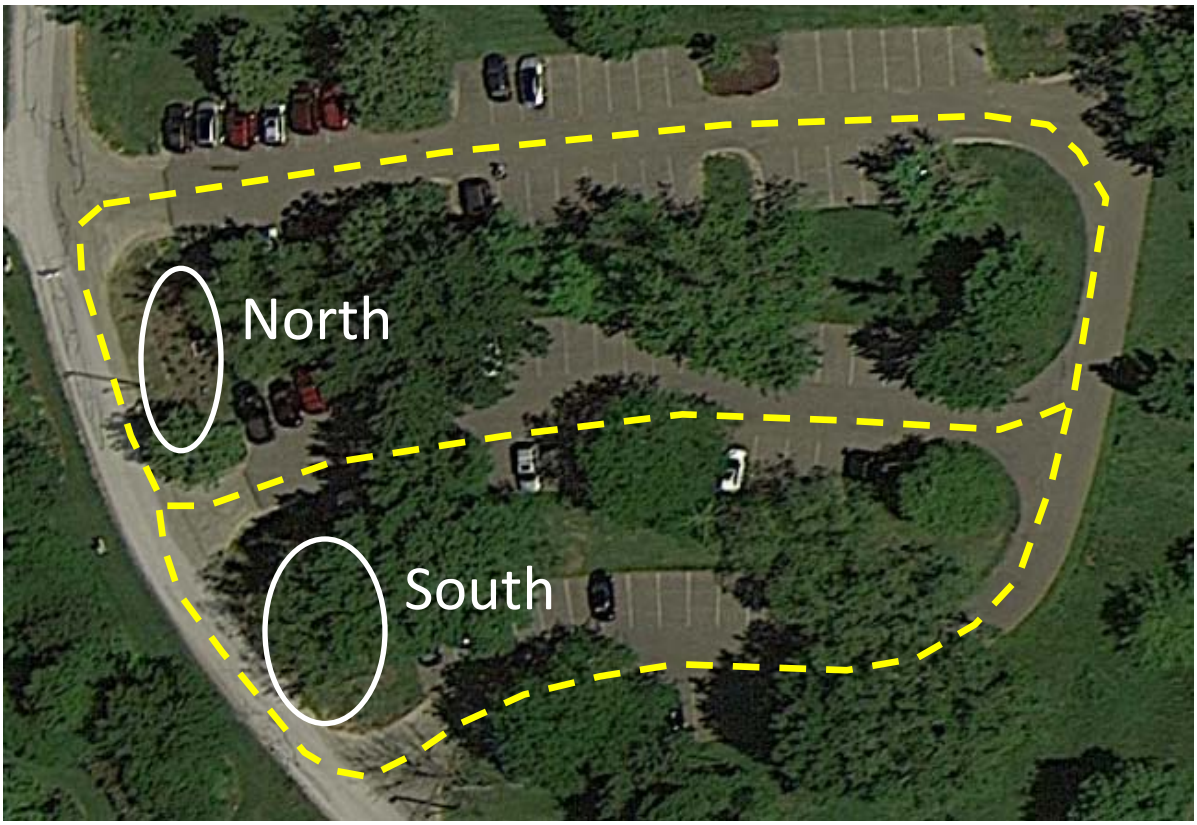

Figure 23. Watersheds (outlined in yellow dashed polygons) and bioretention cell locations (white ellipses) at Holden Arboretum.

The media depth for both Holden Arboretum BRCs was 2.75 feet for the South cell and 3 feet for the North cell. The media for both of the cells was locally sourced and had the same mineral fraction composition of: 88% sand, 2% silt, and 10% clay by mass (Table 13). The media in the South and North cells included 1.4% and 1.0% organic matter by weight, respectively. Similar to the bioretention cell at Ursuline College, the media was underlain with 3 inches of coarse sand, 3 inches of pea gravel, and 12 inches of #57 aggregate. Three inches of hardwood mulch was placed on top of the media. Underdrains were 4 inches in diameter and were tied into the existing catch basins located within each cell. IWS zones of 15 and 18-in depths were incorporated into the South and North cells, respectively. Thus, the IWS zone did not extend into the media at either of the two cells (Table 12).

The bioretention cells were vegetated with a mixture of trees and shrubs (woody plants) in the North cell and forbs and perennial grasses (herbaceous species) in the South cell (Table 14). The shrubs and perennials planted in both cells were from 1 gallon pots. A total of 27 shrubs were planted in the north cell, while 172 specimens were planted in the south cell. One tree was planted in the North cell (a honey locust) which was approximately 6 ft tall at planting.

2.3 Materials and Methods

2.3.1 Data Collection

Instrumentation was installed at each bioretention cell site to monitor rainfall, climatic parameters, and cell hydrology. Rainfall was measured at each site using a 0.01-in resolution tipping-bucket rain gauge affixed approximately 6 feet above the ground (Davis Instruments, Hayward, California). Rainfall data were stored in a Hobo U30 data logger attached to the nearby weather station (Figure 24). A 6 foot tall, Hobo weather station was deployed and included separate sensors for wind speed, wind direction, air temperature, relative humidity, and solar radiation (Figure 24, Onset Computer Corporation, Bourne, MA). Rain gauges and weather stations were located in an open area, free from overhanging trees. All rainfall and climatic parameters were recorded on a 1-minute interval.

Figure 24. Hobo U30 data logger attached to weather station mast (left). Wintertime photo of rain gauge and weather station located at Holden Arboretum (right).

Combined overflow and drainage from each bioretention cell was monitored using a sharp crested, v-notch weir and a Hobo U20 pressure transducer (Onset Computer Corporation, Bourne, MA). Each outlet structure had an internal baffle to calm the flow upstream of the weir and an awning structure to force all overflow and drainage behind the baffle (Figure 25). The pressure transducer was placed immediately downstream of the baffle, as far upstream from the weir as possible. A variety of v-notch weirs were utilized depending on the expected flow rates from the bioretention cells (Table 15). Water level in the bioretention media was measured as a function of time using a Hobo U20 pressure transducer within 1" diameter water table wells located in each bioretention cell. Since the pressure transducers were non-vented, an additional U20 pressure transducer was placed in the rain gauge housing at each site to measure local barometric pressure. All pressure transducer measurements were obtained on a 2-minute interval. Data at each site were downloaded approximately every 3 weeks. Upon arrival at the office, data QA/QC was performed, data were backed up on a server, and data sent to NCSU staff for analysis.

Figure 25. Weir installed in the outlet structure of the south bioretention cell at Holden Arboretum (left) and top view of weir installed in Ursuline College outlet structure (right).

Table 15. Devices used to monitor hydrologic and climatic parameters by site.

Measurement	UC	HA North	HA South
Rainfall	Davis 0.01" tipping bucket	Davis 0.01" tipping bucket	
Climatic Parameters	Hobo weather station	Hobo weather station	
Drainage and Overflow	60˚ v-notch weir	45˚ v-notch weir	60˚ v-notch weir
Internal Water Level	Yes	Yes	Yes

2.3.2 Data Analysis

Data QA/QC was performed in Hoboware Pro version 3.7.0 (Onset Computer Corporation, Bourne, MA) by visually checking for anomalies in the data while in the field. This allowed for replacement of any broken data loggers without an additional trip to the field site. Rainfall and weather parameters were immediately exported from Hoboware Pro and stored in an Excel spreadsheet for analysis. Discrete storm events were identified by a minimum antecedent dry period (ADP) of 6 hours and a minimum rainfall depth of 0.1 inches. Rainfall data were further analyzed for total storm event rainfall depth (inches), average rainfall intensity (in/hr), peak 5-minute rainfall intensity (in/hr), and antecedent dry period (days).

Since inflow to each bioretention cell entered in a diffuse manner (a mixture of sheet and shallow concentrated flow), this precluded the use of a weir or flume to measure inflow.

Therefore, inflow was estimated using a rainfall-runoff model, the NRCS Curve Number method (NRCS 1986):

$$Q = \frac{(P-I_a)^2}{(P-I_a+S)} * A \quad (2.2)$$

where Q is runoff volume (ft^3), P is precipitation depth (in), I_a is the initial abstraction (inches) in the watershed (I_a = 0.2*S), CN is the curve number for the watershed, and S is the potential maximum soil moisture retention (inches) and is related to the CN by:

$$S = \frac{1000}{CN} - 10 \quad (2.3)$$

Using equations 11 and 12, inflow volumes were calculated for each runoff producing event (i.e. P > I_a). Impervious areas within each watershed were assigned the standard CN of 98 (i.e. almost all rainfall becomes runoff), while pervious areas were assigned a CN of 80. This is equivalent to open space in good condition (>75% grass cover) for a HSG D soil (Fangmeier et al. 2006). Discrete runoff volumes for permeable and impermeable watershed areas were calculated and summed, rather than calculating a composite CN, as suggested in Chin (2006). Additionally, antecedent moisture corrections were applied to the CN for dry and wet moisture conditions. ADPs less than two days and greater than 5 days were considered wet and dry antecedent moisture conditions, respectively.

Peak inflow rates were estimated using the Rational Method (Mulvany 1851), a commonly used engineering method that relates rainfall intensity to flow rate:

$$Q_p = C * i * A \quad (2.4)$$

where Q_p is the peak flow rate (ft^3/s), C is the rational runoff coefficient, i is the rainfall intensity measured during the storm (in/hr), and A is the watershed area (acres). The rational coefficient is customarily taken to be 0.9 for impervious areas, while pervious areas were given a

rational coefficient of 0.2, equivalent to that for lawns on average slope and heavy soil (Chin 2006).

Hoboware Pro software was utilized to offset all pressure transducer measurements by barometric pressure measured by a separate, on-site logger. This corrected pressure was then converted to feet of water at that particular monitoring location, and exported to a spreadsheet for further analysis. Weir equations corresponding to the particular weir geometries (Table 15) were utilized to calculate discharge as a function of depth of flow above the weir crest (Grant and Dawson 2001):

$$Q = 1.035 * H^{2.5}, 45^{\circ} \text{ v-notch weir} \quad (2.5)$$

$$Q = 1.443 * H^{2.5}, 60^{\circ} \text{ v-notch weir} \quad (2.6)$$

where Q is flow rate (ft^3/s) and H is head (ft) above the weir crest. Flow rates were calculated on a 2-minute interval, and the area under the hydrograph integrated over time to calculate total outflow volumes on a storm-by-storm basis. Hydrograph analysis was performed to separate the drainage and overflow volumes. The peak outflow rate for each storm event was the instantaneous 2-minute maximum value. Annual inflow and outflow volumes were calculated as the sum of the storm-by-storm volumes.

To determine the volume of exfiltration, water table measurements within the media of each BRC were utilized to calculate the drawdown rate. Following each storm, the water level and date/time of the end of drainage (i.e. when the water level reached the invert of the underdrain) was recorded. Immediately preceding the commencement of the following rain event, the water level and date/time were also recorded. This allowed for a total drawdown time and depth to be calculated. The drawdown rate (in/hr) is defined as the quotient of these values. The volume of exfiltration can then be calculated using:

$$V_{EX} = \frac{\sum_{i=1}^{n}(Q_{DD,i} * DD_{time,i} * \phi) * f_{drain} * A_{IS}}{12} \quad (2.7)$$

where V_{EX} is the stormwater volume exfiltrated over the monitoring period (ft^3), n is the total number of inter-event periods, Q_{DD} is the drawdown rate (in/hr), DD_{time} is the inter-event period (hr), ϕ is the porosity of the aggregate (equal to 0.4) or bioretention soil media (equal to 0.32), f_{drain} is the quotient of the total monitoring period duration to the total dry period duration, and A_{IS} is the area of the infiltrative surface. This allowed for estimation of drawdown while drainage was occurring.

To complete the water balance, equation 17 was utilized to determine the evaporation provided by the BRC:

$$\sum_{i=1}^{n} V_{in} = \sum_{i=1}^{n}(V_D + V_O + V_{EX} + V_{EVAP}) \quad (2.8)$$

where V_{in} is the runoff volume from the watershed, V_D is the drainage volume, V_O is the volume of bypass or overflow, V_{EX} is the volume of exfiltration, and V_{EVAP} is the volume of evapotranspiration from the BRC. The V_{EVAP} term is the only term not measured or estimated, and therefore can be calculated to complete the water balance.

2.4 Results and Discussion

2.4.1 Rainfall

Over the course of the seven month monitoring period at Ursuline College (May to November 2014), fifty storm events were monitored to assess the hydrologic performance of the bioretention cell. The monitoring period at Holden Arboretum lasted nine months from October 2013 through November 2014, during which 90 separate storms were observed. During this time, the climatic and hydrologic data collected from December 2013 through March 2014 were deemed unreliable due to equipment failure or error induced by sub-freezing temperatures.

Summary statistics for rainfall event depth, average intensity, peak five-minute intensity, and antecedent dry period are presented in Table 16. Total rainfall depths during the monitoring periods as Ursuline College and Holden Arboretum were 29.21 and 46.24 inches, respectively.

At both Ursuline College and Holden Arboretum, median rainfall depths were around one-third of an inch, with mean event depths skewed to around one-half inches by the largest events. Maximum observed rainfall depths were 3.51 inches at Ursuline College and 2.79 inches at Holden Arboretum. Median and mean antecedent dry periods were between 2-4 days at each site; these values provide reasonable estimates of the available dewatering time in this region of Ohio to ensure an SCM has storage available for subsequent storm events.

At Ursuline College, the 79th percentile rainfall depth (0.74 inches) was representative of the 0.75 inch water quality event in Ohio. The 80th percentile event at Holden Arboretum (0.76 inches) was representative of the water quality event depth in Ohio. Because all three bioretention SCMs were oversized due to larger-than-required surface area or bowl storage depth, the Ursuline College, Holden South, and Holden North were sized such that they captured and treated without overflow the 86th, 96th, and 96th percentile monitored storm depths, respectively. Therefore, the hydrologic performance of these bioretention stormwater controls is expected to exceed that of the typical bioretention design in northeast Ohio.

Table 16. Summary statistics for rainfall events measured at Ursuline College and Holden Arboretum.

Monitoring Site	Statistic	Depth (in)	Average Intensity (in/hr)	Peak 5-minute Intensity (in/hr)	Antecedent Dry Period (days)
Ursuline College	Minimum	0.10	0.01	0.12	0.3
	Median	0.32	0.05	0.60	2.3
	Mean	0.58	0.09	1.14	3.7
	90th percentile	1.67	0.20	2.58	8.1
	Maximum	3.51	0.51	6.00	20.0
Holden Arboretum	Minimum	0.10	0.01	0.12	0.3
	Median	0.30	0.05	0.48	2.6
	Mean	0.52	0.12	0.95	3.4
	90th percentile	1.27	0.25	2.89	7.6
	Maximum	2.79	1.95	4.08	18.6

2.4.2 Drawdown Rate

During the design phase, understanding the properties of the soil surrounding a bioretention cell is extremely important. *In situ* soils with higher hydraulic conductivities, such as sands and sandy loams, can accept exfiltration from the bioretention media at a much faster rate than a clayey soil (Rawls et al. 1982). Therefore, pre-construction soil testing is critical to predicting and understanding the post-installation performance of bioretention SCMs (Brown and Hunt 2010). If compaction during construction is prevented, these pre-construction soil tests can be an excellent indicator of the long-term hydrologic performance of the SCM (Pitt et al. 2008; Tyner et al. 2009; Wardynski et al. 2012).

At Ursuline College, construction was halted for one day as the excavation reached the final subgrade elevation to undertake soil infiltration testing (Figure 26). Prior to construction at Holden Arboretum, test pits were excavated at the locations of proposed BRCs to conduct infiltration tests. Two single-ring, constant head hydraulic conductivity tests were completed in the subsoils beneath each of the Holden Arboretum cells; three such tests were undertaken at

Ursuline College. At Ursuline College, the subsoils had been raked with the excavator bucket teeth to reduce compaction; at each site, a hoe was used to remove loose soil and create a level test surface, and so the tests were run on uncompacted subsoil. A Mariotte bottle was used to keep a constant head (ponding depth of 6 inches), and mathematical corrections were used based on methods in Reynolds et al. (2002) to account for lateral water flow. Thus, the tests provided estimates of the hydraulic conductivity through the bottom of the BRC.

Figure 26. Single ring infiltrometer with Mariotte bottle used for pre-construction infiltration testing (left) and monitoring well used for post-construction drawdown rate measurement.

Measured saturated hydraulic conductivity at each of the bioretention cells was representative of HSG D soils (Table 17; USDA 2007). Subsoil at Holden North had 0.02 and 0.02 in/hr, Holden South had 0.02 and 0.08 in/hr, and Ursuline College had 0.02, 0.02, and 0.03 in/hr measured saturated hydraulic conductivity. Soil hydraulic conductivity is highly variable spatially (i.e. up to two orders of magnitude within a given SCM, e.g. Asleson et al. 2009 and Olson et al. 2013), and 2-3 tests per bioretention cell may not wholly characterize the capacity of the subsoil to exfiltration stormwater. However, there are practical limits (cost and time) on the number of soil tests that can be carried out for a given stormwater practice.

Average post-construction drawdown rates are also presented in Table 17 for the three bioretention cells; drawdown rates for the bioretention cells were non-linear, but the average

values presented over the monitoring period were used in subsequent modeling (Smolek et al. 2015). These rates were calculated for water table depths below the invert of the underdrain, so drawdown could be isolated from drainage. In each case, the post-construction drawdown rate was *higher* than the K_{sat} measured during construction.

Table 17. Comparison of saturated hydraulic conductivity measured during construction to post-construction drawdown rate.

Site	K_{sat} Measured During Construction (in/hr)	Average Measured Drawdown Rate (in/hr)
Holden North	0.02, 0.02	0.065
Holden South	0.02, 0.08	0.08
Ursuline	0.02, 0.02, 0.03	0.17

There are a number of potential reasons for the disparity between during and post-construction rates of water movement. Since compaction was reduced through dragging the excavator bucket teeth through the subsoil, it apparently did not negatively impact the vertical water transmission rate. As stated previously, the small number of pre-construction K_{sat} tests may not provide a representative average rate, since water stored in an IWS zone will find the path of least resistance for exfiltration. Because the bioretention cells were either irregularly shaped (Holden) or long and thin (Ursuline), the proportion of side wall area was quite high, allowing lateral exfiltration to occur. When the IWS zones were completely full, side wall surface area represented 27%, 20%, and 22% of the bottom surface area of the bioretention cells at Ursuline, Holden South, and Holden North, respectively. Lateral exfiltration, which is not accounted for in the single-ring tests, occurs at a rate proportional to the horizontal saturated hydraulic conductivity. The ratio of vertical to lateral hydraulic conductivity varies spatially and as a function of soil horizon (Bathke and Cassel 1991), but horizontal conductivity is generally higher than that of vertical conductivity in clay soils. Often this difference is 10-fold, but can be

as much as 25-fold (Bathke and Cassel 1991). This is further supported by modeling of exfiltration from urban SCMs, which has shown lateral exfiltration can be the dominant force in providing volume reduction (Browne et al. 2008; Lee et al. 2015). Additionally, while it is probably a small factor when water is stored 18 to 36 inches from the soil surface in an IWS zone and when the plant rooting depth is shallow, ET will be responsible for some fraction of the drawdown measured in each bioretention cell, especially during the summer. For these reasons, drawdown post-construction was higher than vertical K_{sat} measurements obtained during construction; a similar result was not found for permeable pavements in this region of Ohio (see section 1.4.2 for further discussion).

Examples of water table drawdown curves are shown for Ursuline College in Figure 27 and for the two Holden Arboretum cells in Figure 28. Excerpts of the entire data set, which focus on three storm events, are shown in each figure; in each case, 0 feet represents the interface with the subsoil. For Ursuline, the top of the IWS zone was located at 2 feet (horizontal line in Figure 27), and water level above this point corresponded to periods of drainage. A near-vertical exfiltration rate existed between 2 and 1.25 feet elevation, perhaps due to changes in lateral hydraulic conductivity with soil horizon (Bathke and Cassel 1991) or to lateral seepage from the media to the adjacent stream (located 25 feet laterally and 15 feet below the bioretention cell). A slope break in the drawdown curve was present at 1.25 feet, and below this point exfiltration occurred at a lower rate that could be approximated by an exponential decay. Drawdown was very slow below 0.1 feet and may represent the transition from head driven exfiltration to capillary flow.

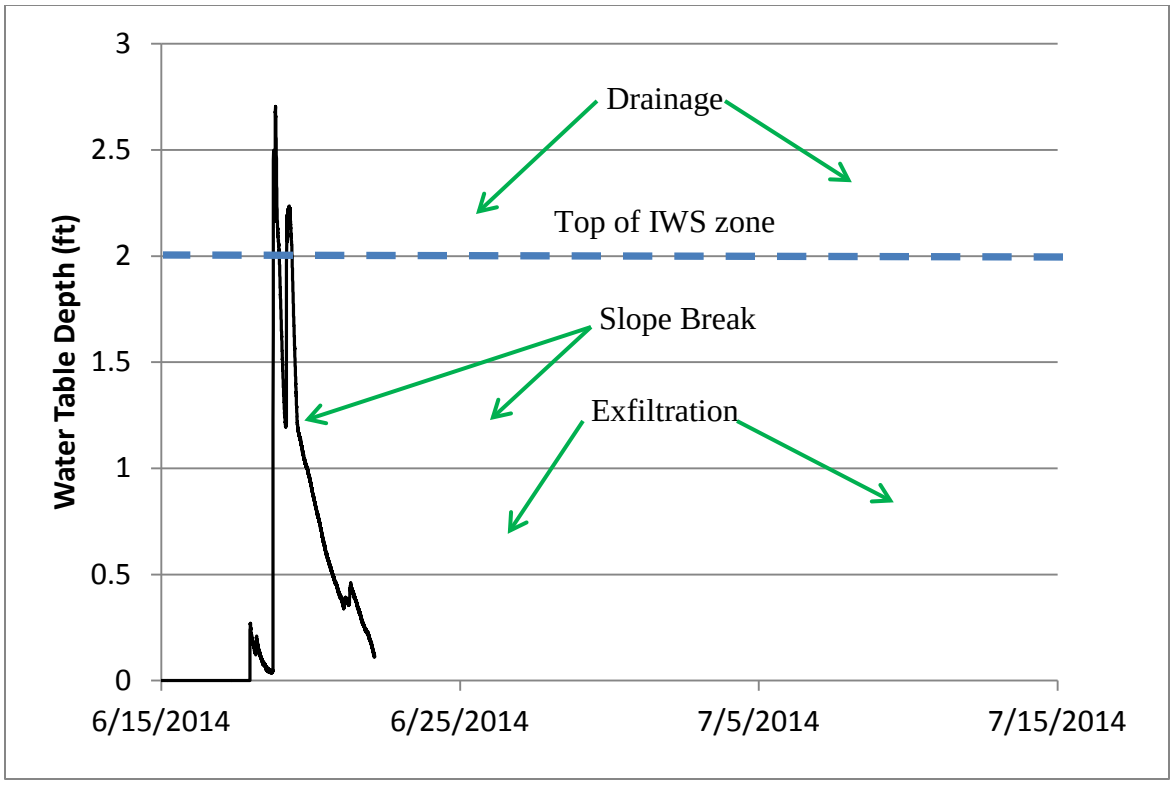

Figure 27. Excerpt of Ursuline water table during June-July 2014. The top of the IWS zone is noted with a horizontal line.

The Holden south and north cells had their respective IWS zone inverts at 15 and 18 inches above the subgrade elevation (shown as horizontal lines in Figure 28). As rainfall and runoff processes occurred, the water table depth increased until the invert of the drain was reached, when drainage began. Once the drain dewatered the bowl and soil storage, exfiltration was the primary process (with ET being minor with a 33 to 36-in depth to the top of the IWS zone at Holden) driving drawdown below the drain invert. Exfiltration rates were about 25% different at Holden South and North cells, showing the spatial variability of soils, given that these SCMs were located approximately 50 feet apart. Even though Holden North had a deeper IWS zone (and therefore more head to drive vertical and lateral exfiltration), the drawdown rate was represented by a shallower exponential decay than the South cell. This resulted in quicker dewatering of the IWS zone in the South cell, ultimately causing the system to perform better for

volume reduction. Both cells tended to shift from head driven exfiltration to capillary flow at around a 0.2 foot water table elevation, resulting in substantial reductions in exfiltration rate.

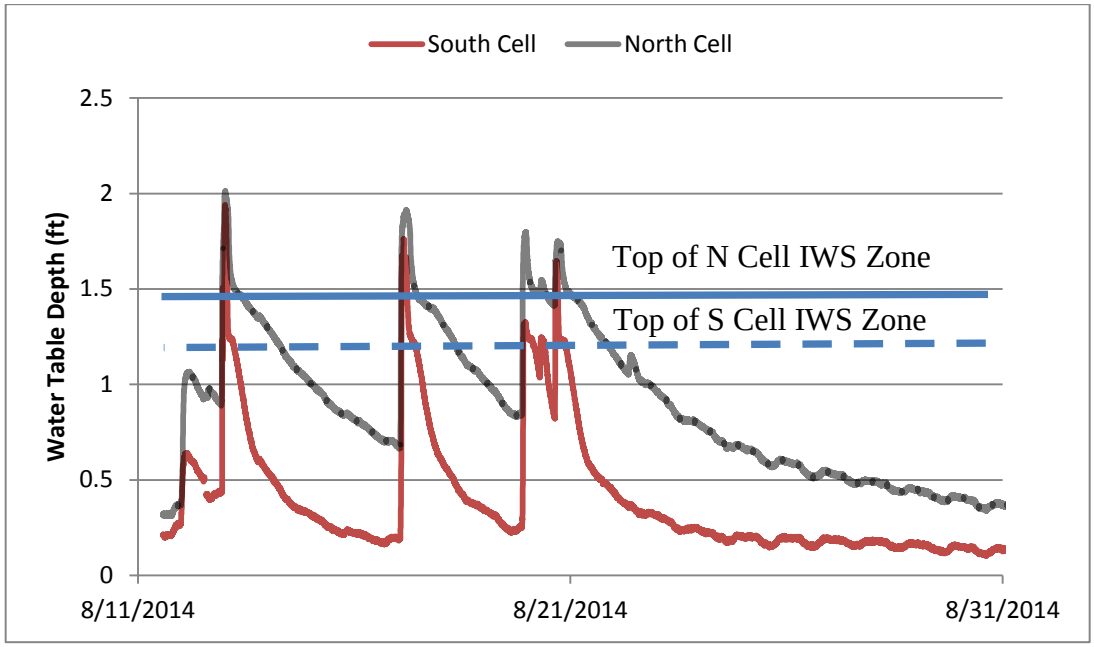

Figure 28. Excerpt of Holden North and South bioretention cell water tables during August 2014. The North cell IWS zone is shown with a solid horizontal line while that of the South cell is shown with a dashed line.

The original intent of the Holden Arboretum study was to observe bioretention SCM performance under two different plant palettes, with all other design parameters the same. However, the differences in underlying soil and exfiltration rates discussed above confounded this effort. Because the plants were juvenile during the monitoring period, the differences in hydrologic performance between the two Holden Arboretum cells discussed below are most likely due to the difference in exfiltration rates.

2.4.3 Volume Reduction

The three monitored bioretention cells had drawdown rates higher than predicted by pre-installation K_{sat} tests. This resulted in total volume reductions (i.e. the sum of exfiltration and

ET) of 60% for Ursuline, 42% for Holden South, and 36% for Holden North (Table 18). The greatest volume reduction was achieved by the cell with the largest drawdown rate and deepest IWS zone. While few similar studies of bioretention cells over poor soils have not been published, Sansalone and Teng (2004) found 55-70% exfiltration from an SCM that they termed a partial exfiltration reactor located in clayey glacial till soils in Cincinnati, OH. Modeling results in DRAINMOD suggested the inclusion of the IWS zone substantially improved the volume reduction of these systems when compared to a standard drainage configuration (Smolek et al. 2015). The total volume reduction for the Holden Arboretum cells was similar to modeled results from long-term simulations of bioretention cells using DRAINMOD (Brown et al. 2011c). Using calibrated bioretention models based on field studies in North Carolina, Brown et al. (2011c) modeled a number of bioretention design scenarios. One scenario with a drawdown rate of 0.04 in/hr and a 1 foot IWS zone - similar to the design characteristics of the Holden Arboretum cells - predicted a total volume reduction of 45%, which was in the range of those observed at Holden Arboretum. Additionally, they modeled a 72% volume reduction for a bioretention cell with a 0.2 in/hr exfiltration rate and a 12-in IWS zone. These results and input parameters compare to those from Ursuline College. Thus, the field monitoring results presented herein are supported by results in the literature.

Table 18. Summary statistics for volume and percentage of inflow, drainage, overflow, and exfiltration+ET.

Site Name	Cell Name	Total Inflow (ft^3)	Drainage (ft^3)	Overflow (ft^3)	Exfiltration + ET (ft^3)	Drainage (%)	Overflow (%)	Runoff Reduction (%)
Ursuline College	-	100700	28300	12500	61700	28.1	12.4	59.5
Holden Arboretum	South	35100	17900	2400	12900	51.1	6.8	42.1
	North	50300	28800	3500	18100	57.2	6.9	36.0

Combined drainage and overflow for each cell were monitored using a single weir; therefore, hydrograph analysis was employed to separate drainage and overflow hydrographs. This was supported by calibrated USEPA SWMM V5.1 models, which predicted the drainage hydrographs reliably, especially for the Ursuline College site (which had higher soil K_{sat}, providing less resistance to flow through the media). This analysis is presented below in Figure 29. From the modeled drainage and measured outflow, one can mathematically separate the volume of drainage from the overflow. A similar method was used at Holden Arboretum. Drainage, or the fraction of water filtered and treated by the soil media, represented 28-57% of the overall water balance, depending on the bioretention cell. Overflow was around 7% of the water balance at Holden Arboretum, a lower percentage of the overall water balance than past studies on bioretention (Brown and Hunt 2012). This is probably due to the fact that these BRCs were sized to capture the 1.76 and 1.78-in events, about nearly 2.5 times the water quality event in Ohio. Additionally, the peak flows at Holden Arboretum could have been dampened by the larger percentage of pervious areas and the impervious area disconnection present in the watersheds. Overflow represented a higher proportion of the water balance at Ursuline (12.4%), perhaps because the impervious watershed area was directly connected at this site. This cell had long-term percentages of overflow similar to those from other studies on BRCs (Li et al. 2009); however, it too was over-sized for the water quality volume, perhaps meaning that a standard BRC in Ohio would have more than 12% overflow under similar conditions.

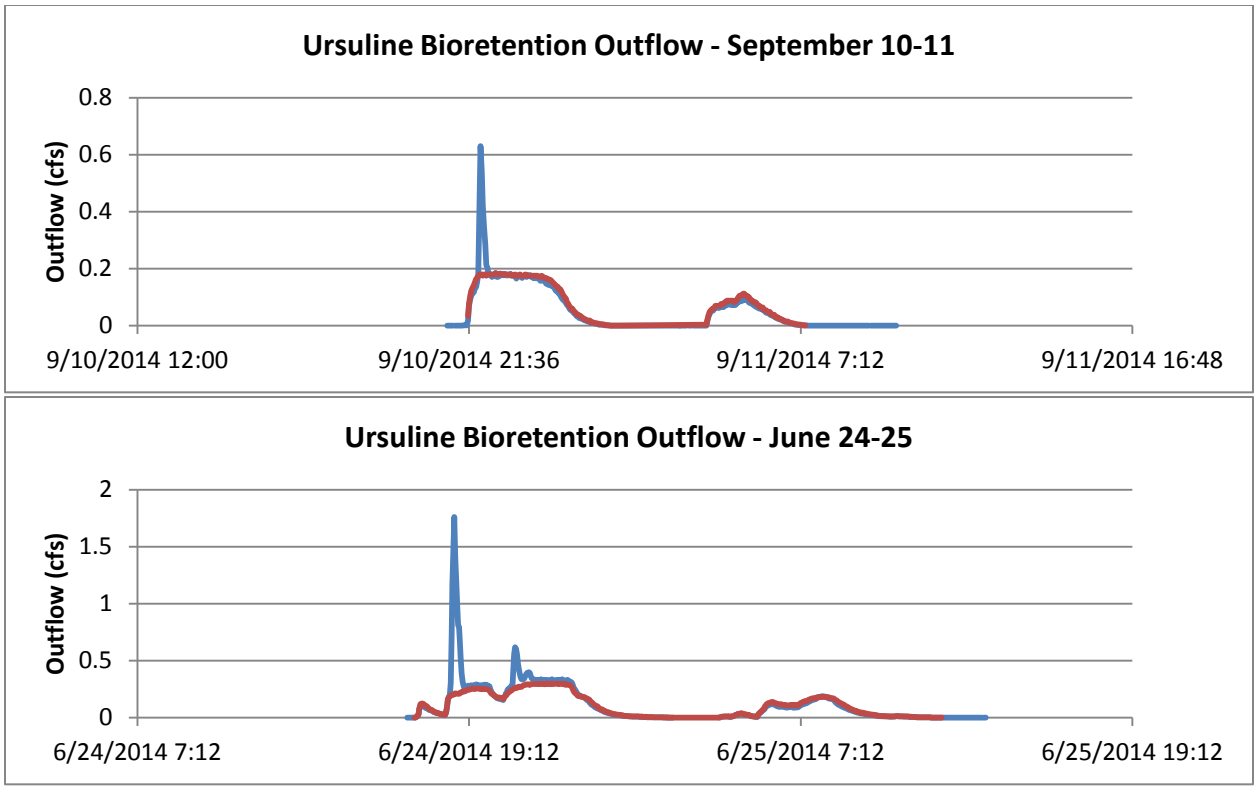

Figure 29. Measured (blue) outflow and modeled (red) drainage hydrographs for Ursuline College. Modeling was completed in US EPA SWMM model V5.1.

When using Low Impact Development (LID) strategies, one of the goals is abstraction of small storm events to restrict the volume of stormwater entering the drainage network (Davis 2008). Data were compiled on the number of events completely captured by the bioretention cells (Table 19). These events produced no drainage or overflow, and represented between one-third and two-thirds of the monitored storm events, depending on the bioretention cell. The completely captured events were up to 0.5 inches in size, albeit the antecedent dry period for this size storm to be captured was a minimum of 9 days at Holden Arboretum and 1.5 days at Ursuline College. This shows the impact of higher exfiltration rates, which dewater the IWS zone more quickly and allow for greater storage and abstraction during short ADPs.

Table 19. Completely captured storm events (i.e. no outflow) for the three monitored bioretention cells.

Site Name	Cell Name	Events Completely Captured (#)	Storm Size of Completely Captured Events (in)	Percentage of Events Completely Captured
Ursuline College	-	33/50	0.1-0.56	66
Holden Arboretum	South	44/90	0.1-0.51	49
	North	28/90	0.1-0.51	31

The idea of a runoff threshold for SCMs was initially proposed by Hood et al. (2007), defined as the minimum rainfall that initiates in discharge from a catchment. Here, we define the discharge threshold (D_T) as the minimum amount of rainfall that produced outflow from a bioretention cell. The outflow from each monitored storm event was plotted against rainfall depth in Figure 30. Two phases of bioretention cell performance exist: (1) abstraction and (2) outflow production. During the abstraction phase, practically all events are captured below a threshold rainfall depth, the D_T. Using segmented linear regression, the discharge thresholds were 0.63, 0.32, and 0.25 inches for Ursuline, Holden South, and Holden North, respectively. While Ursuline was designed to capture a smaller water quality volume than the Holden cells (Table 12), the deeper IWS zone depth and 2-2.5 times higher exfiltration rate resulted in abstraction of larger storm events. Once the systems entered the outflow production phase, the Ursuline College bioretention cell had a steeper slope of the outflow volume trend line, indicative of the larger watershed area and greater directly connected impervious area for this cell.

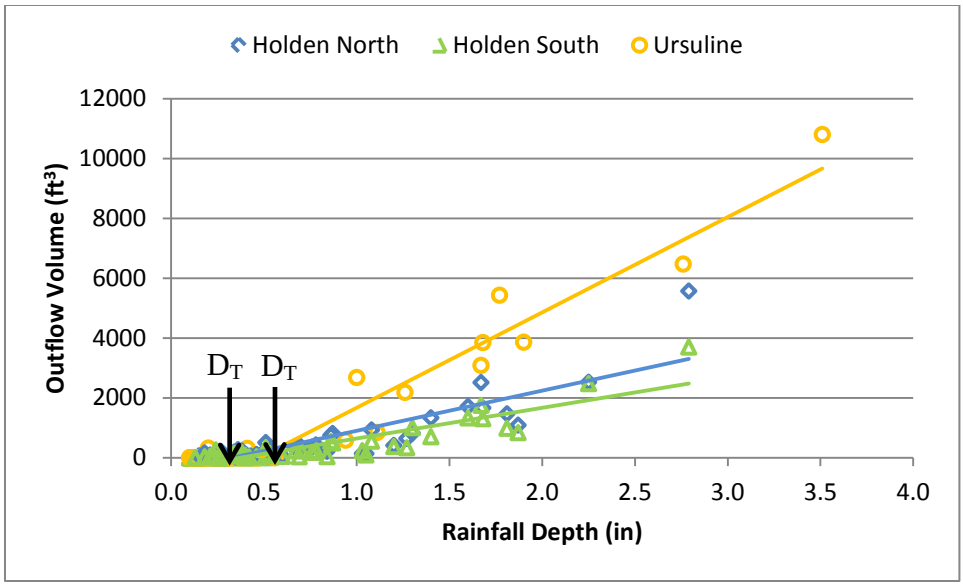

Figure 30. Determination of the discharge threshold at each bioretention monitoring site.

Exceedance probability plots are useful tools to analyze the ranked volume of inflow and outflow (i.e. sum of drainage and overflow) over the monitoring period (Figure 31). Because data are ranked, corresponding inflow and outflow points are not necessarily from the same storm event. However, the distribution of data allow for general conclusions about system performance. For Ursuline, 8 events (or 16% of the total) had substantial outflow, an additional 20% produced minor amounts of outflow, and 66% were completely captured. This can be visually contrasted against the two Holden Arboretum cells, which were situated in more poorly draining soils. These cells had substantial outflow 40-50% of the time; however, every storm had at least a minor volume reduction, with the bioretention cells abstracting at minimum 5% of the inflow volume.

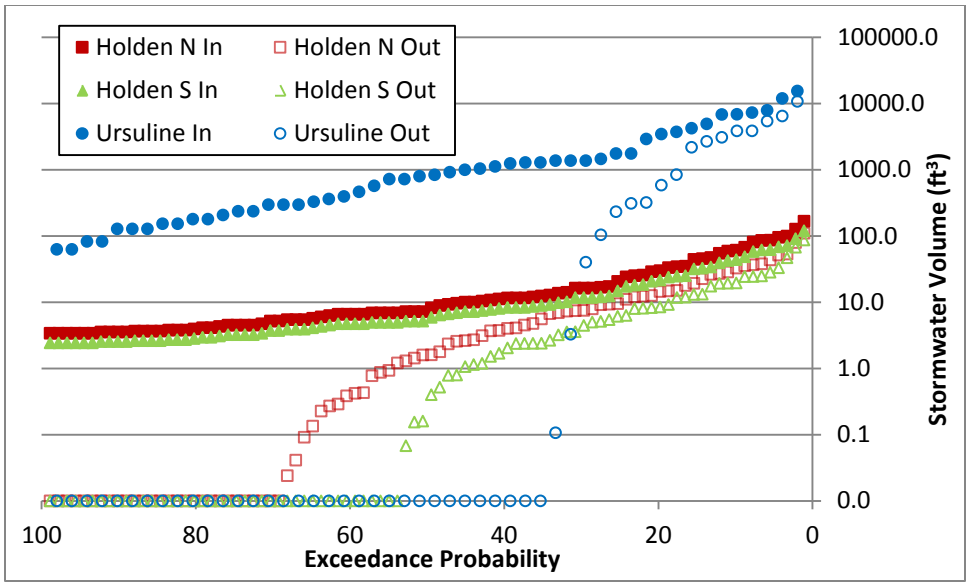

Figure 31. Exceedance probability for inflow and outflow volume over the monitoring periods.

Engineers typically use curve numbers (CN) to determine expected volumes of runoff from a development project (NRCS 1986). They vary from 30 for a forested watershed in good condition located in sandy soils to 98 for an impervious parking lot or rooftop. While volumes of data exist on CNs as a function of land use and HSG, little data are available on the effect of SCM implementation on watershed CN. In Table 20, the composite watershed curve number for the Holden North, Holden South, and Ursuline watersheds are presented. It should be noted that the discrete curve number method is more appropriate for design in both instances (and was used in all other analyses herein), but this does not allow for comparison against a back-calculated CN based upon monitored outflow volumes from each bioretention SCM (Table 20). Methods used to back-calculate the CN for each watershed post-SCM implementation are discussed in Hawkins (1993). The storage parameter, S, was calculated using a quadratic formula originally proposed by Hawkins (1973):

$$S = 5 * [P + 2Q - (4Q^2 + 5PQ)^{1/2}] \quad (2.9)$$

where P is rainfall and Q is runoff (i.e. outflow from the bioretention cell). Equation 12 can then be used to calculate a CN for each storm event. In all cases, CNs were very high for the smallest events, and then approached a horizontal asymptote when rainfall depths were greater than 2 inches. The constant value that is asymptotically approached is defined as the CN and is used for design purposes. Using the field-collected data, watershed CNs post-bioretention implementation were between 87-90. This represented a decrease in CN of between 3-10 for each BRC; because these systems were oversized with respect to the water quality volume, it is expected that a bioretention SCM designed for the 0.75-in water quality volume would have less impact on the watershed CN. These post-installation CNs could be compared against a surrogate CN for pre-development hydrology in Ohio, such as that for a forest in good condition over an HSG D soil (i.e. CN of 77, NRCS 1986). While the BRCs do not completely return the watersheds to a pre-development state, they do aid in reducing the watershed CN. Perhaps a treatment train of SCMs could provide greater volume reduction and meet this particular metric of pre-development hydrology (Wilson et al. 2015).

Table 20. Comparison of pre- and post-bioretention implementation curve numbers for the watersheds.

Effective Curve Number			
Site	Watershed	Median Watershed + BRC	Average Watershed + BRC
Holden North	93.1	87.2	86.7
Holden South	93.1	90	88.8
Ursuline	98.5	89.7	88.1

2.4.4 Peak Flow Mitigation

Peak flow rates from a watershed affect flooding and stream channel stability. Engineers typically implement large-scale retention and detention practices to mitigate peak flow rates from design storm events; however, these systems release runoff at attenuated flow rates over a longer period of time. These lower discharge rates are often above those which cause stream bank

erosion (Tillinghast et al. 2011). DeBusk et al. (2010) found drainage from bioretention cells was released at rates similar to shallow interflow from reference watersheds, suggesting watershed scale implementation of bioretention could benefit stream health through disconnection of imperviousness (Walsh et al. 2009; Burns et al. 2012).

Statistics for peak flow mitigation for the three monitored bioretention cells are presented in Table 21. Peak inflow and outflow rates are presented for the median, 75th percentile, 90th percentile, and maximum flow rates recorded during the respective monitoring periods. Peak flow mitigation was greatest for the smallest rainfall depths, as the bowl storage completely captured the event and the outflow rate was limited by the drainage capacity of the underdrain. Generally, as rainfall intensity increased, peak flow mitigation decreased, especially for storms with overflow. For the three bioretention cells, peak flow mitigation was at minimum 29%, except for one storm at Holden North with no peak flow mitigation. This is probably because these BRCs were sized to capture events larger than 1.16 inches, providing between 50%-150% more storage than a system designed for the 0.75-in water quality volume. Over-sizing a bioretention cell with respect to its watershed area caused the most marked changes in fraction of overflow in DRAINMOD simulations to predict the long-term hydrology of bioretention cells in Ohio (Smolek et al. 2015). Oversized bioretention systems decrease the potential number of overflow producing events by providing greater bowl storage volume; for instance, only 10, 12, and 12 events at Ursuline, Holden South, and Holden North, respectively, exceeded the design storage capacity of the bowl (neglecting storage in the media and IWS zone). This would have increased to 11, 19, and 19 if the cells were sized to capture only the 0.75-in water quality volume.

Table 21. Statistics for peak flow mitigation at the Ursuline College and Holden Arboretum bioretention cells.

Site Name	Cell Name	Location	Median Peak Flow Rate (cfs)	75th Percentile Peak Flow Rate (cfs)	90th Percentile Peak Flow Rate (cfs)	Maximum Peak Flow Rate (cfs)	Median Peak Flow Reduction (%)	Range of Peak Flow Reduction (%)
Ursuline College	-	Inlet	0.37	0.89	1.60	3.71	100	50-100
		Outlet	0.00	0.01	0.28	1.76		
Holden Arboretum	South	Inlet	0.14	0.31	0.82	1.16	98.9	29-100
		Outlet	0.00	0.02	0.06	0.82		
	North	Inlet	0.22	0.48	1.30	1.83	96.6	0-100
		Outlet	0.01	0.03	0.10	1.29		

Peak ratio, defined as the ratio of the outlet peak to the inlet peak, has been suggested to be an important performance metric for bioretention cells (Davis 2008). The author suggested a 0.33 peak ratio should be targeted, as this is the ratio of the rational runoff coefficient for the pre-development condition (0.3) to that for an impervious surface (0.9). Exceedance probability for peak ratio was plotted in Figure 32 for the three monitored bioretention cells. Mean peak ratios were 5% at Ursuline and 8% at Holden Arboretum; median peak ratios were zero at Ursuline, 1% at Holden South, and 3% at Holden North. This suggested for most events, peak flow mitigation was excellent. The mean and median peak ratios were 42 and 51% and 40 and 48%, respectively, for two bioretention cells in Maryland (Davis 2008). Mean peak flow reductions for bioretention cells in New Hampshire (UNHSC 2006) and Charlotte, NC (Hunt et al. 2008) were 85% and 99%, respectively. The bioretention cells met the target peak ratio of 0.33 during 95, 94, and 94% of the monitored events at Ursuline, Holden North, and Holden South, respectively. This compared favorably to the two cells in Maryland, which met this target for 25 and 43% of the storms. This suggested oversized bioretention cells and those which employed IWS zones further aid in peak flow mitigation.

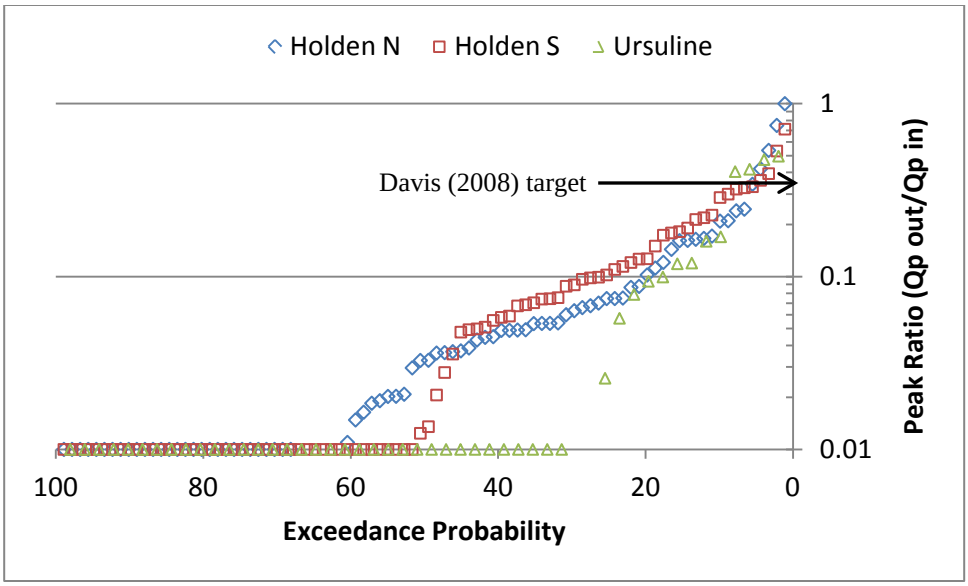

Figure 32. Analysis of peak ratio for monitored storm events at Holden Arboretum and Ursuline College.

Engineers usually design SCMs for peak flow mitigation using infrequent return interval events. Rainfall intensities for design purposes are typically gleaned from NOAA Atlas 14 databases (NOAA 2015); design rainfall event intensities were obtained for Cleveland Hopkins International airport, the nearest reliable source of long term data (located approximately 24 miles from Ursuline College and 37 miles from Holden Arboretum). Because the times of concentration from the catchments of interest were small (i.e. less than 5 minutes), a 5-minute rainfall duration was used for the analysis that follows. During the monitoring period, 5 events occurred at Holden Arboretum with peak rainfall intensities that exceeded the 1 year, 5-minute rainfall intensity (3.88 in/hr); four such events occurred at Ursuline College – of those, one event exceeded the 5-yr, 5-minute (5.56 in/hr) rainfall intensity. While all four events at Ursuline College exceeding design rainfall intensities had rainfall depths exceeding the bowl storage capacity of 1.16 inch at Ursuline, peak outflow rates were still reduced by 53-88%. There were several reasons this degree of peak reduction occurred. In all cases, the peak rainfall intensity occurred within the first few hours of the hyetograph, when the bowl volume had not yet filled.

The high media conductivity (6.6 in/hr) at Ursuline College allowed a significant amount of runoff to be routed through the media even when the bowl volume was full. Drainage rates are then restricted by the capacity of the drain to convey water under a given driving head. At Holden Arboretum, only 3 of these 5 events had rainfall depths that exceeded the design bowl storage volume, meaning they could potentially produce overflow. Peak flow reductions during these high intensity events were between 24-96% at this site. The highest percentage peak flow mitigation was related to the peak rainfall intensity occurring within the first hour of the hyetograph, allowing for capture of the volume without overflow occurring. To summarize, even during events with overflow, substantial peak flow mitigation occurred at both the Ursuline College (worst case 53%) and Holden Arboretum (worst case 24%) bioretention cells.

Flow duration curves are used to summarize the hydraulic response of bioretention cells by amalgamating flow rates measured on a 2-minute interval across all observed storm events into a single distribution (Figure 33; Davis et al. 2012). The curves can be used to compare effluent flow rates against threshold erosion rates. The total monitoring period length was 209 days at Ursuline College and 304 days at Holden Arboretum. Outflow (drainage and/or outflow) from the Ursuline College bioretention cell occurred for 82 hours, or 1.6% of the monitoring period. For the South and North cells at Holden Arboretum, outflow occurred during 495 and 1340 hours, which represented 6.8 and 18.3% of the monitoring periods. The total duration of rainfall during the monitoring periods was 452 and 821 hours at Ursuline College and Holden Arboretum, respectively. Thus, for systems with higher exfiltration rates, the duration of outflow will be substantially reduced, while lower drawdown rates (i.e. Holden North) result in periods of drainage extending well beyond the rainfall duration.

The duration of outflow is related primarily to the IWS zone depth, exfiltration rate, and bowl storage depth. Higher exfiltration rates lead to quicker dewatering of the media post-event, and provide additional storage for follow-on rainfall events. Slower drawdown rates shunt more water to the underdrain as water moves through the bioretention cell following the cessation of rainfall.

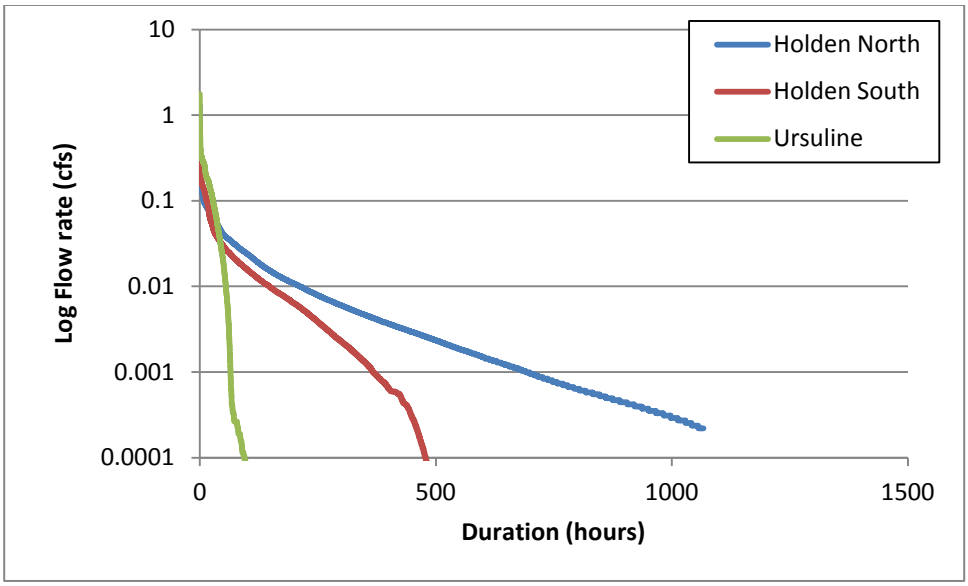

Figure 33. Flow duration curves for outflow from the monitored bioretention cells.

2.5 Summary and Conclusions

Three bioretention cells were monitored for their hydrologic performance over a period of at least seven months in northeast Ohio. The water balance was quantified at each site, and volume reduction and peak flow mitigation were related to design characteristics. The following conclusions can be drawn from this study:

1) The measured post-construction drawdown rates for all three bioretention cells exceeded the vertical saturated hydraulic conductivities of the soils underlying the bioretention cells measured during construction. The authors suggest this was due to head driven flow during

exfiltration due to the 15 to 24-in depth IWS zones, lateral exfiltration from the side walls of the bioretention cells, and minor amounts of evapotranspiration. The importance of lateral exfiltration will wane as the ratio of surface area to perimeter length increases and as the IWS depth decreases. While the soils were mapped as HSG D, measured post-construction drawdown rates were in the range of HSG C soils (0.065-0.17 in/hr).

2) Runoff reduction for the Ursuline College, Holden South, and Holden North cells was 60%, 42%, and 36%, and was primarily related to the exfiltration rate of the underlying soil. These SCMs were oversized and could store the 1.16, 1.78, and 1.76 inch events without overflow, contributing to improved performance. However, volume reduction does occur when bioretention cells are sited over poorly draining soils; the implementation of an IWS zone allows for continued exfiltration over inter-event periods.

3) Discharge thresholds were 0.63, 0.32, and 0.25 inches for the Ursuline College, Holden South, and Holden North cells, respectively. The maximum rainfall depth that could be abstracted without outflow likely is a result of storage capacity in the IWS, a function of IWS depth and exfiltration rate; other factors such as bowl storage depth and HLR will also impact this parameter.

4) Curve numbers were calculated for each watershed both pre- and post-bioretention installation. In each case, the watershed CN was reduced by 3-10 points from the value derived from watershed land use. The post-installation CN was compared to an HSG D soil CN under good quality forested conditions. This comparison showed these bioretention cells were not able to fully restore pre-development hydrology, but provided a marginal benefit.

5) Median peak flow reduction for the three cells was 96% or greater. The smallest storms were either completely captured with no outflow or outflow rates were throttled by the

underdrain. Peak flow mitigation was aided because these SCMs were oversized, which has been shown in bioretention modeling to be a substantial controlling factor for peak attenuation. The peak ratio standard of 0.33 suggested for meeting LID targets was met by the three bioretention cells during 94-95% of storm events. During events that exceeded the 1-yr, 5-minute rainfall intensity, the Ursuline College and Holden Arboretum cells provided 53-88% and 24-96% peak flow mitigation, respectively. This was from the peak rainfall rate occurring well before the centroid of the rainfall volume, meaning there was adequate bowl storage to mitigate peak inflow rates without overflow.

6) Flow duration curves were created for the three bioretention cells. The duration of outflow represented 1.6%, 6.8%, and 18.3% of the monitoring period at Ursuline College, Holden South, and Holden North bioretention cells, respectively. While the Holden Arboretum cells had similar design characteristics, the underlying soils were slightly divergent, resulting in greater exfiltration rates for the South cell. This resulted in a reduced duration of drainage for the South cell when compared to the North cell. The Ursuline College cell produced outflow during 18% of the total rainfall duration, which shows the benefit of siting bioretention cells over higher hydraulic conductivity soils.

2.6 References

Asleson, B.C., Nestingen, R.S., Gulliver, J.S., Hozalski, R.M., and Nieber, J.L. (2009). "Assessment of rain gardens by visual inspection and controlled testing." *Journal of the American Water Resources Association*. 45,1019–1031.

Bathke, G.R., and Cassel, D.K. (1991). "Anisotropic variation of profile characteristics and saturated hydraulic conductivity in an Ultisol landscape." *Soil Science Society of America Journal*. 55(2), 333-339.

Bledsoe, B., and Watson, C. (2001). "Effects of urbanization on channel instability." *Journal of the American Water Resources Association*, 37(2), 255–270.

Booth, D. B. (1990). "Stream-channel incision following drainage-basin urbanization." *Journal of the American Water Resources Association*. 26(3), 407-417.

Booth, D., Hartley, D., and Jackson, R. (2002). "Forest cover, impervious surface area, and the mitigation of storm-water impacts." *Journal of the American Water Resources Association*, 38(3), 835–845.

Bratieres, K., Fletcher, T.D., Deletic, A., and Zinger, Y. (2008). "Nutrient and sediment removal by stormwater biofilters: A large-scale design optimisation study." *Water Research*. 42(14), 3930-3940.

Brown, R.A., and Hunt, W.F. (2010). "Impacts of construction activity on bioretention performance." *Journal of Hydrologic Engineering*. 15(6), 386-394.

Brown, R.A. and Hunt, W.F. (2011a). "Impacts of media depth on effluent water quality and hydrologic performance of under-sized bioretention cells." *Journal of Irrigation and Drainage Engineering.* 137(3), 132-143.

Brown, R.A. and Hunt, W.F. (2011b). "Underdrain configuration to enhance bioretention exfiltration to reduce pollutant loads." *Journal of Environmental Engineering*. 137(11), 1082-1091.

Brown, R.A., Hunt, W.F., and Skaggs, R.W. (2011c). *Long-term modeling of bioretention hydrology with DRAINMOD*. Final Report, Water Resources Research Institute of the University of North Carolina. Report No 415.

Brown, R.A., and Hunt, W.F. (2012). "Improving bioretention/biofiltration performance with restorative maintenance." *Water Science and Technology*. 65(2), 361-367.

Brown, R.A., R.W. Skaggs, and W.F. Hunt. (2013). "Calibration and validation of DRAINMOD to model bioretention hydrology." *Journal of Hydrology*. 486, 430-442.

Browne, D., Deletic, A., Mudd, G.M., and Fletcher, T.D. (2008). "A new saturated/unsaturated model for stormwater infiltration systems." *Hydrological Processes*. 22(25), 4838–4849.

Burns, M.J., Fletcher, T.D., Walsh, C.J., Ladson, A.R., and Hatt, B.E. (2012). "Hydrologic shortcomings of conventional urban stormwater management and opportunities for reform." *Landscape and Urban Planning*. 105(3), 230-240.

Chin, D.A. (2006). *Water resources engineering*. 2nd edition. Pearson Prentice Hall, Upper Saddle River, NJ.

Davis, A.P. (2008). "Field performance of bioretention: hydrology impacts." *Journal of Hydrologic Engineering*. 13(2), 90-95.

Davis, A.P., Hunt, W.F., Traver, R.G., and Clar, M. (2009). "Bioretention technology: Overview of current practice and future needs." *Journal of Environmental Engineering*. *135*(3), 109-117.

Davis, A.P., Stagge, J.H., Jamil, E., and Kim, H. (2012). "Hydraulic performance of grass swales for managing highway runoff." *Water Research*. 46(20), 6775-6786.

DeBusk, K.M., Hunt, W.F., and Line, D.E. (2010). "Bioretention outflow: Does it mimic nonurban watershed shallow interflow?" *Journal of Hydrologic Engineering*. 16(3), 274-279.

Dietz, M.E. and Clausen, J.C. (2005). "A field evaluation of rain garden flow and pollutant treatment." *Water, Air, and Soil Pollution*. 167(1-4), 123-138.

Dietz, M.E. and Clausen, J.C. (2006). "Saturation to improve pollutant retention in a rain garden." *Environmental Science and Technology.* 40(4), 1335-1340.

Eisenberg, B.E., Lindow, K.C., Smith, D.R. (2015). *Permeable pavements*. 1st Ed., American Society of Civil Engineers, Reston, VA.

Emerson, C. and Traver, R. (2008). "Multiyear and seasonal variation of infiltration from storm-water best management practices." *Journal of Irrigation and Drainage Engineering*. 134(5), 598-605.

Fangmeier, D.D., Elliot, W.J., Workman, S.R., Huffman, R.L., Schwab, G.O. (2006). *Soil and water conservation engineering*. 5th edition. Thomson Delmar learning, Clifton Park, NY.

Gilbert Jenkins, J.K., Wadzuk, B.M., and Welker, A.L. (2010). "Fines accumulation and distribution in a storm-water rain garden nine years postconstruction." *Journal of Irrigation and Drainage Engineering*. 136(12), 862-869.

Grant, D.M. and Dawson, B.D. (2001). *Isco open channel flow measurement handbook*. 5th edition. Isco, Inc., Lincoln, NE.

Hammer, T.R. (1972). *Stream channel enlargement due to urbanization*. Regional Science Research Institute Discussion Paper Series, No. 55. Philadelphia, PA, 41 pp.

Hawkins, R.H. (1973). "Improved prediction of storm runoff in mountain watersheds." *Journal of the Irrigation and Drainage Division*. 99(4), 519-523.

Hawkins, R.H. (1993). “Asymptotic determination of runoff curve numbers from data.” *Journal of Irrigation and Drainage Engineering.* 119(2), 334-345.

Hood, M.J., Clausen, J.C., and Warner, G.S. (2007). "Comparison of stormwater lag times for low impact and traditional residential development." *Journal of the American Water Resources Association.* 43(4), 1036-1046.

Hunt, W.F., Jarrett, A.R., Smith, J.T., and Sharkey, L.J. (2006). “Evaluating bioretention hydrology and nutrient removal at three field sites in North Carolina.” *Journal of Irrigation and Drainage Engineering*. 132(6), 600–608.

Hunt, W.F., Smith, J.T., Jadlocki, S.J., Hathaway, J.M., and Eubanks, P.R. (2008). “Pollutant removal and peak flow mitigation by a bioretention cell in urban Charlotte, NC.” *Journal of Environmental Engineering*. 134(5), 403-408.

Hunt, W.F., Davis, A.P., and Traver, R.G. (2012). “Meeting hydrologic and water quality goals through targeted bioretention design.” *Journal of Environmental Engineering*. 138(6), 698-707.

Jones, M.P. and Hunt, W.F. (2009). “Bioretention impact on runoff temperature in trout sensitive waters.” *Journal of Environmental Engineering*. 135(8), 577-585.

Lee, J.G., Borst, M., Brown, R.A., Rossman, L., and Simon, M.A. (2015). “Modeling the hydrologic processes of a permeable pavement system.” *Journal of Hydrologic Engineering*, 20(5), 1-9.

Li, H., Sharkey, L.J., Hunt, W.F., and Davis, A.P. (2009). “Mitigation of impervious surface hydrology using bioretention in North Carolina and Maryland.” *Journal of Hydrologic Engineering*. 14(4), 407–415.

Luell, S.K. (2011). *Evaluating the impact of bioretention cell size and swale design in treating highway bridge deck runoff*. M.S. thesis, Department of Biological and Agricultural Engineering, North Carolina State University.

Mulvany, T.J. (1851). “On the use of self-registering rain and flood gauges in making observations of the relation of rainfall and flood discharges in a given catchment.” *Transactions of the Institution of Civil Engineers of Ireland*. 4, 18-33.

National Oceanic and Atmospheric Administration (NOAA). (2015). *NOAA Atlas 14 point precipitation frequency estimates, Ohio.* Hydrometeorological Design Studies Center, Precipitation Frequency Data Server. Available: http://dipper.nws.noaa.gov/hdsc/pfds/pfds_map_cont.html?bkmrk=oh

Natural Resources Conservation Service (NRCS). (1986). *Urban hydrology for small watersheds*. Technical Release 55 (TR-55). 2nd edition. United States Department of Agriculture (USDA), Natural Resources Conservation Service, Conservation Engineering Division.

Ohio Department of Natural Resources (ODNR), Division of Soil and Water Conservation. (2006). *Rainwater and land development: Ohio's standards for stormwater management, low impact development, and urban stream protection*. 3rd edition. Ed: John Mathews.

Olson, N.C., Gulliver, J.S., Nieber, J.L., and M. Kayhanian. (2013). "Remediation to improve infiltration into compact soils." *Journal of Environmental Management*. 117,85–95.

Palhegyi, G. E. (2009). "Designing storm-water controls to promote sustainable ecosystems: science and application." *Journal of Hydrologic Engineering*. 15(6), 504-511.

Passeport, E., Hunt, W.F., Line, D.E., Smith, R.A., and Brown, R.A. (2009). "Field study of the ability of two grassed bioretention basins to reduce storm-water runoff pollution." *Journal of Irrigation and Drainage Engineering.* 135(4), 505-510.

Pitt, R., Chen, S.E., Clark, S.E., Swenson, J., and Ong, C.K. (2008). "Compaction's impacts on urban storm-water infiltration." *Journal of Irrigation and Drainage Engineering*. 134(5), 652-658.

Rawls, W.J., Brakensiek, D.L., and Saxton, K.E. (1982). "Estimation of soil water properties." *Transaction of the American Society of Agricultural Engineers.* 25(5), 1316-1320.

Reynolds, W.D., Elrick, D.E., Youngs, E.G., and Amoozegar, A. (2002). "Ring or cylinder infiltrometers (vadose zone)." *Methods of Soil Analysis - Part 4: Physical Methods,* J.H. Dane and G.C. Topp, eds., Soil Science Society of America. Madison, WI.

Sansalone, J.J., and Teng, Z. (2004). "In situ partial exfiltration of rainfall runoff. I: Quality and quantity attenuation." *Journal of Environmental Engineering*, 130(9), 990–1007.

Schueler, T.R., Fraley-McNeal, L., and Cappiella, K. (2009). "Is impervious cover still important? Review of recent research." *Journal of Hydrologic Engineering.* 14(4), 309–315.

Smolek, A.P.*, Winston, R.J.*, Dorsey, J.D., and Hunt, W.F. (2015). *Modeling the hydrologic performance of bioretention and permeable pavement stormwater controls in northern Ohio using DRAINMOD: Calibration, validation, sensitivity analysis, and future climate scenarios.* Final report submitted to the University of New Hampshire and the Chagrin River Watershed Partners. In fulfilment of NOAA Award number NA09NOS4190153. *These authors contributed equally to this work.

Soil Survey Staff, Natural Resources Conservation Service, United States Department of Agriculture. (2015). Web Soil Survey. http://websoilsurvey.nrcs.usda.gov/. Accessed 28 January 2015.

Tillinghast, E.D., Hunt, W.F., and Jennings, G.D. (2011). "Stormwater control measure (SCM) design standards to limit stream erosion for Piedmont North Carolina." *Journal of Hydrology*. 411(3), 185-196.

Tyner, J.S., Wright, W.C., and Dobbs, P.A. (2009). “Increasing exfiltration from pervious concrete and temperature monitoring.” *Journal of Environmental Management.* 90(8), 2636-2641.

United States Department of Agriculture (USDA). (2007). *Hydrologic Soil Groups*. Part 630, Chapter 7, National Engineering Handbook. Natural Resources Conservation Service.

United States Environmental Protection Agency (USEPA). (2007). “Reducing storm-water costs through low impact development strategies and practices.” *Rep. No. EPA 841-F-07-006*, EPA, Washington, D.C. www.epa.gov/nps/lid. Accessed Feb 2012.

University of New Hampshire Stormwater Center (UNHSC). (2006). *2005 Data Report*, CICEET, Durham, N.H.

Walsh, C.J., Fletcher, T.D., and Ladson, A.R. (2009). “Retention capacity: a metric to link stream ecology and storm-water management.” *Journal of Hydrologic Engineering*. 14(4), 399-406.

Wang, L., Lyons, J., Kanehl, P., and Bannerman, R. (2001). “Impacts of urbanization on stream habitat and fish across multiple spatial scales.” *Journal of Environmental Planning and Management*. 28(2), 255–266.

Wardynski, B.J., Winston, R.J., and Hunt, W.F. (2012). “Internal water storage enhances exfiltration and thermal load reduction from permeable pavement in the North Carolina mountains.” *Journal of Environmental Engineering*. 139(2), 187-195.

Wilson, C.E., Hunt, W.F., Winston, R.J., and Smith, P. (2015). “Comparison of runoff quality and quantity from a commercial low-impact and conventional development in Raleigh, North Carolina.” *Journal of Environmental Engineering*. 141(2), 05014005.

3 WATER QUALITY PERFORMANCE OF PERMEABLE PAVEMENT

3.1 Review of Literature

Based on 2014 estimates, less than half (46%) of the world's population resides in rural areas; the rural to urban population shift is projected to continue such that two-thirds of the world's population will reside in urban centers by 2050 (United Nations 2014). Urban development results in the introduction of impervious cover, which has been directly linked to stream health declines (Wolman 1967; Morse et al. 2003; Schueler et al. 2009). Parking surfaces represent about 10% of the impervious surfaces in residential watersheds, and as much as 50% of imperviousness in commercial developments (Arnold and Gibbons 1996). In the United States, it has been estimated that approximately 3500 km^2 of land is utilized for parking lots (Ben-Joseph 2012) Therefore, management of parking lot runoff is critical to watershed health and restoration of pre-development hydrology, the overall goal of Low Impact Development (Dietz 2007).

To combat the deleterious effects of impervious cover, engineers have developed stormwater control measures (SCMs), such as bioretention and permeable pavement, to attempt to match pre- and post-development hydrologic fates (Li et al. 2009; Fassman and Blackbourn 2010; DeBusk et al. 2010). Permeable pavements permit water to pass through a porous paving layer or gravel-filled spaces between pavers, allowing water to be stored in an underlying aggregate reservoir. They have the unique dual benefits of stormwater treatment and infiltration while maintaining the buildable area of a parcel of land (Pezzaniti et al. 2009). Previous research studies have shown permeable pavements attenuate runoff volume when compared to impervious parking lots, thereby reducing pollutant loading to receiving water bodies (Bean et al. 2007; Collins et al. 2008; Fassman and Blackbourn 2010; Roseen et al. 2012; Drake et al. 2014a).

Several studies have researched the water quality treatment performance of permeable pavements. Reductions in pollutant concentrations are generally observed for total suspended solids (Legret et al. 1996; Roseen et al. 2012; Drake et al. 2014b), metals (Legret et al. 1996; Bean et al. 2007; Roseen et al. 2012; Drake et al. 2014b), and hydrocarbons (Roseen et al. 2012; Drake et al. 2014b). The pavement layer, where sediment and grit are retained, is cited as a major sink for sediment and sediment-bound pollutants (such as the metals lead, cadmium, copper, and zinc) in permeable pavements (Roseen et al. 2012). Additionally, settling, biological degradation, and chemical mechanisms further pollutant retention within permeable pavements, typically at a geotextile layer or at the interface with the *in situ* soil (Franks et al. 2014). Total phosphorus, which is found in both dissolved and particulate-bound phases, was retained at 40-90% rates by permeable pavement (Bean et al. 2007; Roseen et al. 2012; Drake et al. 2014b).

Dissolved constituents, such as chloride from road salts and nitrate and nitrite nitrogen (NO_{2-3}), tend to migrate through the permeable pavement cross-section with little to no treatment (Collins et al. 2010; Borst and Brown 2014). In fact, nitrification often causes export of NO_{2-3} from permeable pavement systems (Collins et al. 2010; Drake et al. 2014b) and buildup of chloride in the permeable pavement cross-section may cause it to be detectable year-round in drainage samples (Borst and Brown 2014). Because porous asphalt provides better skid resistance and improved drainage when compared to dense-mix asphalt, it required four times less winter salt application to achieve the same level-of-service (Roseen et al. 2014).

Given these dissolved pollutants are often cited for causing water quality degradation such as eutrophication (Smith et al. 1999) and chloride toxicity (U.S. EPA 1988; Fay and Shi 2012), novel permeable pavement designs must be developed to further reduce their loading to surface waters. One such design, now common in bioretention, includes an internal water storage (IWS)

zone, which utilizes an upturned elbow in the underdrain to create internal ponding in an SCM (Hunt et al. 2012). The IWS zone has been shown to promote denitrification in bioretention, thereby reducing nitrate concentrations (Kim et al. 2003) and to promote exfiltration of additional stormwater from the permeable pavement system (Wardynski et al. 2012, when compared to traditional drainage configurations), thereby reducing pollutant loads. Given its promising results for water quality in bioretention and initially positive hydrologic results in permeable pavement, this design feature needs to be studied with regard to its impacts on pollutant concentrations and loads for permeable pavements.

Given the prevalence of permeable pavement being installed in Ohio and other states to treat not only direct rainfall but also run-on from impermeable surfaces, research is needed to determine how permeable pavements function for water quality goals under higher hydrologic loading. To date, the authors are not aware of any published literature that focuses on water quality performance of permeable pavements accepting run-on. Additionally, the vast majority of the permeable pavement water quality studies have been carried out on permeable pavements over Hydrologic Soil Group (HSG) A or B, sandy soils characterized by elevated infiltration rates. The goals of this study were to determine the outcomes of different hydrologic loading on the water quality performance of permeable pavements under northeast Ohio climatic conditions. The impact of purposefully-designed IWS zones within permeable pavements on effluent water quality and pollutant loads has not been published in the literature to-date. For instance, does the IWS zone promote denitrification within the permeable pavement? Additionally, how does a poorly-draining HSG D soil affect pollutant retention? To this end, two side-by-side permeable pavement applications with IWS zones situated over poor soils in northeast Ohio were monitored

over a one-year period to ascertain their performance for nutrients, sediment, heavy metals, and chloride.

3.2 Site Descriptions

Two permeable interlocking concrete pavement (PICP) applications were retrofitted into the parking lot at the Willoughby Hills, OH community center in September-October 2013 (Figure 2, Figure 34 and Figure 35). PICP consists of impermeable brick pavers with interstitial void spaces filled with aggregate, allowing water to infiltrate the pavement surface. Both applications employed a 20 inch total aggregate depth, with 2 inches of #89 stone bedding course immediately below the pavers, 6 inches of #57 aggregate beneath that, with 12 inches of #1/#2 aggregate serving as a base course. Common to both PICP applications was a 6-in diameter PVC underdrain with a 6-in upturned elbow, creating an IWS zone within the aggregate beneath the pavement. Given the poor underlying soils, the IWS zone was expected to hold water. This extended ponding within the aggregate allowed for both vertical and lateral exfiltration into the in situ soils.

The Small application, 482 ft^2 in surface area, had a flat subgrade and water could exfiltrate from this entire area (Table 22). The Large application (surface area of 4420 ft^2) had a stepped subgrade to make up for the 1-2% surface slope; this resulted in four, 6-in tall steps in the subgrade with the underdrain at the bottom of the cross-section. Because water could not be stored over the entire subgrade surface area, the effective infiltrative surface area beneath the IWS was reduced to 2210 ft^2. The contributing drainage areas for both the Small and Large applications were impermeable asphalt, except for two parking lot islands in the Large application catchment and a small portion of concrete sidewalk in Small application catchment.

The Willoughby Hills site was located over poorly draining Mahoning silt loam soils, a HSG D according to the soil survey maps (Soil Survey Staff 2015).

The hydrologic loading ratio (HLR) for a permeable pavement is one factor that affects hydrologic and water quality (through hydraulic retention time and pollutant loading) functionality. It is calculated using equation 17:

$$HLR = \frac{A_{PP}+A_{WS}}{A_{PP}} \quad (3.1)$$

Where A_{PP} is the surface area of the permeable pavement and A_{WS} is the surface area of the watershed. The HLR for the Small application was 8.2, while that of the Large application was 3.2. Past studies of permeable pavement water quality have been on HLRs of 1.0, with no contributing run-on. It should be noted that one of the purposes of this study was to tax the Small application with much higher hydrologic loading than the 3.0 that is currently allowed in the *Ohio Rainwater and Land Development Manual* (ODNR 2006).

Figure 34. Small (left) and Large (right) permeable pavement applications at Willoughby Hills, Ohio community center.

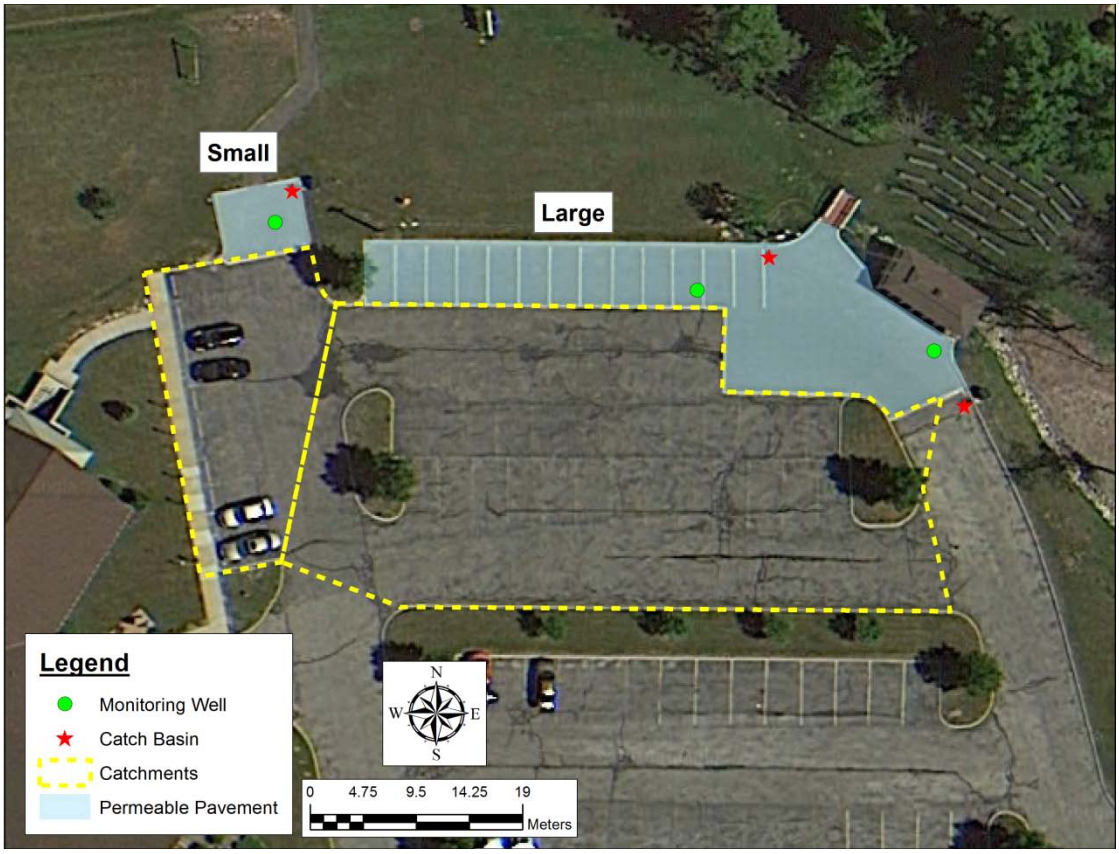

Figure 35. Willoughby Hills site water quality sampling overview. Photo credit: Google earth.

Table 22. Characteristics of the Willoughby Hills permeable pavement applications.

Monitoring Sites	Surface Course	Total Aggregate Depth (in)	Contributing Watershed Area (ac)	Surface Area of Permeable Pavement (ft^2)	Infiltrative Surface Area (ft^2)	Hydrologic Loading Ratio (HLR)
Small Application	PICP	20	0.08	482	482	8.2
Large Application			0.22	4420	2210	3.2

3.3 Materials and Methods

3.3.1 Data Collection

Water quality samples were obtained from three locations at the Willoughby Hills site: a control, impervious asphalt location (representative of the inflow to the permeable pavement) and the underdrain outfall for the Small and Large applications (Figure 35). Samples were

collected within weir boxes used to measure hydrology: a 30° v-notch, a 60° v -notch, and a 1-foot wide, contracted rectangular weir were utilized for the Small application, the Large application, and the control monitoring sites, respectively. ISCO 730 bubbler modules were attached to ISCO 6712 samplers at each monitoring location and used to measure depth of flow over the weir on two minute intervals (Teledyne ISCO, Lincoln, NE). Flow depths were converted to flow rate within each automated sampler using standard weir equations:

$$Q = 0.676 * H^{2.5}, 30^{\circ} \text{ v-notch weir} \quad (3.2)$$

$$Q = 1.443 * H^{2.5}, 60^{\circ} \text{ v-notch weir} \quad (3.3)$$

$$Q = 3.330 * (1 - 0.2H) * H^{1.5}, \text{ 1 ft broad-crested weir} \quad (3.4)$$

where Q is flow rate (ft^3/s) and H is head (ft) over the weir crest. Flow rate was integrated over time to determine stormwater volume at each monitoring location. Cumulative stormwater volume was used to trigger flow-proportional, composite samples obtained in 200mL aliquots. A minimum of five aliquots were obtained from each storm, describing greater than 80% of the pollutograph (U.S. EPA 2002). Sample intake strainers were placed in each weir box where flow was well-mixed. Separate rainfall events were characterized by a minimum antecedent dry period of 6 hours and 0.1-in rainfall depth. Rainfall data were collected at the site using both a manual and a tipping bucket rain gauge.

3.3.2 Laboratory Methods

Samples were obtained from automated sampling equipment within 24 hours of the cessation of rainfall. They were shaken vigorously in the composite 10 L jar to re-suspend solids, and were then subsampled into laboratory sample bottles. Composite samples were divided among two 1L plastic jars for total suspended solids (TSS) analysis, one 500 mL pre-acidified bottle for

nutrient analysis, and one 500 mL pre-acidified bottle for metals analysis. Orthophosphate (OP) analysis was completed in the lab by subsampling from the TSS bottle and filtering out solids using a 0.45 μm filter. Samples were placed immediately on ice and chilled to less than 4°C for transport to the Northeast Ohio Regional Sewer District Laboratory. Samples were delivered to the laboratory within 18 hours of sample collection. Samples were analyzed using U.S. EPA (1983) or American Public Health Association (APHA et al. 2012) methods for: total Kjeldahl nitrogen (TKN), $NO_{2\text{-}3}$, total ammoniacal nitrogen (TAN), OP, total phosphorus (TP), TSS, chloride, and the metals aluminum, calcium, copper, iron, magnesium, manganese, sodium, lead, and zinc (Table 23). Total nitrogen (TN), organic nitrogen (ON), and particle-bound phosphorus (PBP) were calculated using methods in Table 23.

Table 23. Laboratory testing and preservation methods as well as method detection limits (MDL) and practical quantification limits (PQL) for pollutants of concern.

Parameter	Laboratory Method	Preservation	MDL (mg/L)	PQL (mg/L)
TKN	EPA Method 351.2[1]	H_2SO_4 (<2 pH), <4˚C	0.122	0.5
NO_{2-3}	EPA Method 353.2	H_2SO_4 (<2 pH), <4˚C	0.003	0.02
TN	Calculated as TKN + NO_{2-3}	N/A	N/A	N/A
TAN	EPA Method 350.1	H_2SO_4 (<2 pH), <4˚C	0.003	0.02
ON	Calculated as TKN-TAN	N/A	N/A	N/A
OP	EPA Method 300.0	<4˚C	0.03	0.082
PBP	Calculated as TP-OP	N/A	N/A	N/A
TP	EPA Method 365.1	H_2SO_4 (<2 pH), <4˚C	0.001	0.01
Chloride	EPA Method 300.0	<4˚C	1	5
TSS	Standard Methods 2540D[2]	<4˚C	1	1
Parameter	**Laboratory Method**	**Preservation**	**MDL (µg/L)**	**PQL (µg/L)**
Al	EPA Method 200.8	HNO_3 (<2 pH), <4˚C	0.96	10
Ca			35.8	250
Cu			0.22	2
Fe			1.76	10
Mg			13.42	250
Mn			0.46	2
Pb			0.174	1
Zn			1.3	10

[1]U.S. EPA 1983
[2]APHA et al. 2012

3.3.3 Data Analysis

The performance of the two permeable pavement applications at Willoughby Hills was determined by comparing event mean concentrations from the impermeable asphalt drainage area and the underdrain flow from each of the PICP applications. Reductions in event mean concentrations (EMC) were determined using summary statistics, including the range of pollutant concentrations, mean ($\bar{x}$), median ($\tilde{x}$), standard deviation (s), skewness (C_s), the coefficient of variation (CV), the efficiency ratio (ER), and the median relative efficiency (RE_{median}). The latter three metrics are defined below:

$$CV = \frac{s}{\bar{x}} \tag{3.5}$$

$$ER = 1 - \frac{\sum_{i=1}^{n}(Eff\ EMC_i)/n}{\sum_{i=1}^{n}(Inf\ EMC_i)/n} \tag{3.6}$$

$$RE_{median} = 1 - \frac{Eff\ EMC_{median}}{Inf\ EMC_{median}} \tag{3.7}$$

where Eff EMC is the effluent EMC from the SCM, Inf EMC is the influent EMC associated with the watershed, and n is the number of storm events. The efficiency ratio is a commonly used metric for SCM performance, but is influenced by low or irreducible influent concentrations (Strecker et al. 2001). Boxplots were created to examine differences in water quality entering and draining from each permeable pavement application. These analyses were performed for all pollutants studied, including metals, nutrients, sediment, and chloride.

Pollutant loads were also explored since they take into account volume reduction through exfiltration and evaporation within a permeable pavement system and because they factor into total maximum daily load (TMDL) regulations. To calculate pollutant loads during a given storm, the product of stormwater volume and EMC was calculated at a given monitoring location. Sixteen events were sampled for water quality analysis and thus considered for loading calculations. Storms with no outflow, which only occurred in the Large application, contributed influent but not effluent pollutant load. The sum of each storm event load at the inlet and outlet for each permeable pavement was then calculated and compared using a relative percent difference. All pollutant loads were normalized by watershed area.

Kruskal-Wallis k-sample tests were utilized to determine whether seasonality of rainfall depth and intensity was statistically significant. If this omnibus test was significant, pair-wise comparisons were made using Dunn's test to determine seasons in which greater storm depth or

intensity occurred. Rainfall depths and intensities for sampled and non-sampled storms were also compared using unpaired Wilcoxon rank sum tests.

Statistical analysis was undertaken to determine the significance of pollutant concentration and load reductions; paired inlet and outlet values were compared statistically. If data were normal or log-normal, a paired t-test was utilized to determine significance. Normality was determined using Anderson-Darling and Shapiro-Wilkes tests and through visual analysis of quantile-quantile plots. If data were non-normal, a Wilcoxon rank sum test was applied to determine statistical significance. Effluent concentrations from the Small and Large applications were also tested for differences, since influent concentrations were presumably the same for both permeable pavements.

All data analysis was completed using R version 3.1.2 (R Core Team, 2014). A criterion of 95% confidence (α=0.05) was used for this research. For all pollutants except TAN and OP, all laboratory-reported concentrations for the 16 sampled storms were above the PQL, and were analyzed without transformation. For six storms for OP and one for TAN, a value of one-half the detection limit was substituted for concentration data that were below the PQL (Antweiler and Taylor 2008).

3.4 Results and Discussion

3.4.1 Sampled Storm Events

Over the 13 month monitoring period in 2014, 77 storms over 0.1 inch in rainfall depth occurred at Willoughby Hills (Table 24). Water quality sampling equipment was installed in April 2014. Eighteen storms were sampled for water quality for the Small application, while 12 storms were sampled at the Large application (5 storms had no outflow and 1 had sampler

errors). The rainfall characteristics of all monitored and sampled events in 2014 are shown in Figure 36 and Table 24; snowfall occurred during the winter months and was not included in this analysis. Sampled storms tended to be larger and more intense than the overall distribution of storms, but the largest three storms at the site were not sampled. The majority of sampled rainfall events fell in the late spring and summer seasons, when rainfall intensities were highest. The Kruskal-Wallis k-sample test showed no significant difference for seasonality of rainfall depth (p-value=0.55) or rainfall intensity (p-value=0.08). Unpaired Wilcoxon rank sum tests suggested that statistically significant differences in rainfall depth (p-value = 0.0007) and rainfall intensity (p-value = 0.042) existed between the sampled and not-sampled storm events. Further supporting the statistical tests were the median storm depths (0.30 vs. 0.65 inches for all and sampled storms, respectively) and rainfall intensities (0.48 and 1.44 in/hr for all and sampled storms, respectively). Sampled storms tended to be larger and more intense than the overall distribution of storms (Table 24), suggesting that data presented herein may be conservative for water quality performance, since smaller storms would more likely be completely captured and have a larger average hydraulic retention time within the permeable pavements.

Table 24. Summary statistics for sampled storms and all monitored storms at Willoughby Hills.

Statistic	All Storms		Sampled Storms	
	Rainfall Depth (in)	Rainfall Intensity (in/hr)	Rainfall Depth (in)	Rainfall Intensity (in/hr)
Minimum	0.10	0.12	0.34	0.12
Median	0.30	0.48	0.65	1.44
Mean	0.51	1.02	0.85	1.77
Maximum	3.42	6.60	2.07	6.60

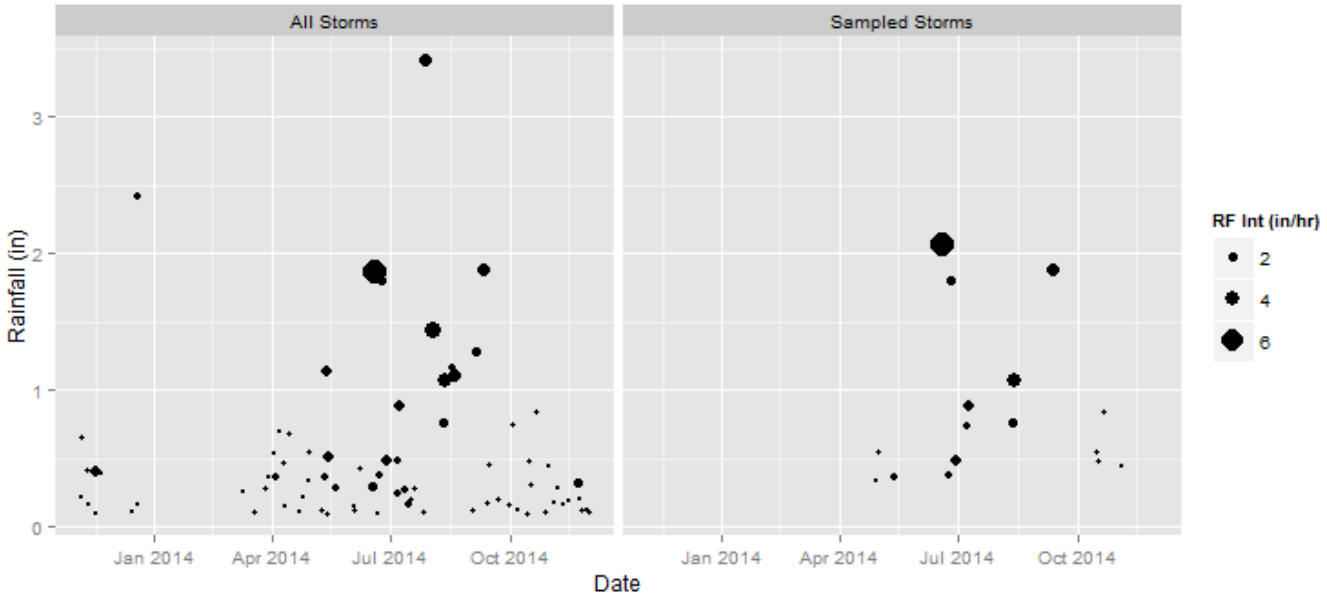

Figure 36. Distribution of sampled (samp) and all monitored storms at Willoughby Hills with rainfall intensity (in/hr) shown by the diameter of the marker.

3.4.2 Pollutant Concentrations

Summary statistics and boxplots for nutrient and TSS concentrations from the Willoughby Hills untreated asphalt runoff (inlet), Small application drainage (Sm Out), and Large application drainage (Lg Out) monitoring sites are presented in Table 25 and Figure 37. ER and RE_{median} for the permeable pavements for nitrogen and phosphorus species were close to zero, suggesting little treatment of the influent stormwater; the boxplots in Figure 37 also support this conclusion. Particulate ON appeared to be trapped, probably near the pavement surface and in the cross-section, resulting in non-significant reductions of ON and TKN in both the Small and Large applications. Paired statistical testing (Table 26) showed that treatment provided by the permeable pavement was not significant for all nutrients except NO_{2-3}, whose concentration significantly increased for the Small application (ER = -1.14). Similar increases in NO_{2-3} concentrations were observed in Bean et al. (2007) and Drake et al. (2014b). Aerobic transformation of TAN and ON to dissolved NO_{2-3} has been cited as a probable cause for this

export of NO_{2-3} from permeable pavements (Collins et al. 2010; Tota-Maharaj and Scholz 2010). An anaerobic zone with a carbon source would be needed to encourage denitrification; while the IWS zones *always* had water ponded within them, air entry through the PICP interstitial spaces probably kept the dissolved oxygen levels above 0.5 mg/L, generally accepted to be the value needed for denitrification to occur (Van Haandel and Van der Lubbe 2012). Additionally, the IWS zone lacked a carbon source, such as mulch or other organic matter, needed to drive denitrification (Knowles 1982). A smaller (ER = -0.1) and not statistically significant export of NO_{2-3} was observed in the Large application. The effluent concentration of NO_{2-3} from the Large application was significantly different from that of the Small application, suggesting hydrologic loading may influence NO_{2-3} export from permeable pavements. Other than NO_{2-3}, no significant differences existed between effluent concentrations of nutrients and TSS for the two permeable pavements.

Statistically significant *increases* in TSS concentrations occurred for both the Small and Large applications of permeable pavement at Willoughby Hills; this has not been observed by other field or lab studies on permeable pavements (Legret et al. 1996; Bean et al. 2007; Roseen et al. 2012; Drake et al. 2014b; Drake et al. 2014c). ERs were -4.1 and -5.1, respectively, for the Small and Large applications. The median effluent concentrations of these permeable pavements exceeded those presented in the literature for permeable pavements by at least a factor of ten (Bean et al. 2007; Roseen et al. 2011; Drake et al. 2014b; Drake et al. 2014c). Median effluent concentrations were 97 and 154 mg/L, respectively, for the Small and Large applications. Legret et al. (1996) observed effluent concentrations up to 139 mg/L for a permeable pavement in France; however, the mean effluent concentration was 12 mg/L – no reasoning was given for this apparent outlier.

The increases in TSS concentrations suggested that sediment was being entrained by the stormwater as it passed through the cross-section of the permeable pavements. Perhaps the Large application had a higher median effluent concentration (with a smaller hydrologic loading) because the system had stair-steps in the subgrade, which may have allowed for higher velocities in the subgrade than the flat-bottomed Small application. It is hypothesized that water passing over the in-situ soil collected the clayey subsoil sediment, helping to export metals, significantly in some cases. Since the soil was 24 inches below grade, the subgrade soil would be part of the B horizon of the clay Mahoning soil (National Cooperative Soil Survey 2014), with very little organic nitrogen. This supposition is supported by the (non-statistically significant) 11% and 32% ERs for ON for the Small and Large applications, respectively.

Table 25. Summary statistics for nutrient and sediment concentrations at the Willoughby Hills permeable pavement stormwater controls.

Pollutant	Location	Range (mg/L)	$\bar{X}$	$\tilde{X}$	s (mg/L)	C_s (mg/L)	CV (mg/L)	ER	RE_{median}
TKN	Inlet	0.24-5	0.99	0.63	1.07	3.35	1.09	-	-
	Sm Out	0.24-2.7	0.86	0.59	0.69	1.45	0.81	0.13	0.07
	Lg Out	0.14-1.5	0.74	0.81	0.47	0.25	0.64	0.25	-0.28
NO_{2-3}	Inlet	0.1-1.7	0.42	0.38	0.33	3.34	0.79	-	-
	Sm Out	0.2-1.9	0.90	0.63	0.60	0.71	0.67	-1.14	-0.66
	Lg Out	0.11-0.9	0.46	0.46	0.30	0.51	0.64	-0.1	-0.20
TN	Inlet	0.43-5.4	1.41	1.01	1.20	2.59	0.86	-	-
	Sm Out	0.64-3.6	1.76	1.22	1.08	0.58	0.62	-0.25	-0.20
	Lg Out	0.36-2.4	1.21	1.00	0.70	0.57	0.58	0.14	0.02
TAN	Inlet	0-1.2	0.23	0.14	0.31	2.39	1.32	-	-
	Sm Out	0.002-0.8	0.19	0.12	0.21	1.65	1.11	0.19	0.18
	Lg Out	0.01-0.5	0.23	0.28	0.14	-0.37	0.59	-0.01	-0.95
ON	Inlet	0.23-3.7	0.76	0.54	0.79	3.54	1.04	-	-
	Sm Out	0.11-2.3	0.67	0.43	0.55	1.84	0.82	0.11	0.21
	Lg Out	0.05-1	0.51	0.54	0.37	0.27	0.73	0.32	0.00
OP	Inlet	0.002-0.056	0.019	0.0167	0.016	1.34	0.86	-	-
	Sm Out	0.003-0.045	0.013	0.01667	0.010	2.04	0.78	0.29	0.00
	Lg Out	0.004-0.017	0.013	0.0167	0.005	-1.06	0.37	0.29	0.00
PBP	Inlet	0.007-0.092	0.04	0.05	0.02	0.33	0.47	-	-
	Sm Out	0.005-0.164	0.04	0.03	0.04	2.57	1.01	0.10	0.41
	Lg Out	0.019-0.164	0.06	0.04	0.04	1.90	0.78	-0.29	0.14
TP	Inlet	0.02-0.1	0.05	0.05	0.02	0.03	0.41	-	-
	Sm Out	0.02-0.18	0.05	0.04	0.04	2.38	0.77	0.03	0.25
	Lg Out	0.02-0.18	0.07	0.05	0.05	1.81	0.71	-0.21	0.10
TSS	Inlet	4-154	26	12	35	3.01	1.36	-	-
	Sm Out	5-723	131	97	166	2.88	1.26	-4.06	-6.92
	Lg Out	12-360	159	154	89	0.81	0.56	-5.1	-11.5

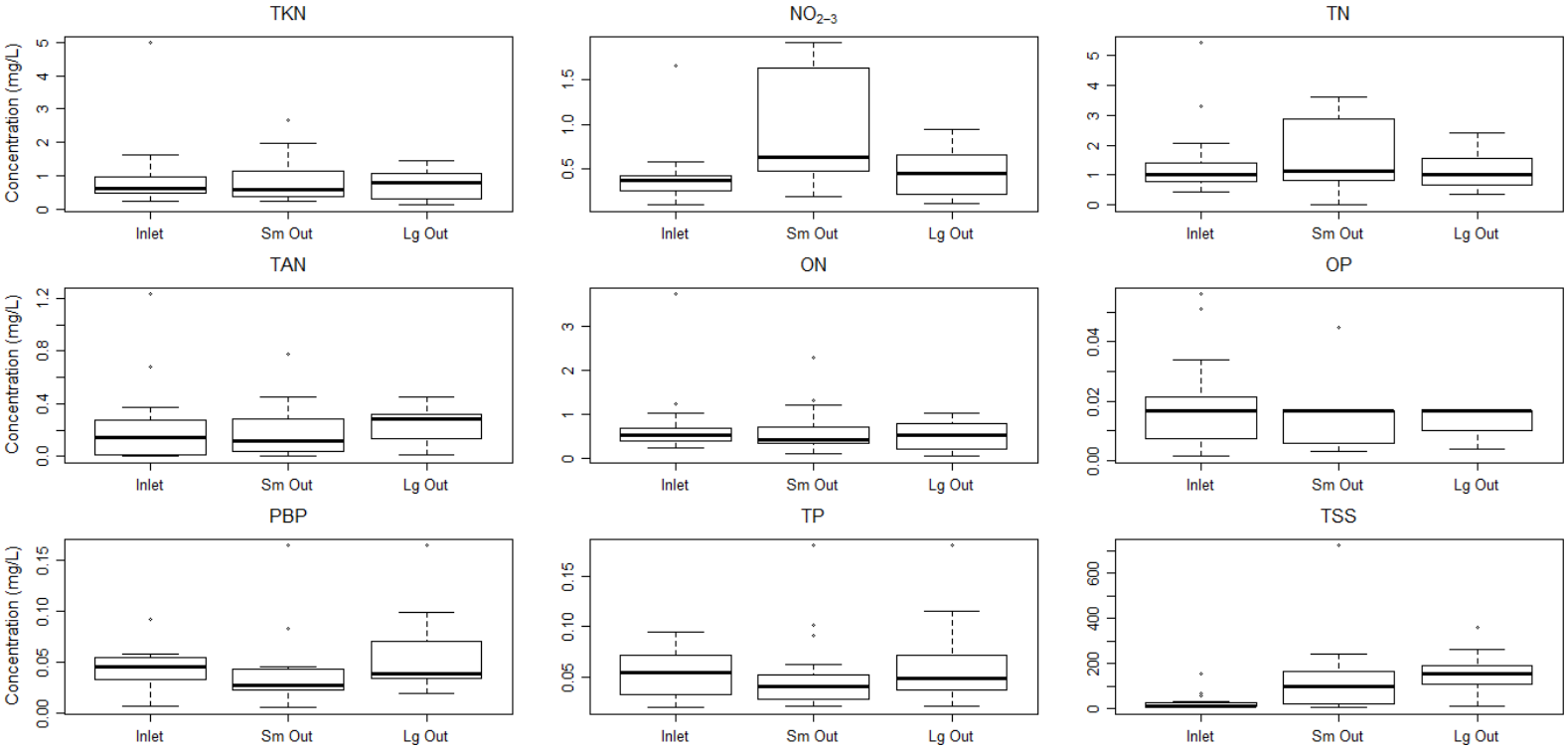

Figure 37. Boxplots of nutrient and sediment concentrations showing asphalt (inlet), Small application outlet (Sm Out), and Large application outlet (Lg Out) concentrations for Willoughby Hills.

Table 26. Summary of statistical testing for pollutant concentrations at Willoughby Hills.

Parameter	Location	Pollutant																	
		Cl	Al	Ca	Cu	Fe	Mg	Mn	Pb	Zn	TKN	NO_{2-3}	TN	TAN	ON	TP	OP	PBP	TSS
Statistical Test	Small	t	WRS	t	t	t	t	WRS	t	t	t	t	WRS	t	WRS	t	t	WRS	t
p-value		**	**	***	0.94	***	***	0.89	0.45	***	0.56	**	0.09	0.79	0.30	0.40	0.75	0.09	**
Statistically Significant?		Yes	Yes	Yes	No	Yes	Yes	No	No	Yes	No	Yes	No	No	No	No	No	No	Yes
Statistical Test	Large	t	WRS	t	WRS	t	t	WRS	WRS	t	WSR	t	WRS	WRS	WRS	t	WRS	t	t
p-value		0.46	**	***	0.84	***	0.13	*	**	0.544	0.313	0.94	0.74	0.46	0.15	0.68	0.08	0.20	***
Statistically Significant?		No	Yes	Yes	No	Yes	No	Yes	Yes	No	No	No	No	No	No	No	No	No	Yes
Statistical Test	Large vs. Small	WRS	t	t	t	t	t	t	t	t	t	t	t	t	t	t	t	t	t
p-value		**	***	***	***	***	**	0.08	**	0.14	0.39	*	0.054	0.15	0.10	0.81	0.18	0.78	0.45
Statistically Significant?		Yes	Yes	Yes	Yes	Yes	Yes	No	Yes	No	No	Yes	No	No	No	No	No	No	No
Lower Eff Conc		Large	Small	Small	Small	Small	Large	N/A	Small	N/A	N/A	Large	N/A	N/A	N/A	N/A	N/A	N/A	N/A

*significant at α=0.05, ** significant at α=0.01, *** significant at α=0.001
Yes = significant export, Yes = significant reduction
WRS = Wilcoxon rank sum test
t = student's t-test

Given the export of TSS from the permeable pavement systems, which has not been consistently observed in the literature (Legret et al. 1996; Bean et al. 2007; Roseen et al. 2012; Drake et al. 2014b; Drake et al. 2014c), further exploration of these results was warranted (Figure 39). For the first 4 months of the monitoring window, effluent concentrations were consistently above those from the asphalt runoff. Influent concentrations were quite low, consistently below 25 mg/L, well below those from parking lots in past studies (Bannerman et al. 1993; Drake et al. 2014b). Toward the end of 2014, effluent concentration decreased substantially to below 25 mg/L. Similar trends were observed for Pb and Cu, whose effluent concentrations trended downward in a linear fashion over the monitoring period, while influent concentrations remained the same (Figure 40). This suggested a potential maturation period for permeable pavement water quality performance, as suggested previously by Drake et al. 2014b, and could have been due to *in situ* soil beneath the aggregate being resuspended as flow entered the permeable pavement reservoir. Soils were raked during construction with the excavator bucket's teeth (Figure 38), and no geotextile was used to separate the aggregate from the underlying soil (due to concerns with clogging of the geotextile; Boving et al. 2004). Therefore, loose sediment could become entrained in the stormwater as it flowed through the cross-section, imparting additional TSS on the drainage samples of the permeable pavements. As the loose sediment is depleted in the IWS zone, effluent concentrations from these permeable pavements would be expected to decrease.

To further test this theory, additional water quality sampling was undertaken in the spring and early summer of 2015. If low effluent concentrations continued, then the maturation period theory would be confirmed. For both the Small and Large applications, effluent TSS concentrations were markedly higher than influent during the 2015 sampling campaign. Effluent

concentrations were quite high, at 723 mg/L for the Small application and 360 and 197 mg/L for the Large application. This suggested that sediment was again being suspended within the cross-section of the pavement, and that this trend was more pronounced following winter. A possible explanation was the application of salt to the watersheds; deicing salt was applied liberally at Willoughby Hills during winter months. The application of sodium-based deicing salts increases the interaction of sodium with the clayey subsoils; this in turn augments both sodium adsorption ratio (SAR) and exchangeable sodium percentage (ESP). These chemical soil parameters are measures of the amount of sodium as a function of other cations, such as Ca^{2+}, Mg^{2+}, and K^{+}. As SAR and ESP increase, deflocculation of clay particles occurs, increasing soil dispersibility. Agassi et al. (1981) found that the impacts of rain drops cause greater dispersion under sodic soil conditions; this means that water in the IWS zone could easily re-suspend the dispersed clay subsoils. Thus, it is expected that this seasonal trend in performance for TSS and metals will continue, where performance will suffer immediately after winter due to salt application and will improve as time passes from winter.

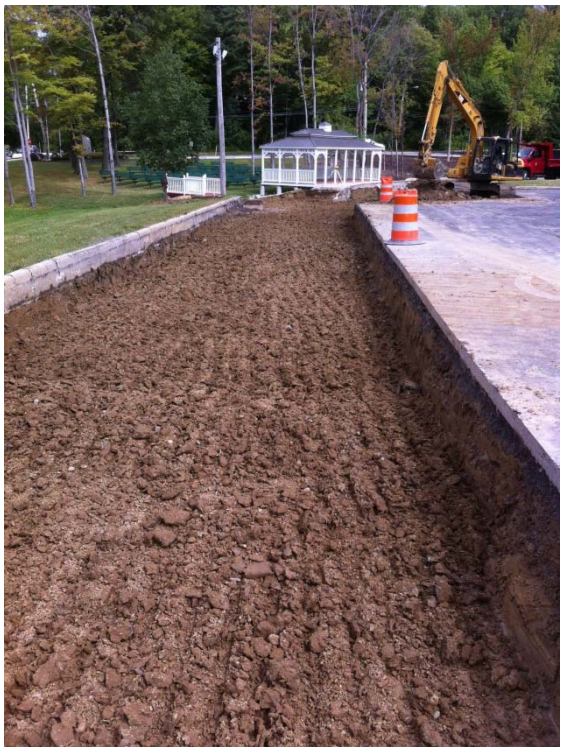

Figure 38. Raked soil at the bottom of the subgrade at Willoughby Hills.

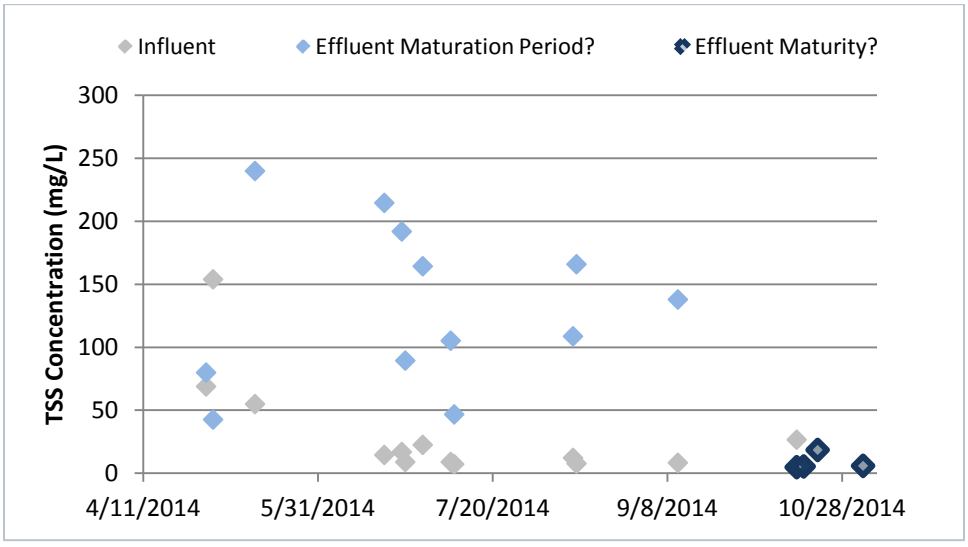

Figure 39. TSS concentrations from the Small application at Willoughby Hills showing potential maturation of the SCM. Maturity was not reached as 2015 sampling again showed elevated effluent TSS concentrations.

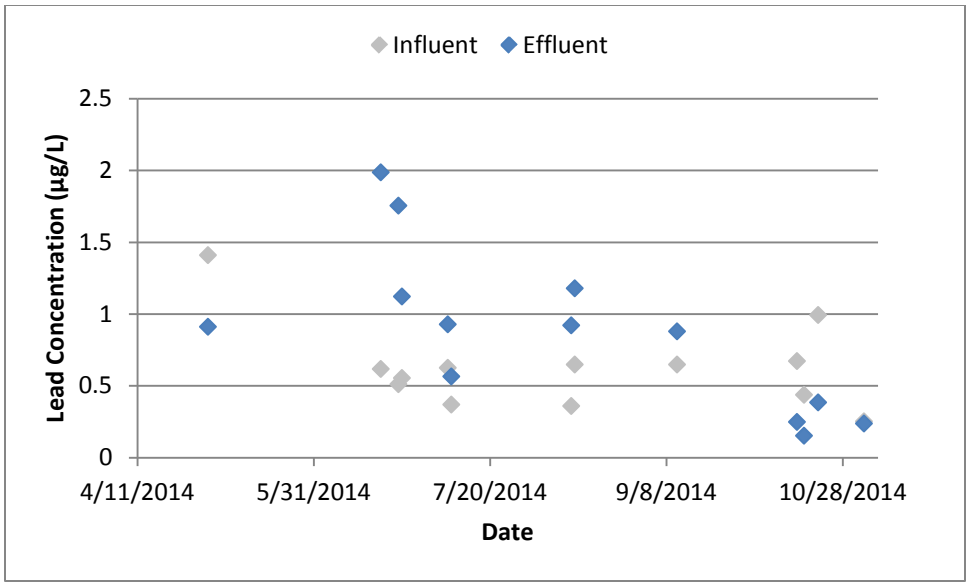

Figure 40. Lead effluent concentrations from the Small application at Willoughby Hills improve as a function of time. Maturity was not reached as 2015 sampling again showed elevated effluent metals concentrations.

Summary statistics and boxplots of chloride and metals concentrations for the Small and Large PICP applications are presented in Table 27 and Figure 41. Chloride was significantly exported from the Small application, with an ER of -3.6 (Table 26). Similar exports of Cl^- were observed in Hogland et al. (1987) and Roseen et al. (2012), while Drake et al. (2014c) suggested that permeable pavement provided mechanisms for storage and dilution of Cl^-. The Large application provided 10% (not statistically significant) lower mean drainage concentrations than that of the influent; since Cl^- is nearly impossible to remove once in the aqueous phase; dilution was suggested as the primary mechanism for this reduction (Drake et al. 2014c). Effluent concentrations of Cl^- from the Large application were significantly less than those from the Small application. Perhaps differences between the two applications can be tied to application of deicing salt in the watersheds; with more walkways present in the Small application watershed, it is plausible that higher chloride applications were undertaken in this watershed (Figure 35).

Al, Ca, and Fe were significantly exported from both the Small and Large applications, with ERs and RE_{median} less than -2.8 and -3.0, respectively. The SCMs were installed in the subsoil of Mahoning silt loam, and given the loss of TSS from these SCMs, it is likely that clay-bound Al and Fe were simultaneously lost (Hunt et al. 2008). The underlying soils are high in Fe and Al oxides due to its 35-45% clay content in the Bt horizon, corresponding with the depth of the subgrade (National Cooperative Soil Survey 2014). Ca could either be leaching from the limestone aggregate (more probable) or from the subsoil, with depth to carbonates (such as $CaCO_3$) reported as 20-42 inches in the B horizon (Kim and Park 2008; National Cooperative Soil Survey 2014). Given that the IWS zone constantly held water within both permeable pavement applications, the Ca has adequate time to leach into the stormwater inter-event. Mg, Mn, and Pb had elevated effluent concentrations when compared to influent, with significant export of Mg for the Small application and Mn and Pb for the Large application. The permeable pavements were a net-zero for Cu treatment. Mean Zn concentration was significantly reduced (by 37%) by the Small application, while the Large application provided 10% treatment (not statistically significant).

In general, metals reduction from the Willoughby Hills site was poor compared to published literature on field performance of permeable pavement (Brattebo and Booth 2003; Roseen et al. 2012; Drake et al 2014b; Drake et al 2014c). The export of sediment from the two permeable pavements following each winter of the sampling window probably led to substantial sediment-bound metals exports. This is supported by the following: the Large application, which had a 57 mg/L higher median effluent TSS concentration than the Small application, had higher median metals concentrations for every metal studied except Mg.

Table 27. Summary statistics for chloride and metals concentrations at the Willoughby Hills permeable pavement applications.

Pollutant	Location	Range (µg/L)	$\bar{X}$	$\tilde{X}$	s (µg/L)	C_s (µg/L)	CV (µg/L)	ER	RE_{median}
Cl	Inlet	1.6-128	36.8	23.96	37.4	1.63	1.02	-	-
	Sm Out	13.8-588	170.8	100.9	167.6	1.57	0.98	-3.6	-3.2
	Lg Out	3.7-91.8	33	24	27.2	1.08	0.82	0.10	0.00
Al	Inlet	29-363	126	91	98	1.72	0.78	-	-
	Sm Out	88-1585	663	701	455	0.43	0.69	-4.28	-6.70
	Lg Out	116-1442	976	1080	444	-0.88	0.46	-6.8	-10.9
Ca	Inlet	7366-31370	16588	14590	7274	0.98	0.44	-	-
	Sm Out	21080-231600	63225	52730	51476	2.77	0.81	-2.8	-2.6
	Lg Out	14850-122700	66570	54220	34048	0.38	0.51	-3.0	-2.7
Cu	Inlet	1.4-11.8	4.56	3.75	2.80	1.62	0.62	-	-
	Sm Out	1.7-10.4	4.36	4.39	2.35	1.15	0.54	0.04	-0.17
	Lg Out	1.9-9.6	5.28	5.40	2.31	0.30	0.44	-0.16	-0.44
Fe	Inlet	91-658	204	164	154	2.25	0.75	-	-
	Sm Out	116-3210	926	740	847	1.62	0.92	-3.54	-3.50
	Lg Out	235-2506	1486	1538	721	-0.28	0.48	-6.3	-8.4
Mg	Inlet	856-3289	1786	1484	773	1.16	0.43	-	-
	Sm Out	1951-8318	3635	3396	1536	2.16	0.42	-1.04	-1.29
	Lg Out	787-5403	2970	2500	1541	0.52	0.52	-0.66	-0.7
Mn	Inlet	6-76	21	9	19	1.84	0.91	-	-
	Sm Out	2.2-79.8	21	18	19	2.26	0.92	-0.01	-0.92
	Lg Out	14.2-79.6	35	27	20	1.35	0.57	-0.68	-1.83
Pb	Inlet	0.25-1.9	0.69	0.62	0.42	1.99	0.61	-	-
	Sm Out	0.15-4.6	1.09	0.91	1.10	2.49	1.01	-0.57	-0.48
	Lg Out	0.62-3.5	1.86	1.51	0.99	0.56	0.53	-1.69	-1.44
Zn	Inlet	12.6-50.3	23	21	10	1.68	0.42	-	-
	Sm Out	5.8-37.3	15	13	8	1.73	0.54	0.37	0.36
	Lg Out	13.5-34.8	21	16	8	0.87	0.38	0.10	0.20

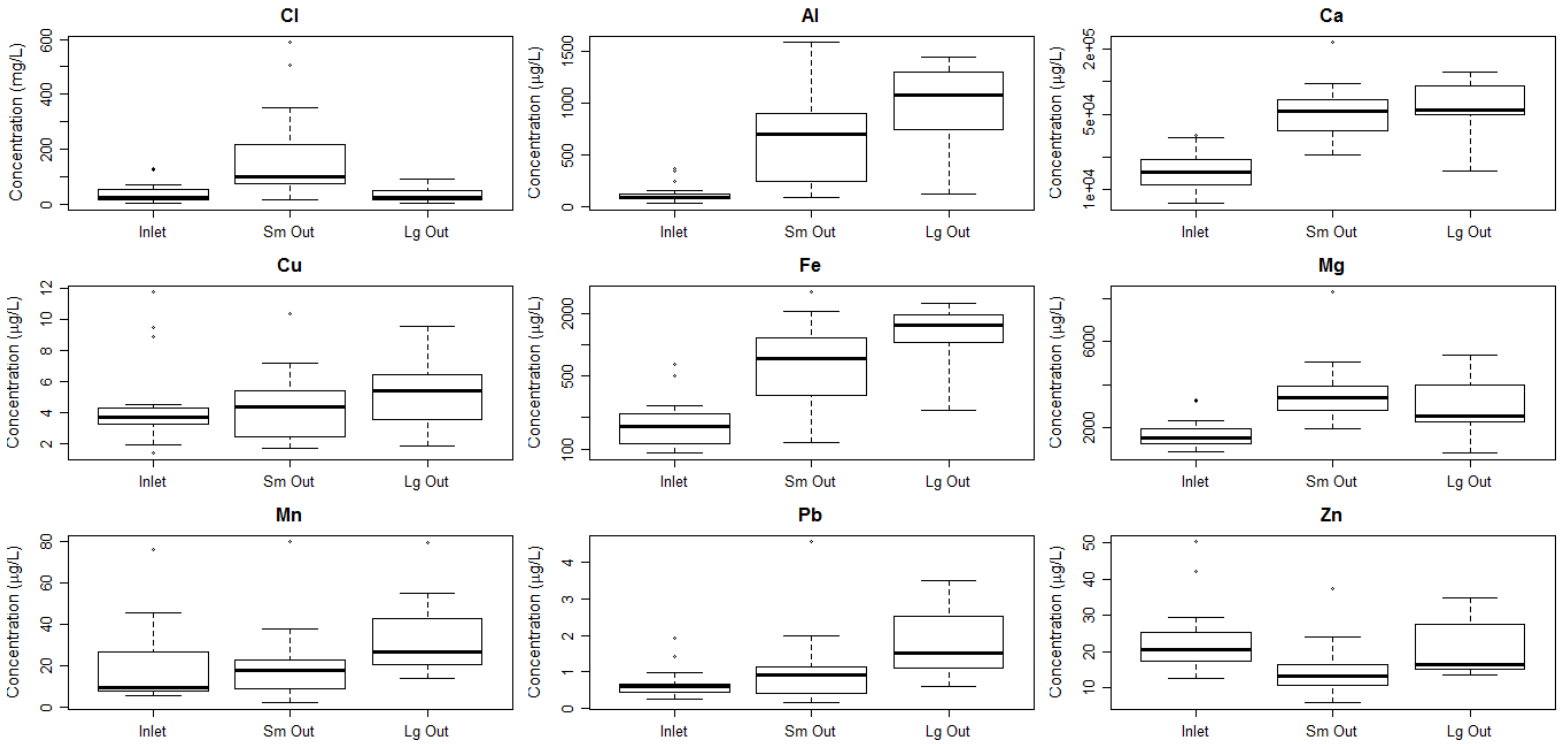

Figure 41. Boxplots of chloride and metals concentrations at the asphalt (inlet), Small application outlet (Sm Out), and Large application outlet (Lg Out) monitoring locations at Willoughby Hills.

3.4.3 Pollutant Loads

Pollutant loads for each of the 15, 17, 17, and 18 storm events sampled for metals, chloride, nutrients, and TSS, respectively, were calculated as the product of stormwater volume and concentration at the inlet and drainage monitoring location for both permeable pavements. A substantial volume of surface runoff (24% of the water balance) occurred for the Large application; no pollutant attenuation was assumed for the surface runoff fraction. The storm event loads were summed for each monitoring location and normalized by watershed area. The pollutant loads presented in Table 28 are representative of the 13.97 inches of rainfall, 14.68 inches, 14.57 inches, and 15.05 inches of rainfall sampled for metals, chloride, nutrients, and sediment, respectively. Table 29 summarizes statistical testing to determine significant differences between inlet and outlet loads for each permeable pavement application. Differences

in watershed area normalized effluent loads were also evaluated, since these are the values that would be used in TMDL calculations.

Of the 77 storms at Willoughby Hills, only 3 were completely captured (i.e. no outflow from the underdrain) within the Small application, all of which were smaller than 0.13 inches in depth. For the Large application, 30 events were completely captured, with a maximum rainfall depth of 0.42 inches. Cumulative volume reductions over the monitoring period for the Small and Large applications were 16 and 32%, respectively. These volume reductions factored into the loading calculations, as 6 sampled storms were completely captured by the Large application, while the Small application had outflow for all 18 sampled events. Of sampled storms, 33% were completely captured in the Large application, fairly representative of the 39% of overall events completely captured.

Chloride load increased by 54% (non-significant) as stormwater passed through the Small permeable pavement application, but decreased significantly by 53% in the Large application. This was attributed mainly to infiltration, though a 10% decrease in Cl^- concentration was observed in the Large application. It should be noted that Cl^- is recalcitrant in the environment, and was probably transferred to groundwater through exfiltration, rather than sequestered within the SCM. TKN and ON were significantly reduced in both permeable pavements, with greater load reduction for the Large application (56 and 61%) versus the Small application (42 and 41%), respectively. This suggested trapping of particulate nitrogen at the surface of the permeable pavement, functioning similarly to a sand filter, as suggested by Collins et al. (2010). Dissolved $NO_{2\text{-}3}$ loading was significantly reduced by 42% in the Large application, and increased by 23% for the Small application (not statistically significant); this was directly related to the additional volumetric reduction in the Large application. $NO_{2\text{-}3}$ is likely being exported to

groundwater from this SCM due to exfiltration. Similarly mixed results for NO_{2-3} loading were observed in Collins et al. (2010) and Drake et al. (2014b). TN was significantly reduced by 52% by the Large application, while the Small application provided 23% reduction (not significantly different from zero), showing the importance of HLR for permeable pavement performance.

Dissolved, particle-bound, and total P loads were reduced between 22 and 40% by the Large application, and it always providing superior or similar performance than the Small application (range of 1-30% for the same pollutants). TSS mass increased by 525% and 329% due to the aforementioned loss of sediment from the permeable pavement subgrade for the Small and Large applications, respectively; however, neither of these were statistically different from zero. Five and eight out of 18 storms for the Small and Large applications, respectively, had lower effluent load than influent load. Ten-fold export of TSS mass during five storms for both the Small and Large applications resulted in the observed export of TSS. The lower export of TSS from the Large application is related to the greater fraction of surface runoff, which could not entrain sediment from the permeable pavement subgrade.

These results suggested that larger HLR for permeable pavements located over clay soils generally provides reduced mitigation of pollutants. It should be noted, however, the Small application often provided greater than half the load reduction of the Large application, even though the HLR of the Small application was more than twice that of the Large application. Similar results have been shown for undersized bioretention cells in Luell et al. (2011), where a half-sized bioretention cell provided more than half the load reduction of the full sized cell. This is due to treatment and infiltration of stormwater for the more frequent, small storms by undersized SCMs. However, surface clogging of heavily-loaded permeable pavements must be

considered in design, as this increases the onerousness and frequency of maintenance to prevent surface runoff.

Loads of Al, Ca, Fe, and Pb increased as stormwater moved through both the Small and Large permeable pavement applications (Table 28). Al, Ca, and Fe concentrations increased more than two-fold. Al (significant for both applications) and Ca (significant for Small application only) leaching was statistically significant and perhaps related to the aggregate or to the red clay subsoil being leached as part of the aforementioned TSS export, subsequently leaching particulate bound Al, Ca, and Fe. The Small application had lower normalized effluent loads of Al, Fe, and Zn which was due to the lower hydraulic retention time (and therefore less contact time with the subsoil) due to the higher HLR when compared to the Large application. All other pollutants studied had effluent loads that were either not significantly different between the two applications, or the Large application had the statistically lower effluent load. Because HLR was the factor that most affected the percentage of water exfiltrated (given similar soils between the two applications), this result was logical. Increases in Pb load (not statistically significant) through a permeable pavement have not been observed previously in the literature (Legret et al. 1996; Gilbert and Clausen 2006; Drake et al 2014c), and may be related to the export of TSS from these SCMs.

Copper load was reduced by 13% for the Small application, but this was not statistically different from zero. The Large application significantly reduced Cu loads by 30%, well below load reductions in other field research on permeable pavements (Bean et al. 2007; Drake et al. 2014b; Drake et al. 2014c). Magnesium was slightly exported by the Small application, but the Large application reduced Mg loads by 16%, neither of which were statistically significant. Statistically significant Zn load reduction was observed for both the Small (37%) and Large

(53%) applications. Zn load reductions in past studies on permeable pavement have been greater than 70% (Legret et al. 1996; Bean et al. 2007; Drake et al. 2014b).

Table 28. Pollutant loads normalized by watershed area for metals, nutrients, and sediment for the permeable pavement applications at Willoughby Hills.

Monitoring Location	Pollutant Loads (g/ha)									
	Al	Ca	Cu	Fe	Mg	Mn	Pb		Zn	
Small Inlet	316	41122	10	469	5031	41	1.6		50	
Small Outlet	1462	134492	9	2192	6669	48	2.5		32	
Large Inlet	478	62140	16	729	7439	65	2.5		190	
Large Outlet	1839	123900	11	2801	6224	68	3.6		90	
% Reduction Small	-363	-227	13	-367	-33	-16	-55		37	
% Reduction Large	-285	-99	30	-284	16	-4	-47		53	
Monitoring Location	Pollutant Loads (kg/ha)									
	Cl	TKN	NO_{2-3}	TN	TAN	ON	TP	OP	PBP	TSS
Small Inlet	135	2.59	1.12	3.71	0.61	1.98	0.11	0.05	0.09	51
Small Outlet	208	1.49	1.37	2.86	0.33	1.16	0.08	0.05	0.08	320
Large Inlet	190	3.63	1.61	5.24	0.85	2.78	0.17	0.07	0.14	76
Large Outlet	90	1.60	0.93	2.53	0.51	1.09	0.10	0.06	0.10	325
% Reduction Small	-54	42	-23	23	46	41	30	1	14	-525
% Reduction Large	53	56	42	52	40	61	40	22	33	-329

Table 29. Summary of statistical testing for normalized pollutant loads at Willoughby Hills.

Parameter	Location	Pollutant																	
		Cl	Al	Ca	Cu	Fe	Mg	Mn	Pb	Zn	TKN	NO_{2-3}	TN	TAN	ON	TP	OP	PBP	TSS
Statistical Test	Small	WRS	t	WRS	t	t	WRS	t	WRS	WRS	WRS	WRS	WRS	WRS	WRS	t	WRS	WRS	t
p-value		0.30	**	**	0.40	**	0.41	0.31	0.54	**	**	0.16	0.12	0.52	***	0.06	0.08	0.07	0.06
Statistically Significant?		No	Yes	Yes	No	Yes	No	No	No	Yes	Yes	No	No	No	Yes	No	No	No	No
Statistical Test	Large	WRS	WRS	WRS	WRS	WRS	WRS	WRS	WRS	WRS	WRS	WRS	WRS	WRS	WRS	WRS	WRS	WRS	WRS
p-value		*	*	0.08	**	*	0.34	0.54	0.24	***	***	**	***	0.42	***	**	**	*	0.09
Statistically Significant?		Yes	Yes	No	Yes	Yes	No	No	No	Yes	Yes	Yes	Yes	No	Yes	Yes	Yes	Yes	No
Statistical Test	Large vs. Small	WRS	WRS	WRS	WRS	WRS	WRS	WRS	WRS	WRS	WRS	WRS	WRS	WRS	WRS	WRS	WRS	WRS	WRS
p-value		*	*	0.08	**	*	0.34	0.54	0.31	***	0.44	**	***	0.41	***	**	0.10	*	0.09
Statistically Significant?		Yes	Yes	No	Yes	Yes	No	No	No	Yes	No	Yes	Yes	No	Yes	Yes	No	Yes	No
Lower Norm Eff Load		Large	Large	N/A	Small	Small	N/A	N/A	N/A	Small	N/A	Large	Large	N/A	Large	Large	N/A	Large	N/A

*significant at α=0.05, ** significant at α=0.01, *** significant at α=0.001
Yes = significant export, Yes = significant reduction
WRS = Wilcoxon signed rank test
t = student's t-test

3.5 Summary and Conclusions

Two PICP retrofits were installed to treat runoff from an impermeable asphalt parking lot at the Willoughby Hills community center in northeast Ohio. Both permeable pavements were situated over HSG D soils, employed IWS zones, and treated runoff from parking lots 2.2 (Large application) and 7.2 (Small application) times their surface areas. Stormwater samples were obtained from three locations: the impervious asphalt (representative of run-on to the permeable pavement) and from the underdrains of both the Large and Small application. Based on laboratory testing of the samples for pollutant concentrations and subsequent calculation of pollutant loads, the following conclusions can be drawn from this study:

1) The concentration of TSS significantly increased through the permeable pavements, a finding that has not been reported in the literature to-date. While trapping of TSS may have occurred in the interstitial spaces of the PICP, loss of sediment from the subgrade far outweighed any filtration by the pavement course. Subsequent significant increases in certain metals concentrations suggested loss of particulate-bound metals as stormwater moved through the permeable pavement cross-section and came in contact with the clay subsoil. This could be related to the raking of the subgrade *in situ* soil performed during construction to reduce compaction and promote exfiltration. Initially, it was thought that a maturation period might have existed for TSS, where loose sediment from the subgrade was contributed to the runoff as it passed through the permeable pavement cross-section. However, further sampling in spring and summer 2015 showed that the export of TSS may be related to the effects of deicing salts, which tend to deflocculate clays, on the subgrade soils. This would allow sediment to be entrained in the runoff as it passed through the permeable pavement SCM.

2) For most nutrient concentrations, the permeable pavements were a net zero, neither aiding nor impairing nutrient removal. No significant reductions in nutrient forms were observed for N and P species, though NO_{2-3} concentrations significantly increased from the Small permeable pavement application. While not statistically significant, ERs for the Large application were between 20-40% for TKN, TN, ON, OP, PBP, and TP.

3) Six storms were completely captured by the Large application, while the Small application had outflow for each storm event sampled. This aided the Large application in having lower or equivalent watershed area-normalized effluent load than the Small application for all but Al and Fe. Nitrogen loads were generally reduced by upwards of 30% for the Small application, with the notable exception of a not-statistically-significant export of 24% of NO_{2-3} for the Small application. Both TKN and ON loads were reduced significantly, suggesting trapping of particulate nitrogen at the pavement surface. The Large application reduced nitrogen loads by greater than 40%, showing the benefit of additional exfiltration resulting from the lower HLR. Load reductions were more often significant for the Large application, with NO_{2-3}, TN, TP, and PBP loads reduced significantly, in addition to those pollutants reduced significantly for the Small application. Export of TSS was 525% and 329% by mass for the Small and Large applications over the monitoring window, neither of which was statistically significant. Export of sediment was related to proximity to winter and therefore salt application.

4) In terms of pollutant loading, Al, Ca, and Fe mass significantly increased as stormwater moved through the permeable pavement, suggesting (1) leaching of Ca from the limestone aggregate used to structurally support the PICP and (2) loss of Al and Fe from the clay subsoils, comprising some fraction of the TSS that washed out of the permeable pavements. Cu was significantly reduced (30% reduction) by the Large application, and Zn was significantly

sequestered by both the Small and Large applications, with 37 and 53% reduction, respectively. Chloride load reduction was significant for the Large permeable pavement application, but it was suggested this was probably lost mostly to exfiltration, where chloride would remain in the groundwater.

5) Results show the importance of HLR for permeable pavements, with generally greater pollutant retention at lower HLR. That said, the Small application did perform at least half as well as the Large application for loads of all nutrient forms (when the HLR was greater than 2 times that of the Large application), suggesting that undersized SCMs perform proportionately better than larger systems. However, at an HLR of 8.2, blinding of the pavement surface of the Small application is expected to occur much more quickly than for the Large application, with an HLR of 3.2.

3.6 References

American Public Health Association (APHA), American Water Works Association (AWWA), and Water Environment Federation (WEF). (2012). *Standard methods for the examination of water and wastewater*, Ed. Laura Bridgewater. 22nd ed., Washington, DC.

Antweiler, R.C., and Taylor, H.E. (2008). "Evaluation of statistical treatments of left-censored environmental data using coincident uncensored data sets: 1. Summary statistics." *Environmental Science and Technology*. 42(10), 3732‑3738.

Arnold Jr, C.L., and Gibbons, C.J. (1996). "Impervious surface coverage: the emergence of a key environmental indicator." *Journal of the American Planning Association*. 62(2), 243-258.

Bannerman, R.T., Owens, D.W., Dodds, R.B., and Hornewer, N.J. (1993). "Sources of pollutants in Wisconsin stormwater." *Water Science and Technology*. 28(3), 241-259.

Bean, E.Z., Hunt, W.F., and Bidelspach, D.A. (2007). "Evaluation of four permeable pavement sites in eastern North Carolina for runoff reduction and water quality impacts." *Journal of Irrigation and Drainage Engineering*. 133(6), 583-592

Ben-Joseph, E., (2012). *ReThinking a Lot: the Design and Culture of Parking*. MIT Press, Cambridge, Massachusetts, USA.

Borst, M., and Brown, R. A. (2014). "Chloride released from three permeable pavement surfaces after winter salt application." *Journal of the American Water Resources Association*. 50(1), 29-41.

Boving, T., Stolt, M., and Augenstern, J. (2004). "Investigation of the University of Rhode Island, Kingston, RI, porous pavement parking lot and its impact on subsurface water quality." *Proceedings of the 33 Annual Meeting, Int. Association of Hydrologists,* Zacatecas, Mexico.

Brattebo, B.O., and Booth, D.B. (2003). "Long-term stormwater quantity and quality performance of permeable pavement systems." *Water Research*. 37(18), 4369-4376.

Collins, K.A., Hunt, W.F., and Hathaway, J.M. (2008). "Hydrologic comparison of four types of permeable pavement and standard asphalt in eastern North Carolina." *Journal of Hydrologic Engineering*. 13(12), 1146-1157.

Collins, K. A., Hunt, W. F., and Hathaway, J. M. (2010). "Side-by-side comparison of nitrogen species removal for four types of permeable pavement and standard asphalt in eastern North Carolina." *Journal of Hydrologic Engineering*. 15(6), 512-521.

DeBusk, K. M., Hunt, W.F., and Line, D.E. (2010). "Bioretention outflow: Does it mimic nonurban watershed shallow interflow?" *Journal of Hydrologic Engineering*. 16(3), 274-279.

Dietz, M.E. (2007). "Low impact development practices: A review of current research and recommendations for future directions." *Water, Air, and Soil Pollution*. 186(1-4), 351-363.

Drake, J., Bradford, A., and Van Seters, T. (2014a). “Hydrologic performance of three partial-infiltration permeable pavements in a cold climate over low permeability soil.” *Journal of Hydrologic Engineering*. 19(9), 04014016.

Drake, J., Bradford, A., and Van Seters, T. (2014b). “Stormwater quality of spring–summer-fall effluent from three partial-infiltration permeable pavement systems and conventional asphalt pavement.” *Journal of Environmental Management*. 139, 69-79.

Drake, J., Bradford, A., and Van Seters, T. (2014c). “Winter effluent quality from partial-infiltration permeable pavement systems.” *Journal of Environmental Engineering*, 140(11), 04014036.

Fassman, E.A., and Blackbourn, S. (2010). “Urban runoff mitigation by a permeable pavement system over impermeable soils.” *Journal of Hydrologic Engineering*. 15(6), 475-485.

Fay, L., and Shi, X. (2012). “Environmental impacts of chemicals for snow and ice control: State of the knowledge.” *Water Air and Soil Pollution.* 223(5), 2751–2770.

Franks, C.A., Davis, A.P., and Aydilek, A.H. (2014). “Effects of runoff characteristics and filter type on geotextile storm water treatment.” *Journal of Irrigation and Drainage Engineering*. 140(2), 04013014.

Gilbert, J. K., and Clausen, J. C. (2006). “Stormwater runoff quality and quantity from asphalt, paver, and crushed stone driveways in Connecticut.” *Water Research*. *40*(4), 826-832.

Hogland, W., Niemczynowicz, J., and Wajlman, T. (1987). “The unit superstructure during the construction period.” *The Science of the Total Environment*. 59, 411–424.

Hunt, W.F., Smith, J.T., Jadlocki, S.J., Hathaway, J.M., and Eubanks, P.R. (2008). “Pollutant removal and peak flow mitigation by a bioretention cell in urban Charlotte, NC.” *Journal of Environmental Engineering*. 134(5), 403-408.

Hunt, W.F., Davis, A.P., and Traver, R.G. (2012). “Meeting hydrologic and water quality goals through targeted bioretention design.” *Journal of Environmental Engineering*. 138(6), 698-707.

Kim, H., Seagren, E.A., and Davis, A.P. (2003). “Engineered bioretention for removal of nitrate from stormwater runoff.” *Water Environment Research*. 75(4), 355-367.

Kim, H.S., and Park, J. (2008). “Effects of limestone on the dissolution of phosphate from sediments under anaerobic condition.” *Environmental technology*. 29(4), 375-380.

Knowles, R. (1982). “Denitrification.” *Microbiological reviews.* 46(1), 43-70.

Legret, M., Colandini, V., and LeMarc, C. (1996). “Effects of a porous pavement with reservoir structure on the quality of runoff water and soil.” *The Science of the Total Environment.* 190, 335–340.

Li, H., Sharkey, L.J., Hunt, W.F., and Davis, A.P. (2009). “Mitigation of impervious surface hydrology using bioretention in North Carolina and Maryland.” *Journal of Hydrologic Engineering*. 14(4), 407-415.

Luell, S.K., Hunt, W.F., and Winston, R.J. (2011). “Evaluation of undersized bioretention stormwater control measures for treatment of highway bridge deck runoff.” *Water Science and Technology*. 64(4), 974-979.

Morse, C.C., Huryn, A.D., and Cronan, C. (2003). “Impervious surface area as a predictor of the effects of urbanization on stream insect communities in Maine, USA.” *Environmental Monitoring and Assessment*. 89(1), 95-127.

National Cooperative Soil Survey, United States Department of Agriculture. (2014). *Mahoning soil series description*. Rev. AR-DMc-RAR. Available: https://soilseries.sc.egov.usda.gov/OSD_Docs/M/MAHONING.html

Ohio Department of Natural Resources (ODNR), Division of Soil and Water Conservation. (2006). *Rainwater and land development: Ohio’s standards for stormwater management, low impact development, and urban stream protection*. 3rd edition. Ed: John Mathews.

Pezzaniti, D., Beecham, S., and Kandasamy, J. (2009). “Influence of clogging on the effective life of permeable pavements.” *Proceedings of the ICE-Water Management*. 162(3), 211-220.

R Core Team. (2014). *A language and environment for statistical computing*. R Foundation for Statistical Computing. Vienna, Austria.

Roseen, R.M., Ballestero, T.P., Houle, J.J., Briggs, J.F., and Houle, K.M. (2012). “Water quality and hydrologic performance of a porous asphalt pavement as a storm-water treatment strategy in a cold climate.” *Journal of Environmental Engineering*. 138(1), 81-89.

Roseen, R. M., Ballestero, T.P., Houle, K.M., Heath, D., and Houle, J.J. (2014). “Assessment of winter maintenance of porous asphalt and its function for chloride source control.” *Journal of Transportation Engineering.* 140(2), 04013007.

Schueler, T.R., Fraley-McNeal, L., and Cappiella, K. (2009). “Is impervious cover still important? Review of recent research.” *Journal of Hydrologic Engineering*.14(4), 309-315.

Smith, V.H., Tilman, G.D., and Nekola, J.C. (1999). “Eutrophication: impacts of excess nutrient inputs on freshwater, marine, and terrestrial ecosystems.” *Environmental Pollution*. 100(1), 179-196.

Soil Survey Staff, Natural Resources Conservation Service, United States Department of Agriculture. (2015). Web Soil Survey. http://websoilsurvey.nrcs.usda.gov/. Accessed 28 January 2015.

Strecker, E.W., Quigley, M.M., Urbonas, B.R., Jones, J.E., and Clary, J.K. (2001). “Determining urban storm water BMP effectiveness.” *Journal of Water Resources Planning and Management*. 127(3), 144-149.

Tota-Maharaj, K., and Scholz, M. (2010). “Efficiency of permeable pavement systems for the removal of urban runoff pollutants under varying environmental conditions.” *Environmental Progress and Sustainable Energy*. 29, 358-369.

United Nations, Department of Economic and Social Affairs, Population Division. (2014). *World Urbanization Prospects: The 2014 revision, highlights*. ST/ESA/SER.A/352.

U.S. Environmental Protection Agency (U.S. EPA). (1983). *Methods of chemical analysis of water and waste*. EPA-600/4-79-020, Cincinnati, Ohio.

United States Environmental Protection Agency (U.S. EPA). (1988). “Ambient water quality criteria for chloride-1988.” EPA 440/5-88-001, Office of Water Regulations and Standards, Criteria and Standards Division, Washington, DC.

U.S. EPA. (2002). *Urban storm water BMP performance monitoring: a guidance manual for meeting the national storm water BMP database requirements*. EPA-821-B- 02-001. U.S. Environmental Protection Agency, Washington, DC.

Van Haandel, A.C., and Van der Lubbe, J.G.M. (2012). *Handbook of biological wastewater treatment: design and optimisation of activated sludge systems*. 2nd ed. IWA Publishing, London, UK.

Wardynski, B.J., Winston, R.J., and Hunt, W.F. (2012). “Internal water storage enhances exfiltration and thermal load reduction from permeable pavement in the North Carolina mountains.” *Journal of Environmental Engineering*. 139(2), 187-195.

Wolman, M.G. (1967). “A cycle of sedimentation and erosion in urban river channels.” *Geografiska Annaler. Series A. Physical Geography*. 385-395.

4 PERFORMANCE OF PERMEABLE PAVEMENT AS PRETREATMENT TO AN UNDERGROUND CISTERN AT OLD WOMAN CREEK NATIONAL ESTUARINE RESEARCH RESERVE

4.1 Review of Literature

Urbanization transforms open space into hardened infrastructure, including residential, commercial, and industrial land uses. It modifies the characteristics of the watershed, reducing or eliminating the A horizon of the soil, changing topography through mass grading, diminishing vegetative cover, canopy interception, and evapotranspiration, and introducing impervious cover (Palhegyi 2009). These changes intensify stream bank erosion and channel incision, reduce baseflow, and impact in-stream biota (Bledsoe and Watson 2001; Walsh et al. 2005; White and Greer 2006). The increase in stormwater runoff volume exacerbates nutrient, sediment, bacteria, heavy metal, and chloride pollutant loads, all of which pose threats to surface water quality (Bannerman et al. 1993; Davis et al. 2001; Diaz 2001; Taebi and Droste 2004).

To combat the deleterious effects of hydromodification and impacts of heightened pollutant loading, engineers implement stormwater controls measures (SCMs). SCMs may be targeted at small watersheds and frequent storm events (Low Impact Development [LID] philosophy; Rushton 2001; Wilson et al. 2015) or may aim to treat large watersheds and infrequent return interval events (wet and dry ponds; Emerson et al. 2005). Two commonly implemented LID stormwater controls are permeable pavement, which allows water to soak through rather than runoff the pavement surface, and water harvesting, which provides water for beneficial use on-site (Brattebo and Booth 2003; Jones and Hunt 2010). Increasingly, stormwater controls are being placed in series using a “treatment train” approach to further benefit urban hydrology and water quality.

Permeable pavement consists of a permeable surface course of concrete, asphalt, or interlocking concrete pavers that allows water to infiltrate the pavement surface. Beneath the surface course are layers of aggregate which provide both structural support and void space for stormwater storage. Permeable pavements have been shown to substantially reduce flow volumes and peak flow rates when treating direct rainfall, even over relatively impermeable soils (Bean et al. 2007; Collins et al. 2008; Ball and Rankin, 2009; Fassman and Blackbourn 2010; Roseen et al. 2012; Wardysnki et al. 2012; Drake et al. 2014a). Additionally, permeable pavements remove particulate and particulate-bound pollutants effectively, including heavy metals. This occurs through filtration of the stormwater as it passes through the surface course and sedimentation within the underlying aggregate (Legret et al. 1996; Bean et al. 2007; Roseen et al. 2012; Drake et al. 2014b). Wardynski et al. (2012) illustrated that an upturned elbow in the underdrain, which creates an internal water storage (IWS) zone within the aggregate, can substantially improve exfiltration. Therefore, permeable pavements may provide a first level of water quality and hydrologic mitigation within a treatment train approach.

Rainwater harvesting as a stormwater control involves rooftop runoff being directed to a tank for storage and reuse during inter-event periods. In ancient and present times, these systems have been used for water supply in arid and semi-arid climates (Radhakrishna 2003; Abdulla and Al-Shareef 2009). Recent droughts across the U.S. have sparked interest in rainwater harvesting in humid regions; however, recent research by Jones and Hunt (2010) and DeBusk et al. (2013) showed that small-scale rainwater harvesting systems are intermittently and inconsistently used unless a dedicated, reliable (all year), and automated use is provided. DeBusk and Hunt (2014) found stormwater quality benefits within rainwater harvesting systems, with significant reductions in both N and P species within the tanks; others have also found improvements in

water quality due to settling and chemical processes within the tank (Despins et al. 2009; Sung et al. 2010). Given the desire to reduce potable water costs, it seems permeable pavement followed by an underground cistern could prove to be a useful treatment train. Until recently, this type of stormwater harvesting for non-potable uses had not been considered as a viable option, because parking lot runoff was viewed as too "dirty" for beneficial use (McArdle et al. 2011; Wilson et al. 2014; Nnadi et al. 2015). Gomez-Ullate et al. (2011) presented the idea of reusing permeable pavement exfiltrate as a resource for non-potable water supply. However, no research studies have been carried out to-date on these two SCMs in series.

Recently, the literature has burgeoned with studies on treatment trains, with co-benefits of two SCMs with different hydrologic benefits and pollutant removal mechanisms being greater than the sum of their parts (Brown et al. 2011; Winston et al. 2012; Wilson et al. 2015). This is not the case, however, if the same SCM or SCMs with similar pollutant removal mechanisms are used in the treatment train (Hathaway and Hunt 2010).

The goal of this study was to evaluate the hydrologic and water quality performance of a permeable pavement and underground water harvesting system treatment train. The permeable pavement was utilized as a pretreatment for the cistern, with cistern water used for landscape irrigation and vehicle washing. The amount of inflow, drainage from the permeable pavement, storage in the cistern, and overflow from the treatment train were monitored from mid-July to early December 2014. Additionally, water quality samples were obtained and analyzed for nutrients, sediment, metals, and chloride retention.

4.2 Site Description

A permeable interlocking concrete paver (PICP) parking lot underlain by two interconnected concrete vault cisterns was installed in June and July 2014 at the Old Woman Creek National Estuarine Research Reserve (NERR) visitor center parking lot located near Huron, Ohio (Figure 42 and Figure 43). The cisterns were each three feet tall, 8 feet wide, and 16 feet in length. The six inch concrete wall thickness resulted in 210 cubic feet of storage within each cistern, or 3140 gallons in total (Table 30). The two cisterns were hydraulically connected with three booted 4-in PVC pipes. They were fitted with concrete tops (Figure 42) and eccentric cone manways to allow access from the surface for maintenance purposes. The cisterns were covered with 1.5 feet of clay soil, which was compacted to 95% Proctor compaction. The aggregate layers for the PICP extended across the top of this compacted clay. A Hobo U20 pressure transducer measured water level within the cisterns as a function of time, so that outflow, including withdrawals from the spigot for irrigation and car washing, and inflows (stormwater runoff passed through the permeable pavement system) could be determined.

Pretreatment for the cistern was provided by a PICP system, with a 2900 ft^2 surface area (Figure 42 and Table 30). The adjacent asphalt parking lot watershed was 0.115 acres (5014 ft^2). The impervious cisterns reduced the effective infiltrative surface area to 2650 ft^2. The hydrologic loading ratio (HLR), or the ratio of the contributing watershed area to the infiltrative surface area of the SCM, was 3.0. From the bottom to top of the cross-section, the permeable pavement aggregate layers included 18-22 inches of #4 stone, 4 inches of #57 stone, and 2 inches of #89 stone. Aggregate was placed in 6-in lifts and compacted with a 10 ton roller, with the pavers installed on the surface of the #89 stone. Two water table wells were installed to measure water depth within the aggregate as a function of time (Figure 43); Hobo U20 pressure

transducers were used to record water levels. The underdrain for the permeable pavement was a 6-in diameter perforated PVC pipe elevated 3 inches above the bottom of the cross-section, creating an IWS zone. The underdrain was tied into a catch basin located outside the boundaries of the permeable pavement, where drainage was measured in a weir box. Flow then entered the cisterns until they were full, at which point overflow would occur, measured using a weir and pressure transducer (Hobo U20; Figure 43).

The Old Woman Creek NERR site was located over poorly draining hydrologic soil group (HSG) D soils (Del Ray, silty clay soil texture at the excavated depth) according to the soil survey (Soil Survey Staff 2015).

Figure 42. Permeable interlocking concrete pavers (PICP) with standard asphalt watershed (left) and underground cisterns located beneath PICP (right) at Old Woman Creek NERR.

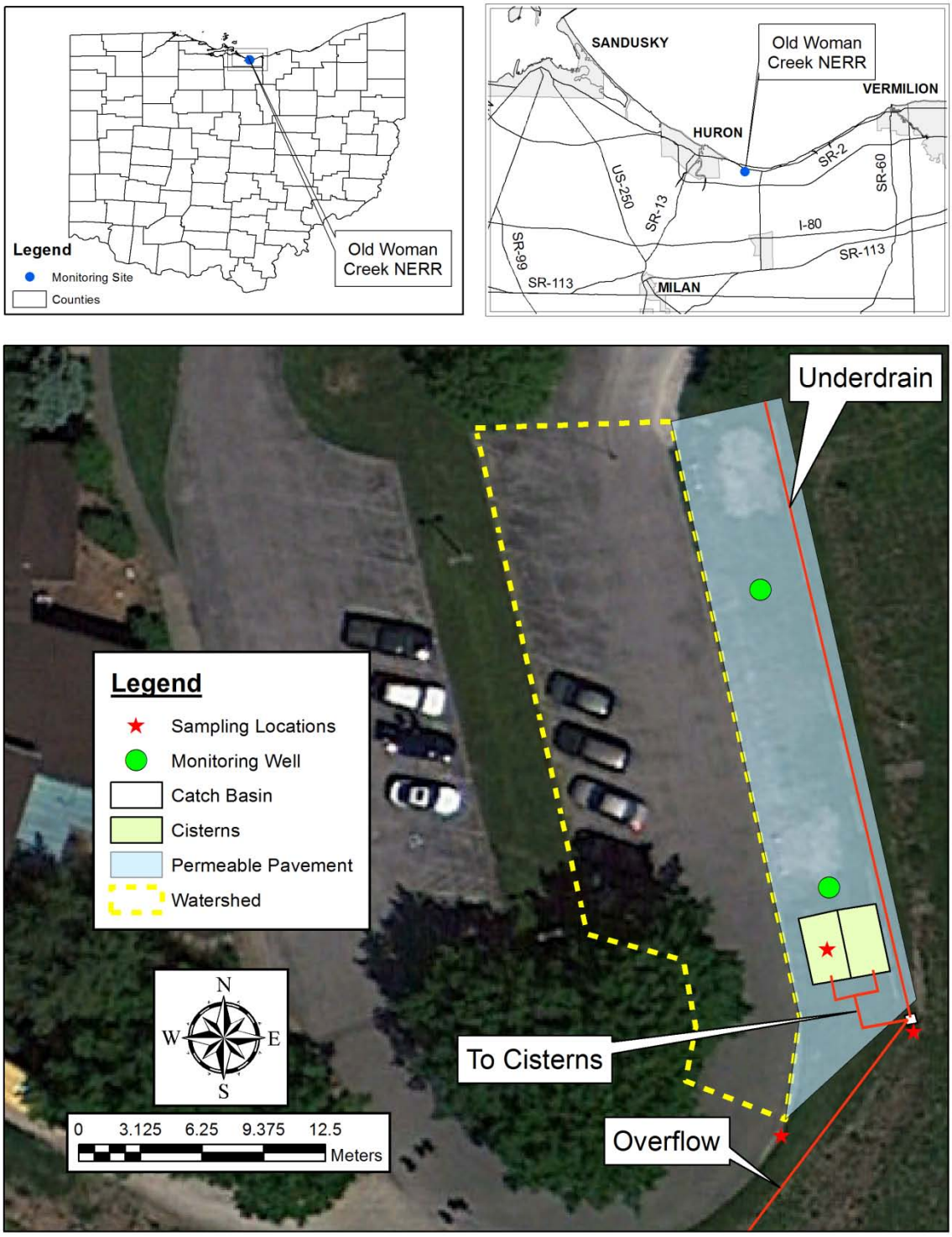

Figure 43. Old Woman Creek NERR site aerial view and location within Ohio.

Table 30. Characteristics of the Old Woman Creek NERR permeable pavement and cistern treatment train.

Surface Course	Total Aggregate Depth (in)	Contributing Watershed Area (ac)	Permeable Pavement Surface Area (ft^2)	Infiltrative Surface Area (ft^2)	Hydrologic Loading Ratio (HLR)	Internal Water Storage Zone Depth (inches)	Cistern Volume (ft^3)
PICP	24-28	0.115	2900	2650	3.0	3	420

4.3 Materials and Methods

4.3.1 Data Collection

Water quality samples were obtained from three locations at the Old Woman Creek NERR site: a control, impervious asphalt location (representative of the inflow to the permeable pavement), from the underdrain of the permeable pavement, and from the spigot which collected water from a submersible pump in the cistern (Figure 43). A sampling trough was installed at the edge of the asphalt parking lot to obtain samples from a representative small catchment, with a small notch cut into the adjacent concrete to direct flow into the sampling trough (Figure 44). Influent samples were paced based on rainfall depth, a direct indicator of runoff volume (Chin 2006). An ISCO 6712 sampler was utilized to obtain a 200 mL sample aliquot from the sampling trough after each 0.05 inches of rainfall, thus obtaining flow proportional, composite samples (Teledyne ISCO, Lincoln, NE). The Curve Number method was used to calculate inflow volume to the permeable pavement from the 100% impervious watershed (NRCS 1986).

Samples were collected from a purpose-built weir-box attached to the underdrain, which included a 30˚ v-notch weir (Figure 45 at left). An ISCO 730 bubbler module was attached to an ISCO 6712 sampler at the underdrain monitoring location and used to measure depth of flow over the weir on two minute intervals (Teledyne ISCO, Lincoln, NE). Overflow was measured using a 60˚ v -notch weir and Hobo U20 pressure transducer in the catch basin (Figure 45 at

right). Using standard weir equations, flow depths above the weir crest were converted to flow rate:

$$Q = 0.676 * H^{2.5}, 30^{\circ} \text{ v-notch weir} \quad (4.1)$$

$$Q = 1.443 * H^{2.5}, 60^{\circ} \text{ v-notch weir} \quad (4.2)$$

where Q is flow rate (ft3/s) and H is head (ft) above the weir crest. Flow rate was integrated over time to calculate volume as a function of time at the overflow and drainage monitoring locations. For drainage sampling, cumulative stormwater volume was used to trigger flow-proportional, composite samples obtained in 200 mL aliquots.

Figure 44. Sampling trough with sample intake to sample runoff quality from the asphalt pavement (left) and the spigot from which water quality samples were obtained to characterize the quality of the water at the point-of-use (right) at Old Woman Creek NERR.

Figure 45. Weirs for drainage (at left) and overflow (at right) measurement in the monitoring vault at Old Woman Creek NERR.

To represent the quality of stormwater as it exited the cistern, water quality samples were obtained from the spigot, which utilized an on-demand, submersible pump to provide pressure (Figure 44). The pump intake had a basic gross solids filter, but lacked UV or grit filtration. Therefore, samples were representative of the quality of the water at the point-of-use. A grab sample was taken from the spigot (in conjunction with sample collection from the water quality samplers) 30 seconds after opening the spigot to obtain a well-mixed sample.

All composite samples had a minimum of five aliquots during the storm to describe greater than 80% of the pollutograph (U.S. EPA 2002). Sample intakes were placed in representative locations where flow was well-mixed and strainers were used to remove gross solids. Separate rainfall events were characterized by a minimum antecedent dry period of 6 hours and rainfall

depth of 0.1 inches. Rainfall data were collected at the site using both a manual and a tipping bucket rain gauge.

4.3.2 Laboratory Methods

Samples were obtained from automated sampling equipment and from the spigot within 24 hours of the cessation of rainfall. Composite samples were shaken vigorously in the 10 L sampling jar to re-suspend solids, and were then subsampled into laboratory sample bottles. Composite samples were divided among two 1L plastic jars for TSS analysis, one 500 mL pre-acidified bottle for nutrient analysis, one 500 mL pre-acidified bottle for metals analysis, and a 50mL glass jar (following filtration through a Whatman Puradisc 0.45 μm filter) for orthophosphate (OP) analysis. Spigot grab samples were dispensed into each sample bottle separately. Samples were placed immediately on ice and chilled to less than 4˚C for transit to the laboratories. Samples destined for the Northeast Ohio Regional Sewer District Laboratory (NEORSD) [total Kjeldahl nitrogen (TKN), and the metals aluminum (Al), calcium (Ca), copper (Cu), iron (Fe), magnesium (Mg), manganese (Mn), sodium (Na), lead (Pb), and zinc (Zn)] were shipped overnight on ice. The following pollutants were analyzed at the onsite water quality laboratory at Old Woman Creek NERR: nitrate and nitrite nitrogen ($NO_{2\text{-}3}$) total ammoniacal nitrogen (TAN), OP, total phosphorus (TP), total suspended solids (TSS), and chloride (Cl). Total nitrogen (TN), organic nitrogen (ON), and particle-bound phosphorus (PBP) were calculated using methods in Table 31. Samples were analyzed using either U.S. EPA (1983) or American Public Health Association (APHA et al. 2012) methods.

Table 31. Laboratory testing and preservation methods as well as method detection limits (MDL) for pollutants of concern.

Parameter	Laboratory Method	Laboratory	Preservation	MDL (mg/L)
TKN	EPA Method 351.2[1]	NEORSD	H_2SO_4 (<2 pH), <4˚C	0.5
NO_{2-3}	EPA Method 353.2	OWC NERR	H_2SO_4 (<2 pH), <4˚C	0.03
TN	Calculated as TKN + NO_{2-3}	Calculated	N/A	N/A
TAN	EPA Method 350.1	OWC NERR	H_2SO_4 (<2 pH), <4˚C	0.003
ON	Calculated as TKN-TAN	Calculated	N/A	N/A
OP	EPA Method 365.2	OWC NERR	<4˚C	0.06
PBP	Calculated as TP-OP	Calculated	N/A	N/A
TP	EPA Method 365.2	OWC NERR	H_2SO_4 (<2 pH), <4˚C	0.008
Chloride	Standard Methods 4500-Cl^- [2]	OWC NERR	<4˚C	1
TSS	Standard Methods 2540D	OWC NERR	<4˚C	1
Parameter	Laboratory Method	Laboratory	Preservation	MDL (µg/L)
Al	EPA 200.8	NEORSD	HNO_3 (<2 pH), <4˚C	0.96
Ca				35.8
Cu				0.22
Fe				1.76
Mg				13.42
Mn				0.46
Pb				0.174
Zn				1.3

[1]U.S. EPA 1983
[2]APHA et al. 2012

4.3.3 Data Analysis

The performance of the Old Woman Creek NERR permeable pavement and cistern treatment train was determined by comparing event mean concentrations from the asphalt, the drainage, and cistern sampling points. Reductions in event mean concentrations (EMC) were determined using summary statistics, including the range of pollutant concentrations, mean ($\bar{x}$), median ($\tilde{x}$), standard deviation (s), skewness (C_s), coefficient of variation (CV), efficiency ratio (ER), and median relative efficiency (RE_{median}). The latter three metrics are defined below:

$$CV = \frac{s}{\bar{x}} \tag{4.3}$$

$$ER = 1 - \frac{\sum_{i=1}^{n}(Eff\ EMC_i)/n}{\sum_{i=1}^{n}(Inf\ EMC_i)/n} \tag{4.4}$$

$$RE_{median} = 1 - \frac{Eff\ EMC_{median}}{Inf\ EMC_{median}} \tag{4.5}$$

where Eff EMC is the effluent EMC from the SCM, Inf EMC is the influent EMC from the watershed, and n is the number of storm events. The efficiency ratio is a commonly used metric for SCM performance, but is influenced by low or irreducible influent concentrations (Strecker et al. 2001). Since the data set was small (7 storm events), the median relative efficiency was assumed to be the better metric to use, as the normal distribution was not assured. Boxplots were created for each pollutant studied to examine differences in water quality entering and leaving the treatment train SCM. These analyses were performed for all pollutants studied, including metals, nutrients, sediment, and chloride.

Pollutant loads were explored since they take into account volume reduction within an SCM and because they factor into total maximum daily load (TMDL) regulations. To calculate pollutant loads during a given storm, the product of stormwater volume and EMC was taken. For events that had outflow but that were not sampled for water quality, the median EMC from sampled storm events was assigned for each pollutant for load calculations. Storms with no outflow (i.e. completely captured within the treatment train) were assumed to contribute pollutant load at the inlet but had zero effluent pollutant load. For the 9.8 inches of rainfall during the monitoring period, the sum of all loading at the inlet and outlet was calculated and compared using a relative percent difference. All pollutant loads were normalized by watershed area.

All data analysis was completed using R statistical software version 2.15.2 (R Core Team, 2014). A value of one-half the detection limit was substituted for concentration data below the detection limit (Antweiler and Taylor 2008). Below detection limit concentrations were rare, and represented less than 15% of the data for all pollutants analyzed.

4.4 Results and Discussion

4.4.1 Sampled Storm Events

Twenty-two separate rainfall events were monitored during August through December 2014. Of the 22 events, water quality samples were obtained from the asphalt and cistern monitoring sites for seven events. Sampled storm events represented 4.78 inches of the 9.80 inches of rainfall that occurred during the monitoring period. Though monitoring equipment was installed to measure drainage from the permeable pavement, drainage did not occur except during the largest storm event (>1.5 inches rainfall), and therefore drainage samples were not obtained during the monitoring period. This was due to multiple leaks in the cistern system, allowing water to be transmitted from the aggregate beneath the pavers, through the backfilled soil on top of the cisterns, and into the cisterns without first draining through the underdrain. The 3-in IWS zone may have exacerbated the problem by allowing ponding (and therefore driving head) within the aggregate. This also meant exfiltration from the permeable pavers could not be quantified during the monitoring period, as water did not remain ponded within the IWS zone inter-event.

However, the system performance as a whole was evaluated, as samples were obtained from the asphalt (representing the quality of the run-on to the permeable pavement) and the cistern (representing the quality of the water at the point-of-use). The seven sampled storm events are shown in Figure 46 in green; for the third event, the rain gage malfunctioned, and hourly on-site

rainfall measurements from a USGS rain gage were used to calculate event depth, but no 5-minute peak intensity could be enumerated. Median sampled storm event depth was 0.57 inches, while the median overall storm depth was 0.47 inches. Median 5-minute peak rainfall intensity for sampled storms was higher than for all observed storms (0.79 in/hr vs. 0.52 in/hr). These data suggest that sampled storms were slightly larger and more intense than the central tendency, but that sampled storms were generally representative of the distribution of rainfall events.

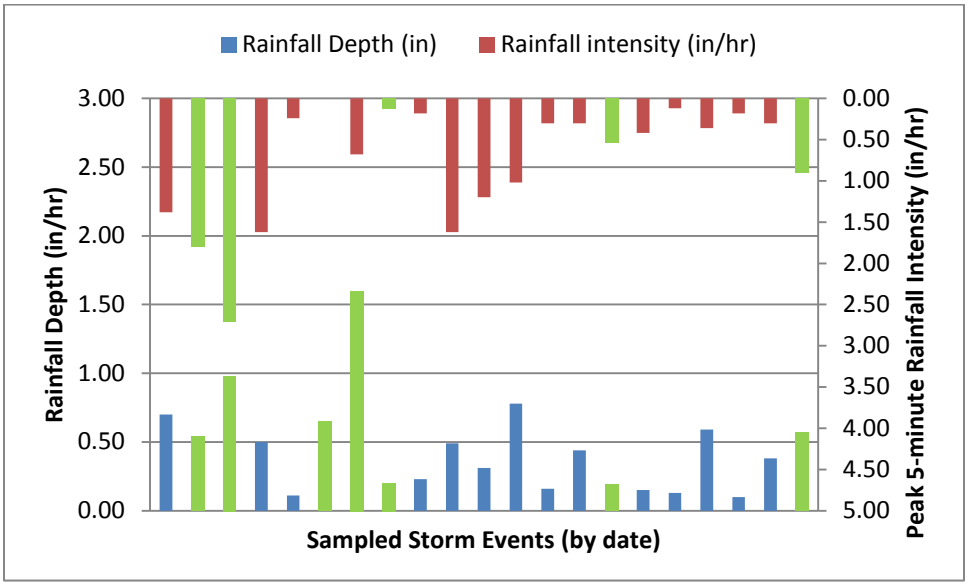

Figure 46. Storm events characteristics at the Old Woman Creek NERR permeable pavement and underground cistern treatment train. Sampled storms are shown in green.

4.4.2 Hydrologic Performance

The cistern remained full during the entirety of the monitoring period because of a lack of use of the stormwater for irrigation and vehicle washing. In Figure 47, the abscissa represents the bottom of the cistern. The cisterns were 2 feet in height (neglecting wall thickness), and so water above this point represented ponding within the access manways. The vertical drop in water level on October 15th, 2014, was due to the cistern being pumped to affect a repair, during which hydraulic cement was utilized in an effort to stop water from leaking from the aggregate beneath the permeable pavement, through the backfilled soil, directly to the cisterns. Based on the

remainder of the data set, this effort did not succeed. No other vertical drops in water level occurred during the monitoring period, suggesting little to no water use from the spigot. There was, however, a slow drawdown in water level following each storm event, typically to about 2-2.5 feet water level (Figure 47). This was due to the two joints in the cistern system, which appeared to both be leaking. The joint between the top concrete slab of the cisterns and the eccentric cone manways was located at 2.5 feet elevation, while the joint between the top and bottom of the cistern storage volume was located at 2.0 feet; these were the two elevations where leaks could have occurred. Because the cistern was one continuous concrete pour below 2.0 feet, no leaks occurred below this elevation and the cistern remained full. Because the soil surrounding the cistern was hydraulically connected to the cistern through the leaks, the drawdown rate within the cistern most likely reflects the exfiltration rate of the surrounding soil. The median drawdown rate from the cistern was 0.068 in/hr. The drawdown rates from the two wells in the permeable pavement aggregate were very slow (0.002 in/hr). This suggests that a more permeable lens in the soil exists at deeper depths at the Old Woman Creek site. Overflow from the permeable pavement and cistern treatment train into Old Woman Creek estuary was observed for 17 of the 22 storm events (Figure 48).

Because the cistern was always full, the stormwater could only fill the volume in the eccentric cone manways, which would then dewater through exfiltration after the storm event (Figure 48). This meant that 55 ft^3 of potential abstraction was present within the system, given the negligible infiltration rates from the permeable pavement and preferential flow pathway to the cistern. This resulted in an overall volume reduction for the system of 16.9% (as a percentage of the total inflow volume). For the seven storms that were sampled for water quality, between 0 and 91% volume reduction was observed. In the future, the performance of this treatment train could be

improved dramatically through the consistent use of stormwater inter-event, perhaps through toilet flushing inside the Old Woman Creek NERR Visitor's Center. Additionally, purposeful leaks within the concrete tanks could be included by drilling holes in their side or bottom.

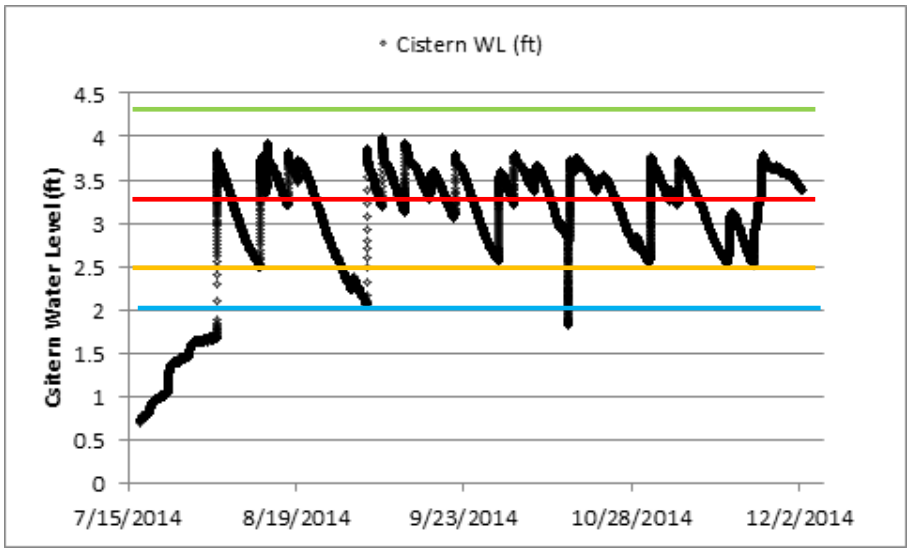

Figure 47. Old Woman Creek NERR cistern water level as a function of time. The successive horizontal lines are the locations of: the invert of the underdrain (4.3 ft, green line), the overflow for the system (3.3 ft, red line), the elevation of the joint between the manway and the top slab of the cistern (2.5 ft, orange line) and the elevation of the top of the cistern storage (2.0 ft, blue line).

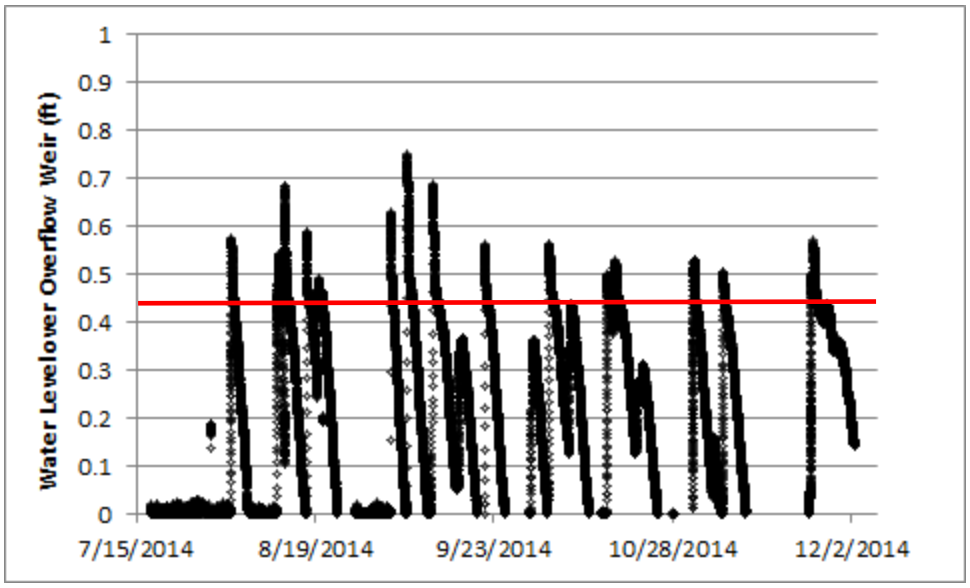

Figure 48. Old Woman Creek flow depth over the overflow weir as a function of time. Note that the invert of the weir is set at 0.44 ft, shown as the horizontal line on the graph. Overflow did not occur until this water level was reached.

4.4.3 Nutrient, Chloride, and Metals Concentrations

Only ***seven*** storm events were able to be sampled for water quality at Old Woman Creek NERR; therefore, caution should be utilized in interpreting the data presented below. They should be viewed as a snapshot of performance, rather than a definitive answer as to how the system would be expected to perform over the long-term. Issues such as seasonality, outliers in pollutant concentrations, or clogging of the permeable pavement will not be captured in this data set, and therefore any conclusions drawn from the data should be interpreted conservatively. Because of the small amount of data, hypothesis testing was not performed.

Generally, the permeable pavement and underground cistern treatment train at Old Woman Creek NERR performed well for nutrient and sediment removal (Table 32 and Figure 49). Positive ER and RE_{median} were observed for all nutrient forms, TSS, and turbidity, except for a net export of NO_{2-3}. This dissolved constituent is often the product of aerobic transformation of TAN through the processes of ammonification and subsequent nitrification within the aggregate

or cistern, and export of this constituent is often observed from SCMs lacking an anaerobic layer (Gisvold et al. 2000; Hunt et al. 2008). This is further supported by the sequestration of TAN which occurred within the permeable pavement and cistern treatment train, suggesting conversion to $NO_{2\text{-}3}$. The reduced concentrations of ON and TKN imply trapping and/or settling of particulate nitrogen, perhaps at the pavement surface (Drake et al. 2014b), within the aggregate underlying the permeable pavement (Roseen et al. 2012), and within the cistern itself (Wilson et al. 2014). The nearly complete sequestration of OP was surprising, given that it is a dissolved constituent. Perhaps the dissolved P adsorbed to the calcium cation in limestone, the primary type of rock that was utilized as the aggregate for the permeable pavement (Kim and Park 2008); it could also adsorb to the *in situ* clay soil as water entered the cistern. PBP, TSS, and turbidity ER and RE_{median} values were all greater than 85%, suggesting excellent retention of sediment in this treatment train SCM. These high removal rates were similar to other cisterns and permeable pavement applications in the literature, and therefore expected (Kim and Han 2011; Roseen et al. 2012; Drake et al. 2014b; Wilson et al. 2014). It should be noted that one substantial influent outlier existed for TSS (3025 mg/L), which can be attributed to sediment in the catchment immediately following construction. Median effluent concentrations of TN, TP, and TSS were low, with values of 0.87, 0.05, and 4 mg/L, respectively. This median effluent TN concentration is marginally higher than what would be expected from biologically based SCMs, such as bioretention, but the TP and TSS median effluent concentrations from this treatment train were better than conventional SCMs reported in the literature (Winston et al. 2015). This was perhaps due to the differing unit processes present in permeable pavement and cisterns, and longer pathway to the cistern.

Table 32. Summary statistics for nutrient and sediment concentrations at the Old Woman Creek permeable pavement and rainwater harvesting system.

Pollutant	Location	Range (mg/L)	$\overline{x}$ (mg/L)	$\tilde{x}$ (mg/L)	s (mg/L)	C_s (mg/L)	CV (mg/L)	ER	RE_{median}
TKN	Inlet	0.67-5.22	2.06	1.59	1.69	1.31	0.82	0.69	0.66
	Outlet	0.4-1.15	0.64	0.54	0.28	1.35	0.44		
NO_{2-3}	Inlet	0.04-0.51	0.17	0.12	0.16	2.37	0.95	-1.42	-1.75
	Outlet	0.03-1.24	0.40	0.33	0.46	1.17	1.15		
TN	Inlet	0.82-5.34	2.23	2.05	1.68	1.21	0.76	0.53	0.58
	Outlet	0.42-1.8	1.04	0.87	0.55	0.43	0.53		
TAN	Inlet	0-0.16	0.05	0.04	0.06	1.66	1.28	0.37	0.19
	Outlet	0-0.06	0.03	0.03	0.02	0.07	0.78		
ON	Inlet	0.62-5.18	1.76	0.81	1.94	2.10	1.10	0.68	0.42
	Outlet	0.37-1.14	0.57	0.47	0.32	2.11	0.57		
OP	Inlet	0.001-0.028	0.011	0.0046	0.011	0.73	0.97	0.90	0.85
	Outlet	0-0.002	0.001	0.0007	0.001	0.17	0.79		
PBP	Inlet	0.03-0.92	0.38	0.35	0.36	0.51	0.92	0.87	0.85
	Outlet	0-0.1	0.05	0.05	0.04	-0.06	0.79		
TP	Inlet	0.03-0.93	0.39	0.36	0.36	0.45	0.91	0.87	0.85
	Outlet	0.01-0.1	0.05	0.05	0.04	-0.03	0.78		
TSS	Inlet	52-3025	766	483	1040	2.22	1.36	0.99	0.99
	Outlet	1-9	4	4	3	0.72	0.69		
Turbidity	Inlet	26-1323	348	145	498	2.06	1.43	0.98	0.97
	Outlet	1-12	6	4	5	0.39	0.81		

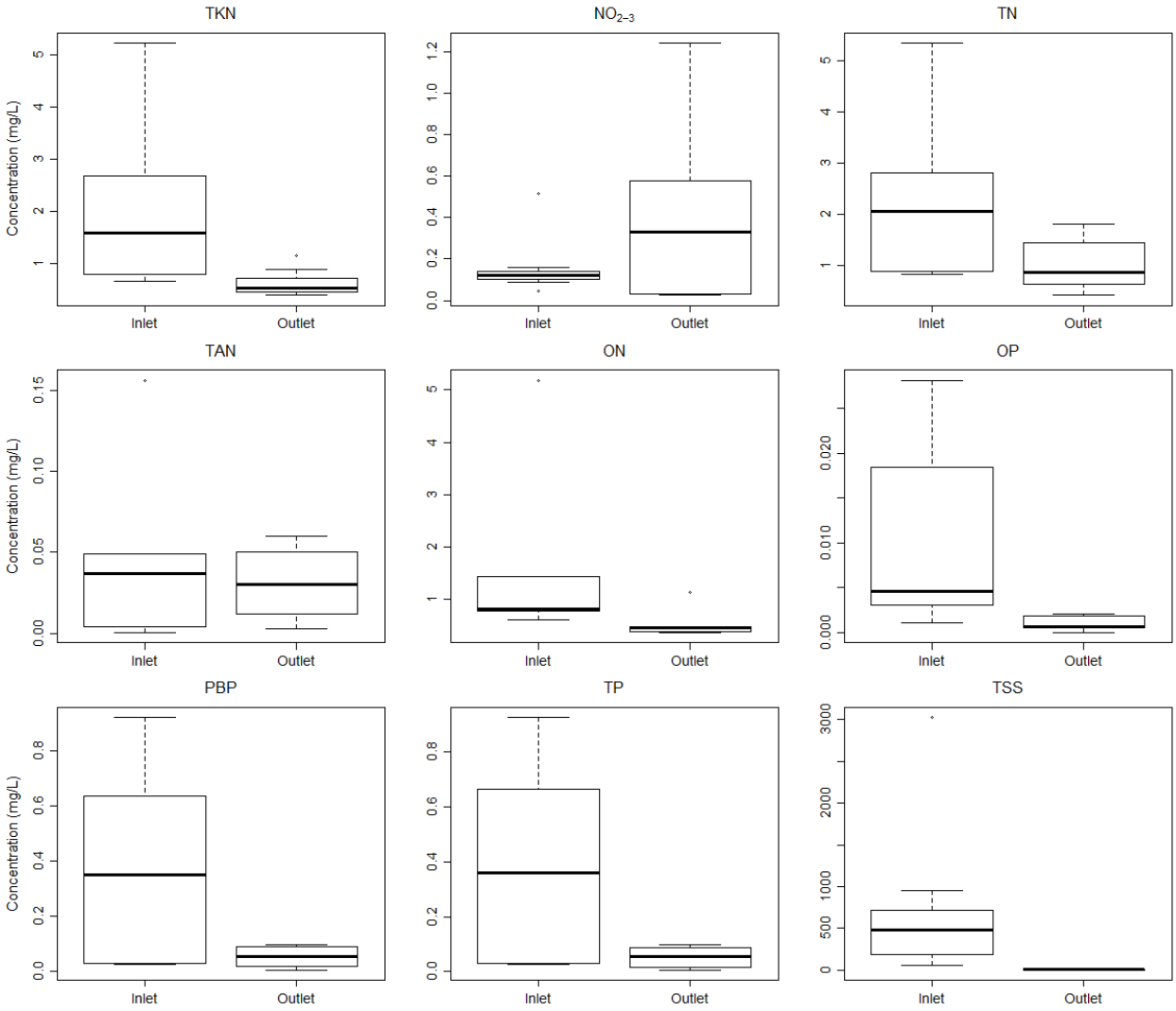

Figure 49. Boxplots of nutrient and sediment concentrations from the asphalt (inlet) and cistern (outlet) at the Old Woman Creek NERR permeable pavement and rainwater harvesting system.

Concentrations of total metals were reduced substantially as water moved through the treatment train SCM, except for Ca and Mg. Al, Mn, and Fe concentrations were reduced by 80% or more, suggesting particulate capture within the system (further supported by the sediment reductions observed). These Al and Fe ERs were higher than those reported in the literature for permeable pavement (Drake et al. 2014b). Cu, Pb, and Zn ERs were 0.61, 0.83, and 0.70, suggesting that these pollutants were well retained. Similar ERs were found for a stand-alone permeable pavement in Drake et al. 2014b, implying that the majority of the heavy metals

removal in this treatment train was occurring in the first stormwater control. This phenomenon has been observed in other studies of SCMs in series (Hathaway and Hunt 2010). The export of Ca and Mg from the permeable pavement and cistern treatment train is probably related to the aggregate used to support the permeable pavers. Quarried rock in north-central Ohio typically is dolomitic limestone, made up of limestone ($CaCO_3$) and dolomite [$CaMg(CO_3)_2$], potential sources of the Ca and Mg as water passed through the SCM (Lamar and Shorde 1953). Chloride concentrations from the parking lot were either below detection limit or near-zero, and chloride was exported from this SCM in all seven sampled storm events (ER of -65). Since all sampled storms occurred in the autumn, no appreciable residual salt was retained in the watershed; however, chloride is often leached from dolomite (Lamar and Shorde 1953). While Drake et al. (2014c) found that permeable pavement was not effective at reducing chloride concentrations in runoff, Roseen et al. (2014) found that porous asphalt reduced the amount of salt that needs to be applied by 64-77% to maintain the same level of skid resistance within a parking lot.

Table 33. Summary statistics for chloride and metals concentrations at the Old Woman Creek permeable pavement and rainwater harvesting system.

Pollutant	Location	Range (µg/L)	$\overline{x}$ (µg/L)	$\tilde{x}$ (µg/L)	s (µg/L)	C_s (µg/L)	CV (µg/L)	ER	RE_{median}
Cl	Inlet	0-2	0.3	0	0.7	2.65	2.65	-65	N/A
	Outlet	4-36	18	13	13.0	0.45	0.73		
Al	Inlet	83-13550	3959	2308	4941	1.51	1.25	0.94	0.90
	Outlet	75-526	247	231	144	1.17	0.58		
Ca	Inlet	12710-152000	59811	48910	50829	1.08	0.85	-0.66	-1.22
	Outlet	62260-133700	99570	108700	25525	-0.51	0.26		
Cu	Inlet	7-23	13.17	10.65	5.99	0.82	0.45	0.61	0.66
	Outlet	3-15	5.13	3.58	4.61	2.54	0.90		
Fe	Inlet	139-21450	6089	3671	7731	1.62	1.27	0.95	0.92
	Outlet	151-493	309	305	116	0.38	0.37		
Mg	Inlet	1129-29260	11534	8068	10842	0.81	0.94	-1.11	-2.21
	Outlet	14240-32430	24300	25930	5778	-0.62	0.24		
Mn	Inlet	43-662	245	217	214	1.40	0.87	0.82	0.86
	Outlet	4-132	43	31	46	1.39	1.06		
Pb	Inlet	0.6-26.04	7.84	5.81	8.95	1.69	1.14	0.83	0.75
	Outlet	0.4-3.06	1.37	1.48	0.90	1.04	0.66		
Zn	Inlet	36-1080	278	151	366	2.31	1.31	0.70	0.43
	Outlet	14-158	84	86	44	0.21	0.52		

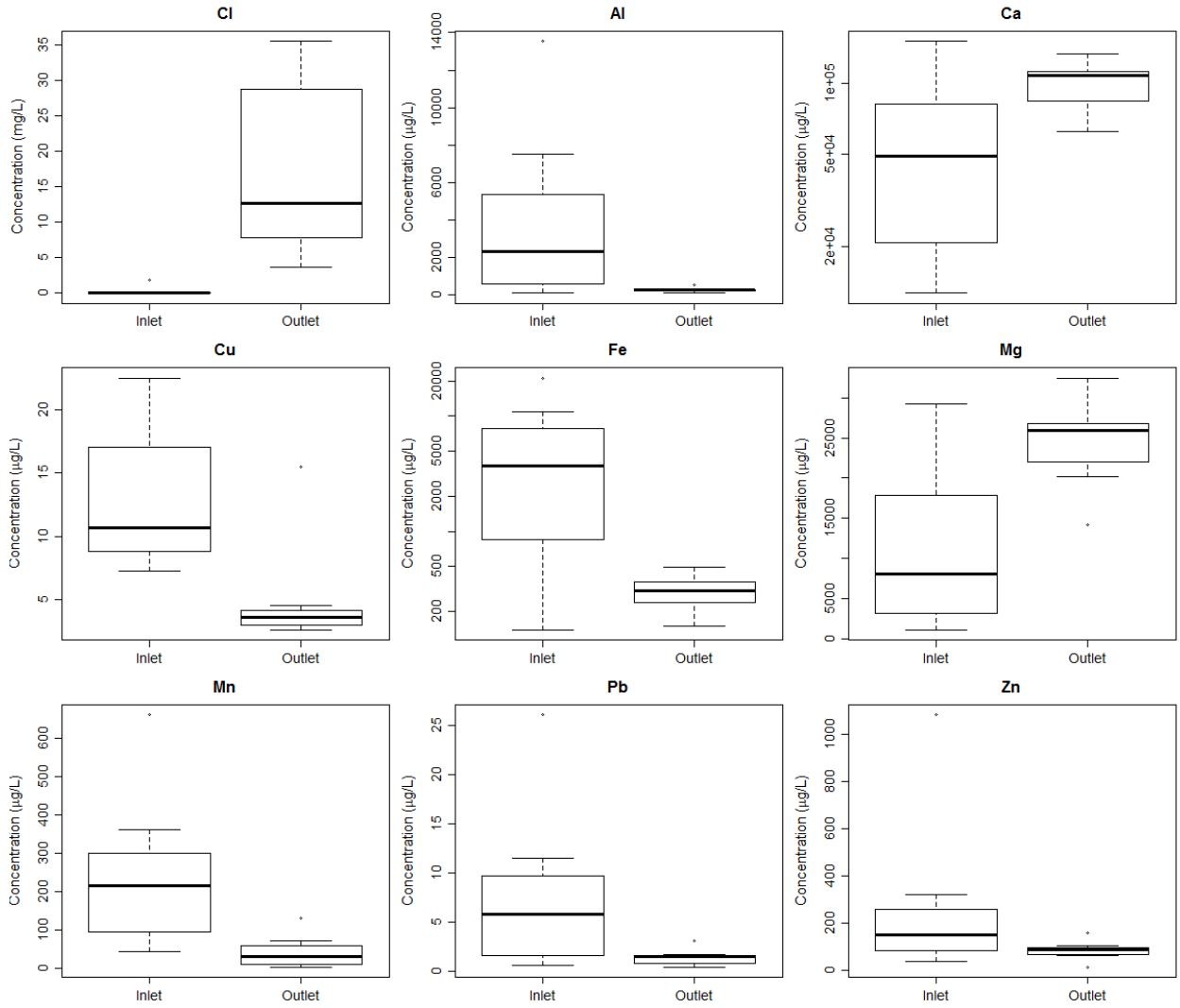

Figure 50. Boxplots of chloride and metals concentrations from the asphalt (inlet) and cistern (outlet) at the Old Woman Creek NERR permeable pavement and rainwater harvesting system.

4.4.4 Pollutant Loads

Only ***seven*** storm events were able to be sampled for water quality at the Old Woman Creek NERR site; therefore, see the caveats at the beginning of the previous section (4.4.3) about the interpretation of data.

Runoff pollutant loading from the asphalt parking lot was compared to effluent pollutant loading from the treatment train SCM (Table 34). An overall 16.9% volume reduction for the SCM and generally positive nutrient, sediment, and metals concentration reductions meant that

pollutant loads were reduced, often by more than 60%. Ca, Mg, and Cl loads all increased as water passed through the SCM because of increases in concentration of these analytes, probably due to leaching from the aggregate underlying the permeable pavement. NO_{2-3} concentrations probably increased due to nitrification within the cistern during inter-event periods. Dissolved P (OP) loads were reduced by 91% through the SCM, suggesting use of limestone aggregate within permeable pavement parking lots along the Lake Erie shoreline could reduce the load of dissolved P to the lake, one potential response to the harmful algal bloom issue (Correll 1998). This could also be a function of filtration through the backfilled soil as water entered the cistern through the aforementioned leaks. TN, TP, and TSS loads were reduced by 68, 86, and 99%, similar to the best performing bioretention cells and permeable pavement systems in the literature (Dietz and Clausen 2005; Davis 2007; Collins et al. 2010; Passeport et al. 2009; Drake et al. 2014b). Overall, the treatment train SCM reduced pollutant mass by retaining/sequestering pollutants of concern before they entered Old Woman Creek estuary.

Table 34. Pollutant load estimation from the parking lot and the outlet of the treatment train at Old Woman Creek NERR.

Monitoring Location	Pollutant Loads (g/ha)									
	Al	Ca	Cu	Fe	Mg	Mn	Pb		Zn	
Inlet	4911	85540	19	7583	15934	356	10		552	
Outlet	249	103450	3.7	400	24168	30	1.9		73	
Percent Reduction	95	-21	80	95	-52	92	82		87	
Monitoring Location	Pollutant Loads (kg/ha)									
	Cl	TKN	NO_{2-3}	TN	TAN	ON	TP	OP	PBP	TSS
Inlet	0.18	2.73	0.23	3.18	0.05	1.56	0.50	0.01	0.49	911
Outlet	17.6	0.54	0.48	1.02	0.02	0.40	0.07	0.00	0.07	5
Percent Reduction	-9453	80	-109	68	60	75	86	91	85	99

4.5 Summary and Conclusions

A permeable pavement and stormwater harvesting treatment train SCM was constructed at the Old Woman Creek NERR visitor center parking lot near Huron, Ohio in June-July, 2014. Four months of extensive hydrologic and water quality monitoring ensued on an innovative treatment train SCM. The conclusions related to water quality presented below are based on a data set of 7 samples, and therefore caution should be used in interpretation and use of the data. The following conclusions were drawn from this study:

1) Overall, the permeable pavement and cistern treatment train reduced runoff volume by 16.9%. This was respectable, given that no discernable water use from the cistern occurred during the monitoring period. The permeable pavement aggregate drained very quickly, and drainage through the underdrain was never observed. Preferential flow pathways through the backfilled soil allowed water to move downward from the IWS zone and into the cistern, which was apparently not properly sealed at two joints in the system. This allowed for leakage to occur from the cistern and into the surrounding soils inter-event, which was the primary source of the volumetric reductions for this SCM.

2) Nitrogen species concentrations were generally reduced through this treatment train, with a 0.53 ER for TN. Export of NO_{2-3} was observed, presumably due to aerobic transformation of TAN. ON, PBP, TP, TSS, and turbidity all showed ERs greater than 66%, suggesting sequestration of particulate matter as water infiltrated the pavement surface and/or settling of particles within the permeable pavement aggregate or the cistern. Median effluent TP (0.05 mg/L) and TSS (4 mg/L) concentrations from these SCMs in series were lower than those from conventional SCMs reported in the literature.

3) Given the particulate capture described above, it was expected a high level of sequestration of particulate-bound metals would occur within the SCM. Efficiency ratios were greater than 60% for Al, Cu, Fe, Mn, Pb, and Zn, suggesting that this treatment train was effective for retention of most heavy metals. Calcium, magnesium, and chloride concentrations had elevated effluent concentrations when compared to those in the influent runoff. This could be related to the types of minerals composing the aggregate used beneath the PICP, primarily dolomitic limestone. These have been shown to leach Ca, Mg, and Cl in previous research studies.

4) Estimates of pollutant loading into and leaving the SCM showed reduction of all pollutants studied except for Ca, Mg, and Cl. Metals retention was greater than 80% in all cases except Ca and Mg. Of TN, TP, and TSS influent pollutant mass, 68%, 86%, and 99% was retained within the SCM, primarily related to concentration reductions. Interestingly, 91% or OP was sequestered within this parking lot SCM, which could prove useful for Lake Erie and other water bodies where phosphorus has been identified as a primary cause of algae blooms.

4.6 References

Abdulla, F.A. and Al-Shareef, A.W.. (2009). "Roof Rainwater Harvesting Systems for Household Water Supply in Jordan." *Desalination*. 243(1-3):195-207.

Antweiler, R.C., and Taylor, H.E. (2008). "Evaluation of statistical treatments of left-censored environmental data using coincident uncensored data sets: 1. Summary statistics." *Environmental Science and Technology*. 42(10), 3732‑3738.

American Public Health Association (APHA), American Water Works Association (AWWA), and Water Environment Federation (WEF). (2012). *Standard methods for the examination of water and wastewater*, Ed. Laura Bridgewater. 22nd ed., Washington, DC.

Ball, J. E., and Rankin, K. (2010). "The hydrological performance of a permeable pavement." *Urban Water Journal*. 7(2), 79-90.

Bannerman, R.T., Owens, D.W., Dodds, R.B., and Hornewer, N.J. (1993). "Sources of pollutants in Wisconsin stormwater." *Water Science and Technology*. 28(3), 241-259.

Bean, E. Z., Hunt, W. F., and Bidelspach, D. A. (2007). "Evaluation of four permeable pavement sites in eastern North Carolina for runoff eduction and water quality impacts." *Journal of Irrigation and Drainage Engineering*. 133(6), 583-592.

Bledsoe, B., and Watson, C. (2001). "Effects of urbanization on channel instability." *Journal of the American Water Resources Association.* 37(2), 255–270.

Brattebo, B.O., and Booth, D.B. (2003). "Long-term stormwater quantity and quality performance of permeable pavement systems." *Water Research*. 37(18), 4369-4376.

Brown, R.A., Line, D.E., and Hunt, W.F. (2011). "LID treatment train: Pervious concrete with subsurface storage in series with bioretention and care with seasonal high water tables." *Journal of Environmental Engineering*. 138(6), 689-697.

Chin, D.A. (2006). *Water-Resources Engineering*. 2nd edition, Pearson Prentice Hall. NJ, USA.

Collins, K. A., Hunt, W. F., and Hathaway, J. M. (2008). "Hydrologic comparison of four types of permeable pavement and standard asphalt in eastern North Carolina." *Journal of Hydrologic Engineering.* 13(12), 1146-1157.

Collins, K.A., Hunt, W.F., and Hathaway, J.M. (2010). "Side-by-side comparison of nitrogen species removal for four types of permeable pavement and standard asphalt in eastern North Carolina." *Journal of Hydrologic Engineering*. 15(6), 512-521.

Correll, D.L. (1998). "The role of phosphorus in the eutrophication of receiving waters: A review." *Journal of Environmental Quality*. 27(2), 261-266.

Davis, A.P., Shokouhian, M., and Ni, S. (2001). "Loading estimates of lead, copper, cadmium, and zinc in urban runoff from specific sources." *Chemosphere*. 44(5), 997-1009.

Davis, A.P. (2007). “Field performance of bioretention: Water quality.” *Environmental Engineering Science*. 24(8), 1048-1064

DeBusk, K.M., Hunt, W.F., and Wright, J.D. (2013). “Characterizing rainwater harvesting performance and demonstrating stormwater management benefits in the humid southeast USA.” *Journal of the American Water Resources Association*. 49(6), 1398-1411.

DeBusk, K.M., and Hunt, W.F. (2014). “Impact of rainwater harvesting systems on nutrient and sediment concentrations in roof runoff.” *Water Science and Technology: Water Supply*. 14(2), 220-229.

Despins, C., Farahbakhsh, K. and Leidl, C. (2009). “Assessment of rainwater quality from rainwater harvesting systems in Ontario, Canada.” *Journal of Water Supply: Research and Technology*. 58 (2), 117–134.

Diaz, R.J. (2001). “Overview of hypoxia around the world.” *Journal of Environmental Quality*. 30(2), 275–281.

Dietz, M.E., and Clausen, J.C. (2005). “A field evaluation of rain garden flow and pollutant treatment.” *Water, Air, and Soil Pollution*. 167(1-4), 123-138.

Drake, J., Bradford, A., and Van Seters, T. (2014a). “Hydrologic performance of three partial-infiltration permeable pavements in a cold climate over low permeability soil.” *Journal of Hydrologic Engineering*, 19(9), 04014016-1.

Drake, J., Bradford, A., and Van Seters, T. (2014b). “Stormwater quality of spring–summer-fall effluent from three partial-infiltration permeable pavement systems and conventional asphalt pavement.” *Journal of Environmental Management*. 139, 69-79.

Drake, J., Bradford, A., and Van Seters, T. (2014c). “Winter Effluent Quality from Partial-Infiltration Permeable Pavement Systems.” *Journal of Environmental Engineering*. 140(11).

Emerson, C.H., Welty, C., and Traver, R.G. (2005). “Watershed-scale evaluation of a system of storm water detention basins.” *Journal of Hydrologic Engineering*. 10(3), 237-242.

Fassman, E. A., and Blackbourn, S. (2010). “Urban runoff mitigation by a permeable pavement system over impermeable soils.” *Journal of Hydrologic Engineering.* 15(6), 475-485.

Gisvold, B., and Fllesdal, M. (2000). “Enhanced removal of ammonium by combined nitrification/adsorption inexpanded clay aggregate filters.” *Water Science and Technology*. 41(4-5), 409-416.

Gomez-Ullate, E., Novo, A.V., Bayon, J.R., Hernandez, J.R., and Castro-Fresno, D. (2011). “Design and construction of an experimental pervious paved parking area to harvest reusable rainwater.” *Water Science and Technology*. 64(9), 1942-1950.

Hathaway, J.M., and Hunt, W.F. (2010). “Evaluation of storm-water wetlands in series in Piedmont North Carolina.” *Journal of Environmental Engineering*.136(1), 140-146.

Hunt, W.F., Smith, J.T., Jadlocki, S.J., Hathaway, J.M., and Eubanks, P.R. (2008). “Pollutant removal and peak flow mitigation by a bioretention cell in urban Charlotte, NC.” *Journal of Environmental Engineering*. 134(5), 403-408.

Jones, M.P., and Hunt, W.F. (2010). “Performance of rainwater harvesting systems in the southeastern United States.” *Resources, Conservation and Recycling*. 54(10), 623-629.

Kim, M. and Han, M. (2011). “Composition and distribution of bacteria in operating rainwater harvesting tank.” *Water Science and Technology*. 63(7): 1524-1530.

Kim, H.S., and Park, J. (2008). “Effects of limestone on the dissolution of phosphate from sediments under anaerobic condition.” *Environmental technology*. 29(4), 375-380.

Lamar, J.E., and Shorde, R.S. (1953). “Water soluble salts in limestone and dolomites.” *Economic Geology*. 48(2), 97-112.

Legret, M., Colandini, V., and LeMarc, C. (1996). “Effects of a porous pavement with reservoir structure on the quality of runoff water and soil.” *The Science of the Total Environment.* 190, 335–340.

McArdle, P., Gleeson, J., Hammond, T., Heslop, E., Holden, R., and Kuczera, G. (2011). “Centralised urban stormwater harvesting for potable reuse.” *Water Science and Technology*. 63(1), 16-24.

Nnadi, E.O., Newman, A.P., Coupe, S.J., and Mbanaso, F.U. (2015). “Stormwater harvesting for irrigation purposes: An investigation of chemical quality of water recycled in pervious pavement system.” *Journal of environmental management*. 147, 246-256.

Natural Resources Conservation Service (NRCS). (1986). *Urban hydrology for small watersheds*. Technical Release 55 (TR-55), 2nd edition. United States Department of Agriculture (USDA), Natural Resources Conservation Service, Conservation Engineering Division.

Palhegyi, G. E. (2009). “Designing storm-water controls to promote sustainable ecosystems: science and application.” *Journal of Hydrologic Engineering*. 15(6), 504-511.

Passeport, E., Hunt, W.F., Line, D.E., Smith, R.A., and Brown, R.A. (2009). “Field study of the ability of two grassed bioretention cells to reduce storm-water runoff pollution.” *Journal of Irrigation and Drainage Engineering*. 135(4), 505-510.

R Core Team. (2014). *A language and environment for statistical computing*. R Foundation for Statistical Computing. Vienna, Austria.

Radhakrishna, B.P. (2003). “Rainwater Harvesting: A Time-Honoured Practice: Need for Revival.” *Current Science.* 85(9):1259-1261.

Roseen, R.M., Ballestero, T.P., Houle, J.J., Briggs, J.F., and Houle, K.M. (2012). “Water quality and hydrologic performance of a porous asphalt pavement as a storm-water treatment strategy in a cold climate.” *Journal of Environmental Engineering*. 138(1), 81-89.

Roseen, R.M., Ballestero, T.P., Houle, K.M., Heath, D., and Houle, J.J. (2014). “Assessment of winter maintenance of porous asphalt and its function for chloride source control.” *Journal of Transportation Engineering*. 140(2), 04013007.

Rushton, B.T. (2001). “Low-impact parking lot design reduces runoff and pollutant loads.” *Journal of Water Resources Planning and Management*. 127(3), 172-179.

Soil Survey Staff, Natural Resources Conservation Service, United States Department of Agriculture. (2015). Web Soil Survey. http://websoilsurvey.nrcs.usda.gov/. Accessed 28 January 2015.

Strecker, E.W., Quigley, M.M., Urbonas, B.R., Jones, J.E., and Clary, J.K. (2001). “Determining urban storm water BMP effectiveness.” *Journal of Water Resources Planning and Management*. 127(3), 144-149.

Sung, M., Kan, C.C., Wan, M.W., Yang, C.R., Wang, J.C., Yu, K.C. and Lee, S.Z. (2010). “Rainwater harvesting in schools in Taiwan: system characteristics and water quality.” *Water Science and Technology*. 61(7), 1767–1778.

Taebi, A., and Droste, R.L. (2004). “Pollution loads in urban runoff and sanitary wastewater.” *Science of the total environment*. 327(1), 175-184

U.S. Environmental Protection Agency (U.S. EPA). (1983). *Methods of chemical analysis of water and waste*. EPA-600/4-79-020, Cincinnati, Ohio.

U.S. EPA. (2002). Urban storm water BMP performance monitoring: a guidance manual for meeting the national storm water BMP database requirements. EPA-821-B- 02-001,Washington, DC.

Walsh, C.J., Roy, A.H., Feminella, J.W., Cottingham, P.D., Groffman, P.M., and Morgan, R.P. (2005). “The urban stream syndrome: current knowledge and the search for a cure.” *Journal of the North American Benthological Society*. 24(3), 706-723.

Wardynski, B. J., Winston, R. J., and Hunt, W. F. (2012). “Internal water storage enhances exfiltration and thermal load reduction from permeable pavement in the North Carolina mountains.” *Journal of Environmental Engineering*, 139(2), 187-195.

White, M.D., and Greer, K.A. (2006). “The effects of watershed urbanization on the stream hydrology and riparian vegetation of Los Penasquitos Creek, California.” *Landscape and Urban Planning*. 74(2), 125-138.

Wilson, C.E., Hunt, W.F., Winston, R.J., and Smith, P. (2014). “Assessment of a rainwater harvesting system for pollutant mitigation at a commercial location in Raleigh, NC, USA.” *Water Science and Technology: Water Supply*. 14(2), 283-290.

Wilson, C.E., Hunt, W.F., Winston, R.J., and Smith, P. (2015). “Comparison of runoff quality and quantity from a commercial low-impact and conventional development in Raleigh, North Carolina.” *Journal of Environmental Engineering*. 141(2), 05014005.

Winston, R.J., Hunt, W.F., Kennedy, S.G., Wright, J.D., and Lauffer, M.S. (2012). “Field evaluation of storm-water control measures for highway runoff treatment.” *Journal of Environmental Engineering*. 138(1), 101-111.

Winston, R.J., Lauffer, M.S., Narayanaswamy, K., McDaniel, A.H., Lipscomb, B.S., Nice, A.J., and Hunt, W.F. (2015). “Comparing bridge deck runoff and stormwater control measure quality in North Carolina.” *Journal of Environmental Engineering.* 141(1), 04014045.

5 WATER QUALITY PERFORMANCE OF A BIORETENTION CELL AT URSULINE COLLEGE

5.1 Review of Literature

Land use change from agricultural or forested watersheds to urban conditions fundamentally modifies the watershed hydrology and poses threats to water quality (Schoonover and Lockaby 2006). Urbanization spurs increases in impervious surface percentage and soil compaction, modifying the long-term hydrologic balance (Meyer 2004). Due to these changes, the urban land use is a primary source of surface water pollution, with concentrations of heavy metals, indicator bacteria, polycyclic aromatic hydrocarbons (PAHs), and suspended solids often exceeding federal water quality regulations (U.S. EPA 1983a; Bannerman et al. 1993). Augmented pollutant loads stress aquatic habitat following conversion from rural to urban land use (Williamson et al. 1993; Finkenbine et al. 2000).

Bioretention is the standard bearer for Low Impact Development, a novel method of development that includes open space preservation, clustering imperviousness, and installing distributed stormwater control measures (SCMs) to treat stormwater at its source (Dietz and Clausen 2008; Wilson et al. 2015). Bioretention cells are vegetated media filters used in urban watersheds to treat the first flush of runoff, thereby ameliorating both hydrologic and water quality impacts of impervious cover (Feng et al. 2012). They are depressed basins in the landscape that allow 9-12 inches of water to pond, contain specialized soil media designed to filter and treat the stormwater, and typically have underdrains to promote de-watering when situated over poor soils (Hunt et al. 2012; Liu et al. 2014). In Ohio, they are designed to store runoff from the 0.75-in event in their bowl without overflow and to have a surface area equivalent to 5% of their impervious watershed area (ODNR 2006).

For bioretention, stormwater volume mitigation benefits have been observed through exfiltration to the native soils and evapotranspiration (Davis et al. 2009). Generally, systems situated in sandy soils are able to exfiltrate larger stormwater volumes due to higher saturated hydraulic conductivity (Davis 2008; Passeport et al. 2009; Brown and Hunt 2011a; Luell et al. 2011); however, this may reduce their performance for pollutant mitigation, due to reduced hydraulic retention time within the media (Brown and Hunt 2011a). Reductions in sediment (Davis 2007; Hunt et al. 2008; Davis et al. 2009) and heavy metal (Davis 2007; Hunt et al. 2008; Davis et al. 2009; Feng et al. 2012) concentrations were observed in nearly every field and lab-based study on bioretention. Nutrient reductions (N and P) are not assured for biofilters, and are observed in some studies (Davis 2007; Hunt et al. 2008; Li et al. 2009; Luell et al. 2011), while export of nutrients is observed in others (Hunt et al. 2006; Dietz and Clausen 2006; Brown and Hunt 2011b). Three major factors influence water quality performance: (1) the media specification, (2) the presence of an internal water storage (IWS) zone, and (3) the type and number of plants.

Media specifications for bioretention vary widely from state to state. Typically, the majority of the media consists of sand, with various additional components, including silt, clay, organic matter, topsoil, compost, and other media enhancements (Carpenter and Hallam 2010). This typically results in a sandy loam or loamy sand soil texture, allowing for relatively high infiltration rates (1-4 in/hr recommended, Hunt et al. 2012) and water quality improvement through interactions with clay particles and organic matter (Hunt et al. 2012). The P content of the media has been shown to be critical to whether the bioretention cell acts as a net P sink or source (Hunt et al. 2006; Hatt et al. 2009). ODNR (2006) requires 60 mg/kg as the maximum P adsorbed P content for bioretention media in Ohio, while NCDENR (2007) provides a range of

12-36 mg/kg for soil test P levels in North Carolina based on research in Hunt et al. (2006). To assure P adsorption, an oxalate ratio of 20-40 has also been suggested based on laboratory studies of bioretention media (O'Neill and Davis 2012). The incorporation of iron or aluminum oxides enhances the P uptake capacity of the bioretention cell (Davis et al. 2006). Zeolite, perlite, water treatment residuals, biochar, and designer media blends, usually containing Fe and Al oxides aimed at adsorption of P, have been evaluated as part of bioretention media mixes (Liu and Davis 2013; Norris et al. 2013; Reddy et al. 2014a; Reddy et al. 2014b; Li et al. 2014; Duranceau and Biscardi 2015).

Nitrogen fate within the media is regulated mainly by the aerobic or anaerobic conditions of the media and plant uptake (Davis et al. 2009). The media as well as the organic layers, formed from the breakdown of mulch near the surface, sequester a fraction of the organic nitrogen (ON). ON then undergoes aerobic transformation to NO_3 by ammonification and subsequent nitrification. Therefore, without an anaerobic layer in the media where denitrification could drive conversion of NO_3 to N_2 gas, export of nitrate from these systems is common (Brown and Hunt 2011b). Particulate matter is captured near the surface of the media through filtration, resulting in good capture of particulate P, TSS, and heavy metals (Davis 2007).

An IWS zone within the media leads to greater exfiltration and evapotranspiration due to increased storage of water during inter-event periods, which aids in pollutant load mitigation (Dietz and Clausen 2006). A deeper, 3 foot IWS zone reduced runoff by 87% in a BRC over a sandy clay loam soil in North Carolina, whereas the same bioretention cell with a shallower IWS zone (2 feet deep) reduced volume by 75% (Brown and Hunt 2011a). Various studies have suggested that the addition of an IWS zone or saturated zone within the media leads to improved N removal, specifically through denitrification of NO_3 (Passeport et al. 2009; Brown and Hunt

2011a; Payne et al. 2014). One study suggested that the storage of water within the IWS zone during inter-event periods could add climate resiliency to bioretention cells, as plants have access to water during longer periods of drought (Payne et al. 2014).

Plants in bioretention cells provide a mechanism for volume reduction through transpiration, take up nutrients and metals from the soil water (Lucas and Greenway 2008), and provide root macropores to enhance long-term hydraulic functionality of these SCMs (Pitt et al. 2008; Jenkins et al. 2010). Planted bioretention cells had higher soil saturated hydraulic conductivity than unplanted bioretention media (Bartens et al. 2008; Lucas and Greenway 2011a). Studies have shown repeatedly that unplanted media filters have lower N (Bratieres et al. 2008; Lucas and Greenway 2011b) and P (Zhang et al. 2011) assimilation when compared to planted systems. It has been suggested that utilizing plants with high nutrient uptake rates may improve bioretention performance (Sharma et al. 2004; Bratieres et al. 2008). Since no transport pathway exists to transform influent P to a gaseous form, plant uptake and retention in the soil media are the two pathways for sequestration (Davis et al. 2006).

While much is known about bioretention, local verification of bioretention performance is key for private-sector engineers and landscape architects to use it for stormwater control. The goals of this study were to monitor field performance of a bioretention cell under northeast Ohio climate conditions for water quality pollutants of concern. Stormwater sampling was conducted using best methods and analysis of these samples occurred for a suite of nutrient and metals constituents, as well as TSS and chloride. These data were utilized to determine changes in pollutant concentration, and, along with concomitantly collected hydrology data, to estimate pollutant loading from this SCM. These data provide effluent concentrations and yearly pollutant loading rates for bioretention systems designed according to ODNR recommendations.

5.2 Site Description

A bioretention cell (BRC) was monitored for water quality performance at Ursuline College (UC) in Pepper Pike, Ohio (Figure 51). The BRC was installed in April-May of 2014 to treat the existing 0.89 acre, 77% impervious parking lot using design guidance in the OH Rainwater and Land Development Manual (Figure 52 and Table 35). The as-built filter bed surface area of the BRC was 1960 ft^2; this SCM was slightly over-designed per ODNR specifications at 6.5% of the contributing impervious watershed area (ODNR 2006). The as-built bowl storage was surveyed with a total station and provided an average of 11.7 inches of ponding before overflow occurred. This resulted in a total storage volume of 2120 ft^3 below the overflow structure, compared to the water quality volume of 1380 ft^3; therefore, the BRC actually was sized to store the 1.16 inch storm event in its bowl storage volume. The BRC was located over Mahoning soils according to the soil survey (Soil Survey Staff 2015); however, analysis of the soil during construction showed that it was relic fill soil, perhaps placed there during construction of the parking lot.

Figure 51. Photographs of the Ursuline College bioretention cell six months post-construction.

Figure 52. Watershed overview for the Ursuline College bioretention cell site. The watershed is outlined in green and the bioretention cell in blue.

Table 35. Characteristics of the Ursuline College bioretention cell and its catchment.

Contributing Impervious Watershed Area (ac)	Contributing Pervious Watershed Area (ac)	Surface Area of Bioretention Cell (ft^2)	Hydraulic Loading Ratio (HLR)	Catchment Percentage Impervious	Avg. Bowl Depth (in)	IWS Zone depth (in)
0.69	0.20	1960	21	77	11.7	24

A single 6-in diameter underdrain was utilized to drain the BRC, which was tied into the outlet structure. The BRC was constructed with an upturned elbow in the underdrain, creating a 24-in deep IWS zone; the top 6 inches of the IWS was located within the filter media (Figure 53). This created a minimum 18 inches of aerobic soil. The bioretention soil mix was sourced locally, and third party testing showed that the mineral fraction was 87% sand, 4% silt, and 9% clay, or a loamy sand soil texture. Organic matter made up 4.3% of the media by mass. The bioretention media was 2 feet deep and was underlain by 3 inches of medium coarse sand, 3 inches of pea gravel, and 12 inches of #57 gravel bedding around the underdrain. The media contained 3 distinct layers: 6 inches of Osorb® amendment and media mixed together sandwiched between two 9-in layers of standard bioretention media. Approximately 0.1%

Osorb® was mixed into the media on a mass basis. Osorb® is a media amendment purported to aid in treatment of oils, volatile organic compounds, pesticides, and nutrients.

The bioretention cell was planted with a mixture of 1450 one-inch plugs spaced 15 inches on center and a 3-in layer of hardwood mulch was spread over the media. The plant palette included *Carex*, *Scirpus*, *Aster*, *Lobelia*, and *Eupatorium* species (among others) that can tolerate both inundated and droughty conditions. During the monitoring period, the plants were juvenile and developed shoots that were less than 1 foot in height; therefore, plant processes were not expected to play a major role in the results presented below.

Figure 53. Internal water storage zone (IWS) installed using an upturned elbow in the underdrain at the Ursuline College bioretention cell.

Given past experiences with N and P leaching from soils with high organic matter or soil-test P concentrations (Hunt et al. 2006; Hatt et al. 2009; Clark and Pitt 2009; Hunt et al. 2012), the soil mix was tested by both a private laboratory and the North Carolina Department of Agriculture Agronomic Division laboratories for soil-bound P. Soil P was tested using a

Mehlich 3 test (Mehlich 1984). The North Carolina laboratory analysis resulted in a soil test P of 70.6 mg/kg for this media. This was considered moderate to high, and is above both the suggested soil test P value in NC (10-36 mg/kg; NCDENR 2007) based on research in Hunt et al. (2006) and above the 60 mg/kg level suggested by ODNR (2006) as the maximum values to observe TP sequestration within a bioretention cell. At higher levels of soil test P, leaching of this parameter is expected.

5.3 Materials and Methods

5.3.1 Data Collection

Instrumentation was installed within the bioretention cell to monitor rainfall, climatic parameters, and hydrologic conditions. Rainfall was measured using a 0.01-in resolution tipping-bucket and a manual rain gauge (Davis Instruments, Hayward, California). Rainfall data were stored in the Hobo U30 data logger attached to the nearby weather station (Onset Computer Corporation, Bourne, MA). Climatic data were collected for the following parameters: wind speed, wind direction, air temperature, relative humidity, and solar radiation. Rain gauges and weather stations were located in an open area, free from overhanging trees. All rainfall and climatic parameters were recorded on a 1-minute interval.

Water quality samples were obtained from the inlet to and outlet from the UC BRC to characterize its performance. A sampling trough was installed in the curb cut separating the asphalt parking lot from the rock-lined forebay of the bioretention cell (Figure 54). Influent samples were paced based on rainfall depth, a direct indicator of runoff volume (Chin 2006). An ISCO 6712 sampler was utilized to obtain 200 mL sample aliquots from the sampling trough after each 0.05 inches of rainfall, thus obtaining flow proportional, composite samples (Teledyne

ISCO, Lincoln, NE). Since a monitoring structure (e.g. weir or flume) was not able to be located at the inlet to this BRC, the Curve Number method was used to calculate inflow volume from the 77% impervious watershed (NRCS 1986). Combined overflow and drainage from the BRC was monitored within the outlet structure using a sharp crested, v-notch weir and an ISCO 730 bubbler module (to measure flow depth) connected to an ISCO 6712 sampler (Figure 54). Flow depths were converted to flow rate by the automated sampler using:

$$Q = 1.443 * H^{2.5}, 60^{\circ} \text{ v-notch weir} \quad (5.1)$$

where Q is flow rate (ft^3/s) and H is head (ft) above the weir crest. Flow rate was integrated over time to determine volume as a function of time at each monitoring location. Cumulative stormwater volume was used at the outlet to trigger flow-proportional, composite samples obtained in 200 mL aliquots. A minimum of five aliquots describing greater than 80% of the pollutograph were obtained for each storm (U.S. EPA 2002). Sample intake strainers were located in the monitoring trough and outlet structure in areas of well-mixed flow. Separate rainfall events were characterized by a minimum antecedent dry period of 6 hours and a 0.1-in rainfall depth. All hydrologic measurements used in pollutant loading analysis were obtained on a 2-minute interval.

Figure 54. Inflow monitoring structure located between the parking lot and the forebay (left) and top view of weir installed in Ursuline College outlet structure (right).

5.3.2 Laboratory Methods

Samples were obtained from automated sampling equipment within 24 hours of the cessation of rainfall. Samples were shaken vigorously in the composite 10 L jar to re-suspend solids, and were then subsampled into laboratory sample bottles. Composite samples were divided among two 1L plastic jars for total suspended solids (TSS) analysis, one 500 mL pre-acidified bottle for nutrient analysis, and one 500 mL pre-acidified bottle for metals analysis. Orthophosphate (OP) analysis was completed in the lab by subsampling from the TSS bottle and filtering out solids using a 0.45 µm filter. Samples were placed immediately on ice and chilled to less than 4°C for transport to the northeast Ohio Regional Sewer District Laboratory. Samples were delivered to the laboratory within 18 hours of sample collection. Samples were analyzed using U.S. EPA (1983b) or American Public Health Association (APHA et al. 2012) methods for: total Kjeldahl nitrogen (TKN), nitrate and nitrite nitrogen ($NO_{2\text{-}3}$) total ammoniacal nitrogen (TAN), OP, total phosphorus (TP), total suspended solids (TSS), chloride (Cl), and the metals aluminum (Al), calcium (Ca), copper (Cu), iron (Fe), magnesium (Mg), manganese (Mn), sodium (Na), lead

(Pb), and zinc (Zn) (Table 36). Total nitrogen (TN), organic nitrogen (ON), and particle-bound phosphorus (PBP) were calculated using methods in Table 36.

Table 36. Laboratory testing and preservation methods as well as method detection limits (MDL) and practical quantification limits (PQL) for pollutants of concern.

Parameter	**Laboratory Method**	**Preservation**	**MDL (mg/L)**	**PQL (mg/L)**
TKN	EPA Method 351.2[1]	H_2SO_4 (<2 pH), <4˚C	0.122	0.5
NO_{2-3}	EPA Method 353.2	H_2SO_4 (<2 pH), <4˚C	0.003	0.02
TN	Calculated as TKN + NO_{2-3}	N/A	N/A	N/A
TAN	EPA Method 350.1	H_2SO_4 (<2 pH), <4˚C	0.003	0.02
ON	Calculated as TKN-TAN	N/A	N/A	N/A
OP	EPA Method 300.0	<4˚C	0.03	0.082
PBP	Calculated as TP-OP	N/A	N/A	N/A
TP	EPA Method 365.1	H_2SO_4 (<2 pH), <4˚C	0.001	0.01
Chloride	EPA Method 300.0	<4˚C	1	5
TSS	Standard Method 2540D[2]	<4˚C	1	1
Parameter	**Laboratory Method**	**Preservation**	**MDL (µg/L)**	**PQL (µg/L)**
Al	EPA Method 200.8	HNO_3 (<2 pH), <4˚C	0.96	10
Ca			35.8	250
Cu			0.22	2
Fe			1.76	10
Mg			13.42	250
Mn			0.46	2
Pb			0.174	1
Zn			1.3	10

[1]U.S. EPA 1983b
[2]APHA et al. 2012

5.3.3 Data Analysis

The performance of the UC BRC was assessed by comparing event mean concentrations (EMC) at the inlet and outlet of the SCM. Reductions in EMC were determined using summary statistics, including the range of pollutant concentrations, mean ($\overline{x}$), median ($\tilde{x}$), standard deviation (s), skewness (C_s), coefficient of variation (CV), efficiency ratio (ER), and median relative efficiency (RE_{median}). The latter three metrics are defined below.

$$CV = \frac{s}{\bar{x}} \tag{5.2}$$

$$ER = 1 - \frac{\sum_{i=1}^{n}(Eff\ EMC_i)/n}{\sum_{i=1}^{n}(Inf\ EMC_i)/n} \tag{5.3}$$

$$RE_{median} = 1 - \frac{Eff\ EMC_{median}}{Inf\ EMC_{median}} \tag{5.4}$$

where Eff EMC is the effluent EMC from the SCM, Inf EMC is the influent EMC from the watershed, and n is the number of storm events. The efficiency ratio is a commonly used metric for SCM performance, but is influenced by low or irreducible influent concentrations (Strecker et al. 2001). Since the data set was so small for the UC BRC (7 storm events), the median relative efficiency may be the better metric to use since the normal distribution is not assured. Boxplots were created for each pollutant to examine differences in water quality entering and leaving the bioretention cell. These analyses were performed for all pollutants studied, including metals, chloride, and nutrients.

Pollutant loads also were explored since they take into account volume reduction within an SCM and because they factor into total maximum daily load (TMDL) regulations. To calculate pollutant loads during a given storm, the product of stormwater volume and EMC was taken. For events that had outflow but that were not sampled for water quality, the median EMC from sampled storm events was assigned for each pollutant for load calculations. Storms with no outflow (i.e. completely captured within the BRC) were assumed to contribute pollutant load at the inlet but had zero effluent pollutant load. Loads were then normalized by watershed area. The sum of normalized inlet and outlet loads for the total of 9.77 inches of rainfall for which water quality samples were obtained were compared using a relative percent difference.

All data analysis was completed using R statistical software version 2.15.2 (R Core Team, 2014). A value of one-half the detection limit was substituted for concentration data below the

detection limit (Antweiler and Taylor 2008). Below detection limit concentrations were rare, and represented less than 25% of the data for all pollutants analyzed.

5.4 Results and Discussion

5.4.1 Sampled Storm Events

Fifty separate hydrologic events were monitored during the May-December 2014 monitoring window. Of the 50 events, 40 had no outflow due to the relatively high exfiltration rate (average 0.17 in/hr) and deep IWS zone (24 inches). Of the ten with outflow, only four events were able to be sampled for water quality (Figure 55). This was due to errors the outlet sampler experienced during approximately the first half of the monitoring period, to weekend storm events not sampled because of a lack of staffing, and to the low rainfall intensities experienced during the last quarter of the monitoring period (Figure 55). The four sampled storm events had rainfall depths of 1.11, 1.56, 1.82, and 2.45 inches. Their peak 5-minute rainfall intensities (similar to the time of concentration of the watershed) were 1.44, 1.56, 1.92, and 4.32 in/hr. All four of the sampled storm events had rainfall depths and peak rainfall intensities above the 75th percentile, suggesting large depth and high intensity rainfall was needed to drive outflow from this bioretention cell.

During 2015 and prior to the end of June, 28 storm hydrologic storm events occurred at the Ursuline College site. Of those, three were able to be sampled for water quality performance. These events had rainfall depths of 0.66, 0.69, and 1.33 inches, with corresponding peak 5-minute rainfall intensities of 1.56, 2.64, and 2.88 in/hr. Sampled rainfall events in 2015 were a bit smaller in depth than those in 2014, but had similar peak rainfall intensity.

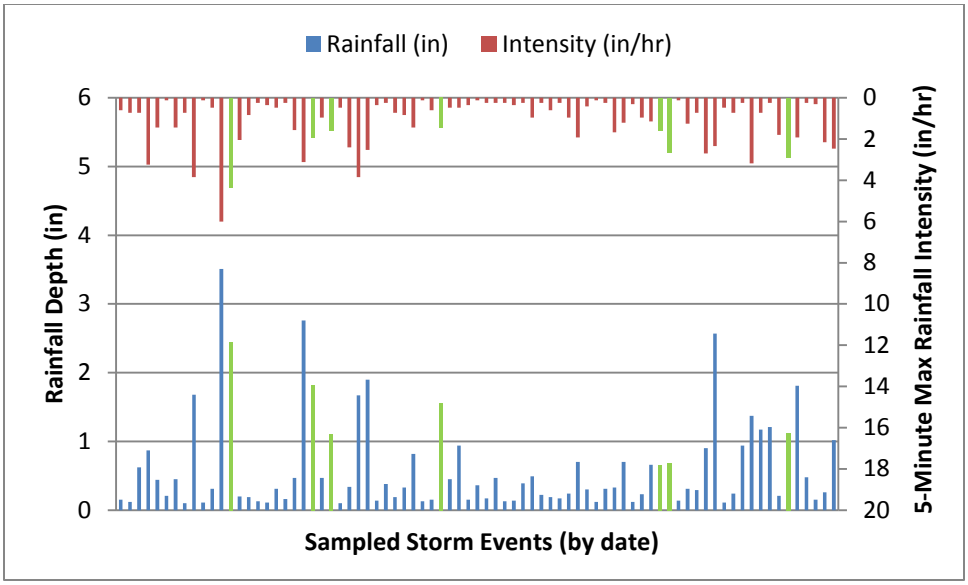

Figure 55. Storm events characteristics at the Ursuline College bioretention cell. Sampled storms are shown in green.

5.4.2 Nutrient, Chloride, and Metals Concentrations

Only ***seven*** storm events were able to be sampled prior to the end of June 2015; therefore, caution should be utilized in interpreting the data presented below. They should be viewed as a snapshot of performance, rather than a definitive answer as to how the system would be expected to perform over the long-term. Issues such as seasonality, outliers in pollutant concentrations, or growth of plants leading to greater pollutant uptake will not be captured in this data set, and therefore any conclusions drawn from the data should be interpreted conservatively. Because of limited data, hypothesis testing will not be performed on pollutant concentration data.

Summary statistics of the data for the UC BRC are shown in Table 37 and Table 38 for nutrients, metals, and sediment concentrations. In general, both ER and RE_{median} suggested the BRC was a source of nitrogen (Figure 56). The increases in nitrate suggest that perhaps (1) not enough of the media was located within the IWS zone (only 6 inches) to effectively promote denitrification, and/or (2) the relatively high exfiltration rate meant that the soil media was not saturated for long periods of time, implying that anaerobic conditions probably did not form

within the media, and/or (3) the plants were not large enough during the 2014 portion of the monitoring period to contribute to nitrate removal through plant uptake (Hunt et al. 2012). NO_{2-3} effluent concentrations decreased over time perhaps due to (1) larger plants took up more NO_{2-3} in the 2015 portion of the monitoring period, and (2) reduced leaching from the compost in the media over time. The relatively high exfiltration rates (average 0.17 in/hr) resulted in low hydraulic retention time within the IWS zone, perhaps resulting in a lack of anoxic conditions, thereby inhibiting denitrification (Brown and Hunt 2011b). Ammonification and nitrification may also have contributed to NO_{2-3} release, but augmented TAN effluent concentrations suggest that this is perhaps not the only pathway. Surprisingly, ON concentrations (and thereby TKN and TN) concentrations increased substantially, suggesting export of particulate N. This is not typical of bioretention cells in the literature (Brown and Hunt 2012), but has been observed in one study where it was suggested that it was caused by the mobilization of organic matter in the media and its discharge in the effluent from the BRC (Hunt et al. 2006). However, TSS capture within the media was upwards of 70% (i.e. sediment-bound nitrogen from the watershed was not the source), implying that some fraction of the organic matter within the media migrated through the profile and out of the BRC. In past studies, it has been observed the type of organic matter used in the media mix affects the export or sequestration of particulate N (Clark and Pitt 2009).

Dissolved (OP) and particulate (PBP) P were released from the Ursuline College BRC (Figure 56). This resulted in an increase in the mean TP concentration from the inlet (0.07 mg/L) to the outlet (0.08 mg/L) of 12%. However, this influent TP concentration was extremely low, well below the average value of 0.19 mg/L for eight parking lots in North Carolina (Passeport and Hunt 2009). Aggregated research from the mid-Atlantic region suggested that median effluent TP concentrations from BRCs were between 0.10-0.18 mg/L, which would suggest that this BRC

was performing well, even in light of the negative ER and RE_{median} (McNett et al. 2011). This suggests an irreducible concentration could have been reached for the bioretention cell, and no further treatment would be expected for TP from this SCM. However, the release of particulate P suggests that this may be related to the loss of organic matter, which would further support the export of ON. The ER for TSS was 0.88, suggesting capture of TSS particles through filtration and sedimentation. This efficiency ratio is in the range of those reported in the literature, (Li and Davis 2008; Li and Davis 2009; Hathaway et al. 2011; Brown and Hunt 2012).

Table 37. Summary statistics for nutrient and sediment concentrations at the Ursuline College bioretention cell.

Pollutant	Location	Range (mg/L)	$\overline{x}$ (mg/L)	$\tilde{x}$ (mg/L)	s (mg/L)	C_s (mg/L)	CV (mg/L)	ER	RE_{median}
TKN	Inlet	0.41-2.04	0.81	0.57	0.57	2.25	0.70	-1.85	-1.36
	Outlet	0.96-6.65	2.30	1.34	2.05	2.04	0.89		
NO_{2-3}	Inlet	0.17-0.32	0.23	0.22	0.04	1.23	0.20	-2.46	-2.23
	Outlet	0.38-1.28	0.79	0.71	0.31	0.58	0.39		
TN	Inlet	0.58-2.36	1.03	0.80	0.61	2.23	0.59	-1.99	-1.44
	Outlet	1.34-7.43	3.09	1.96	2.16	1.64	0.70		
TAN	Inlet	0.09-0.80	0.27	0.23	0.24	2.19	0.88	-1.32	-0.15
	Outlet	0.11-2.39	0.64	0.26	0.81	2.17	1.27		
ON	Inlet	0.18-1.24	0.53	0.43	0.35	1.65	0.65	-2.13	-1.81
	Outlet	0.7-4.27	1.66	1.22	1.25	1.89	0.75		
OP	Inlet	0.0015-0.035	0.01	0.01	0.01	1.64	1.21	0.10	-1.20
	Outlet	0.0015-0.0167	0.01	0.01	0.01	-0.30	0.73		
PBP	Inlet	0.014-0.18	0.06	0.04	0.06	1.78	0.97	-0.22	-0.52
	Outlet	0.04-0.15	0.08	0.06	0.04	1.83	0.48		
TP	Inlet	0.02-0.21	0.07	0.05	0.07	2.01	0.96	-0.12	-0.47
	Outlet	0.04-0.16	0.08	0.07	0.04	1.71	0.51		
TSS	Inlet	25.3-604	145	53	207	2.40	1.43	0.88	0.63
	Outlet	9-25	17.7	19.5	6.1	-0.39	0.34		

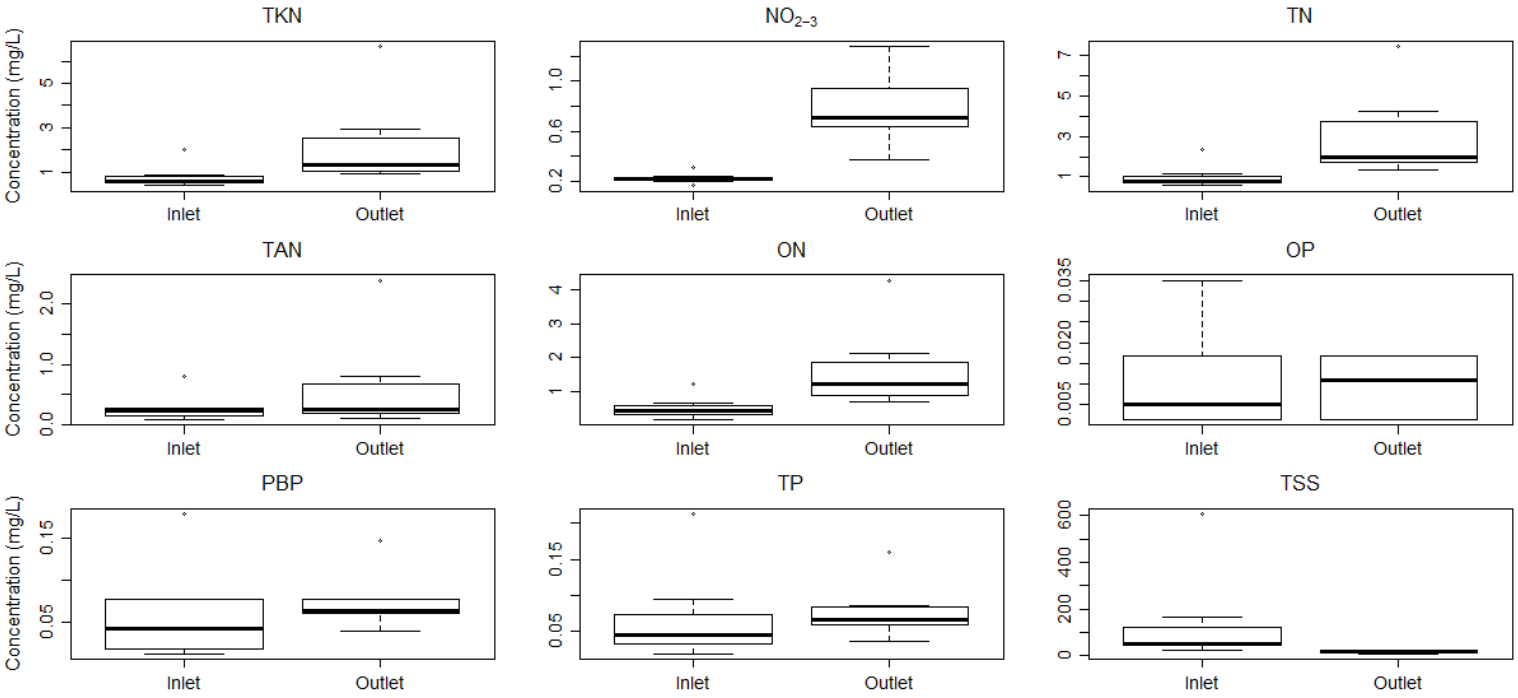

Figure 56. Boxplots of nutrient and sediment concentrations at the inlet and outlet of the bioretention cell at Ursuline College.

Lead and zinc were well sequestered in the Ursuline College bioretention cell, with ERs of 0.83 and 0.68, respectively. These were representative of reductions presented for these pollutants in other studies in the literature; mechanisms for removal include adsorption of dissolved metals to clay and organic matter particles and/or physical trapping of sediment-bound Pb and Zn (Davis 2007; Hunt et al. 2008; Jones and Davis 2013). Aluminum concentrations were little changed, and increases in Ca, Cu, Fe, Mg, and Mn were observed, with effluent concentrations as much as 11 times higher than influent. This was especially surprising given that most of these pollutants are majority sediment-bound, and sediment trapping within the Ursuline College BRC was observed in every sampled storm. Cu concentrations are typically reduced by 70% or more in bioretention cells (Feng et al. 2012; Søberg et al. 2014; Zhang et al. 2014). Feng et al. (2012) also found excellent retention of Fe and Al within bioretention media, with minimum 70% retention. Hunt et al. (2008) showed an ER of 0.54 for Cu for a bioretention

cell draining a commercial parking lot in Charlotte, NC. They also saw large exports of Fe (ER = 3.3); the authors maintained that this was due to the Fe-rich clays used in the media. On average, chloride concentrations increased substantially, and minimum six-fold increases were observed on a storm event basis. Muthanna et al. (2007) found similar results for bioretention cells treating snowmelt. In mesocosm-scale testing, Denich et al. (2013) found that only 10% of influent chloride mass was retained within the media. Sampling date appeared to affect chloride performance at the Ursuline College BRC, with the largest exports of chloride coming closest to winter (July) and the smallest exports were later in the sampling period (October) during both the 2014 and 2015 monitoring periods.

Table 38. Summary statistics for chloride and metals concentrations at the Ursuline College bioretention cell.

Pollutant	Location	Range (µg/L)	$\overline{x}$ (µg/L)	$\tilde{x}$ (µg/L)	s (µg/L)	C_s (µg/L)	CV (µg/L)	ER	RE_{median}
Cl	Inlet	0.5-2.73	1.00	0.50	0.90	1.61	0.90	-10.56	-17.87
	Outlet	2.99-29.6	11.56	9.43	9.31	1.40	0.81		
Al	Inlet	175-3055	821	491	1010	2.38	1.23	0.38	-0.15
	Outlet	242-857	507	565	217	0.33	0.43		
Ca	Inlet	6233-68840	19294	9188	22498	2.36	1.17	-1.93	-4.90
	Outlet	35620-81170	56447	54220	13674	0.56	0.24		
Cu	Inlet	1.96-16.3	6.33	4.26	4.96	1.70	0.78	-0.55	-1.04
	Outlet	4.25-20.2	9.79	8.69	5.11	1.60	0.52		
Fe	Inlet	291-5253	1409	856	1740	2.37	1.23	0.10	-0.59
	Outlet	709-1844	1270	1363	387	-0.05	0.31		
Mg	Inlet	498-17270	3963	1393	6023	2.38	1.52	-2.81	-10.76
	Outlet	8702-24690	15100	16380	5731	0.47	0.38		
Mn	Inlet	21.4-235	96	66	87	1.03	0.91	-3.55	-1.53
	Outlet	82.3-1904	435	168	655	2.53	1.50		
Pb	Inlet	1.57-22.81	6.14	2.93	7.51	2.41	1.22	0.83	0.67
	Outlet	0.54-1.63	1.03	0.98	0.34	0.53	0.33		
Zn	Inlet	19.54-131.5	44	27	39	2.44	0.89	0.68	0.47
	Outlet	6.62-19.69	14.2	14.2	4.1	-0.82	0.29		

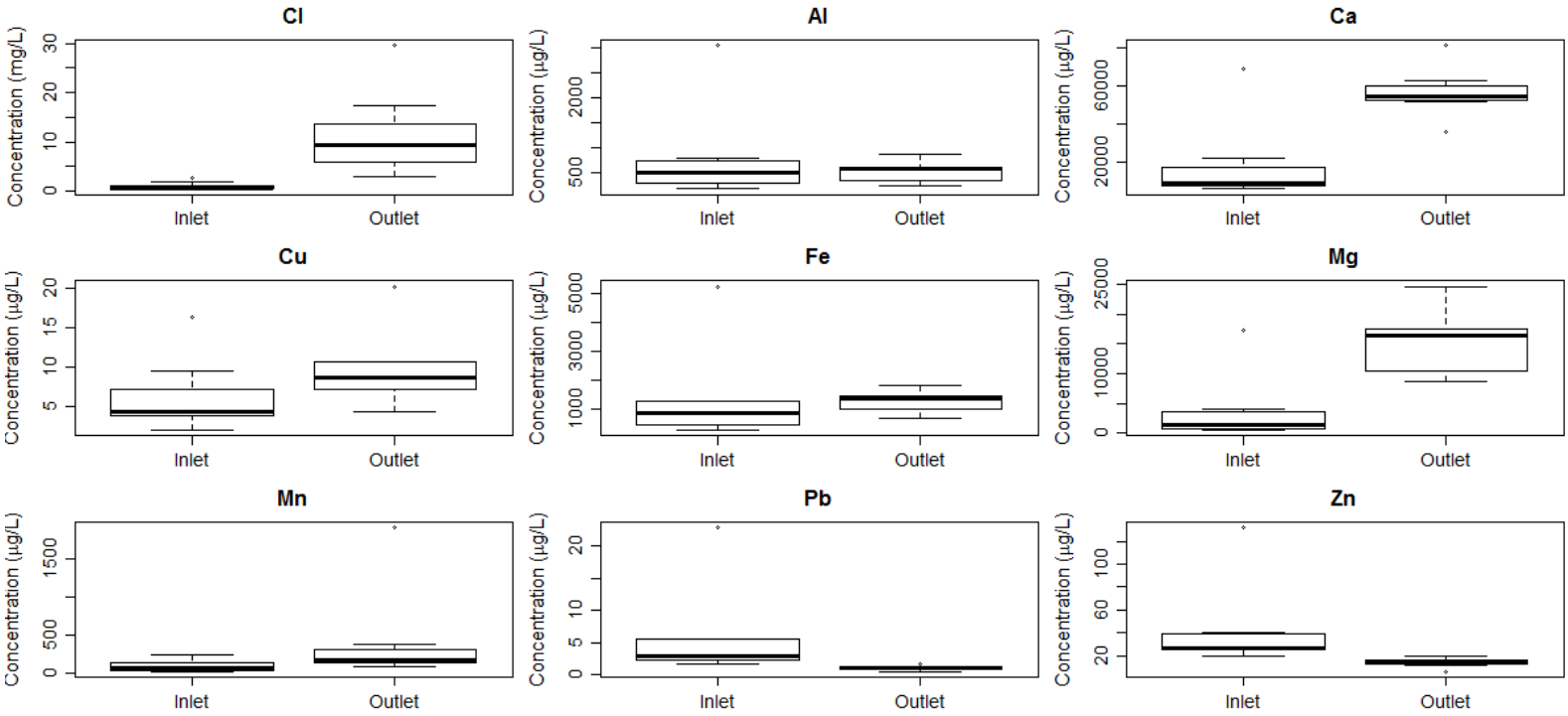

Figure 57. Boxplots of chloride and metals concentrations at the inlet and outlet of the bioretention cell at Ursuline College.

5.4.3 Nutrient, Chloride, and Metals Loading

Only ***seven*** storm events were able to be sampled for water quality at the Ursuline College site; therefore, see the caveats at the beginning of the previous section (5.4.2) about the interpretation of data.

Pollutant loads normalized by watershed area for the seven sampled and 46 non-sampled rainfall events during the 2014-2015 monitoring period at Ursuline College are presented in Table 39. An overall 59.5% volume reduction was observed for this bioretention cell, aiding in pollutant load reduction. The bioretention cell was a benefit for dissolved phosphorus loading, but this represented a very minor portion of the TP. TP mass was reduced by 11%. TSS load reduction was greater than 85%. Chloride load increased by 700%, suggesting leaching from the media after application to the watershed during the two winters. Loads of Al, Pb, and Zn were reduced from 53-87%; Cu, Pb, and Zn load reduction were supported by previous studies in the

literature (Davis 2007; Hunt et al. 2008; Davis et al. 2009; Feng et al. 2012). Total nitrogen loading increased by 40% as stormwater passed through the bioretention cell, even with a 59.5% runoff reduction. This was due to large increases in organic nitrogen concentrations. Pollutant loads also increased (i.e. net loss) for Ca, Mn, Mg, TAN, ON, TKN, and NO_{2-3}, as water passed through the bioretention cell. The leaching of certain metals, N, and lack of substantial capture of PBP indicated that perhaps organic matter was leaching (either solid phase or dissolved) from the media into the stormwater as it passed through the media. The color of the influent (left) and effluent (right) samples in Figure 58 supported this supposition. The 0.88 ER for TSS indicated general capture of solids in the bioretention cell, perhaps suggesting leaching of dissolved metals or metals adsorbed to organic matter. Careful selection of the type of organic matter used in bioretention media is needed to prevent resuspension and leaching as water moves through the media. Organic matter could be mixed only in the upper layers of the media, perhaps preventing its movement from the media and into the effluent from the BRC.

Table 39. Estimation of pollutant loading normalized by watershed area for the Ursuline College Bioretention Cell.

Monitoring Location	Pollutant Loads (g/ha)									
	Al	Ca	Cu	Fe	Mg	Mn	Pb		Zn	
Inlet	2212	44779	19.1	3827	7333	296	14.2		124	
Outlet	1041	98335	17.9	2489	30071	715	1.9		26	
Percent Difference	53	-120	6	35	-310	-142	87		79	
Monitoring Location	Pollutant Loads (kg/ha)									
	Cl	TKN	NO_{2-3}	TN	TAN	ON	TP	OP	PBP	TSS
Inlet	3	2.53	0.93	3.51	0.98	1.84	0.11	0.11	0.19	277
Outlet	20	3.70	1.32	4.90	0.98	2.89	0.09	0.05	0.14	35
Percent Difference	-704	-46	-41	-40	-1	-57	11	57	24	87

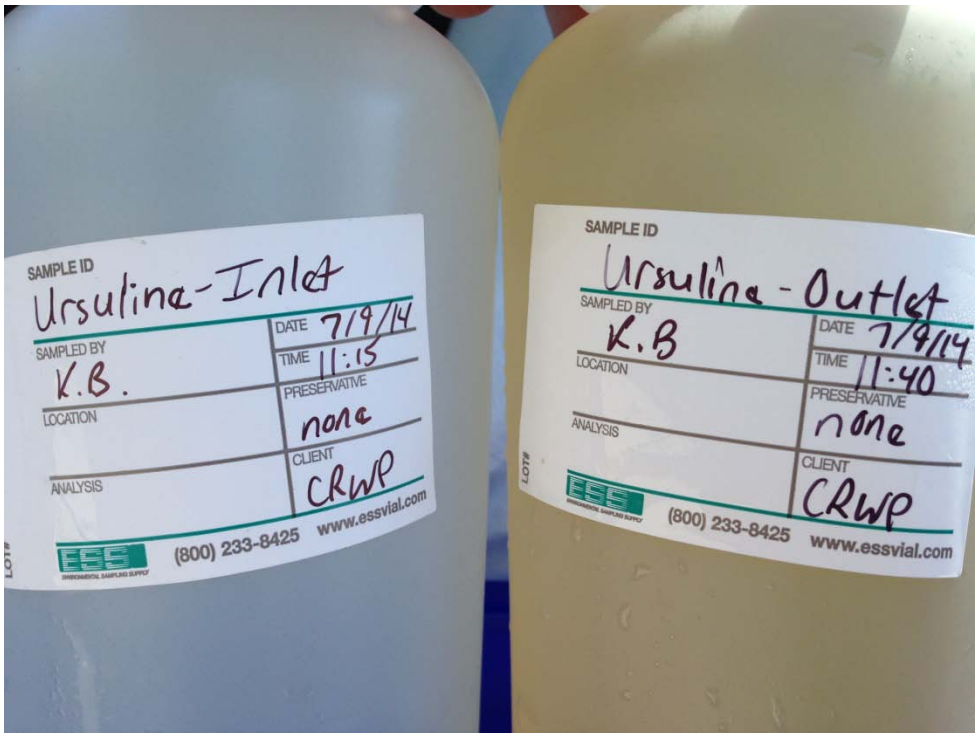

Figure 58. Color of inlet and outlet samples during July 9, 2014 storm event.

5.5 Summary and Conclusions

A bioretention cell was constructed to treat stormwater runoff from a parking lot on the campus of Ursuline College in Pepper Pike, Ohio in April-May, 2014. Seven months of

hydrologic and water quality monitoring of this system ensued in 2014, with an additional 3 months of monitoring in 2015. It should be noted that the conclusions related to water quality presented below are based on a data set of 7 water quality samples, and therefore caution should be used in interpretation and use of the data. The following preliminary conclusions can be drawn from this study:

1) The bioretention cell was a net source of nutrients (N and P), including both organic and inorganic N, and particle bound P (OP concentrations were essentially unchanged through the bioretention cell). Median influent TN and TP concentrations were low compared with those from typical parking lots at 0.80 and 0.05 mg/L; however, effluent TN concentrations were much higher than other studies on bioretention in the literature, suggesting that the media was leaching N into the stormwater. This limited data set suggests that if N and P capture are a primary goal, the media mix for the state of Ohio may need to be modified. The ER for TSS was 0.88, suggesting stilling of flow within the bioretention cell and filtration through the media allowed for particle capture.

2) Sequestration of lead and zinc occurred within the bioretention cell; each of the other five metals analyzed as well as chloride had higher median effluent concentrations than influent. Efficiency ratios for Ca, Mg, Mn, and, and chloride were all greater than -2.0. This may be related to an apparent loss of organic matter from the media. Chloride median effluent concentrations appeared to be related to season, and appeared to be directly related to the elapsed time since the last salt application in the parking lot. The addition of Osorb® appeared to have little impact on the pollutants studied.

3) Volume reduction in the Ursuline College bioretention cell was quite high given the underlying soil type, at 59.5%; this helped improve mass retention of pollutants. Estimates of

pollutant loading from the parking lot and exiting the bioretention system suggested excellent retention of solids and that it was a net zero for inorganic nitrogen. Metals retention was mixed, with net capture of Pb, Zn, Al, Cu and Fe, but net export of Ca, Mg, and Mn. Chloride mass increased by nearly 700% through the bioretention cell, suggesting leaching of chloride from the media. Mass of all forms of P was reduced by at least 11%. Loads of all forms of nitrogen increased as water passed through the bioretention cell. This along with the color of water quality samples suggested that the media was leaching dissolved and/or solid phase organic matter. The type and/or amount of organic matter in the typical bioretention mix in Ohio may need to be adjusted to prevent this from occurring in the future.

5.6 References

American Public Health Association (APHA), American Water Works Association (AWWA), and Water Environment Federation (WEF). (2012). *Standard methods for the examination of water and wastewater*, Ed. Laura Bridgewater. 22nd ed., Washington, DC.

Antweiler, R.C., and Taylor, H.E. (2008). "Evaluation of statistical treatments of left-censored environmental data using coincident uncensored data sets: 1. Summary statistics." *Environmental Science and Technology*. 42(10), 3732‑3738.

Bannerman, R.T., Owens, D.W., Dodds, R.B., and Hornewer, N.J. (1993). "Sources of pollutants in Wisconsin stormwater." *Water Science and Technology*. 28(3), 241-259.

Bartens, J., Day, S.D., Harris, J.R., Dove, J.E., and Wynn, T.M. (2008). "Can urban tree roots improve infiltration through compacted subsoils for stormwater management?" *Journal of Environmental Quality*, 37(6), 2048-2057.

Bratieres, K., Fletcher, T.D., Deletic, A., and Zinger, Y. (2008). "Nutrient and sediment removal by stormwater biofilters: A large-scale design optimisation study." *Water Research*. 42(14), 3930-3940.

Brown, R.A., and Hunt, W.F. (2011a). "Underdrain configuration to enhance bioretention exfiltration to reduce pollutant loads." *Journal of Environmental Engineering*. 137(11), 1082-1091.

Brown, R. A., and Hunt, W. F. (2011b). "Impacts of media depth on effluent water quality and hydrologic performance of undersized bioretention cells." *Journal of Irrigation and Drainage Engineering*. 137(3), 132-143.

Brown, R.A., and Hunt, W.F. (2012). "Improving bioretention/biofiltration performance with restorative maintenance." *Water Science and Technology*. 65(2), 361-367.

Carpenter, D.D., and Hallam, L. (2010). "Influence of planting soil mix characteristics on bioretention cell design and performance." *Journal of Hydrologic Engineering*. 15(6), 404-416.

Chin, D.A. (2006). *Water-Resources Engineering*. 2nd edition, Pearson Prentice Hall. NJ, USA.

Clark, S.E., and Pitt, R. (2009). "Storm-water filter media pollutant retention under aerobic versus anaerobic conditions." *Journal of Environmental Engineering*. 135(5), 367–371.

Davis, A.P., Shokouhian, M., Sharma, H., and Minami, C. (2006). "Water quality improvement through bioretention media: Nitrogen and phosphorus removal." *Water Environment Research*. 78(3), 284-293.

Davis, A.P. (2007). "Field performance of bioretention: Water quality." *Environmental Engineering Science*. 24(8), 1048-1064.

Davis, A.P. (2008). "Field performance of bioretention: Hydrology impacts." *Journal of Hydrologic Engineering*. 13(2), 90-95.

Davis, A.P., Hunt, W.F., Traver, R.G., and Clar, M. (2009). “Bioretention technology: Overview of current practice and future needs.” *Journal of Environmental Engineering*. *135*(3), 109-117.

Denich, C., Bradford, A., and Drake, J. (2013). “Bioretention: assessing effects of winter salt and aggregate application on plant health, media clogging and effluent quality.” *Water Quality Research Journal of Canada*. 48(4), 387-399.

Dietz, M.E., and Clausen, J.C. (2006). “Saturation to improve pollutant retention in a rain garden.” *Environmental Science and Technology*. 40(4), 1335-1340.

Dietz, M.E., and Clausen, J.C. (2008). “Stormwater runoff and export changes with development in a traditional and low impact subdivision.” *Journal of Environmental Management*. 87(4), 560-566.

Duranceau, S.J., and Biscardi, P.G. (2015). “Comparing adsorptive media use for the direct treatment of phosphorus-impaired surface water.” *Journal of Environmental Engineering*. 04015012.

Feng, W., Hatt, B.E., McCarthy, D.T., Fletcher, T.D., and Deletic, A. (2012). “Biofilters for stormwater harvesting: understanding the treatment performance of key metals that pose a risk for water use.” *Environmental Science and Technology*. 46(9), 5100-5108.

Finkenbine, J.K., Atwater, J.W., Mavinic, D.S. (2000). “Stream health after urbanization.” *Journal of the American Water Resources Association*. 36(5), 1149-1160.

Hathaway, J.M., Hunt, W.F., Graves, A.K., and Wright, J.D. (2011). “Field evaluation of Bioretention indicator bacteria sequestration in Wilmington, North Carolina. *Journal of Environmental Engineering.* 137, 1103–1113.

Hatt, B.E., Fletcher, T.D., and Deletic, A. (2009). “Hydrologic and pollutant removal performance of stormwater biofiltration systems at the field scale.” *Journal of Hydrology*. 365(3), 310-321.

Hunt, W.F., Jarrett, A.R., Smith, J.T., and Sharkey, L.J. (2006). “Evaluating bioretention hydrology and nutrient removal at three field sites in North Carolina.” *Journal of Irrigation and Drainage Engineering*. 132(6), 600–608.

Hunt, W.F., Smith, J.T., Jadlocki, S.J., Hathaway, J.M., and Eubanks, P R. (2008). “Pollutant removal and peak flow mitigation by a bioretention cell in urban Charlotte, NC.” *Journal of Environmental Engineering*. 134(5), 403-408.

Hunt, W.F., Davis, A.P., and Traver, R.G. (2012). “Meeting hydrologic and water quality goals through targeted bioretention design.” *Journal of Environmental Engineering*. 138(6), 698-707.

Jenkins, J.K.G., Wadzuk, B.M., and Welker, A.L. (2010). “Fines accumulation and distribution in a storm-water rain garden nine years postconstruction.” *Journal of Irrigation and Drainage Engineering*. 136(12), 862-869.

Jones, P.S., and Davis, A.P. (2013). “Spatial accumulation and strength of affiliation of heavy metals in Bioretention media.” *Journal of Environmental Engineering*. 139(4), 479-487.

Li, H., and Davis, A.P. (2008). “Urban particle capture in bioretention media I: laboratory and field studies.” *Journal of Environmental Engineering*. 134(6), 409–418.

Li, H., and Davis, A.P. (2009). “Water quality improvement through reductions of pollutant loads using bioretention.” *Journal of Environmental Engineering.* 135(8), 567–576.

Li, H., Sharkey, L.J., Hunt, W.F., and Davis, A.P. (2009). “Mitigation of impervious surface hydrology using bioretention in North Carolina and Maryland.” *Journal of Hydrologic Engineering*. 14(4), 407-415.

Li, Y.L., McCarthy, D.T., and Deletic, A. (2014). “Stable copper-zeolite filter media for bacteria removal in stormwater.” *Journal of Hazardous Materials*. 273, 222-230.

Liu, J., and Davis, A.P. (2013). “Phosphorus speciation and treatment using enhanced phosphorus removal bioretention.” *Environmental Science and Technology*. 48(1), 607-614.

Liu, J., Sample, D.J., Bell, C., and Guan, Y. (2014). “Review and research needs of bioretention used for the treatment of urban stormwater.” *Water*. 6(4), 1069-1099.

Lucas, W.C., and Greenway, M. (2008). “Nutrient retention in vegetated and nonvegetated bioretention mesocosms.” *Journal of Irrigation and Drainage Engineering*. 134(5), 613-623.

Lucas, W.C., and Greenway, M. (2011a). “Hydraulic response and nitrogen retention in bioretention mesocosms with regulated outlets: Part I—hydraulic response.” *Water Environment Research*. 83(8), 692-702.

Lucas, W.C., and Greenway, M. (2011b). “Hydraulic response and nitrogen retention in bioretention mesocosms with regulated outlets: Part II—nitrogen retention.” *Water Environment Research*. 83(8), 703-713.

Luell, S.K., Hunt, W.F., and Winston, R.J. (2011). “Evaluation of undersized bioretention stormwater control measures for treatment of highway bridge deck runoff.” *Water Science and Technology*. 64(4), 974-979.

McNett, J.K., Hunt, W.F., and Davis, A.P. (2011). “Influent pollutant concentrations as predictors of effluent pollutant concentrations for mid-Atlantic bioretention.” *Journal of Environmental Engineering*. 137(9), 790-799.

Mehlich, A. (1984). “Mehlich 3 soil test extractant: A modification of Mehlich 2 extractant.” *Communications in Soil Science and Plant Analysis*. 15(12), 1409-1416.

Meyer, S.C. (2004). “Analysis of base flow trends in urban streams, northeastern Illinois, USA.” *Hydrogeology Journal*. 13(5–6), 871–885.

Muthanna, T.M., Viklander, M., Blecken, G., and Thorolfsson, S.T. (2007). “Snowmelt pollutant removal in bioretention areas.” *Water Research*. 41(18), 4061-4072.

Natural Resources Conservation Service (NRCS). (1986). *Urban hydrology for small watersheds*. Technical Release 55 (TR-55). 2nd edition. United States Department of Agriculture (USDA), Natural Resources Conservation Service, Conservation Engineering Division.

Norris, M.J., Pulford, I.D., Haynes, H., Dorea, C.C., and Phoenix, V.R. (2013). "Treatment of heavy metals by iron oxide coated and natural gravel media in sustainable urban drainage systems." *Water Science and Technology*. 68(3), 674-680.

North Carolina Department of Environment and Natural Resources (NCDENR). (2007). *Stormwater Best Management Practices Manual*. Chapter 12: Bioretention. Raleigh, NC. Available: http://portal.ncdenr.org/web/lr/bmp-manual

Ohio Department of Natural Resources (ODNR), Division of Soil and Water Conservation. (2006). *Rainwater and land development: Ohio's standards for stormwater management, low impact development, and urban stream protection*. 3rd edition. Ed: John Mathews.

O'Neill, S.W., and Davis, A.P. (2012). "Water treatment residual as a bioretention amendment for phosphorus. I: Evaluation studies." *Journal of Environmental Engineering*. 138(3), 318-327.

Passeport, E., Hunt, W.F., Line, D.E., Smith, R.A., and Brown, R.A. (2009). "Field study of the ability of two grassed bioretention basins to reduce storm-water runoff pollution." *Journal of Irrigation and Drainage Engineering.* 135(4), 505-510.

Passeport, E., and Hunt, W.F. (2009). "Asphalt parking lot runoff nutrient characterization for eight sites in North Carolina, USA." *Journal of Hydrologic Engineering*. 14(4), 352-361.

Payne, E.G., Pham, T., Cook, P.L., Fletcher, T.D., Hatt, B.E., and Deletic, A. (2014). "Biofilter design for effective nitrogen removal from stormwater–influence of plant species, inflow hydrology and use of a saturated zone." *Water Science and Technology*. 69(6), 1312-1319.

Pitt, R., Chen, S.E., Clark, S.E., Swenson, J., and Ong, C.K. (2008). "Compaction's impacts on urban storm-water infiltration." *Journal of Irrigation and Drainage Engineering*. 134(5), 652-658.

R Core Team. (2014). *A language and environment for statistical computing*. R Foundation for Statistical Computing. Vienna, Austria.

Reddy, K.R., Xie, T., and Dastgheibi, S. (2014a). "Nutrients removal from urban stormwater by different filter materials." *Water, Air, and Soil Pollution*. 225(1), 1-14.

Reddy, K.R., Xie, T., and Dastgheibi, S. (2014b). "Evaluation of biochar as a potential filter media for the removal of mixed contaminants from urban storm water runoff." *Journal of Environmental Engineering*. 140(12), 04014043.

Schoonover, J.E., and Lockaby, B.G. (2006). "Land cover impacts on stream nutrients and fecal coliform in the lower Piedmont of West Georgia." *Journal of Hydrology*. 331(3–4), 371–382.

Sharma, N.C., Sahi, S.V., Jain, J.C., Raghothama, K. G. (2004) “Enhanced accumulation of phosphate by *Lolium multiflorum* cultivars grown in phosphate-enriched media. *Environmental Science and Technology*. 38 (8), 2443-2448.

Søberg, L.C., Viklander, M., and Blecken, G.T. (2014). “The influence of temperature and salt on metal and sediment removal in stormwater biofilters.” *Water Science and Technology*. 69(11), 2295-2304.

Soil Survey Staff, Natural Resources Conservation Service, United States Department of Agriculture. (2015). Web Soil Survey. http://websoilsurvey.nrcs.usda.gov/. Accessed 28 January 2015.

Strecker, E.W., Quigley, M.M., Urbonas, B.R., Jones, J.E., and Clary, J.K. (2001). “Determining urban storm water BMP effectiveness.” *Journal of Water Resources Planning and Management*. 127(3), 144-149.

U.S. Environmental Protection Agency (U.S. EPA). (1983a). *Results of the nationwide urban runoff program, volume 1*. EPA, Office of Research and Development.

U.S. Environmental Protection Agency (U.S. EPA). (1983b). *Methods of chemical analysis of water and waste*. EPA-600/4-79-020, Cincinnati, Ohio.

U.S. EPA. (2002). Urban storm water BMP performance monitoring: a guidance manual for meeting the national storm water BMP database requirements. EPA-821-B- 02-001,Washington, DC.

Williamson, S. C., Bartholow, J.M., and Stalnaker, C.B. (1993). “Conceptual model for quantifying pre-smolt production from flow- dependent physical habitat and water temperature.” *Regulated Rivers: Research and Management.* 8: 15-28.

Wilson, C.E., Hunt, W.F., Winston, R.J., and Smith, P. (2015). “Comparison of runoff quality and quantity from a commercial low-impact and conventional development in Raleigh, North Carolina.” *Journal of Environmental Engineering*. 141(2), 05014005.

Zhang, Z., Rengel, Z., Liaghati, T., Antoniette, T., and Meney, K. (2014). “Influence of plant species and submerged zone with carbon addition on nutrient removal in stormwater biofilter.” *Ecological Engineering*. 37(11), 1833-1841.

6 PERMEABLE PAVEMENT CLOGGING STUDY

6.1 Review of Literature

Urbanization causes detrimental effects on surface waters through increases in the rate and volume of stormwater conveyed through storm sewer systems (Leopold et al. 1964). Impervious cover, such as rooftops, roadways, and parking lots, reduces the potential for infiltration and evapotranspiration within a watershed. Source-control stormwater management, where small distributed stormwater control measures (SCMs) are placed throughout the watershed, has gained popularity in recent years (Page et al. 2015). One method of reducing effective impervious cover within a watershed is to use permeable pavement, an alternative to traditional asphalt or concrete surfaces.

Permeable interlocking concrete pavers (PICP), pervious concrete (PC), and porous asphalt (PA) are all commonly-used pavements developed to have inherent permeability. In contrast to impermeable pavements, rainfall infiltrates the pavement surface, where it enters an underground storage reservoir. Depending on project goals and site conditions, the underground reservoir can be designed to provide extended detention, exfiltration into the underlying soil, or both. Exfiltrating systems recharge the groundwater (Brattebo and Booth 2003; Gilbert and Clausen 2006; Collins et al. 2008). When compared to conventional pavements, permeable pavements reduce runoff volume and peak rate, while delaying peak flows (Pratt et al. 1989; Fassman and Blackbourn 2010). Because of their hydrologic benefits, permeable pavements are one of the favored tools of Low Impact Development (LID). Permeable pavements also provide a number of water quality benefits, including filtration and settling of sediment and sediment-bound pollutants (Roseen et al. 2012). Given that permeable pavements serve the dual role of parking

surface and SCM, there has been a recent surge in installation of these systems across northern Ohio.

Widespread adoption of permeable pavements has been hampered by concerns about cost, winter performance, and the frequency and effort of maintenance (Roseen et al. 2012). Newly installed pervious concrete (PC) and permeable interlocking concrete pavers (PICP) had surface infiltration rates (SIR) in the range of 800-2600 and 800-1600 in/hr, respectively (Bean et al. 2007). Over time, the pore spaces in permeable pavements begin to clog with organic debris, sediment, and grit, causing a decrease in SIR. As larger particles clog the void spaces, small particles begin to be trapped, resulting in further reduction of SIR (Pratt et al. 1995). Clogging potential is a function of both particle size distribution of the sediment in the runoff and the pore size distribution of the void spaces (Sansalone et al. 2008). Fassman and Blackbourn (2010) suggested clogging is a function of land uses surrounding the permeable pavement, rather than traffic load. Thus, maintenance of permeable pavements is needed to prevent surface runoff and ensure treatment functionality (Bean et al. 2007).

Research has shown in most cases clogging occurs near the surface of the pavement, with removal of clogging material from the top 1 inch (Gerrits and James 2002) or 0.5-0.75 inches (Bean et al. 2007) of pavement resulted in significant increases in SIR. Clogging can cause 100-fold reductions in SIR of permeable pavements (Illgen et al. 2007). In Australia and the Netherlands, research has shown an exponential decay of SIR as a function of age of the permeable pavement, reaching a 20-40 in/hr rate within 3-4 years (Boogaard et al. 2014a). Two porous asphalt sites treating direct rainfall in northern Sweden had SIR of 4420 and 7160 in/hr immediately after construction (Al-Rubaei et al. 2013). Approximately 2 years later (without maintenance), these rates had decreased to 290 in/hr and 107 in/hr, respectively. After 18 and 24

years, SIRs were 7.5 and 3.3 in/hr, showing that without maintenance, a continually decreasing trend in SIR throughout the life of the pavement will occur. Seven years post-construction, eight PICP test sites in the Netherlands had SIRs between 7 and 87 in/hr (Boogaard et al. 2014b).

Maintenance of permeable pavements typically is performed using street sweepers. Various types, including bristle sweepers, regenerative air sweepers, and vacuum trucks may be used to remove the clogging layer. The latter two types also apply suction to the pavement, while bristle sweepers only sweep the pavement surface. Dougherty et al. (2011) studied a heavily clogged pervious concrete sidewalk, and found that pressure washing (200 in/hr post-maintenance SIR) and pressure washing with power blowing (260 in/hr post-maintenance SIR) effective in rejuvenating pavement permeability. A porous asphalt in northern Sweden was maintained using pressure washing and vacuum cleaning, with a subsequent increase in mean SIR from 7.5 to 53 in/hr (Al-Rubaei et al. 2013). Drake and Bradford (2013) found the SIR of PICP responded more to vacuum-cleaning than did pervious concrete or porous asphalt, suggesting more difficult remediation for the latter two pavement types. During destructive testing of PICP in Australia, Lucke (2014) showed sediment migrates to the bedding course beneath the PICP; the authors contended this is the reason that efforts to return SIR to newly-installed rates have not succeeded. While most permeable pavement applications constructed in the USA today accept run-on from impermeable pavement (as opposed to treating only direct rainfall), only *two* research studies have investigated clogging rates in these situations (Pezzaniti et al. 2009; Lucke and Beecham 2011), and *none* have researched maintenance on these more heavily taxed (in terms of sediment loading) systems.

A laboratory study on clogging of pervious concrete by clay-laden runoff was conducted by Haselbach (2010). During laboratory tests, repeated applications of different types of clay-water

mixtures resulted in clogging, with the vast majority of sediment accumulated at the surface of the pavement. After four wet-dry cycles with clay-laden synthetic runoff, SIR was reduced by minimum and maximum factors of 5 and 90, respectively. The SIR was substantially improved using surface sweeping and subsequent washing, albeit the SIRs never returned to their initial rates. Drake and Bradford (2013) also found maintenance of PA, PC, and PICP only achieved partial restoration of initial SIR. This suggests a long-term decline in SIR, even with prescribed maintenance at regular intervals. Brown and Borst (2013) found clogging began at the upgradient end of the permeable pavement on a permeable pavement with a high impermeable to permeable pavement area ratio (9.7:1). Within 12 storm events, the clogging had progressed nearly the entire length of the permeable pavement application, suggesting frequent maintenance would be needed with this level of hydrologic loading.

Given that permeable pavements clog with organic debris, sediment, and grit over time, a study was devised to determine potential factors that affect rates of clogging. Engineers in recent years have begun to design these SCMs to receive run-on from impermeable pavements to reduce their per square foot cost. This, among other factors (such as tree cover, traffic loading, rainfall characteristics, etc.), affects the frequency of maintenance needed to prevent permeable pavements from completely clogging. Based on recommendations in Brown and Borst (2014), five to eight fixed locations were established at each of five permeable pavement sites for quarterly testing of surface infiltration rates (SIR). SIR tests repeated over time at these fixed locations allowed for identification of locations that clog quickly (and may need frequent spot maintenance), as well as assessment of SIR recovery provided by various types of maintenance. Additionally, a comparison of the ASTM standard and a simple infiltrometer (furnished from easily-obtained materials) was made.

6.2 Site Descriptions

Five permeable pavement installations were monitored for SIR, with between 5 and 8 test locations established at each permeable pavement site for repeated infiltration tests over time (Table 40). The SIR monitoring locations were selected to determine the rate at which clogging occurs as a function of several factors, including rainfall depth, impermeable to permeable pavement area ratio, tree cover, run-on from pervious surfaces, locations near the permeable/impermeable pavement interface (PII), raveling of PC, etc. (Table 41). The impervious to pervious ratio was the average for the entire permeable pavement, and was not representative of areas that received preferentially more flow due to grading of the watershed. Because Perkins Township had roof runoff routed to the subgrade of the pavement, it did not contribute to clogging of the pavement surface (see section 1.1.2 for additional detail). Monitoring at three sites located in Ohio (Willoughby Hills, Orange Village, and Perkins Township) was funded by the NERRS Science Collaborative grant, while the two sites in North Carolina (Piney Wood and North Carolina Central University [NCCU]) were funded by other sources. Since the collective data provide a better understanding of where and how fast clogging occurs, data from both Ohio and North Carolina were analyzed.

Table 40. Characteristics of the five permeable pavement sites monitored for clogging using SIR tests.

Site Name	Surface Course	Impervious Pavement Run-on	Impervious to Pervious Ratio	Date Built	Initial Infiltration Tests	Q1 Test Date	Q2 Test Date	Q3 Date	Maintenance Dates
Orange Village	PICP	None	0	Oct 2013	4/24/2014	7/9/2014	10/13/2014	N/A	N/A
Willoughby Hills	PICP	Asphalt	7.23, 2.17	Oct 2013	4/24/2014	7/9/2014	10/13/2014	N/A	8/6/2014
Perkins Township	Pervious Concrete	Concrete	0.62, 0.75	Nov 2012	4/23/2014	7/7/2014	10/14/2014	N/A	N/A
Piney Wood	PICP	Asphalt	1.8	March 2014	4/18/2014	7/18/2014	10/17/2014	1/29/2015	8/15/2014

NCCU	PICP	Asphalt	6.5	July 2013	5/3/2014	10/6/2014	1/22/2015	N/A	10/9/2014, 10/10/2014

Table 41. Characteristics of the SIR monitoring sites.

Site	Test Location	Test Focus Area	Distance from PII (inches)
Orange Village	1	Tree	-
	2	Entry	-
	3	Entry	-
	4	Control	-
	5	Parking	-
Willoughby Hills	1	PII[1]	30
	2	Concentrated	-
	3	Pervious/Sidewalk	-
	4	Control	-
	5	PII	15
	6	PII	72
	7	PII	22
	8	PII	94
Perkins Township	1	Control	-
	2	Control	-
	3	Raveling	-
	4	Parking	-
	5	Parking	-
	6	PII	14
	7	PII	87
Piney Wood	1	PII	48
	2	PII	24
	3	PII	72
	4	Control	-
	5	Tree	-
	6	Control	-
NCCU	1	PII	12
	2	PII	24
	3	Concentrated	-
	4	Sidewalk	-
	5	Concentrated	-

[1] PII is the permeable-impermeable interface.

[2] Test location 4 was located in the middle of the parking stall, while location 5 was in a tire track.

Five locations were established for SIR testing at Orange Village, a PICP parking lot designed with no run-on from impermeable pavement (Figure 59). The first location was chosen due to its location below a tree because clogging from leaves and organic detritus has been cited as an important factor (Hunt 2011; Lucke and Beecham 2011). Locations 2 and 3 were established to determine the clogging that might occur from materials carried by tires as cars enter the permeable pavement; the concrete apron was sloped away from the parking lot, meaning that no run-on occurred near the permeable/impermeable interface (PII). Location 5 was situated in an infrequently used handicapped parking stall. Location 4 was a control location in the middle of the drive aisle, presumably receiving little detritus that might clog the pavement. SIR testing was completed at Orange Village in April, July, and October of 2014. Maintenance was not performed at Orange Village during the monitoring period, as SIRs were adequately high to prevent surface runoff.

Figure 59. Locations of SIR tests conducted at Orange Village, Ohio.

At the Willoughby Hills site, two PICP applications were installed to treat runoff from an approximately 12 year old asphalt parking lot. The PICP was installed in October of 2013 in Small and Large applications (Figure 60), with differing impermeable/permeable run-on ratios of 7.2 and 2.2, respectively. Three SIR test locations were established in the Small application, with one apiece near the PII, near an area receiving run-on from a seal-coated walking trail (and adjacent pervious areas), and one as a control (location 2). Two pairs of PII monitoring locations were established in the Large application (locations 5-8); both of these locations received runoff from upslope parking lot islands whose curbing caused flow to concentrate. Location 4 was established as a control, and did not receive run-on from impermeable asphalt.

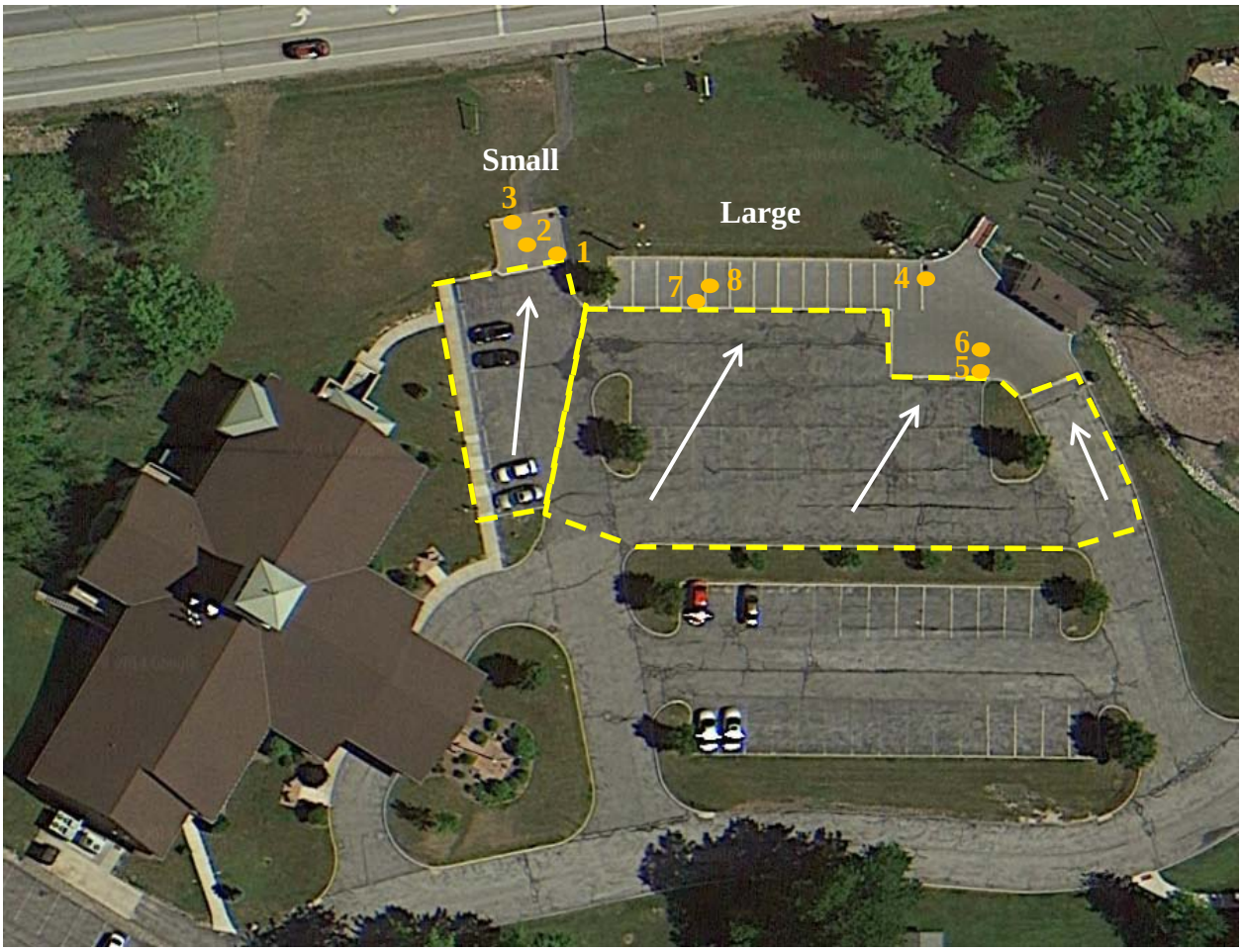

Figure 60. Locations of SIR tests conducted at Willoughby Hills, Ohio.

The Perkins Township pervious concrete site was constructed in October-November 2012, with six different areas of pervious concrete parking stalls installed to drain the standard concrete drive lanes (Figure 61). Seven SIR monitoring locations were established. Very low impermeable to permeable ratios existed at this site, with values of 0.62 and 0.75 for SIR monitoring locations 1-5 and 6-7, respectively. Locations 1 and 2 effectively served as controls for the site, being located in the middle of parking stalls and 10 ft from the PII. Location 3 was located in a bay of PC that did not cure properly, and thus pavement surface raveling was occurring. Locations 4 and 5 were immediately adjacent to one another, with location 5 located in the center of the parking stall and location 4 in an obvious tire path in the PC caused by

deposition of sediment from vehicle tires. This parking stall was used daily during the business week. Locations 6 and 7 were chosen to determine the progression of clogging from the PII.

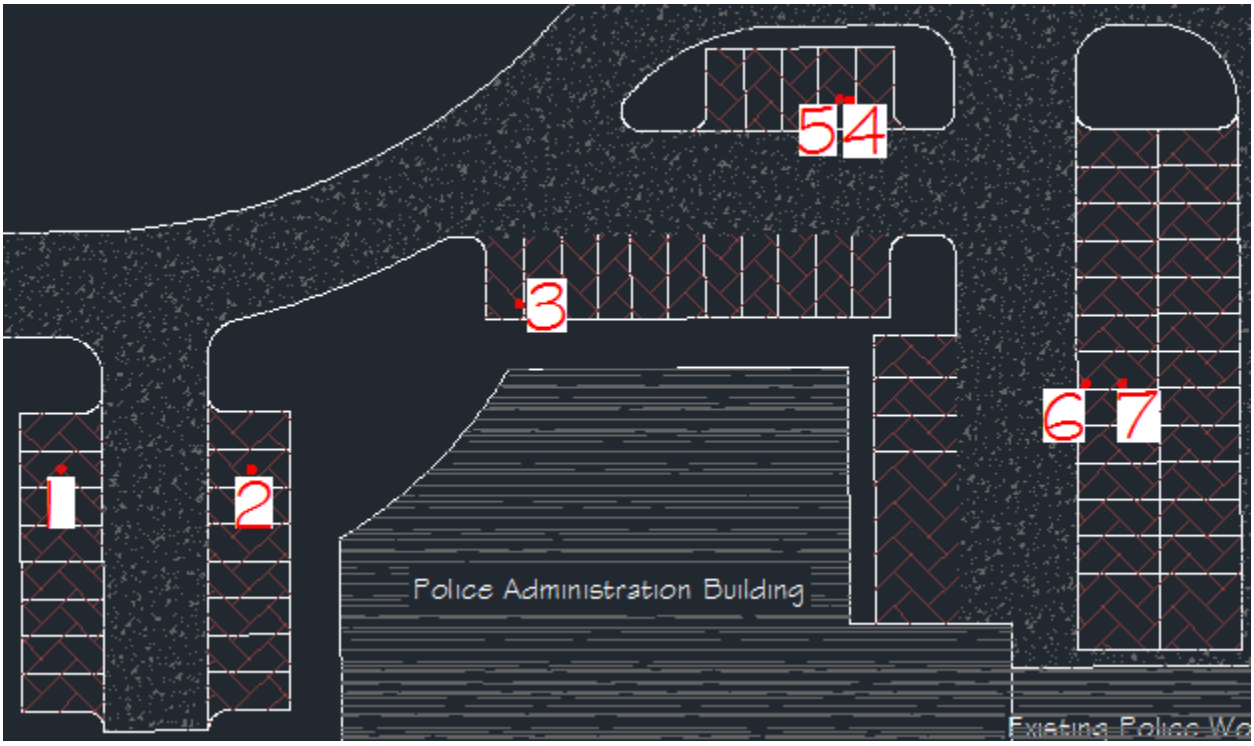

Figure 61. Locations of SIR tests conducted at the Perkins Township, Ohio site. PC is shown in brown hatching. Concrete drive aisles were crowned in the center and drained to the PC.

The NCCU law school parking lot in Durham, North Carolina, was retrofitted with 5 PICP parking stalls to treat runoff from a catchment with impervious area 6.5 times larger than the permeable pavement surface area (Figure 62). Due to a surface cross-slope of the existing parking lot, a speed bump was installed in the watershed to prevent flow from bypassing the permeable pavement. This resulted in a concentrated flow regime as water entered the PICP. Locations 1 and 2 were chosen to determine the progression of clogging as water was shunted onto the PICP by the speed bump. Locations 3 and 5 were located along the cross-slope to determine the progression of clogging from the concentrated flow path (assumed to occur at a greater rate than for diffuse flow onto permeable pavement). Location 4 was originally selected

as a control, but it received flow from the adjacent slope and sidewalk, and so did not serve that purpose.

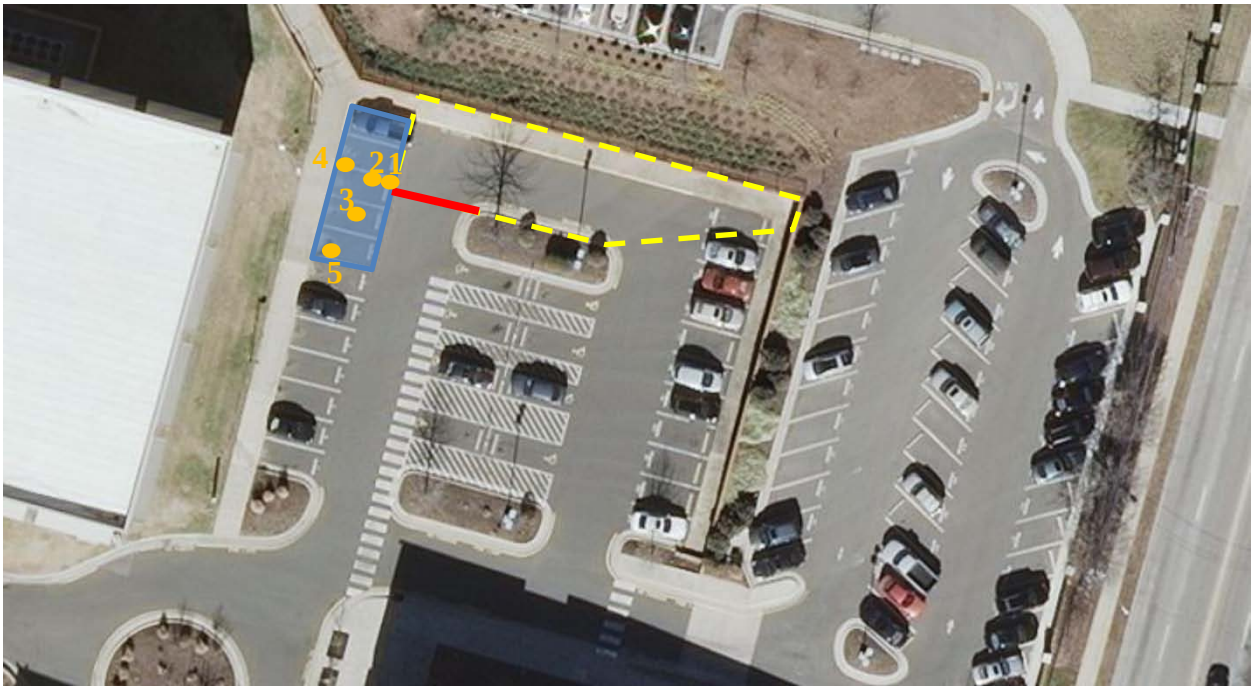

Figure 62. Locations of SIR tests conducted at the NCCU permeable pavement parking lot. Location of the PICP lot is hatched in blue. The speed bump is shown in red. The watershed is outlined with hashed yellow lines.

Four stalls of PICP were installed as a retrofit at an existing asphalt parking lot at Piney Wood park in Durham, North Carolina (Figure 63). The watershed was approximately 1.8 times larger than the surface area of the permeable pavement; this was difficult to judge, however, as the parking lot was so flat as to complicate catchment delineation and flow path determination, even with a total station survey of the watershed. Run-on entered the permeable pavement in a diffuse manner, with SIR monitoring locations 1-3 chosen to determine clogging at the PII. Sites 4 and 6 served as controls for the site, while site 5 was located beneath a tree.

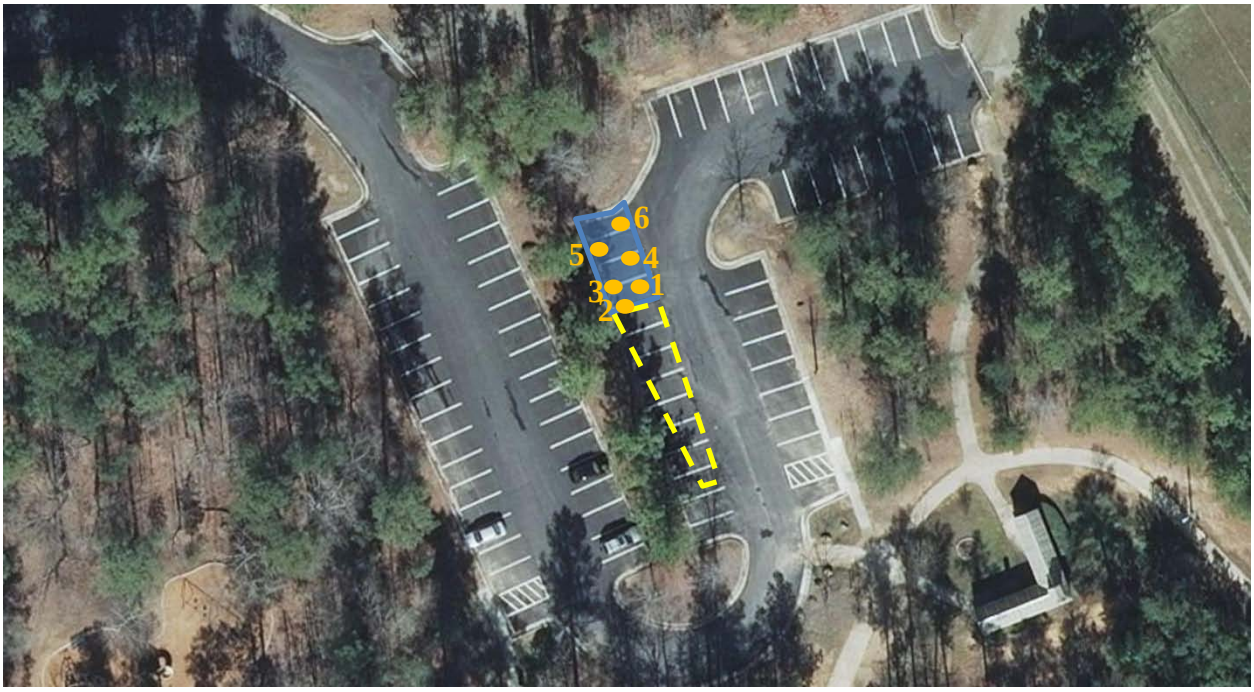

Figure 63. Locations of SIR testing at Piney Wood park in Durham, NC. The PICP parking lot is hatched in blue, with the watershed outlined using a yellow dashed line.

All five permeable pavement sites were visited quarterly to conduct SIR testing. Sites were not regularly maintained with street sweepers, but were maintained as needed when SIR tests showed substantial clogging (Table 40). Maintenance was not required at either Orange Village (due to the site receiving little run-on) or Perkins Township (perhaps due to clean influent or due to run-on ratios <1). Winter maintenance at the three Ohio sites consisted of road salt application as needed and snow plowing following each winter weather event. In North Carolina, snowfall happened much more infrequently, and neither plowing nor salting occurred during the monitoring period. By the time SIR testing commenced, Perkins Township had experienced two winters, while Orange Village and Willoughby Hills had endured one apiece.

The first SIR tests were conducted in April-May 2014. This was 8 months post-construction for Orange Village and Willoughby Hills, 28 months for Perkins Township, 1 month for Piney Wood, and ten months for NCCU, respectively. From that point, infiltration tests were

conducted approximately quarterly, except during the winter at the Ohio sites, when snow accumulation precluded testing. Infiltration testing at all locations at a monitoring site also was conducted immediately following maintenance.

6.3 Materials and Methods

6.3.1 Data Collection

Testing of SIR at the five sites utilized two different methods to compare a standard method with a newly-developed simple infiltration test (SIT) method. The single ring, constant head test described in ASTM C1781 for PICP (ASTM 2013) and ASTM C1701 for PC (ASTM 2009) was utilized as a baseline for SIR. This method is simpler than the double ring infiltrometer method used by Bean et al. (2007) and Drake and Bradford (2013) for permeable pavement SIR testing in that only one 12-in diameter infiltrometer must be sealed to the pavement surface using plumber's putty (Figure 64). To create an effective seal, both the inner and outer edges of the infiltrometer where it contacted the permeable pavement were sealed in this fashion. A ruler was used to measure water depth in a nearly-full bucket (typically about 4.75 gallons) and a rating curve used to determine the volume of water applied to the pavement. Water was transferred from the bucket into the infiltrometer by pouring as close to the pavement surface as possible, to prevent dislodging of the crusted clogging material near the pavement surface. The water level was kept at a constant head within the infiltrometer between 0.4 and 0.6 inches above the pavement surface. Typically, the entire volume of water was poured through the infiltrometer and total time recorded, thus allowing the calculation of infiltration rate. However, for heavily clogged permeable pavements, this could take several hours per test. Thus, the testing method was modified to pour as much water as possible within 15 minutes while still meeting other

aforementioned requirements, and the leftover volume in the bucket was recorded. This was deducted from the initial volume before calculating infiltration rate (Equation 6.1). This facilitated shorter duration tests lasting less than 1 hour in all cases.

$$I = \frac{K*(M_i - M_f)}{D^2*t} \quad (6.1)$$

where I is surface infiltration rate (SIR, in/hr), K is a conversion factor (126870 in^3*s/(lb*hr)) M_i is the initial mass of water (lb), M_f is the final mass of water (zero unless pavement was clogged, lb), D is the diameter of the infiltrometer (in), and t is the time for infiltration to occur (seconds).

Figure 64. ASTM surface infiltration rate tests on PC (left) and PICP (right).

The SIT methods can be carried out with materials purchased from a home improvement store. The infiltrometer was constructed by cutting an 8 ft long 2" by 4" board into four equal lengths, and screwing them together to make a square (Figure 65). All other testing methodologies were similar to those for the ASTM method, except the SIT was a falling head test. The entire initial volume (approximately 4.75 gallons of water) was placed in the infiltrometer, and the time to infiltrate that volume recorded. The infiltration rate was calculated as the depth of water applied over the time:

$$I = \frac{K*M}{L^2*t} \quad (6.2)$$

where I is surface infiltration rate (SIR, in/hr), K is a conversion factor (161536 $in^{3*}s/lb*hr$)), M is the initial mass of water (lb), L is the length of each side of the infiltrometer (in), and t is the time for infiltration to occur (seconds).

The SIT method resulted in much quicker quantification of SIR because in the SIT (1) a greater head is applied initially and (2) the SIT had a 440% greater surface area than that of the ASTM test. This would allow maintenance personnel to more efficiently and cost-effectively determine when and where maintenance is needed within a particular permeable pavement application.

Figure 65. Surface infiltration rate testing using the SIT method on PC (left) and PICP (right).

During each round of SIR tests, three SIT and two ASTM replicates were completed at each testing location at each of the five monitored permeable pavements. Greater replication was needed for the SIT, as the test would often last less than 30 seconds under optimal pavement conditions, meaning that the error in timing was magnified. SIR testing was performed within the same day at each site, with the order of testing (SIT and ASTM) randomized. Testing was

also conducted following any maintenance of the pavement to determine the potential improvements in SIR and assess remediation of clogging.

6.3.2 Data Analysis

Field collected data were utilized to calculate SIR for each test performed in the field. Within a permeable pavement parking lot, large spatial variability in SIR has been observed (Drake and Bradford 2013). To determine locations where clogging occurs most quickly (and therefore should be prioritized for maintenance), data were categorized by location. Reduction in SIR was characterized from the start to the end of each quarter (i.e. the testing window), and any maintenance activities signified the beginning of a new quarter; otherwise, the infiltration rate at the end of the first quarter also served as the initial infiltration rate for the second quarter, and so on. Summary statistics for each location were calculated, including the absolute change and percent change in SIR during each testing window. Locations expected to clog (near the PII, under trees, in tire tracks in a parking space, etc.) were compared against control locations at each site. When infiltration rates increased over a quarter (due to error inherent in testing methodologies, especially at very high infiltration rates), the change was assumed to be zero. Paired statistical tests were utilized to determine if reductions in SIR over the testing windows at each location type (near the PII, control, concentrated flow, etc.) were statistically significant. The t-test was used if data were normal or log-normal; otherwise the Wilcoxon signed rank test was used. The Shapiro-Wilk and Anderson-Darling normality tests as well as quantile-quantile plots aided in assessing normality.

Since clogging was apparent near the PII, further analysis of the locations near the PII was undertaken to develop a relationship for how fast these areas clog. Data at all locations near the

PII were aggregated across sites. Relationships between the percent change and absolute change in infiltration rate over the testing window were explored as a function of rainfall depth and loading ratio, as these two factors were presumed responsible for conveyance of sediment onto the permeable pavement, thereby clogging it. A linear relationship over each quarterly SIR testing window was developed between initial SIR and the change in SIR normalized by total rainfall depth during the monitoring window.

In order to relate the performance of the SIT to the ASTM test, the median value for each type of test was calculated for each monitoring date. These two values were paired, with a resulting 123 paired median infiltration rates. A linear regression was applied to develop a relationship between the two tests, with the intent to use the SIT and to predict ASTM equivalent infiltration rates.

Pre- and post-maintenance infiltration testing was completed during the monitoring period at Willoughby Hills, NCCU, and Piney Wood. This allowed for quantification of the improvement in SIR provided by various maintenance schemes, including: a standard bristle street sweeper (no suction), a regenerative air street sweeper, and a vacuum truck. Absolute change and percent change in infiltration rate were summarized for each maintenance type. Separate paired statistical tests (either t-test or Wilcoxon signed rank) were used to determine if improvements to SIR post-maintenance were statistically significant.

All data analysis was completed using R version 3.1.2 (R Core Team 2014). A criterion of 95% confidence (α=0.05) was used for this research.

6.4 Results and Discussion

6.4.1 Prevalence of Clogging by Test Location

Surface infiltration rate data were combined by test location over all testing windows to analyze where and to what extent clogging occurred within the five permeable pavement applications (Figure 66 and Table 42). Measures of central tendency suggested very little clogging at the control sites from beginning to end of the testing windows. These sites received very little, if any, surface flow from impermeable pavement, and essentially treated direct rainfall. A median 11% change in SIR and median absolute change of 66 in/hr was experienced for these locations on a quarterly basis, which was not statistically significant (p-value = 0.20). Control site SIRs were generally within the ranges observed by Bean et al. (2007) for properly functioning PC (800-2600 in/hr) and PICP (800-1600 in/hr). Thus, for sites treating only direct rainfall and without substantial tree cover, the clogging rate should be quite small, and the initial maintenance interval will be years after installation.

Locations beneath trees were present at Piney Wood and Orange Village. A statistically significant decrease in SIR occurred beneath trees over the testing windows, presumably due to the additional organic matter deposited on the pavement surface. Median absolute and percentage reduction from the beginning to end of the quarterly testing windows were 261 in/hr and 66%, respectively. Locations with concentrated flow that were not near the PII were only present at NCCU, and were already clogged in April 2014 (median SIR = 28 in/hr), the date of the first set of SIR tests. However, additional clogging occurred during the monitoring period, with median final SIR in January 2015 of 10 in/hr. This represented a median percentage change of 72%, which was statistically significant. Rapid clogging of locations receiving concentrated run-on also was observed by Pezzaniti et al. (2009). Since unstable watersheds have been

suggested as a cause for surface clogging of permeable pavements (Bean et al. 2007), one test location at Willoughby Hills selected because it had a small chipseal walkway draining to it, which contributed sediment to the permeable pavement. While SIRs significantly declined for PII, tree, concentrated flow, and chipseal sidewalk testing locations during the testing windows, the median absolute change was only 24 in/hr. The median initial infiltration rate was 206 in/hr, suggesting that this site had partially clogged prior to the first round of infiltration tests. Perhaps the chipseal on the walkway prevented the clayey *in situ* soil from badly clogging the pavement surface, but grass clipping, twigs, and other organic matter were noted in the interstitial spaces at this location. Two locations at Orange Village were at the entry to the parking lot, but did not receive run-on from impermeable pavement. No significant difference (p-value = 0.70) in initial and final infiltration rates over the testing windows was observed for these two sites, and median percentage change (5%) in infiltration rate was near that of control sites. This suggests traffic may be a minor factor in clogging of permeable pavements, as suggested by Fassman and Blackbourn (2010).

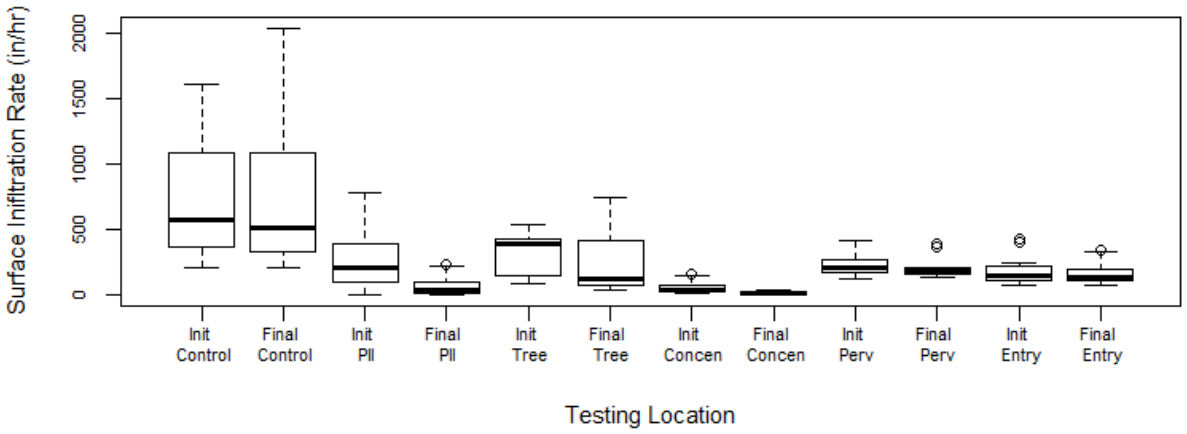

Figure 66. Boxplots of SIR by location across all monitoring sites. Paired initial and final data are presented for the permeable/impermeable interface (PII), control (direct rainfall only), locations underneath trees, locations receiving concentrated flow, locations receiving flow from pervious areas, and locations in entryways that receive no run-on, respectively.

Table 42. Summary statistics for SIR by location across all monitoring sites.

Parameter	Control		PII		Tree		Concentrated Flow		Chipseal Sidewalk/Pervious		Entryway	
	Initial	Final	Initial	Final	Initial	Final	Initial	Final	Initial	Final	Initial	Final
Number of Tests	80		122		25		23		19		20	
Range (in/hr)	208-1600	204-2033	3.8-775	0.6-225	78-539	38-743	7.4-158	1.1-39	118-408	132-394	73-428	73-341
Mean (in/hr)	727	721	258	58	324	249	55	14	230	213	177	161
Median (in/hr)	576	510	207	37	383	122	39	11	206	181	141	134
Median Absolute Change (in/hr)	66		170		261		28		24		7	
Median % Change	11		82		68		72		12		5	
Statistical Test	Wilcoxon Signed Rank		Wilcoxon Signed Rank		Wilcoxon Signed Rank		Wilcoxon Signed Rank		t-test		t-test	
p-value	0.20		2.00E-16		0.03		3.33E-06		0.01		0.70	
Significantly Different?	No		Yes		Yes		Yes		Yes		No	

Location 3 at Perkins Township was selected to represent an area that experienced improper curing of the pervious concrete due to wind blowing the plastic tarp off of the wet concrete, resulting in raveling of the pavement surface. SIR tests from this location were compared against control locations at Perkins Township (Figure 67). SIR for the raveled location were not significantly different from the control (p-value = 0.11). Median SIR for the raveled location was 1212 in/hr, while that of the control locations was 1290 in/hr. These results suggest raveling may affect the aesthetics and lifespan of pervious concrete, but does not affect the infiltration properties.

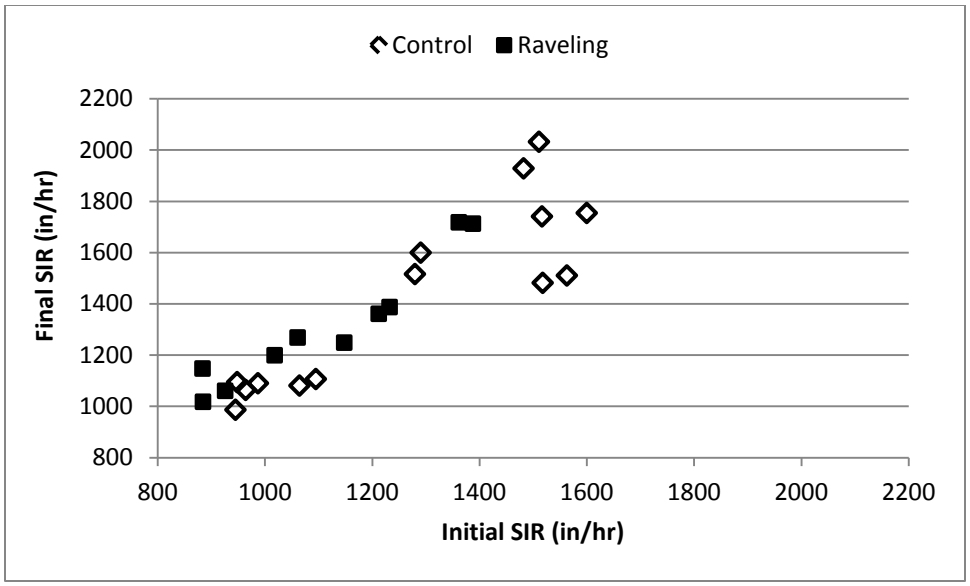

Figure 67. Pervious concrete SIR for control and raveled locations at Perkins Township at the beginning and end of each quarter.

At Perkins Township, locations 4 and 5 were located within the same parking stall. Location 4 was in the middle of the parking stall, with no impacts from traffic. Location 5 was identified by a tire path that had formed within the parking spot, which was utilized nearly every business day. It was 2.75 ft east of location 4, with both SIR testing sites located 5.5 ft downslope from the PII. SIRs at the tire track site were significantly (p-value 3.41×10^{-5}) less than in the center of the parking stall, suggesting that micro-scale clogging does occur within permeable pavement parking lots (Figure 68). Median SIRs were 1103 and 874 in/hr for the no tire track and tire track locations, respectively. Similar reductions in SIR were found in tire tracks in pervious concrete and PICP applications in Lingen, Germany (Illgen et al. 2007). Median SIRs for the tire track location were still quite high, suggesting that while tires may impart additional sediment and debris on the pavement, a tire track is not as substantial a clogging factor as trees, concentrated flow, or the PII.

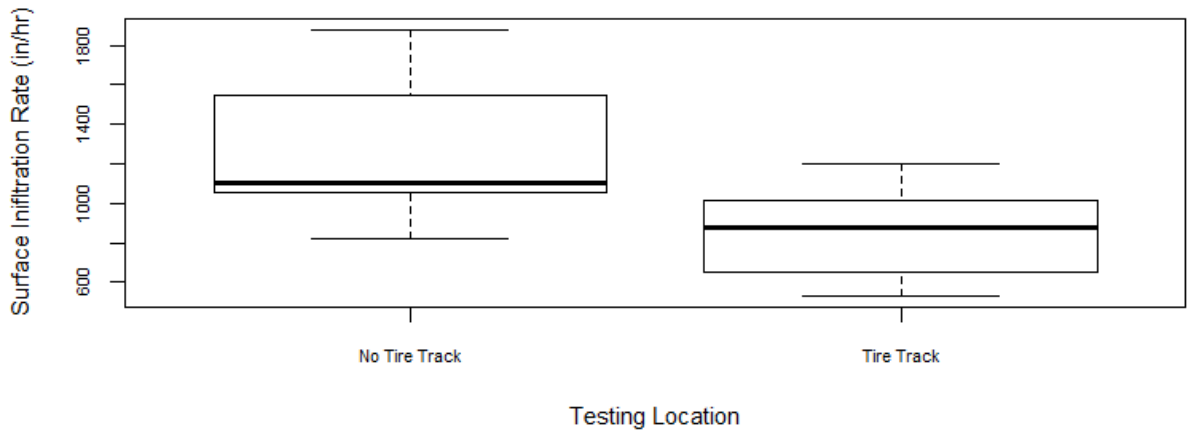

Figure 68. Differences in SIR for pervious concrete in center of parking stall (site 4) and tire track (site 5) at Perkins Township.

The most significant factor for clogging was location near the PII, with a p-value of $2x10^{-16}$. While the control sites fall on or near the 1:1 line, the PII sites often have a 10-fold reduction in SIR over the quarterly testing windows (Figure 70). The median change from the beginning to end of the testing window was an 82% reduction in SIR for sites within 8 feet of the PII, the highest of any location studied. Additionally, minimum SIRs were an order of magnitude lower than those from control, tree, pervious, or entryway locations, suggesting that clogging was concentrated at the PII (Figure 66). Many of the PII locations were substantially clogged within the first 6 months of operation, with SIRs less than 150 in/hr. SIRs were often less than 20 in/hr at locations within 2 feet of the PII (Figure 70). This rate is high enough to infiltrate most rainfall if the pavement is only treating direct rainfall (as noted in Al-Rubaei et al. 2013), but results in surface runoff when run-on ratio is high. Infiltration testing was conducted on July 9, 2014, at Willoughby Hills with two locations near the PII having median SIRs of 8.5 and 97 in/hr at locations 7 and 8, respectively (Figure 69). From the photographs, it can be seen infiltration rates were not high enough to infiltrate all of the water before surface bypass occurred, even though this storm was quite small (0.2 inches) and was not particularly intense

(peak 5-minute intensity 0.36 in/hr). This along with the results from NCCU suggest shallow concentrated or concentrated flow regimes should be avoided for flow entering permeable pavement.

Figure 69. Runoff entering PICP at Willoughby Hills on July 17th, 9 days after infiltration testing. Shallow concentrated flow created by parking lot island (left) and flow passing all the way to the catch basin, bypassing treatment (right).

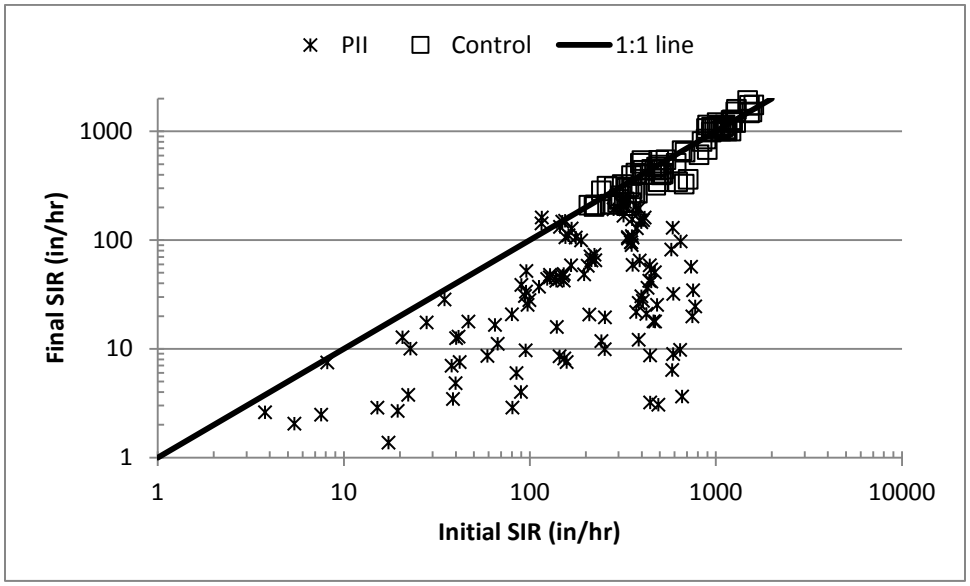

Figure 70. SIR for PII and control locations across sites shown at the beginning and end of each quarterly testing window, with the 1:1 line shown.

Since the PII was the focus of the most substantial clogging in this study, further analysis of the clogging rate at these locations was warranted. Relationships between initial and final infiltration rates across the testing window were explored. This included both absolute change

and percentage change in infiltration rate. These were regressed with and normalized by various factors including loading ratio, rainfall depth, and others. The best predictor of final infiltration rate (based on goodness of fit) was a relationship between initial infiltration rate and the absolute change in infiltration rate over the testing window normalized by rainfall depth (Figure 71). This relationship explained 83% of the variability in the data, with limits on initial infiltration rates between 0-800 in/hr for sites within 8 ft of the PII. Thus, as long as the initial infiltration rate and the total rainfall depth over a period of interest are known, the expected final infiltration rate can be estimated.

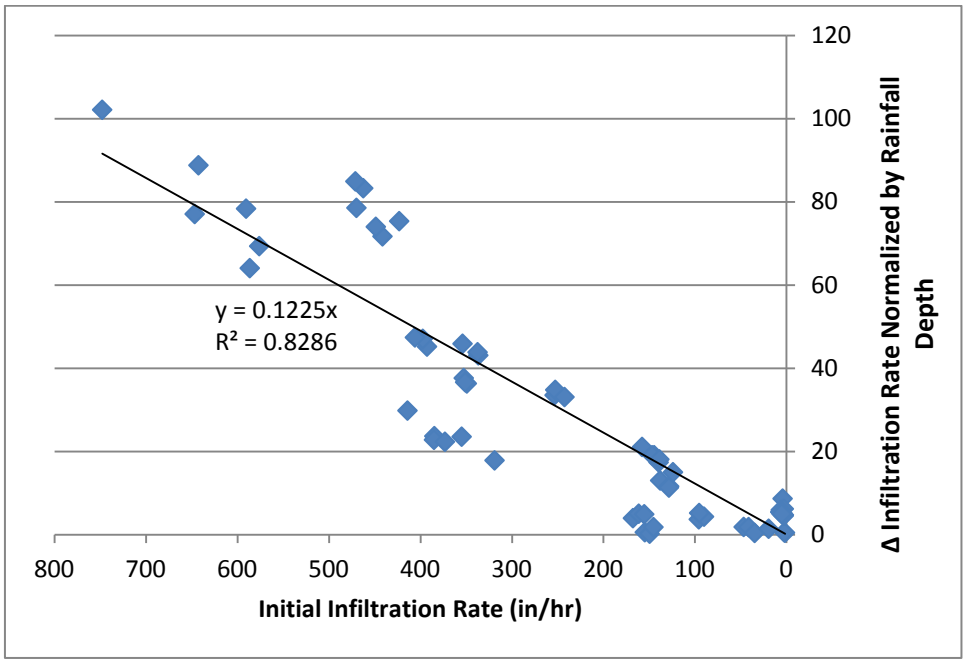

Figure 71. Change in infiltration rate for sites near the PII normalized by rainfall depth as a function of initial infiltration rate of the permeable pavement.

In order to predict maintenance intervals near the PII, this model (which is valid only within 8 feet of the PII) was applied using initial infiltration rates between 1000-1500 in/hr, to represent newly constructed permeable pavements. After the first 6 inches of rainfall, SIRs were predicted to be 265-398 in/hr. After 12 inches of rainfall (roughly 1/3rd of the yearly rainfall depth in northern Ohio), SIRs were in the range of 70-105 in/hr. Given that surface bypass occurred near

the PII at Willoughby Hills at 100 in/hr SIR, this might be an appropriate target to signal maintenance is needed near the PII. Thus, the initial maintenance interval for sites with run-on for impermeable/permeable ratios greater than 2.15 would be 4 months. However, maintenance has *not* been shown to rejuvenate the pavement SIR entirely (i.e. to SIRs of a newly-installed permeable pavement; Bean et al. 2007; Chopra et al. 2010; Al-Rubaei et al. 2013; Drake and Bradford 2013). This means the maintenance schedule thereafter would be non-linear and the time would need to be shortened after each successive maintenance activity.

While normalizing the change in SIR by both rainfall and loading ratio reduced the R^2 value (and was therefore not the best model) in Figure 71, the loading ratio does factor into clogging. At higher loading ratios, runoff is characterized by greater volumes, flow rates, and velocities, entraining more pore-clogging sediment. At every site, locations further from the PII had higher SIRs than those closer to the PII (Figure 72). At the site with the lowest loading ratio (0.75, Perkins Township), the progression of clogging had not made it to the downslope PII monitoring point (location 7), situated 87 inches from the PII. SIRs at this point were all above 900 in/hr during the last SIR tests in October 2014. Location 6 (nearest the PII) at Perkins Township has clogged over time, from median infiltration rates of 355 in/hr in April to 161 in/hr in July to 111 in/hr in October 2014. This site has not yet required maintenance of the pavement, even though it is the oldest of the sites monitored (constructed November 2012). Sites with higher loading ratios (1.8-7.2) and concentrated or shallow concentrated flow entering the permeable pavement (Willoughby Hills, NCCU, and Piney Wood) required maintenance within the first six months of operation. This suggested that lower loading ratios will result in correspondingly lower maintenance frequency.

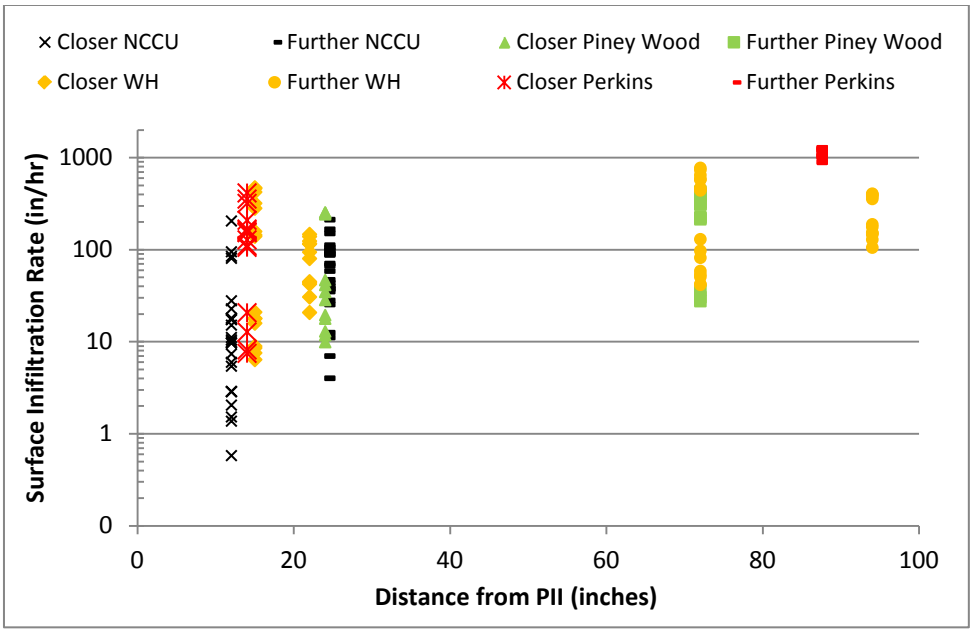

Figure 72. SIR as a function of distance from the PII by site. Symbols of similar color are from the same site.

6.4.2 Comparison of SIT and ASTM Tests

A linear relationship was established between SIR measured using the ASTM method and SIR measured using the SIT (Figure 73), to allow prediction of ASTM-equivalent SIR as a function of SIT SIR. For each set of SIT and ASTM data at a particular monitoring location on a given day, the median value was calculated for SIR and ASTM tests. These data were then paired and used in the linear regression, resulting in a total of 123 paired data points from Willoughby Hills, Orange Village, Perkins Township, NCCU, and Piney Wood park. A linear model fit the data well, with measured SIR of the SIT explaining 92.2% of the variability in the ASTM measured SIR. The F test statistic was highly significant (p-value < 2.2E-16), suggesting that both the slope and intercept were different from zero. It should be noted the SIT and ASTM tests measure SIR on different pavement surface areas, resulting in some of the variability in Figure 73.

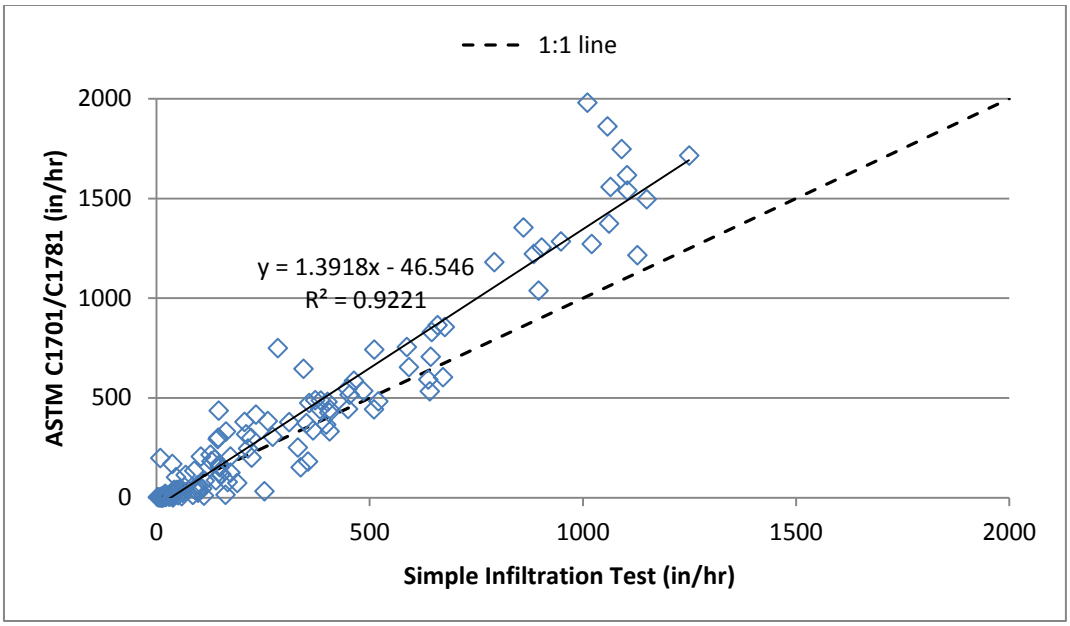

Figure 73. Linear relationship between surface infiltration rates among SIT and ASTM tests.

Because the surface area of the SIT is 440% greater than that for the ASTM test, while the volume of water applied during the tests is the same, the ASTM test takes longer to complete ($\bar{x}$ = 10.7 ± 19.9 minutes, range 0.1-47.6 minutes) than the SIT ($\bar{x}$ = 2.3 ± 4.6 minutes, range 0.3-176 minutes). SIR test duration for the most clogged locations, represented by the 90th percentile duration of testing, were 6.5 minutes for the SIT and 30.2 minutes for the ASTM test. Practically, this means maintenance personnel can determine maintenance needs for a permeable pavement application approximately 5 times more quickly using the SIT. Results could then be converted from the SIT to the ASTM infiltration rate using the relationship presented in Figure 73.

To determine the repeatability of both tests, the coefficient of variation (CV) was calculated for each test site at each location on each test date. The CV was plotted against mean SIR in Figure 74, which showed a much higher variability in measured infiltration rates at lower SIR. Especially for sites with SIR less than 10 in/hr, the organic material and accumulated sediment in

the pore spaces caused a decrease in infiltration rate as its water content increased. This meant for each successive test, SIR would often decrease as the water content of the clogged pore spaces approached saturation. At very high SIR (>100 in/hr), little variability existed in the measurements, and CV approached zero asymptotically. Paired CV values for ASTM and SIT methods were compared using a Wilcoxon signed rank test, and were statistically different (p-value 0.002). The mean CV for the ASTM test was 0.103, while that for the SIT was 0.035. These results suggest that the SIT is at least as repeatable as the ASTM test (if not more), and given its other advantages (shorter time to complete, cheaper and simpler to build the infiltrometer), it could be a preferable method.

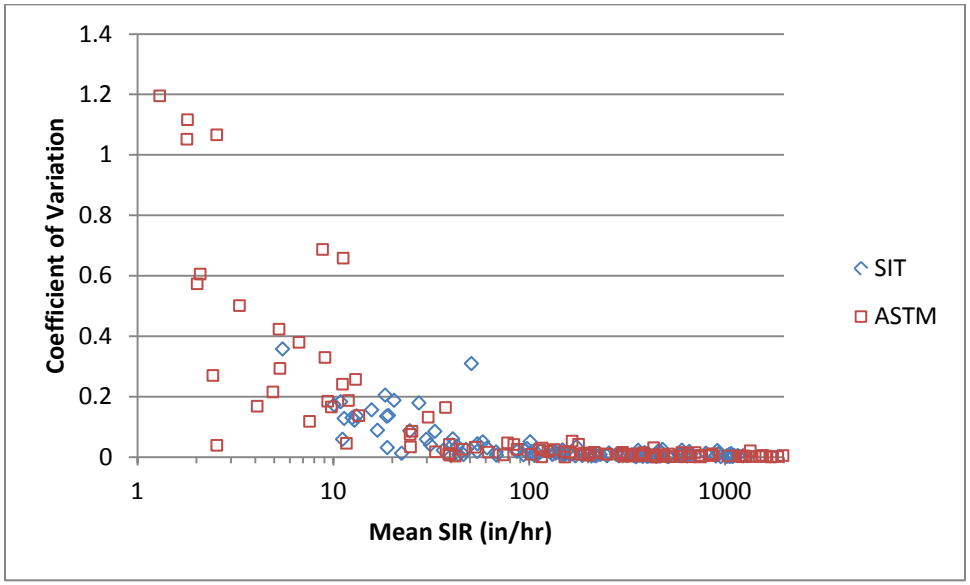

Figure 74. Coefficient of variation for SIT and ASTM surface infiltration rate measurements.

6.4.3 Improvements in Surface Infiltration Rate due to Maintenance

Two types of maintenance were performed over a two day period at the NCCU site, as all five of the SIR testing sites were badly clogged (median SIR <10 in/hr by the ASTM test). The first attempt at maintenance was made on October 9, 2014, and was carried out by making 4-5 passes

over the permeable pavement using a standard bristle street sweeper (Figure 75). This type of street sweeper applies pressure to the surface of the pavement through rotating bristles, dislodging material accumulated in the interstitial spaces. It does not have a suction component intended to collect sediment responsible for clogging, and observations showed it dislodged only the uppermost 1/4-1/2 inches of clogging material. Immediately following maintenance, infiltration testing was completed to measure the improvement in infiltration rate. The median improvement in SIR was 54% using the SIT test (range of -38% to 347%) and 223% using the ASTM test (range of -58% to 1902%, Table 43). The larger percentage improvements for the ASTM tests likely resulted from the lower pre-maintenance infiltration rates (median 2.5 in/hr) versus the SIT test (median 15.5 in/hr). Post-maintenance, median infiltration rates for the 5 monitoring locations approximately doubled to 5.3 and 29 in/hr, respectively for the ASTM and SIT (Table 43). Using a hose, water was applied to the pavement surface, and surface runoff still occurred from the permeable pavement surface; therefore, further maintenance was scheduled.

Figure 75. Standard bristle street sweeper (left) and regenerative air street sweeper (right) performing maintenance at NCCU.

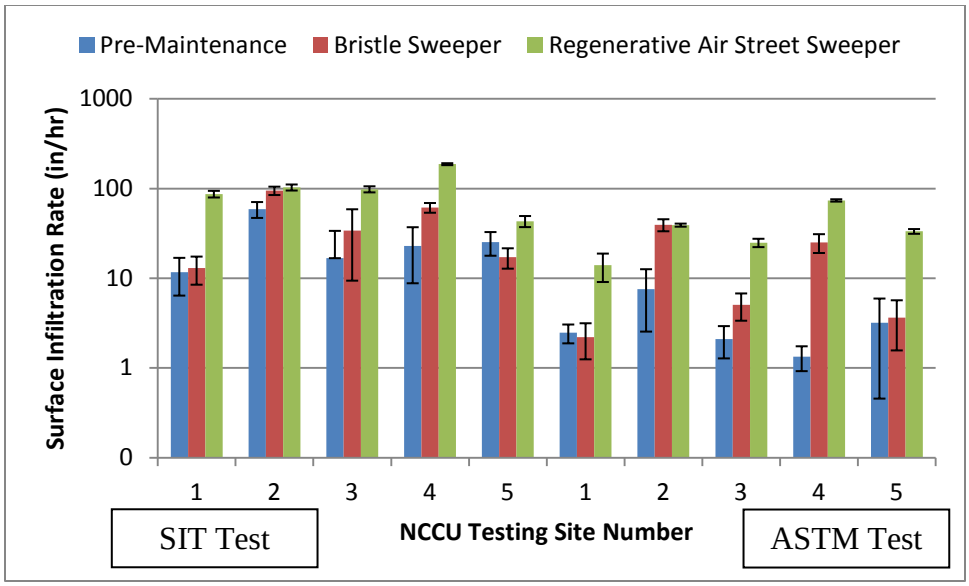

Figure 76. Improvements to SIR using a standard bristle street sweeper (10/9/2014) and a regenerative air street sweeper (10/10/2014) at NCCU.

Table 43. Measured surface infiltration rates (in/hr) for clogged locations pre- and post-maintenance. Pre = pre-maintenance, RA = regenerative air street sweeper, Bristle = bristle street sweeper (no suction), and Vacuum = vacuum truck.

Site	Type of Test	Location	Date/Type of Test		
			7/18 Pre	8/15 RA	
Piney Wood	SIT	1	22	351	
		2	18	253	
		3	30	311	
	ASTM	1	14	373	
		2	4	32	
		3	6	379	
Site	Type of Test	Location	10/6 Pre	10/9 Bristle	10/10/2014 RA
NCCU	SIT	1	10	11	85
		2	59	90	100
		3	14	29	97
		4	15	61	189
		5	22	16	40
	ASTM	1	2.5	2.2	14
		2	7.6	39	39
		3	2.1	5.1	25
		4	1.3	25.	74
		5	3.2	3.6	33
Site	Type of Test	Location	7/9 Pre	8/6 Vacuum	
Willoughby Hills	SIT	1	20	338	
		2	37	592	
		3	206	173	
		5	9	463	
		6	97	449	
		7	148	139	
		8	45	398	
	ASTM	1	19	152	
		2	169	654	
		3	380	125	
		5	199	586	
		6	41	444	
		7	152	87	
		8	103	366	

Since the bristle sweeper did not provide enough improvement in SIR to prevent surface bypass, a regenerative air street sweeper was used to perform maintenance the following day, October 10, 2014 (Figure 75). Two to three passes were made over the parking lot, except for site 5, which was blocked by an adjacent parked car. Mechanical agitation was also applied to the interstitial spaces using a pocket knife to dislodge clogging sediment. Both the SIT and ASTM tests were performed again immediately following this maintenance. Median percentage improvement from the prior day (post bristle sweeper maintenance) was 192% for the SIT test (range 5% to 735%) and 411% for the ASTM test (range -8% to 1369%, Table 43). Post regenerative air sweeper maintenance, median SIRs were 96.9 in/hr and 33.3 in/hr, respectively, for the SIT and ASTM tests (Figure 76). These larger gains in SIR suggested the suction provided by the regenerative air street sweeper was able to dislodge clogging material at deeper depths, thereby providing better rejuvenation of the pavement SIR.

At Piney Wood, maintenance was performed using a regenerative air street sweeper in the fall of 2014. The three testing locations closest to the PII (sites 1-3, Figure 77) had pre-maintenance median SIRs of 14, 4, and 6 in/hr for the ASTM test (22, 18, and 30 in/hr using the SIT). These locations were swept with 5-6 passes of the street sweeper, with the sweeper moving slowly and stopping over heavily clogged areas. Post-maintenance, median percentage improvement in SIR was 1318% for the SIT and 2525% for the ASTM test (sites 1-3 only, Table 43). Median post-maintenance infiltration rates were improved significantly to 311 in/hr for the SIT and 373 in/hr for the ASTM test. Sites 4-6 were furthest from the PII, and did not appear clogged visually; therefore, maintenance made little difference in SIR (Figure 77).

Similar pre- and post-maintenance infiltration testing was undertaken at Willoughby Hills using an Elgin Megawind vacuum truck during August 2014 (Figure 77 and Table 43). This

type of sweeper provides greater suction than a regenerative air street sweeper. Maintenance consisted of one pass over the entire parking lot, and a second pass over the more heavily clogged PII locations, with replacement of stone in the interstitial spaces following maintenance. Post-maintenance, the median SIRs increased by 568% for the SIT (range -16% to 5308%) and 208% for the ASTM test (range -43% to 990%). This was in the range of the 200% increase observed for combined power washing and power blowing utilized in PC maintenance by Dougherty et al. (2011). For three sites, SIR did not improve substantially post- maintenance: locations 3, 4, and 7. Location 4 was the control monitoring location, and was not clogged (pre-maintenance median SIRs of 650-800 in/hr). Locations 3 and 7 were located in the Small and Large applications, respectively, and were less than 2 ft from the PII. Given the large loading ratios to these locations, frequent and heavy maintenance will be needed to keep sites near the PII from clogging. It was suggested by Drake and Bradford (2013) that sites with severely degraded permeability (i.e. clogging several inches into the PICP joints) were not able to be rejuvenated by regenerative air street sweepers. They suggested frequent maintenance at these sites receiving high particulate loading to maintain acceptable SIRs.

For most clogged locations (1-3 and 5-8 at Willoughby Hills, 1-3 at Piney Wood), the vacuum truck and regenerative air street sweepers performed similarly for restoration of post-maintenance SIRs. At Willoughby Hills, median post-maintenance SIRs were 398 and 366 in/hr for the SIT and ASTM tests, respectively (Table 43). These rates were 311 and 373 in/hr for Piney Wood. However, the Piney Wood maintenance was more intensive, with 5-6 passes of the regenerative air sweeper and focused maintenance on heavily clogged areas, including the use of a pocket knife to mechanically loosen debris. At Willoughby Hills, the vacuum truck made two passes over the PII and one over the rest of the lot, and achieved the same results. This

suggested a vacuum truck was more effective for maintenance of PICP when run-on was part of the design.

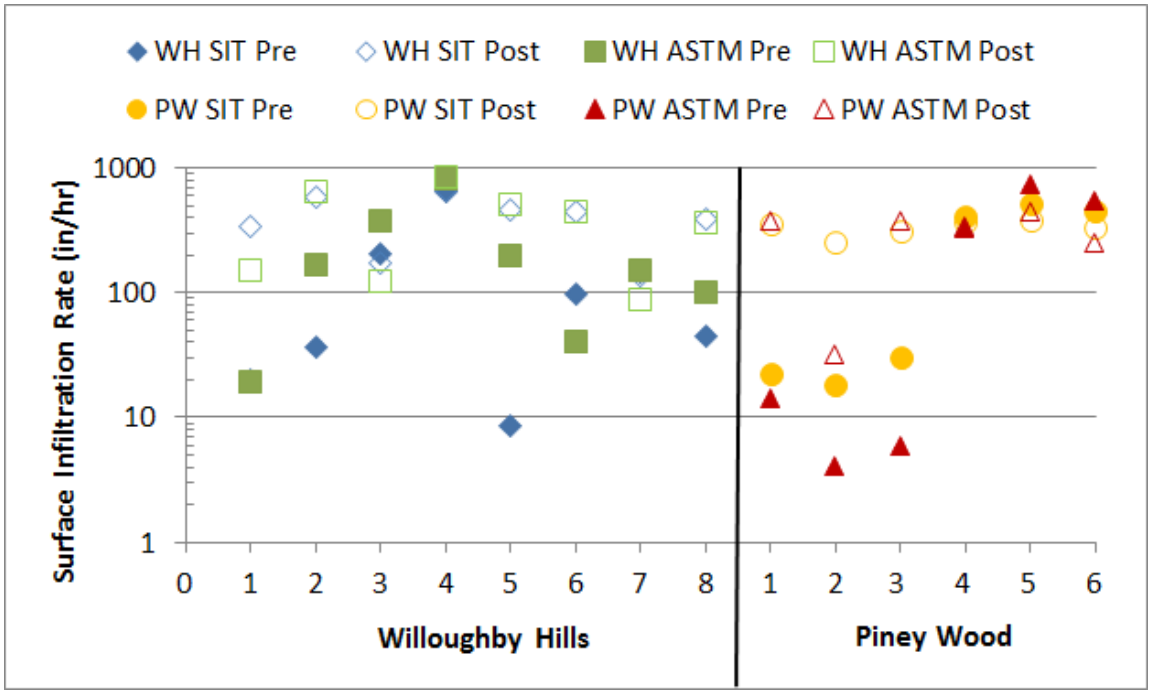

Figure 77. Pre- and post-maintenance SIR for locations at Willoughby Hills (vacuum truck) and Piney Wood park (regenerative air).

Statistical testing was undertaken to determine the impacts of street sweeping on surface infiltration rate of PICPs (Table 44). Data were pooled by site and by date of maintenance. All data sets were log normal except for the post-maintenance ASTM test data at Willoughby Hills, which could not be rendered normal using standard transformations. Paired pre- and post-maintenance data were tested using Student's t-tests for all data sets except the Willoughby Hills ASTM data, which were tested using the Wilcoxon signed-rank test. The use of the bristle sweeper at NCCU significantly improved the SIR (Figure 76). However, the follow-on maintenance the follow day using a regenerative air street sweeper provided greater removal of organic material that accumulated in the interstitial spaces (Figure 76). Improvements in SIR

also were statistically significant at Piney Wood and Willoughby Hills for both SIT and ASTM tests (Table 44), meaning all types of maintenance were able to significantly improve SIR.

Table 44. Results of statistical comparisons between pre- and post-maintenance surface infiltration rates.

Parameter	Bristle Sweeper		Regenerative Air Sweeper				Vacuum Truck	
	NCCU		Piney Wood		NCCU		Willoughby Hills	
	SIT	ASTM	SIT	ASTM	SIT	ASTM	SIT	ASTM
p-value	0.0143	0.021	0.00345	0.04	1.55E-05	0.00069	1.65E-05	0.021
Significant?	Yes	Yes	Yes	Yes	Yes	Yes	Yes	Yes
Test	Student's t-test	Student's t-test	Student's t-test	Student's t-test	Student's t-test	Student's t-test	Student's t-test	Wilcoxon Signed Rank

6.5 Summary and Conclusions

A series of monitoring locations were established for surface infiltration rate testing at 5 permeable pavement applications in Ohio and North Carolina. Testing locations were chosen to evaluate clogging. SIR tests were conducted quarterly to determine the progression of clogging over time. Additionally, maintenance was performed on permeable pavements to determine its impact on SIRs. Two different types of infiltrometers were utilized in this study: a single ring, constant head method, and a simple infiltration test employing falling head techniques. The following conclusions can be drawn from this study:

1) The rate of clogging at control sites, which did not receive run-on or additional stressors, was not statistically significant and was relatively low at 66 in/hr per over each quarterly testing window. The presence of trees, concentrated flow onto the permeable pavement, and the PII caused statistically significant reductions in SIR. Entryways onto permeable pavement, where tires might be expected to drop sediment and organic debris, were not a factor in increasing clogging rates. Raveling of pervious concrete was shown to not significantly impact SIR, while the presence of a tire track from repeated wear and deposition of sediment on pervious concrete significantly decreased SIR by 21% over an adjacent unimpacted location.

2) A relationship was derived to predict clogging at the PII, the most heavily stressed location in terms of sediment load, as a function of the initial infiltration rate and the total rainfall depth during the period of interest. To prevent surface runoff, it was suggested, at loading rates studied herein (2-7:1), the PII would require maintenance within 4 months post-construction, and then subsequent maintenance would need to become more and more frequent.

3) A linear relationship was developed between SIRs measured using the SIT and the ASTM methods, so contractors could predict ASTM infiltration rates based on the SIT, which takes less time to complete. The ASTM test generally predicted lower infiltration rates than the SIT test, and the relationship developed herein would need to be applied to the SIT to predict ASTM test results.

4) Maintenance was conducted at three of the monitoring sites: Piney Wood, NCCU, and Willoughby Hills. Different methods of maintenance were utilized, including a standard bristle street sweeper (no suction), a regenerative air street sweeper, and a vacuum truck. Street sweepers with greater suction should be utilized for maintenance (regenerative air sweeper or vacuum truck), especially near the PII, which may need frequent maintenance with a vacuum truck. Maintenance did *not* return SIR to 800-1600 in/hr or 800-2600 in/hr, which have been suggested to be the SIR for newly-constructed PICP and PC, respectively (Bean et al. 2007). This suggested maintenance was not 100% effective at removing clogging material, meaning that more frequent maintenance of permeable pavements will be needed over time to meet a threshold SIR.

6.6 References

Al-Rubaei, A.M., Stenglein, A.L., Viklander, M., and Blecken, G.T. (2013). "Long-term hydraulic performance of porous asphalt pavements in northern Sweden." *Journal of Irrigation and Drainage Engineering*. 139(6), 499-505.

American Society for Testing and Materials (ASTM). (2009). *Standard test method for infiltration rate of in place pervious concrete.* ASTM C1701/C1701M-09.

American Society for Testing and Materials (ASTM). (2013). Standard test method for surface infiltration rate of permeable unit pavement systems. C1781/C1781M-13.

Bean, E.Z., Hunt, W.F., and Bidelspach, D.A. (2007). "Field survey of permeable pavement surface infiltration rates." *Journal of Irrigation and Drainage Engineering*. 133(3), 249-255.

Boogaard, F., Lucke, T., and Beecham, S. (2014a). "Effect of age of permeable pavements on their infiltration function." *CLEAN–Soil, Air, Water*. 42(2), 146-152.

Boogaard, F., Lucke, T., van de Giesen, N., and van de Ven, F. (2014b). "Evaluating the infiltration performance of eight Dutch permeable pavements using a new full-scale infiltration testing method. *Water*. 6(7), 2070-2083.

Brattebo, B. O., and Booth, D. B. (2003). "Long-term stormwater quantity and quality performance of permeable pavement systems." *Water Research.* 37(18), 4369-4376.

Brown, R.A., and Borst, M. (2013). "Assessment of clogging dynamics in permeable pavement systems with time domain reflectometers." *Journal of Environmental Engineering*. 139(10), 1255-1265.

Brown, R.A., and Borst, M. (2014). "Evaluation of surface infiltration testing procedures in permeable pavement systems." *Journal of Environmental Engineering*. 140(3), 04014001.

Chopra, M., Kakuturu, S., Ballock, C., Spence, J., and Wanielista, M. (2010). "Effect of rejuvenation methods on the infiltration rates of pervious concrete pavements." *Journal of Hydrologic Engineering*. 15(6), 426-433.

Collins, K. A., Hunt, W. F., and Hathaway, J. M. (2008). "Hydrologic comparison of four types of permeable pavement and standard asphalt in eastern North Carolina." *Journal of Hydrologic Engineering.* 13(12), 1146-1157.

Dougherty, M., Hein, M., Martina, B.A., and Ferguson, B.K. (2011). "Quick surface infiltration test to assess maintenance needs on small pervious concrete sites." *Journal of Irrigation and Drainage Engineering*. 137(8), 553-563.

Drake, J., and Bradford, A. (2013). "Assessing the potential for restoration of surface permeability for permeable pavements through maintenance." *Water Science and Technology*. 68(8), 1950-1958.

Fassman, E. A., and Blackbourn, S. (2010). “Urban runoff mitigation by a permeable pavement system over impermeable soils.” *Journal of Hydrologic Engineering.* 15(6), 475-485.

Gerrits, C., and James, W. (2002). “Restoration of infiltration capacity of permeable pavers.” *Proceedings of the 9th International Conference on Urban Drainage*. ASCE, Portland, Ore.

Gilbert, J. K., and Clausen, J. C. (2006). “Stormwater runoff quality and quantity from asphalt, paver, and crushed stone driveways in Connecticut.” *Water research*. *40*(4), 826-832.

Haselbach, L.M. (2010). “Potential for clay clogging of pervious concrete under extreme conditions.” *Journal of Hydrologic Engineering*. 15(1), 67-69.

Hunt, W.F. (2011). *Maintaining permeable pavements*. North Carolina Cooperative Extension Urban Waterways fact sheet series. AG-588-23 W.

Illgen, M., Harting, K., Schmitt, T.G., and Welker, A. (2007). “Runoff and infiltration characteristics of permeable pavements – Review of an intensive monitoring program.” *Water Science and Technology*. 56(10), 133-40.

Leopold, L.B., Wolman, M.G., and Miller, J.P. (1964). *Fluvial processes in geomorphology*. W.H. Freeman and Company, San Francisco, USA.

Lucke, T., and Beecham, S. (2011). “Field investigation of clogging in a permeable pavement system.” *Building Research and Information*. 39(6), 603-615.

Lucke, T. (2014). “Using drainage slots in permeable paving blocks to delay the effects of clogging: Proof of concept study.” *Water*. 6(9), 2660-2670.

Page, J.L., Winston, R.J., Mayes, D.B., Perrin, C., and Hunt, W.F. (2015). “Hydrologic mitigation of impervious cover in the municipal right-of-way through innovative stormwater control measures.” *Journal of Hydrology.* 527, 923-932.

Pezzaniti, D., Beecham, S., and Kandasamy, J. (2009). “Influence of clogging on the effective life of permeable pavements.” *Proceedings of the Institution of Civil Engineers-Water Management*, 162(3), 211-220.

Pratt, C.J., Mantle, J.D.G., and Schofield, P.A. (1989). “Urban stormwater reduction and quality improvement through the use of permeable pavements.” *Water Science and Technology*, 21(8), 769–778.

Pratt, C.J., Mantle, J.D.G., and Schofield, P.A. (1995). “UK research into the performance of permeable pavement, reservoir structures in controlling stormwater discharge quantity and quality.” *Water Science and Technology*, 32(1), 63–69.

R Core Team. (2014). *A language and environment for statistical computing*. R Foundation for Statistical Computing. Vienna, Austria.

Roseen, R.M., Ballestero, T.P., Houle, J.J., Briggs, J.F., and Houle, K.M. (2012). “Water quality and hydrologic performance of a porous asphalt pavement as a storm-water treatment strategy in a cold climate.” *Journal of Environmental Engineering*. 138(1), 81-89.

Sansalone, J., Kuang, X., and Ranieri, V. (2008). “Permeable pavement as a hydraulic filtration interface for urban drainage.” *Journal of Irrigation and Drainage Engineering*. 134(5), 666–674.

7 SUMMARY AND CONCLUSIONS

An extensive study of LID stormwater controls was undertaken along the Lake Erie shoreline in northern Ohio. Four permeable pavement applications and three bioretention cells were extensively monitored at the direction of a Collaborative Learning Group of stormwater professionals. The following over-arching conclusions can be drawn from this work:

1) Both bioretention and permeable pavements can be implemented successfully in the poorly draining soils and harsh winter climate of northern Ohio.

2) Volume reductions for permeable pavements varied from 13% to nearly 99%, showing that a one-size-fits-all approach for crediting these systems may not be appropriate. Factors that contributed to greater volume reductions were: (1) lower hydrologic loading ratio, (2) incorporation of an IWS zone, and (3) higher permeability underlying soils.

3) Volume reductions for the three bioretention cells were 36%, 42%, and 60%. While drawdown rates were relatively low, the deep IWS zones (15-24 inches) employed at each site helped to improve exfiltration.

4) Peak flow mitigation occurred in both permeable pavements and bioretention cells, even during the most intense rainfall events. This was generally due to the fact that the peak rainfall intensity often occurred before the centroid of the rainfall depth, meaning that there was still bowl storage or aggregate storage available to reduce the outflow peak. Also, the outflow rate is limited by the underdrain, as long as overflow from bioretention or surface bypass (due to clogging) in permeable pavement does not occur.

5) Sampling of water quality during storm events provided interesting insight into SCM performance. For instance, two permeable pavements leached sediment into their drainage, which was potentially related to either a maturation period following construction or sediment

deflocculation following deicing salt use. Permeable pavements provided the vast majority of their water quality benefit through reduction in outflow volume. The addition of a cistern in a treatment train with permeable pavement provided additional hydraulic retention time and excellent effluent water quality. Water quality samples from the bioretention cell at Ursuline College suggested leaching of organic matter from the media. Other parameters such as metals and sediment were well sequestered by the SCM.

6) A study carried out on clogging of permeable pavement suggested that the permeable/impermeable interface will be the location receiving the largest sediment load, and therefore the most apt to clog. Locations beneath trees, draining pervious areas, and with higher traffic load were also more apt to clog. A simple infiltration test was developed that may provide quicker estimation of where (spatially) maintenance is needed within a permeable pavement application. Maintenance with street sweepers was shown to be effective in increasing surface infiltration rate through removal of clogging materials. However, diligent maintenance over time will be needed to maintain pavement permeability.

8 ACKNOWLEDGEMENTS AND DISCLAIMER

This final report is based upon work supported by the University of New Hampshire under Cooperative Agreement No. NA09NOS4190153 (CFDA No. 11.419) from the National Oceanic and Atmospheric Association. Financial assistance was also provided under award number DNRFP038 from the National Oceanic and Atmospheric Administration, U.S. Department of Commerce through the Old Woman Creek National Estuarine Research Reserve, administered by the Ohio Department of Natural Resources, Division of Wildlife. The Old Woman Creek National Estuarine Research Reserve is part of the National Estuarine Research Reserve System, (NERRS), established by Section 315 of the Coastal Zone Management Act, as amended. Additional information about the system can be obtained from the Estuarine Reserves Division, Office of Ocean and Coastal Resource Management, National Oceanic and Atmospheric Administration, US Department of Commerce, 1305 East West Highway – N/ORM5, Silver Spring, MD 20910. Any opinions, findings, and conclusions or recommendations expressed in this publication are those of the author(s) and do not necessarily reflect the views of the University of New Hampshire or the National Oceanic and Atmospheric Association.

The authors wish to thank a number of people for their aid throughout the project. The project team, consisting of Frank Lopez, Breann Hohmann, Crystal Dymond, Heather Elmer, Jay Dorsey, Ona Ferguson, and Ryan Winston, contributed greatly to the project goals and outcomes. The current and former staff of the Chagrin River Watershed Partners, including Amy Brennan, Heather Elmer, Keely Davidson-Bennett, Kristen Buccier, Christina Znidarsic, and Linda Moran all contributed in various ways, from aiding in surface infiltration testing of permeable pavements to collecting water quality samples to providing various GIS layers. Amy and Dan Brennan saved the grant thousands of dollars by providing housing pro-bono, allowing for the

addition of several studies beyond the original project scope. The laboratory staff at both the Northeast Ohio Regional Sewer District and Old Woman Creek National Estuarine Research Reserve (OWC NERR) are appreciated for their hard work analyzing water quality samples from the bioretention and permeable pavement monitoring sites. The cities of Willoughby Hills and Pepper Pike, Orange Village, Perkins Township, Holden Arboretum, and OWC NERR were very gracious in hosting the research sites and providing aid at various junctures to the project team. Rebecca Jacobson and Will Brown, formerly of the University of New Hampshire, were very helpful in aiding with field work for the project. Kristi Arend of OWC NERR, Rebecca Jacobson, Kristen Buccier, and Keely Davidson-Bennett are thanked for their collection of water quality samples in support of chapters 3-5 of this document. Some of the SCM installations monitored were funded by Ohio EPA under the Surface Water Improvement Fund. We thank them for this financial contribution to the project.

Finally, the authors wish to thank the Collaborative Learning Group (CLG) of stormwater professionals, who met with the project team and guided our project from start to finish. They provided 3-4 days per year of their time to meet, review our progress, and provide critical feedback that helped us to provide meaningful results in a northern Ohio context. Thanks also go to the rest of the project team for their help in making this project the success that it was.